DESIGN AND NUMERICAL EVALUATION OF FULL–AUTHORITY FLIGHT CONTROL SYSTEMS FOR CONVENTIONAL AND THRUSTER–AUGMENTED HELICOPTERS EMPLOYED IN NOE OPERATIONS

Todd A. Perri
R. M. McKillip, Jr.
H. C. Curtiss, Jr.

Department of Mechanical and Aerospace Engineering
Princeton University, Princeton, NJ 08544–5263

Principal Investigator: H. C. Curtiss, Jr.

Technical Report No. 1789T

NASA Ames Research Center Grant No. NAG 2–244
Studies in Helicopter Aerodynamics and Control

NASA Technical Officer for this Grant: W. A. Decker

INTERIM REPORT

August 1987

ABSTRACT

This study presents the development and methodology for development of full-authority implicit model-following and explicit model-following optimal controllers for use on helicopters operating in the Nap-of-the Earth (NOE) environment. The controllers were designed based on NOE handling qualities requirements and the longitudinal dynamics of the conventional AH-1G and the AH-1G fitted with a simplified longitudinal auxiliary propulsion system. Pole placement, input-output frequency response, and step input response were used to evaluate handling qualities performance. The pilot was equipped with velocity-command inputs.

A mathematical/computational "trajectory optimization" method was employed to evaluate the ability of each controller to fly NOE maneuvers. The method determines the optimal swashplate and thruster input histories from the helicopter's dynamics and the prescribed geometry and desired flying qualities of the maneuver. Minimization of a cost function which incorporates these dynamic, geometric, and flying qualities constraints resulted in the optimal control histories. From the control law for each controller, these optimal helicopter control histories were used to "back out" the pilot input histories. The helicopter state histories and pilot input histories were used to evaluate the controllers in terms of their abilities to meet the flying qualities criteria and to minimize pilot workload; pilot workload

was measured by the integral cost of stick input rates. The method avoids the time and cost constraints, and biases, associated with piloted simulation studies.

Three maneuvers were investigated for both the implicit and explicit controllers with and without auxiliary propulsion installed: pop-up/dash/descent, bob-up at 40 knots, and glideslope. The pop-up and bob-up clearly showed the advantages that the use of auxiliary propulsion has in reducing the time to complete a task and in providing increased longitudinal acceleration/deceleration while not requiring excessive pitch attitudes.

The explicit controller proved to be superior to the implicit controller in performance and ease of design. The design sythesis showed that, in most cases, it was necessary only to weight the diagonal elements of the state and control weighting matrices; guidelines for selecting these elements is included in the study. Pilot inputs using the explicit controller were smooth, decoupled, and in proportion to the desired horizontal and vertical velocities of the helicopter.

TABLE OF CONTENTS

LIST OF TABLES

LIST OF FIGURES

NOMENCLATURE

A	stability derivative matrix of open-loop helicopter
AC	Attitude Command
AH	Attitude Hold
B	control derivative matrix of open-loop helicopter
B_{1s}	perturbation longitudinal cyclic swashplate input (inches)
$\mathbb{B}_{1s}$	total longitudinal cyclic swashplate position (inches)
cos	cosine
C	control constraint function
$C_{\#}$	controller feedback or feedforward matrix
$C_{\#_{i,i}}$	element [i.i] of the $C_{\#}$ matrix
d	differential operator
deg	degrees
d	perturbation pilot input control vector
e	2.7182818
f	function dynamics
ft	feet
F	state matrix of dynamic handling qualities model
g	gravity; 32.174 ft/sec^2
G	control matrix of dynamic handling qualities model
Hz	Hertz
$\mathcal{H}$	Hamiltonian of a cost function
$\mathcal{H}_u$	control gradient
$\mathcal{H}_u'$	control gradient during control saturation

I	number of specified interior points; moment of inertia
J	scalar cost function
k	index element
k	vector of gradient fractions
K_u	cost function control weighting matrix
K_x	cost function state weighting matrix
K_{xu}	cost function state/control weighting matrix
l	adjoint operator on system dynamics
LQR	Linear Quadratic Regulator
$\mathcal{L}$	Lagrangian of a cost function
m	scalar control dimension; helicopter mass
m	control constraint adjoint vector
M	perturbation aerodynamic moments about the Y_B axis
M_u, M_w, M_q	pitching moment stability derivatives
M_{θ_0}, M_{B1s}	pitching moment control derivatives
$\mathbb{M}$	total aerodynamic moments about the Y_B axis
n	scalar state dimension; number of discrete entries in time history
NA	Not Applicable
P	Riccati matrix; roll rate
P_1	Riccati matrix
P_2	adjoint matrix for model vector (explicit controller)
PIO	Pilot Induced Oscillations
q	perturbation body axis pitch rate
Q	total body axis pitch rate; cost function state weighting matrix
Q'	augmented state weighting matrix for explicit controller
r	pilot command dimension; resultant axis in x-y plane for three-dimensional search routine

rad	radians
R	cost function control weighting matrix; yaw rate
RC	Rate Command
s, sec	seconds
sin	sine
S	adjoint matrix for pilot vector
t	time
t_i^+	time infinitesimally after t_i
t_i^-	time infinitesimally before t_i
T	perturbation thruster input (inches)
u	perturbation body axis forward velocity; scalar control variable
u_{com}	perturbation pilot horizontal velocity command
U_{com}	total pilot horizontal velocity command
$\mathbf{u}$	helicopter open-loop control vector
u_{max}	upper bound on perturbation control
u_{min}	lower bound on perturbation control
U	total body axis forward velocity
v	a variable
w	perturbation body axis downward velocity
w_{com}	perturbation pilot vertical velocity command
W_{com}	total pilot vertical velocity command
W	total body axis downward velocity
W_{xx}	implicit controller state weighting matrix
W_{xu}	implicit controller state/control weighting matrix
W_{du}	implicit controller pilot/control weighting matrix

W_{xd}	implicit controller state/pilot weighting matrix
W_{uu}	implicit controller control weighting matrix
W_{dd}	implicit controller pilot weighting matrix
x	perturbation body axis forward position; an axis for the three-dimensional search routine
$\mathbf{x}$	perturbation helicopter state vector
$\mathbf{x}_{fd}$	desired state vector at final time
$\mathbf{x}_{id}$	desired state vector at interior point time
$\mathbf{x}_m$	perturbation model state vector
X	perturbation aerodynamic forces along the X_B axis; total inertial horizontal position
X_B	forward body axis direction
X_I	horizontal inertial direction
X_T	auxiliary thruster X-force control derivative
X_u, X_w, X_q	X-force stability derivatives
X_{θ_c}, X_{B1s}	X-force control derivatives
$\mathbb{X}$	total aerodynamic forces along the X_B axis
y	perturbation downward body axis position; a variable; an axis for the three-dimensional search routine
Y	total downward inertial position
Y_B	sideward body axis direction
Y_I	sideward inertial direction
z	an axis for the three-dimensional search routine
Z	perturbation aerodynamic forces along the Z_B axis
Z_B	downward body axis direction
Z_I	downward inertial direction
Z_u, Z_w, Z_q	Z-force stability derivatives

$Z_{\theta_c}, Z_{B_{1s}}$	Z-force control derivatives
$\mathbb{Z}$	total aerodynamic forces along the Z_B axis
∂	partial differential operator
$\Delta( )$	the change in ( )
ϕ	final state penalty function
τ	handling qualities time-constant
τ_θ	collective actuator lag time-constant
τ_B	longitudinal cyclic actuator lag time-constant
τ_T	thruster actuator lag time-constant
θ	perturbation body axis pitch angle
θ_c	perturbation collective swashplate input (inches)
θ_i	i^{th} interior point penalty function
Θ	total body axis pitch angle
Θ_c	total collective swashplate position (inches)
ζ	damping ratio
$( )_0$	trim in the body axis system; value of variable at time t_o
$( )_f$	variable at final time t
$( )_t$	partial derivative with respect to t
$( )_u$	partial derivative with respect to **u**
$( )_{uu}$	second derivative with respect to **u**
$( )_x$	partial derivative with respect to **x**
$( )^T$	vector or matrix transpose
$(\dot{})$	derivative with respect to time
$( )^{-1}$	inverse

$( )^{L}$ left pseudo-inverse

$( )^{*}$ optimal point

Chapter I

INTRODUCTION

1.1 Background and Motivation for this Study

Today's battlefield helicopters need to be highly maneuverable. In particular, the maneuvers that must be performed for successful Nap-of-the-Earth (NOE) tasks require a high level of helicopter agility, good handling qualities, and reasonable levels of pilot workload. These agility and handling qualities criteria often dictate both the required response characterisitics of the control system, and the required acceleration potential of the helicopter. Such specifications can often only begin to be realized through a full-authority controller, one that can utilize the full control power of the helicopter. Additional requirements to rapidly transition from one point to the next suggests the need for higher acceleration/deceleration levels, which may make the inclusion of auxiliary propulsion mandatory.

Motivated by these considerations, the aim of this study was to:

1. define the "operational effectiveness" criteria for NOE operations;
2. investigate suitable controller structures for full-authority control of the helicopter which meet the established criteria and which are sufficiently easy to design;
3. investigate the advantages incurred by using

auxiliary longitudinal propulsion in NOE operations;

4. introduce a mathematical/computational method for evaluating the performance of a controller and auxiliary propulsion system for NOE applications which does not employ human pilots or pilot models. This method is called the trajectory optimization method.

1.2 Definitions Of Handling Qualities and Agility

At the onset, it is necessary to define and distinquish several terms which are used throughout this work.

Handling qualities are "those qualities or characteristics of an aircraft that govern the ease and precision with which a pilot is able to perform the tasks in support of the aircraft role." [14] Agility is "a measure of the ease with which a helicopter can change its state." [10]

There is an important distinction between handling qualities and agility. Handling qualities are allied with the dynamic response of the helicopter, and as such, handling qualities criteria define the helicopter's response to a given control input; quantitatively, they define how the controller should perform in terms of damping ratio, bandwidth, control sensitivities, pole/zero locations, control force gradients, et cetera. Agility is more closely allied with translational motion. Quantitatively, agility can be measured in terms of particular aspects of the helicopter's state time histories, most notably its accelerations. Handling qualities criteria, agility, and pilot workload are the three measures used to evaluate the performance of the helicopter and controller over a prescribed mission. These

three measures collectively constitute what may be called the mission's "operational effectiveness."

1.3 Overview of this Study

This study addresses the application of full-authority optimal controllers and auxiliary propulsion to helicopter NOE operations. Chapter II describes the NOE environment and gives both a qualitative and quantitative account of the desired flying qualities and handling qualities within this environment. In view of these criteria, the advantages of using auxiliary propulsion are discussed, as is the preferred controller command structure.

Chapter III presents the formal development of the explicit model-following and implicit model-following controller structures. They are developed using the linearized equations of motion of the helicopter. Chapter IV explains how the controller and auxiliary propulsion system are evaluated for a given maneuver. A trajectory optimization method is used to compute the optimal helicopter input control histories. The pilot input histories are found from these control histories and the control law; pilot workload is measured from the pilot input histories. Chapter V presents a detailed description of the mathematics and computational solution for the trajectory optimization method.

The implicit and explicit model-following controllers are applied to the AH-1G helicopter. The selection of the controller gains for both of these controller structures, at the hover trim condition, is presented in Chapter VI. The examples in this chapter are given for both the conventional helicopter and for the helicopter equipped with auxiliary propulsion.

Three NOE maneuvers are investigated in this study: bob-up/dash/descent, pop-up at 40 knots, and glideslope. The optimal control input histories, computed using the trajectory optimization program, are shown in Chapter VII along with the histories of the state variables. Finally, in Chapter VIII, the pilot input histories are shown for each of the three NOE maneuvers, using both of the controller structures, and for the helicopter with and without auxiliary propulsion. The "operational effectiveness" of all of these helicopter/controller configurations is evaluated in this chapter.

Chapter II

THE NOE ENVIRONMENT

2.1 General Attributes of NOE Missions/Maneuvers

The roles of the pilot and helicopter vary in the battlefield environment. But in general, NOE maneuvers are employed chiefly to avoid detection by the use of cover. [10,14] The helicopter moves discretely from one point to the next. Maneuvers may be elusive, as during air-to-air combat; they may be operational, as in transporting troops and/or cargo; or they may be of the scout/attack type, for example air-to-air combat and anti-tank missions. The latter usually employ target search and weapons delivery; many employ navigation. A generalized list of necessary attributes for flying NOE maneuvers is: [10,12,13]

* high dash speed
* good longitudinal/vertical acceleration/deceleration
* small turn radius
* good handling qualities and controllability
* low pilot workload

2.2 Typical NOE Maneuvers

The literature commonly defines a list of 15-20 high and low speed maneuvers descriptive of NOE flight: [10,12,13,15,19,28]

Low speed	High speed
* precision hover	* box pattern (four turns)
* taxi	* longitudinal accel/decel
* lateral jink	* pull-up/push-over
* rearward flight	* turning approach
* bob-up	* straight approach
* dash	* lateral accel/decel
* slalom	
* quick-stop	
* liftoff and landing (including ship deck liftoff/landing)	
* pop-up (zero forward velocity)	
* hover about a point/masked hover	

This work is concerned with the longitudinal degrees of freedom of the helicopter. We therefore investigate tasks that include the bob-up and pop-up, dash, quick-stop, longitudinal acceleration/deceleration, and straight approach maneuvers. Actually, our purpose in selecting this group of maneuvers is twofold. This group reflects representative longitudinal maneuvers, and it also reflects those maneuvers for which auxiliary longitudinal propulsion is perceived to be most useful. Sample trajectories are computed and shown in Chapter VII.

The bob-up is usually associated with a quick ascent from behind tree cover or other terrain cover; pop-ups are like bob-ups but begin from hover. The dash is a sprint maneuver typically from fifty feet to a half mile. The dash is most commonly employed to rapidly transition from one point to another; as such, it is often accompanied by a quick-stop and descent to hover.

Other longitudinal maneuvers require high speed flight over longer distances. A typical bob-up maneuver at high speed is obstacle avoidance, for example in "hurdling" a bridge while flying low over a river.

2.3 Desired NOE Flying Qualities

Two flying qualities issues stand out as being very important in NOE flight. These are the pitch attitude constraint and acceleration/deceleration potential.

2.3.1 Pitch Attitude Constraint

It is important in NOE maneuvers to maintain a desirable pitch attitude. Most often this attitude is close to zero. These small pitch attitudes are very important for carrying out secondary operations, armament and navigation in particular: [10,13]

- For weapons delivery, maintaining near-constant pitch attitude is crucial for radar "locked on" tolerances.
- Large nose-up and nose-down pitch attitudes are undesirable for navigation and target search.
- Large pitch forward attitudes raise the the tail rotor above tree-line, making it easier to be seen and heard.
- Pitching must be small for the pilot to maintain visual cues.
- There are dangers of tail rotor ground strike and autorotation with excessive nose-up attitudes.

Though there is not universal agreement on exactly what are the permissible attitudes for NOE maneuvers, the literature suggests that pilots prefer nose-down attitudes in the 0° to 15° range and

nose-up attitudes from 0° to 10°. [10,12,19]

2.3.2 Acceleration/Deceleration Requirements

Time is the most important agility parameter. Most tasks are performed in minimum time, or, at the highest possible accelerations and decelerations. But because conventional helicopters require large attitude changes for acceleration and deceleration, the acceleration/deceleration levels are restrained because of the pitch attitude constraints outlined above. In a survey of Army, Navy, and Air Force pilots [10,19], the ability to accelerate and decelerate -- at higher rates and with less pitch attitude -- was sighted as the issue in which they would like to see the biggest improvement.

Figure 2-1 plots acceleration versus airspeed for a typical helicopter. The plot shows that acceleration potential decreases with airspeed. Particularly for battlefield operations, pilots prefer to have higher acceleration potential across the airspeed spectrum. The current ABC [25,29] and Tilt-Rotor [28] aircraft increase the acceleration potential at higher airspeeds. These programs, and the studies conducted in References 10, 16, 24, 25, and 29 define the desired potential acceleration level, across all airspeeds, at 0.3 to 0.5g.

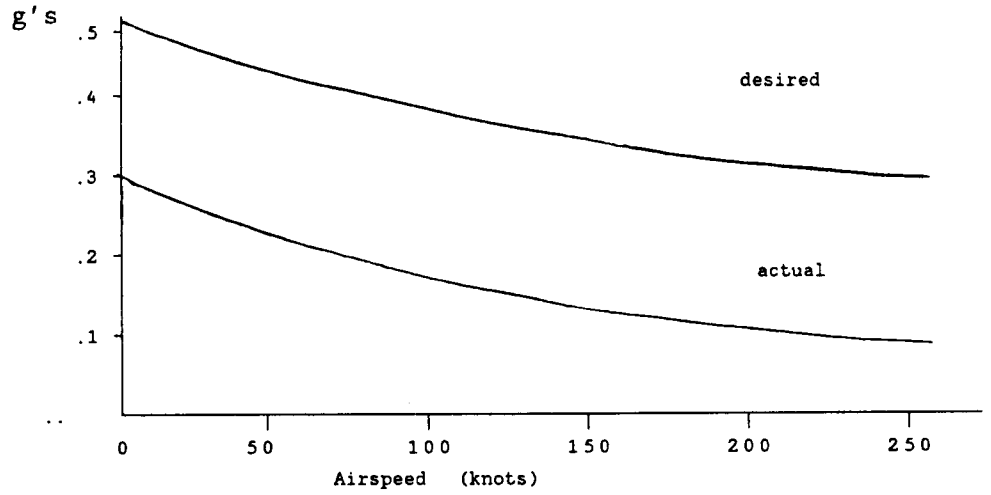

Figure 2-1 Available acceleration vs airspeed
(Figure adapted from References 24 and 25)

2.4 Potential Benefits of Auxiliary Propulsion

In light of these flying qualities criteria, we can predict the improvement in agility that would result using an auxiliary longitudinal thruster on a helicopter operating in this environment. The addition of an additional X-force via a longitudinal thruster would increase available acceleration levels, so that the acceleration potential of the helicopter looks like the upper line in Figure 2-1. And, because this X-force is thruster-generated rather than rotor-generated, large pitch attitudes are not required to achieve greater acceleration/deceleration levels, so that pitch attitude constraints should be met. These predictions are substantiated in Chapters VII and VIII.

2.5 Handling Qualities and Controller Selection

As one might expect, there is a direct connection between the type of maneuver the pilot is expected to perform and the type of command input which the pilot prefers to have. For the

longitudinal degrees of freedom, the flight (i.e. state) variables are the helicopter horizontal and vertical velocities, and pitch attitude and pitch rate. Numerous studies have investigated longitudinal controllers with various command inputs. The two basic configurations are velocity command configurations and attitude/attitude-rate command configurations. From the literature available, it is determined that for the types of NOE maneuvers investigated in this study, pilots prefer velocity command controllers. The following paragraphs summarize some of the work found in the literature and explain the rational for choosing the velocity command controller configuration over alternative configurations.

The pilot's control over the full longitudinal and lateral-directional motions of the helicopter typically consists of four command inputs; pitch, roll, yaw, and vertical command inputs. For longitudinal motion, these inputs reduce to the pitch and vertical command inputs. Although more (or fewer) pilot inputs may be defined, two inputs is the most efficient for control within this horizontal-vertical plane. Ideally, one input should control vertical motion, and one input should control horizontal motion. [6,11,12,13,15,28]

Most NOE tasks require the pilot to govern the speed and position of the helicopter; other tasks, notably air-to-air combat, require attitude control. It is, of course, logical to equip the pilot with command inputs that will best enable him to perform the tasks at hand. For the maneuvers of interest in this study, which are velocity/position based, we find that pilots prefer a rate (velocity) command controller, with possible

modifications. The results from a literature review of controller structures for NOE tasks, outlined below, show that velocity command systems are best for maneuvering, and attitude command systems are best for precision hover tasks.

References 17, 28, and 31 conclude that pilots prefer velocity command over attitude command (AC) for tracking tasks. Typically, both velocity command and attitude command systems have a vertical velocity command as one input; for the other input, the velocity command system uses a horizontal velocity command and the attitude command uses a pitch attitude command. This preference also holds for low speed precision pointing tasks; reference 19 found that an AC controller degraded the helicopter's handling qualities during precision pointing tasks. The study conducted in that reference also found that the addition of attitude hold (AH) to the velocity command controller results in a high level of agility, as measured by achievable rates and accelerations.

For chase and aquisition, reference 31 finds that pilots prefer the velocity controller. For these types of tasks, the large stick inputs necessary with the AC controller are found to be objectionable; the AC controller is preferred for tasks where precision maneuvering is critical. This reference, and references 11, 13, and 15 note that the best handling qualities are achieved when the two velocity commands in the the velocity system are decoupled; decoupled contols is highly desirable for good handling qualities. Hence, the study conducted in this thesis uses an velocity controller.

With the control structure thus defined, it was then possible to set some quantitative response criteria for the velocity

controller that would result in good handling qualities. Many of the defining handling qualities criteria used in this work were taken from the Army's Advanced Digital/Optical Control System (ADOCS) program. [11,15] This control system is being designed to provide satisfactory handling qualities for attack helicopters. The ADOCS report itself includes an extensive literature search to define applicable handling qualities criteria for attack helicopters.

At the onset, the two velocity command inputs should be decoupled, and should produce responses that closely approximate the outputs of two first-order systems. Specifications for the two first order time-constants vary strongly according to pilot and task, but the literature generally agrees that the accepted range for the vertical response time constant is from 1 to 4 seconds, while the horizontal response time-constant ranges from 2 to 5 seconds. [11,13] When a first-order response cannot be achieved, a second-order response should have a damping ratio equal to or greater than 0.7; the minimum acceptable damping ratio is 0.5.

The input frequency band of concern does not vary greatly among the references [11,13,15,18,20], and thus the band was taken to be from 0 to 1 Hz (6.26 radians/second). In addition, the transfer function phase response should follow that of a first-order system, with a suitable time-constant as specified above. Too much phase shift can result in pilot induced oscillations (PIO). [20]

For the velocity-command controller, the vertical velocity command input sensitivity should range from 13 to 16 ft/sec per

inch of stick, for the vertical response time-constants listed above. [11,13]; the horizontal velocity input sensitivity ranges from 12 to 16 ft/sec per inch, for the related time-constants. This range is again due to the variation in tasks from which these data were taken. These inputs should not produce pitch accelerations in the helicopter which exceed 0.69 rad/s^2.

The handling qualities criteria are summarized in Table 2-1 below:

	horizontal velocity command	vertical velocity command
first-order time-constant	2-5 sec	1-5 sec
damping ratio	$\geq$ 0.7	$\geq$ 0.7
minimum damping ratio	0.5	0.5
bandwidth	0-6 rad/s	0-6 rad/s
control sensitivity	12-16 ft/s/inch	13-16 ft/s/inch
maximum pitch rate sensitivity	.69 rad/s/inch	.69 rad/s/inch

Table 2-1

Handling qualities criteria for velocity-command controller

Chapter III

CONTROLLER DEVELOPMENT

3.1 Linearized Equations of Motion

Aircraft performance analyses and controller development are commonly accomplished using the linearized equations of motion of the vehicle about a trim point. These linearized equations can very closely approximate the total nonlinear equations of motion, and are much easier to use in application. In addition, linearized numerical data for many aircraft is readily available. The controller development methods and trajectory optimization procedure of this study utilized the helicopter's linearized equations of motion. All numerical data was derived for the AH-1G helicopter, which typifies helicopters that are used for the roles discussed in this study.

Appendix A reviews the procedure and assumptions used in the linearization of the helicopter's nonlinear equations of motion. It is shown below that the helicopter's total state variables are the sums of the trim states and the linearized (perturbation) states. Appendix B contains the numerical (linearized) stability and control derivatives for the AH-1G at twenty-two trim points from reference 1. A realistic representation of the helicopter states at all points and times in space requires that these derivatives be scheduled between trim points. Appendix B discusses how these data are scheduled according to flight condition.

The speed, position, acceleration, and orientation of the helicopter are described in terms of its nominal (trim) and perturbation state variables. Figure 3-1 shows the total and perturbation states of the helicopter. Because of the small angle assumption used in the linearization of the equations of motion, the total state variables U, W, Q, and Θ are the sums of their trim values (U_o, W_o, Q_o, θ_o) and perturbation values (u, w, q, θ). Since perturbation positions (x and y) are measured along the trimmed body axis, their contribution to the total inertial referenced positions must take into account the trim attitude θ_o. Therefore,

$$X = X_o + x\cos\theta_o \quad \text{and} \quad Y = Y_o + y\sin\theta_o .$$

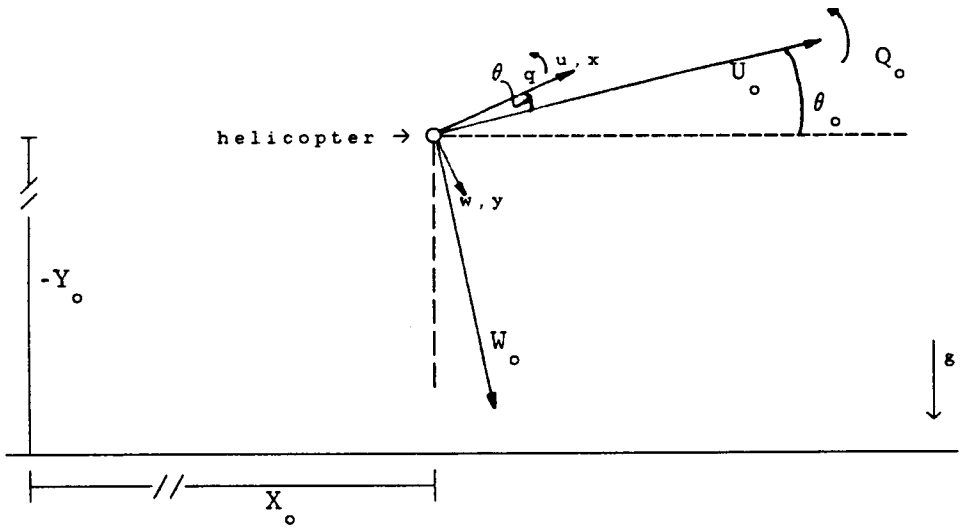

Figure 3-1 Longitudinal Body Axis System

3.2 Design Objectives

The objective of this study was to design a controller for helicopters that perform NOE tasks, or other demanding tasks, utilizing the full available control power of the helicopter. Such a controller is a "full-authority" controller, one which is

capable of exploiting the full control potential of the helicopter, rather than one which limits the controls to less than their full range of travel (as is often done in stability-augmentation systems). There are numerous controller structures which can potentially fit this bill. For controller design using the helicopter's linearized equations of motion, several popular and promising controller structures are those referred to as linear-quadratic optimal controllers.

A suitable controller structure is one that satisfies the prescribed input/output response criteria (handling qualities criteria). But it is also of concern that the controller be sufficiently easy to design , and that it is adaptable to changing flight conditions (i.e., easy to schedule within the flight envelope). Linear-quadratic implicit and explicit model-following optimal controllers prove to meet these requirements.

Pilots have shown favorable responses in studies conducted on aircraft using model-following controller structures. Reference 18 shows that pilots rated model-following better than response feedback mode control, producing respective Cooper-Harper ratings of 3 versus 3.5. The pilots described a sense that the model-follower controller was "locking on" when it was engaged. Reference 17 also notes pilots' preferences for model-following over response feedback control because of the ability of the model-following system to provide inter-axis control to compensate for undesirable cross-coupling affects in the vertical and horizontal axes.

The ADOCS program [11,13] used a model-following concept to achieve the desired command responses. In that study, classical

control methods were used to design feedback paths that met the stability requirements. However, based on the desired command/response characteristics, a command reponse model was used to provide the desired response. It achieved good pilot ratings, falling within Level 1 of the Cooper-Harper ratings scale. This feedforward command augmentation and shaping performs the same function as the feedforward gains of the model-following controllers presented below. The feedforward structure provides control mixing (to achieve decoupled modes) and prefiltering, but does not affect the level of feedback stabilization. The model-follower structure also facilitates easy flight condition scheduling.

3.3 Linear-Quadratic Optimal Controllers

The method employed in the design of optimal controllers is to minimize a predetermined cost function, subject to the system's dynamic constraint, for the purpose of generating an optimal control law, i.e., an optimal relationship between the states and controls, that gives the resulting closed-loop system the desired control/response characteristics. The general method is to define, from the cost function and system dynamics, the equations that establish necessary and sufficient conditions for minimum cost. [2,4] The necessary conditions are derived by equating the cost function's linear sensitivity to zero through a procedure known as the Calculus of Variations. The cost function is typically comprised of a final state penalty and an integral penalty function of the state and control. Parameters of the integrand, or Lagrangian ($\mathcal{L}$), define the nature of the optimizing

solution. The cost function is written as:

$$J = \phi[\mathbf{x}(t_f),t_f] + \int_{t_o}^{t_f} \mathcal{L}[\mathbf{x}(t),\mathbf{u}(t),t]dt \qquad (3\text{-}1)$$

The system dynamics: $\dot{\mathbf{x}} = \mathbf{f}[\mathbf{x}(t),\mathbf{u}(t),t]$ (3-2)

and initial condition: $\mathbf{x}(t_o) = \mathbf{x}_o$ (3-3)

must be satisfied while J is being minimized. To assure adherence to this "dynamic constraint," these dynamics are adjoined to the cost function via an adjoint (or influence) vector $\mathbf{1}(t)$.

$$J = \phi[\mathbf{x}(t_f),t_f] + \int_{t_o}^{t_f} \Big\{ \mathcal{L}[\mathbf{x}(t),\mathbf{u}(t),t] + \mathbf{1}^T(t)(\mathbf{f}[\mathbf{x}(t),\mathbf{u}(t),t]-\dot{\mathbf{x}}(t)) \Big\} dt \qquad (3\text{-}4)$$

$\mathbf{f}[\mathbf{x}(t),\mathbf{u}(t),t]-\dot{\mathbf{x}}(t)$ is adjoined to the integrand because it must be satisfied over the entire interval $<t_o,t_f>$. And because it equals zero when satisfied, the numerical value of J is not changed. $\mathbf{1}(t)$, then, acts as an influence function, and expresses the cost function's sensitivity to dynamic effects.

The Hamiltonian, $\mathcal{H}$, of the integrand is defined as:

$$\mathcal{H}[\mathbf{x}(t),\mathbf{u}(t),t] = \mathcal{L}[\mathbf{x}(t),\mathbf{u}(t),t] + \mathbf{1}^T(t)\mathbf{f}[\mathbf{x}(t),\mathbf{u}(t),t] \qquad (3\text{-}5)$$

and J can be rewritten as

$$J = \phi[\mathbf{x}(t_f),t_f] + \int_{t_o}^{t_f} \Big\{ \mathcal{H}[\mathbf{x}(t),\mathbf{u}(t),t] - \mathbf{1}^T(t)\dot{\mathbf{x}} \Big\} dt \qquad (3\text{-}6)$$

(Explicit reference to time is dropped here; variables at the final time t_f are denoted by the subscript $_f$).

Using the Calculus of Variations, three necessary conditions are derived from the cost function. These are:

1. $0 = (\frac{\partial \mathcal{H}}{\partial \mathbf{u}})^T$ (3-7a)

2. $\dot{\mathbf{l}} = (-\frac{\partial \mathcal{H}}{\partial \mathbf{x}})^T$ (3-7b)

3. $\mathbf{l}_f^T = (\frac{\partial \phi}{\partial \mathbf{x}_f})^T$ (3-7c)

These equations are also known as the Euler-Lagrange equations. When satisfied, the Hamiltonian is stable for infinitesimal control variations. These conditions are therefore local, rather than global criteria. The sufficient condition is that $\mathcal{H}_{uu}>0$. For linear-quadratic cost functions (defined below), $\mathcal{H}_{uu}>0$ is guaranteed to be satisfied. Therefore, the formal mathematics for this sufficient condition are not pursued here.

Inspection of Equations 3-2 and 3-3 and Equations 3-7b and 3-7c shows that this optimization problem is two-point boundary value problem; the state integration constants are specified at t_o and the adjoint integration constants are specified at t_f.

For linear-quadratic controllers, the dynamics are linear and the Lagrangian consists of weighted quadratic norms. A quadratic, time-invariant, final state penalty takes the form $\phi[\mathbf{x}_f] = \mathbf{x}_f^T P_f \mathbf{x}_f$, and the third Euler-Lagrange equation becomes $\mathbf{l}_f = P_f \mathbf{x}_f$. However, the integration interval is taken from 0 to t_f, as t_f approaches infinity. This means that the final state penalty is presumably insignificant. [4] With this in mind, and recalling that $\mathbf{l}$ and $\mathbf{x}$ are adjoint and therefore hold over the entire interval $<0,\infty>$, we drop the final time subscript for the third Euler-Lagrange equation, and now have a more suitable, yet wholely correct, condition that $\mathbf{l} = P\mathbf{x}$.

The sufficient condition, $\mathcal{H}_{uu}>0$, is guaranteed to be satisfied

for quadratic cost functions as long as the weighting matrices are positive-definite. The elements of the weighting matrices are parameters that are chosen to meet the closed-loop response criteria; a *unique* optimal controller results for *each set* of weighting matrices chosen for the giver system dynamics. The relationship of weighting matrices parameters and control objectives is not direct nor is parameter selection intuitive. However, linear-quadratic model-following optimal controllers prove to be easy to develop because one usually needs only to adjust the diagonal elements of the weighting matrices, and perhaps an off-diagonal element for obviously coupled variables.

3.4 Implicit Model-Following Controller

The system (in our case, the helicopter) is described by the dynamics:

$$\dot{\mathbf{x}} = \mathbf{A}\mathbf{x} + \mathbf{B}\mathbf{u} \tag{3-8}$$

where for our application

$$\mathbf{x} = \begin{bmatrix} u \\ w \\ q \\ \theta \end{bmatrix} \quad \text{and} \quad \mathbf{u} = \begin{bmatrix} \theta_c \\ B_{1s} \\ T \end{bmatrix} \tag{3-9}$$

and A and B are the stability and control derivative matrices, respectively. Note that we include an auxilary longitudinal thrust control, T (inclusion of T does not alter the derivation).

The model, whose state response ($\mathbf{x}_m$) to control inputs (**d**) we want the system (helicopter) to emulate, is expressed as

$$\dot{\mathbf{x}}_m = \mathbf{F}\mathbf{x} + \mathbf{G}\mathbf{d} \tag{3-10}$$

where **x** is the plant state vector as given above and **d** is the vector of (pilot) inputs. For the velocity-command controller, **d** contains horizontal and vertical commands:

$$\mathbf{d} = \begin{bmatrix} u_{com} \\ w_{com} \end{bmatrix} \tag{3-11}$$

This is an *implicit* model-follower structure because the error -- in this case, the rate error -- between the system and the model is penalyzed *inside* the cost function, rather than as part of the control system in the closed-loop system dynamics. [9,21]

The cost function is:

$$J = \frac{1}{2}\int_0^\infty \left\{ (\dot{\mathbf{x}}-\dot{\mathbf{x}}_m)^T Q(\dot{\mathbf{x}}-\dot{\mathbf{x}}_m) + \mathbf{u}^T R\mathbf{u} + \mathbf{l}^T(A\mathbf{x}+B\mathbf{u}) - \mathbf{l}^T\dot{\mathbf{x}} \right\} dt \tag{3-12}$$

where $\mathbf{x}$ and $\mathbf{x}_m$ are $n \times 1$, Q is $n \times n$, $\mathbf{u}$ is $m \times 1$, and R is $m \times m$.

Substituting for $\dot{\mathbf{x}}$ and $\dot{\mathbf{x}}_m$ from Equations 3-7 and 3-8,

$$J = \frac{1}{2}\int_0^\infty \left\{ (A\mathbf{x}+B\mathbf{u}-F\mathbf{x}-G\mathbf{d})^T Q(A\mathbf{x}+B\mathbf{u}-F\mathbf{x}-G\mathbf{d}) + \mathbf{u}^T R\mathbf{u} \right\} dt$$

$$= \frac{1}{2}\int_0^\infty \left\{ (\mathbf{x}^T[A-F]^T+\mathbf{u}^T B^T-\mathbf{d}^T G^T) Q([A-F]\mathbf{x}+B\mathbf{u}-G\mathbf{d}) + \mathbf{u}^T R\mathbf{u} \right\} dt$$

$$= \frac{1}{2}\int_0^\infty \left\{ \mathbf{x}^T(A-F)^T Q(A-F)\mathbf{x} + \mathbf{u}^T(B^T QB+R)\mathbf{u} + \mathbf{d}^T G^T QG\mathbf{d} \right.$$

$$\left. + 2\mathbf{x}^T(A-F)^T QB\mathbf{u} - 2\mathbf{x}^T(A-F)^T QG\mathbf{d} - 2\mathbf{d}^T G^T QB\mathbf{u} \right\} dt \tag{3-13}$$

Using the following definitions,

$$W_{xx} = (A-F)^T Q(A-F) \qquad W_{xu} = (A-F)^T QB \qquad W_{du} = G^T QB$$

$$W_{xd} = (A-F)^T QG \qquad W_{uu} = BQB+R \qquad W_{dd} = GQG \tag{3-14}$$

the cost function becomes

$$J = \frac{1}{2}\int^\infty \left\{ \mathbf{x}^T W_{xx}\mathbf{x} + \mathbf{u}^T W_{uu}\mathbf{u} + \mathbf{d}^T W_{dd}\mathbf{d} + 2\mathbf{x}^T W_{xu}\mathbf{u} - 2\mathbf{x}^T W_{xd}\mathbf{d} \right.$$

$$\left. - 2\mathbf{d}^T W_{du}\mathbf{u} + \mathbf{l}^T(A\mathbf{x}+B\mathbf{u}) - \mathbf{l}^T\dot{\mathbf{x}} \right\} dt \tag{3-15}$$

and the Hamiltonian is

$$\mathcal{H} = \frac{1}{2}\Big\{\mathbf{x}^T W_{xx}\mathbf{x} + \mathbf{u}^T W_{uu}\mathbf{u} + \mathbf{d}^T W_{dd}\mathbf{d} + 2\mathbf{x}^T W_{xu}\mathbf{u} - 2\mathbf{x}^T W_{xd}\mathbf{d} - 2\mathbf{d}^T W_{du}\mathbf{u} + \mathbf{l}^T(A\mathbf{x}+B\mathbf{u})\Big\} \qquad (3\text{-}16)$$

Employing the three optimality conditions, we have

$$1. \quad 0 = \left(\frac{\partial \mathcal{H}}{\partial \mathbf{u}}\right)^T = W_{uu}\mathbf{u} + W_{xu}^T\mathbf{x} - W_{du}^T\mathbf{d} + B^T\mathbf{l} \qquad (3\text{-}17)$$

$$2. \quad \dot{\mathbf{l}} = \left(\frac{-\partial \mathcal{H}}{\partial \mathbf{x}}\right)^T = -W_{xx}\mathbf{x} - W_{xu}\mathbf{u} + W_{xd}\mathbf{d} - A^T\mathbf{l} \qquad (3\text{-}18)$$

At this point we observe that the integrand contains the variables **l**, **u**, **x**, *and* **d**. Therefore, we revise the algebraic expression for **l** to include effects of the model input **d**. This is done by adding a linear inhomogeneous term to the (linear) homogeneous expression for **l** from the previous section [22]:

$$3. \quad \mathbf{l} = P\mathbf{x} - S\mathbf{d} \qquad (3\text{-}19)$$

P is n × n and S is n × r. Solving Equation 3-15 for **u** yields

$$\mathbf{u} = -W_{uu}^{-1}(W_{xu}^T\mathbf{x} - W_{du}^T\mathbf{d} + B^T\mathbf{l}) \qquad (3\text{-}20)$$

Using Equation 3-19 we substitute for **l** in Equation 3-20 to obtain the optimal control law in terms of the desired variables **x** and **d**:

$$\mathbf{u} = -W_{uu}^{-1}(W_{xu}^T\mathbf{x} - W_{du}^T\mathbf{d} + B^TP\mathbf{x} - B^TS\mathbf{d})$$

$$= -W_{uu}^{-1}(W_{xu}^T + B^TP)\mathbf{x} + W_{uu}^{-1}(W_{du}^T + B^TS)\mathbf{d} \qquad (3\text{-}21)$$

$$= -C_1\mathbf{x} + C_2\mathbf{d} \qquad (3\text{-}22)$$

The expressions for P and S are found from the dynamic equation for **l**. Sustituting **u** from Equation 3-21 and **l** from Equation 3-19

into Equation 3-18, we have

$$\dot{\mathbf{i}} = -\mathbf{W}_{xx}\mathbf{x} - \mathbf{W}_{xu}[-\mathbf{W}_{uu}^{-1}(\mathbf{W}_{xu}^{T}+\mathbf{B}^{T}\mathbf{P})\mathbf{x}+\mathbf{W}_{uu}^{-1}(\mathbf{W}_{du}^{T}+\mathbf{B}^{T}\mathbf{S})\mathbf{d}] + \mathbf{W}_{xd}\mathbf{d} - \mathbf{A}^{T}(\mathbf{P}\mathbf{x}-\mathbf{S}\mathbf{d})$$

$$= [-\mathbf{W}_{xx}+\mathbf{W}_{xu}\mathbf{W}_{uu}^{-1}\mathbf{W}_{xu}^{T}+\mathbf{W}_{xu}\mathbf{W}_{uu}^{-1}\mathbf{B}^{T}\mathbf{P}]\mathbf{x}$$

$$+ [-\mathbf{W}_{xu}\mathbf{W}_{uu}^{-1}\mathbf{W}_{du}^{T}-\mathbf{W}_{xu}\mathbf{W}_{uu}^{-1}\mathbf{B}^{T}\mathbf{S}+\mathbf{W}_{xd}+\mathbf{A}^{T}\mathbf{S}]\mathbf{d} \qquad (3\text{-}23)$$

Taking the derivative of Equation 3-19 with respect to time, and noting that the best estimate of $\dot{\mathbf{d}}$ is zero (since it is unpredictable [22]), we have

$$\dot{\mathbf{i}} = \dot{\mathbf{P}}\mathbf{x} + \mathbf{P}\dot{\mathbf{x}} - \dot{\mathbf{S}}\mathbf{d} \qquad (3\text{-}24)$$

Substituting for $\dot{\mathbf{x}}$ from Equation 3-8 and then for $\mathbf{u}$ from Equation 3-21, and collecting like terms, Equation 3-24 becomes

$$\dot{\mathbf{i}} = [\dot{\mathbf{P}}+\mathbf{P}\mathbf{A}-\mathbf{P}\mathbf{B}\mathbf{W}_{uu}^{-1}\mathbf{W}_{xu}^{T}-\mathbf{P}\mathbf{B}\mathbf{W}_{uu}^{-1}\mathbf{B}^{T}\mathbf{P}]\mathbf{x}$$

$$+ [\mathbf{P}\mathbf{B}\mathbf{W}_{uu}^{-1}\mathbf{W}_{du}^{T}+\mathbf{P}\mathbf{B}\mathbf{W}_{uu}^{-1}\mathbf{B}^{T}\mathbf{S}-\dot{\mathbf{S}}]\mathbf{d} \qquad (3\text{-}25)$$

Equating the right hand sides of Equations 3-23 and 3-25, and recognizing that, for minimum cost, the resulting equation will hold true irrespective of the values of $\mathbf{x}$ and $\mathbf{d}$, we generate two separate equations by equating the coefficients of $\mathbf{x}$ and the coefficients of $\mathbf{d}$ in these equations:

$$\dot{\mathbf{P}} = -\mathbf{P}[\mathbf{A}-\mathbf{B}\mathbf{W}_{uu}^{-1}\mathbf{W}_{xu}^{T}] - [\mathbf{A}-\mathbf{B}\mathbf{W}_{uu}^{-1}\mathbf{W}_{xu}^{T}]^{T}\mathbf{P}$$

$$+ [-\mathbf{W}_{xx}+\mathbf{W}_{xu}\mathbf{W}_{uu}^{-1}\mathbf{W}_{xu}^{T}] + \mathbf{P}[\mathbf{B}\mathbf{W}_{uu}^{-1}\mathbf{B}^{T}]\mathbf{P} \qquad (3\text{-}26)$$

$$\dot{\mathbf{S}} = -[\mathbf{A}-\mathbf{B}\mathbf{W}_{uu}^{-1}\mathbf{W}_{xu}^{T}]^{T}\mathbf{S} + \mathbf{P}[\mathbf{B}\mathbf{W}_{uu}^{-1}\mathbf{B}^{T}]\mathbf{S}$$

$$+ \mathbf{P}[\mathbf{B}\mathbf{W}_{uu}^{-1}\mathbf{W}_{du}^{T}] - [\mathbf{W}_{xd}-\mathbf{W}_{xu}\mathbf{W}_{uu}^{-1}\mathbf{W}_{du}^{T}] \qquad (3\text{-}27)$$

Equation 3-26 takes the form $\dot{\mathbf{P}} = -\mathbf{P}\mathbf{M} - \mathbf{M}^{T}\mathbf{P} + \mathbf{P}\mathbf{N}\mathbf{P} + \mathbf{K}$ and is

recognized to be a matrix Riccati equation in P. The steady-state P matrix is solved according to the diagonalization method [26] outlined in Appendix C. Once P is determined, the steady-state solution for S ($\dot{S} = 0$) is determined from Equation 3-27 using simple matrix algebra.

Equation 3-22 is the control law for the implicit model-follower. Substituting this expression for **u** into the open-loop dynamics, the closed-loop dynamics are

$$\dot{\mathbf{x}} = A\mathbf{x} + B\mathbf{u} = A\mathbf{x} + B(-C_1\mathbf{x}+C_2\mathbf{d}) = (A-BC_1)\mathbf{x} + BC_2\mathbf{d} \qquad (3\text{-}28)$$

Figure 3-2 shows a block diagram of the open-loop helicopter, and the closed-loop helicopter with feedback gains C_2 on the measured states **x**, and feedforward gains from the pilot inputs **d**.

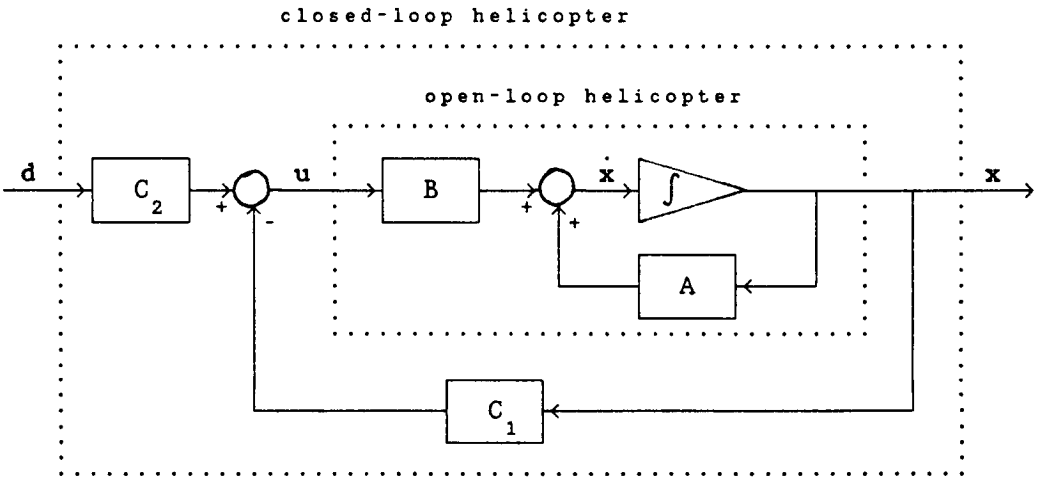

Figure 3-2 Implicit Model Controller

3.5 Explicit Model-following Controller

The open-loop dynamics of course do not depend on the controller structure, and are again given by Equation 3-8. The idealized model dynamics are

$$\dot{x}_m = Fx_m + Gd \tag{3-29}$$

where x_m is the model state vector and d is the pilot control input vector.

The linear-quadratic cost function for the explicit model-follower penalizes control excursions and the error between the actual state and the model state. [2,21]

$$J = \frac{1}{2}\int_0^\infty \left\{(x-x_m)^T Q(x-x_m) + u^T Ru + 1^T(Ax+Bu) - 1^T\dot{x}\right\}dt \tag{3-30}$$

$$= \frac{1}{2}\int_0^\infty \left\{[x^T Qx - 2x^T Qx_m + x_m^T Qx_m] + 1^T(Ax+Bu) - 1^T\dot{x}\right\}dt \tag{3-31}$$

Because there are two distinct states, we could define an augmented state which includes both x and x_m. The cost function using the augmented state is

$$J = \frac{1}{2}\int_0^\infty \left\{X^T Q' X + u^T Ru + 1^T(Ax+Bu) - 1^T\dot{x}\right\}dt \tag{3-32}$$

where $X = \begin{bmatrix} x \\ x_m \end{bmatrix}$ and $Q' = \begin{bmatrix} Q & -Q \\ -Q & Q \end{bmatrix}$

Minimization of the cost functions given by Equations 3-31 and 3-32 yield dimensionally different optimality equations. The resulting control law in each case, however, yields identical gain coefficients for the state and command vectors x and d. Derivation of the control law using Equation 3-32 is exactly analagous to the derivation for linear quadratic regulators (LQR); this method is not presented here. Instead, the derivation using the "unaugmented " cost function, Equation 3-31, is used as perhaps it best shows how the control law depends on x_m as well as x and d.

The Hamiltonian is

$$\mathcal{H} = \frac{1}{2}\left\{x^T Q x - 2x^T Q x_m + x_m^T Q x_m + u^T R u + l^T(Ax+Bu)\right\} \qquad (3\text{-}33)$$

The first two optimality conditions are

$$1. \quad 0 = \left(\frac{\partial \mathcal{H}}{\partial u}\right)^T = Ru + B^T l \qquad (3\text{-}34)$$

$$2. \quad \dot{l} = \left(-\frac{\partial \mathcal{H}}{\partial x}\right)^T = -Qx + Qx_m - A^T l \qquad (3\text{-}35)$$

As we did in the implicit model-follower development, we assume a linear relationship among l and the variables of the integrand (other than u):

$$3. \quad l = P_1 x + P_2 x_m - Sd \qquad (3\text{-}36)$$

From Equations 3-34 and 3-36, the control law is

$$u = -R^{-1}B^T l = -R^{-1}B^T(P_1 x + P_2 x_m - Sd)$$

$$= -R^{-1}B^T P_1 x - R^{-1}B^T P_2 x_m + R^{-1}B^T Sd \qquad (3\text{-}37)$$

$$= -C_1 x - C_2 x_m + C_3 d \qquad (3\text{-}38)$$

To find expressions for P_1, P_2, and S, solve for $\dot{l}$. Substituting Equation 3-36 into Equation 3-35:

$$\dot{l} = -Qx + Qx_m - A^T(P_1 x + P_2 x_m - Sd)$$

$$= [-Q - A^T P_1]x + [Q - A^T P_2]x_m + [A^T S]d \qquad (3\text{-}39)$$

Taking the derivative of Equation 3-36 with respect to time (and recognizing that the best estimate of $\dot{d}$ is zero), we have

$$\dot{l} = P_1 \dot{x} + \dot{P}_1 x + P_2 \dot{x}_m + \dot{P}_2 x_m - \dot{S}d \qquad (3\text{-}40)$$

Substituting Equation 3-8 for $\dot{\mathbf{x}}$ and Equation 3-29 for $\dot{\mathbf{x}}_m$, and then substituting Equation 3-37 for $\mathbf{u}$ and collecting terms, we have

$$\dot{\mathbf{i}} = [P_1A+\dot{P}_1+P_1BR^{-1}B^TP_1]\mathbf{x} + [P_1BR^{-1}B^TP_2+P_2F+\dot{P}_2]\mathbf{x}_m + [P_1BR^{-1}B^TS+P_2G-\dot{S}]\mathbf{d} \quad (3\text{-}41)$$

Equating the coefficients of $\mathbf{x}$, $\mathbf{x}_m$, and $\mathbf{d}$ from the right hand sides of Equations 3-39 and 3-41 yields the expressions for $\dot{P}_1$, $\dot{P}_2$, and $\dot{S}$:

$$\dot{P}_1 = -P_1A - A^TP_1 + P_1BR^{-1}B^TP_1 - Q \quad (3\text{-}42)$$

$$\dot{P}_2 = -P_2F - A^TP_2 + P_1BR^{-1}B^TP_2 - Q \quad (3\text{-}43)$$

$$\dot{S} = P_2G - A^TS + P_1BR^{-1}B^TS \quad (3\text{-}44)$$

Equation 3-42 is a matrix Riccati equation; the steady-state P_1 matrix is solved according to the diagonalization method [26] described in Appendix C. Once P_1 is determined, steady-state P_2 is solved from Equation 3-43 via a Kronecker product method [30], since P_2 premultiplies *and* postmultiplies other (constant) matrices. With P_1 and P_2 known, steady-state S is solved algebraically:

$$S = [A^T - P_1BR^{-1}B^T]^{-1}P_2G \quad (3\text{-}45)$$

The block diagram for a helicopter equipped with an explicit model-following control law (Figure 3-3) shows that the ideal model acts as a prefilter of pilot inputs $\mathbf{d}$ to the open-loop helicopter.

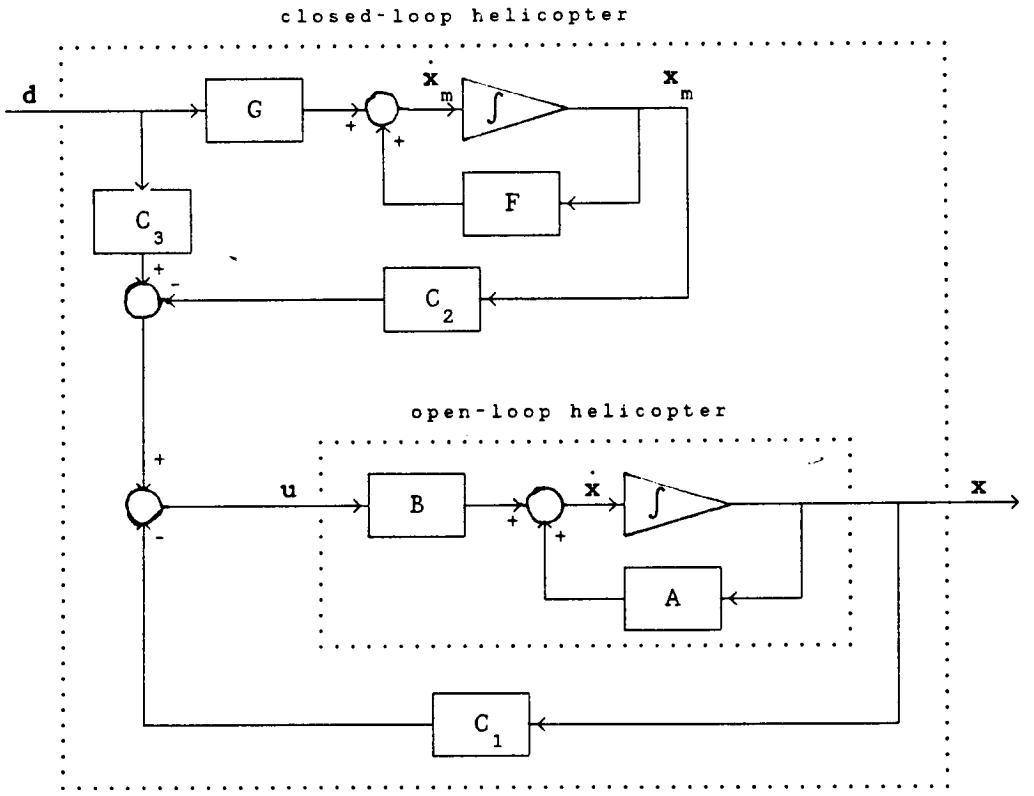

Figure 3-3 Explicit Model Controller

3.6 Other Controller Structures

Other linear-quadratic optimal controller structures were investigated. In particular, the proportional-filter and proportional-integral structures were considered. [2] However, choosing suitable weighting matrices parameters for these two structures proved to be a very laborious assignment. Because of this, and because the response characteristics of these controllers showed no improvement over the model-following controllers, they were eliminated as possible controller structures.

3.7 Gain Scheduling

The controller gains are derived for the linearized dynamics of the helicopter about a trim point. As such, they are only applicable for flight within a region close to this trim condition. For the controller to be effective throughout the entire flight envelope, it became necessary to derive gains for trimmed flight conditions throughout the helicopter's entire flight envelope, and to schedule the gains between these discrete trim points. Scheduling is typically done by expressing the gains as a function of flight condition, e.g., airspeed, advance ratio, and dynamic pressure. [8] Reference 7 suggests a means to select the flight variables and the gains which require scheduling by the use of correlation analysis. Any scheduling method should be chosen to provide accurate gain values throughout the entire envelope, while not being overburdening in terms of computation time and data, or cost.

The data available for this study limits the number of trim data points to twenty-two. This means that twenty-two sets of gains have been derived for each controller structure investigated (see Appendix D). But this limited data set makes it feasible only to schedule the gains in terms of the most obviously influential variables, the helicopter's forward and vertical speeds, U and W. And it is impossible to heuristically argue what functional dependence the gains have with U and W between trim points (unlike what can be done for the stability and control matrices -- see Appendix B). Therefore, the gains are linearly interpolated and extrapolated using the trim data set.

Figure B-1 shows the spread of the data (trim) points in the

U-W plane. In this study, a data set contains the value of every gain element at each of these twenty-two points for each controller. For each [U,W] pair sampled throughout a trajectory, the gain elements are scheduled by first interpolating with respect to U, and then with respect to W. For flight conditions that put [U,W] outside of these data points, the data is simply extrapolated out to the [U,W] point.

Chapter IV

CONTROLLER AND AUXILIARY PROPULSOR EVALUATION

4.1 Method of Evaluation

In Chapter I, we expressed the operational effectiveness of the helicopter/control system as a measure of its ability to perform its prescribed mission. In the context of this study, we are specifically concerned about the abilities of the controller and auxiliary propulsor to meet this goal. System performance, or operational effectiveness, is described by three primary groups of criteria: handling qualities and flying qualities, both of which are outlined in Chapter II for NOE operations, and pilot workload. The handling qualities criteria are evaluated coincident with the development of the controllers (Chapter VI), with one exception, controller sensitivity, discussed below. Flying qualities and pilot workload must, of course, be evaluated over a specific maneuver. This study used a "trajectory optimization" method for evaluating these two categories of criteria. Use of this method avoids the traditionally subjective rating method for evaluating pilot workload and contoller sufficiency.

4.1.1 Trajectory Optimization Method

The trajectory optimization method computes, for a maneuver of specified time, geometry, and flying qualities, the optimal helicopter control histories, i.e., the motion of the helicopter's

physical controls (swashplate and thruster input) throughout the trajectory. The process is purely mathematical, and is performed computationally. Flying qualities and the geometry of the maneuver are incorporated by specifying the helicopter's state vector at various times throughout the trajectory. Excursions from these "constraints" are penalyzed according to their importance, and, using the dynamic equations of motion of the helicopter, the best (optimal) control input history is determined. A pilot implicitly performs exactly the same process in attempting to fly a specified maneuver. [10,12,17,19,33] Chapter V describes the trajectory optimization process and algorithm in detail.

4.1.2 Flying Qualities and Pilot Workload

Using the optimal control histories derived from the optimization, the flying qualities and pilot workload evaluations were then performed as follows:

1.) If an optimal control history could be found that forced the helicopter to fly the prescibed trajectory with the prescibed flying qualities, then we concluded that the helicopter was capable of achieving these qualities. An inability to meet the criteria (e.g., minimum transition time) suggested a deficiency in the helicopter (e.g., lack of sufficient acceleration potential).

2.) From the control law for each controller, we "backed out" the pilot input time histories. These histories enabled us to evaluate the controller for satisfactory control sensitivity (criteria tabulated in Section 2.5) and decoupled response, and enabled us to compare the pilot's "workload" over that trajectory.

The "workload" was a quantitative measure derived from the pilot input-rate histories; the process used here is explained fully in Section 4.3.

The premise for using this method is straightforward, and the method's advantages are readily seen:

1.) This method does not employ human pilots or a simulator. It is purely computational, but much simpler compared to a simulator, though equally effective for preliminary analyses of controllers and the effects of auxiliary propulsion. In addition, the method certainly does not require the cost and time commitments of simulation studies, nor does it depend on the availability of pilots with comparable training.

2.) Taking the pilot out of the loop permits separate and unbiased evaluation of the helicopter attributes (notably agility via available control power) and the control system attributes. The *inherent* ability to satisfy the geometric and flying qualities criteria throughout a trajectory, with *acceptable* pilot workload, is essentially a function of the features of the helicopter, and not of the pilot. But, because human pilots are very adaptable [14], an ill-equipped helicopter may be made to fly as desired at the expense of the pilot's workload. Consequently, the pilot rating system makes it impossible to separate out pilot workload associated with "inadequacies" of the helicopter, from workload associated purely with the functioning of the control system.

In the trajectory optimization method, the trajectory's geometry and flying qualities are easily quantified, and are exactly the same criteria which the pilot attempts to meet when

performing the maneuver. But by specifying the physical control input histories, and not pilot input histories, we *make* the helicopter fly as close to these constraints as possible, and we can therefore evaluate the helicopter's attributes independently of the pilot and the control system.

3.) Pilot workload is effectively described using a simple quantitative measure. We quantify pilot workload by observing that workload is directly related to the amount which the pilot must exercise his controls. That is, workload is directly related to the "area under the curve" of the pilot input-rate histories (we use the integral of the norm of the input rates -- see Section 4.3).

Reference [10] suggests that a quantifiable measure of pilot workload can be related to the amount of time that the helicopter's pitch attitude exceeds specified upper and lower bounds. This may be a good measure, but in the method of this study, we *force* the helicopter to remain within these bounds. Therefore, this type of workload, which is really associated with the control power of the helicopter, can be disregarded, so that our valuation of pilot workload seems to give a better appraisal of the controller itself.

4.) The control histories extracted from the trajectory optimization program are for the open-loop helicopter. Determination of these optimal control histories is therefore independent of the controller. The inputs must come from the control system, but are completely independent of the control system *structure*. To evaluate the performance of *any* control system structure, we take the optimal input histories, and the

control law for that controller, and back out what the pilot input histories to the controller must be to generate the controller *output* histories, which are the optimal *input* histories to the helicopter. This means that, for each maneuver, the optimal histories need to be computed only once, and then any number of controller structures can be evaluated.

4.2 Pilot Input Histories

4.2.1 Implicit Model Controller

Extracting the pilot input history, $\mathbf{d}(t)$, for this controller involves nothing more than simple matrix algebra. From Chapter II, the control law is $\mathbf{u}(t) = -C_1\mathbf{x}(t) + C_2\mathbf{d}(t)$. For a given trajectory, $\mathbf{u}(t)$ is the (optimal) history of swashplate inputs and thruster inputs (if a thruster is included), $\mathbf{x}(t)$ is the state history, i.e., the trajectory that was prescribed and which results from the input history, $\mathbf{u}(t)$, and C_1 and C_2 are the gain matrices. The control law equation is solved for $\mathbf{d}(t)$:

$$\mathbf{d}(t) = C_2^L[\mathbf{u}(t) + C_1\mathbf{x}(t)] \qquad (4\text{-}1)$$

$\mathbf{d}(t)$ is the history of pilot control input commands. This study assigns the pilot two controls, vertical and horizontal velocity command: $\mathbf{d} = \begin{bmatrix} w_{com} \\ u_{com} \end{bmatrix}$. Therefore, when the thruster is employed, there are three helicopter controls, and C_2 is not square. The solution for $\mathbf{d}(t)$ is overdetermined, and we must use the left pseudo-inverse of C_2: $C_2^L = (C_2^T C_2)^{-1} C_2$. C_1 and C_2 are scheduled according to the total flight velocities, U and W.

It is also necessary to scale the command vector, **d**, so that the pilot inputs are within an acceptable range. The obvious choice is to scale W_{com} to the range of the collective stick, and U_{com} to the longitudinal cyclic stick range. These scale factors in no way affect the stability or response characteristics of the control system. The factors form a 2 × 2 diagonal matrix,

$$D = \begin{bmatrix} \theta_{c,range}/w_{com,range} & 0 \\ 0 & B_{1s,range}/u_{com,max} \end{bmatrix},$$ which simply scales **d** by premultiplying the feedforward matrix C_2 (the left pseudo-inverse is now a weighted left pseudo-inverse); see Figure 3-2.

For the thrust augmented helicopter, the helicopter has three control degrees of freedom while the pilot has only two. Using the pseudo-inverse to solve for the pilot histories effectively was a "minimum norm" fit of **d**(t). Therefore, it was necessary to check that the state history that resulted from pilot inputs to the closed-loop system ($\dot{\mathbf{x}} = [A\text{-}BC_1]\mathbf{x} + BC_2\mathbf{d}$) matched the state history determined in the trajectory optimization process. For the trajectories and controllers investigated in this study, the state variables of both histories (i.e., the integrated closed-loop history and optimized history) matched within one percent of each other over the trajectory interval. This was expected because of the good low frequency input-output responses of the controllers. Had these two histories not been consistent, a suitable weight for a weighted left pseudo-inverse transformation that resulted in matching state histories would have been chosen.

4.2.2 Explicit Model Controller

The prefilter in this controller makes the solution for $\mathbf{d}(t)$ slightly more complicated than the solution for the implicit model controller. It is necessary to simultaneously integrate the model dynamics while calculating the pilot input history.

The control law is $\mathbf{u}(t) = -C_1\mathbf{x}(t) - C_2\mathbf{x}_m(t) + C_3\mathbf{d}(t)$. Solving for $\mathbf{d}(t)$:

$$\mathbf{d}(t) = C_3^L[\mathbf{u}(t) + C_1\mathbf{x}(t) + C_2\mathbf{x}_m(t)] \tag{4-2}$$

However, in this equation $\mathbf{x}_m(t)$ is unknown. It must be calculated from its dynamic equation,

$$\dot{\mathbf{x}}_m(t) = A\mathbf{x}_m(t) + G\mathbf{d}(t) \tag{4-3}$$

But since $\mathbf{d}(t)$ is present in this dynamic equation, Equation 4-2 must be solved while Equation 4-3 is being integrated. The procedure is as follows:

The state and model initial conditions are known: $\mathbf{x}(t_o) = \mathbf{x}_m(t_o) = \mathbf{x}_o$. $\mathbf{u}(t)$ and $\mathbf{x}(t)$ are known for all t. Therefore, we can find $\mathbf{d}(t_o)$ from Equation 4-2. Then $\mathbf{x}_m$ at the next step, i.e. $\mathbf{x}_m(t_o+1)$, is found by integrating Equation 4-3. Then solve Equation 4-2 for $\mathbf{d}(t_o+1)$, and so on up to and including time t_f. In general, the procedure is

1. Solve Equation 4-2 for $\mathbf{d}(t_o)$ using the initial conditions.
2. For n discrete time entries in the time history, do the following for k = 1 to n-1:

   integrate Equation 4-3 to get $\mathbf{x}_m(t_{k+1})$

   solve Equation 4-2 to get $\mathbf{d}(t_{k+1})$

Because a fourth-order Runge-Kutta method is used for integration, step 2 of the above iterative procedure is actually

done four times for each integration time step. And, because the gains are dependent on flight condition, they are calculated whenever step 2 is performed.

When **d** is overdetermined , i.e. when C_3 has more nonzero rows than columns because there are more physical controls **u** than pilot commands **d**, the left pseudo-inverse of C_3 is used in Equation 4-2. And, the pilot command vector, **d**, is scaled to the conventional collective and cyclic stick ranges.

The same discussion of the left pseudo-inverse and state history matching of Section 4.2.1 applies to the explicit controller.

4.3 Assessment of Pilot Workload

As stated in Section 4-1, pilot workload is assessed in terms of control sensitivity, decoupled response to commands, and the pilot command input rates. The first two are easily understood, and used without explanation in Chapter VIII.

Intuitively, the more the pilot has to move the sticks, and the higher the rates of movement, the more work he is doing to fly the aircraft. The amount of stick movement, then, is a good quantitative measure of pilot workload. The amount of work performed in moving the sticks is the integral of the stick input rate -- actually, to avoid assigning a negative work value for negative rates, we used the norm of each (scalar) rate history. Thus, this measure of workload is the "cost" of the rate input, using unit weighting:

$$\text{Pilot workload} = \int_{t_o}^{t_f} ||\dot{d}(t)||\,dt \qquad (4\text{-}4)$$

This measure of workload depends on the time and nature of the maneuver. Therefore, it best serves as a means of comparing controllers for the *same* maneuver.

This measure was also applied to the helicopter control rate histories (collective, cyclic, and thruster rate histories). These work "costs" are used as normalizing measures for the controller inputs, and also to compare U_{com} vs B_{1s} workloads and W_{com} vs θ_c workloads.

Chapter V

THE TRAJECTORY OPTIMIZATION METHOD

This chapter is comprised of three sections. The first presents a general description of the formulation and minimization of the cost function used in the trajectory optimization process. In the second part, this general trajectory optimization method is applied to the helicopter problem to determine the optimal control histories for helicopter trajectories; individual terms of the cost function are physically interpreted in the context of the helicopter trajectory optimization problem. These two sections are mathematically formal; optimized sample trajectories are given in Chapter VII. The third part of this chapter describes the algorithm used for the optimization.

5.1 Formal Mathematics

We begin with the dynamics of the plant and initial conditions of the state:

$$\dot{\mathbf{x}} = \mathbf{f}[\mathbf{x}(t),\mathbf{u}(t),t] \tag{5-1}$$

$$\mathbf{x}(t_o) = \mathbf{x}_o \tag{5-2}$$

where $\mathbf{x}$ and $\mathbf{u}$ (for our purposes) are the helicopter state and control vectors, respectively (see Chapter III).

Initially, we define a cost function in the manner used in designing optimal controllers. [4] The cost function J penalizes state, state-control, and control excursions throughout the

interval. The integrand of "penalties" is the Lagrangian, $\mathcal{L}$.

$$J = \int_{t_o}^{t_f} \mathcal{L}[\mathbf{x}(t),\mathbf{u}(t),t]dt \qquad (5\text{-}3)$$

Since we seek the control history $\mathbf{u}(t)$ which yields a stationary minimium of this cost function, subject to Equations 5-1 and 5-2, we adjoin the dynamic equation to the cost function, thus including it in the minimization. Note that when the dynamic equation is satisfied, this additional term in the cost function equals zero, thus the cost function is numerically unchanged.

$$J = \int_{t_o}^{t_f} \left\{ \mathcal{L}[\mathbf{x}(t),\mathbf{u}(t),t] + 1^T\{\mathbf{f}[\mathbf{x}(t),\mathbf{u}(t),t] - \dot{\mathbf{x}}(t)\} \right\} dt \qquad (5\text{-}4)$$

In many applications, one often desires to specify state conditions at the end of the interval and at times along the interval. Mathematically, this is accomplished by including interior point penalty functions, θ, and a final point function, ϕ. Incorporating these penalties (also termed constraints), the redefined cost function becomes

$$J = \phi[\mathbf{x}_f(t),t_f] + \sum^{I} \theta_i[\mathbf{x}_i(t),t_i]$$
$$+ \int_{t_o}^{t_f} \left\{ \mathcal{L}[\mathbf{x}(t),\mathbf{u}(t),t] + 1^T\{\mathbf{f}[\mathbf{x}(t),\mathbf{u}(t),t] - \dot{\mathbf{x}}(t)\} \right\} dt \qquad (5\text{-}5)$$

where I is the number of interior point constraints.

Finally, it is useful (and realistically imperative) to have saturation constraints on the controls. These control constraints are expressed by the function

$$\mathbf{C}[\mathbf{u}(t),t] \leq 0 \qquad (5\text{-}6)$$

As with the dynamic constraint, the control constraint is included in the minimization of the cost function by adjoining it to the

integrand of the cost function; the adjoint vector for control constraint is m(t). The redefined cost function becomes

$$J = \phi[\mathbf{x}_f(t),t_f] + \sum^{I}\theta_i[\mathbf{x}_i(t),t_i] + \int_{t_o}^{t_f}\Big\{\mathcal{L}[\mathbf{x}(t),\mathbf{u}(t),t] + \boldsymbol{\lambda}^T\{\mathbf{f}[\mathbf{x}(t),\mathbf{u}(t),t] - \dot{\mathbf{x}}(t)\} + \mathbf{m}^T(t)\mathbf{C}[\mathbf{u}(t),t]\Big\}dt \quad (5\text{-}7)$$

m(t) is an influence vector, and each element of m takes its value according to whether or not its corresponding control is saturated:

$$m_i(t)\begin{cases}\geq 0 & C_i = 0\\ = 0 & C_i < 0\end{cases} \quad (5\text{-}8)$$

This means that the product of each control/adjoint element pair is zero, or mC = 0, so that the cost function is numerically unchanged. The cost function now incorporates all the desired penalties and constraints.

A Calculus of Variations procedure is used to derive the conditions for optimality. [4] The objective is to find those conditions which will cause the cost function to be at a stationary minimum. Therefore, we begin by taking the first variation (the differential) of J and equating it to zero. Explicit reference of the variables to time is dropped here. And, for simplicity in notation, only one interior point constraint is used; the results are easily generalized to include multiple interior point constraints.

It is convenient at this point to define the Hamiltonian, $\mathcal{H}$, of the cost function:

$$\mathcal{H}[\mathbf{x},t] = \mathcal{L}[\mathbf{x},\mathbf{u},t] + \mathbf{l}^T\mathbf{f}[\mathbf{x},\mathbf{u},t] + \mathbf{m}^T\mathbf{C}(\mathbf{u},t) \qquad (5\text{-}9)$$

The Hamiltonian has the same form as the one used for optimal controllers, with the addition of the control constraint term.

$$\text{Then} \quad J = \phi[\mathbf{x}_f,t_f] + \theta[\mathbf{x}_i,t_i] + \int_{t_o}^{t_f}(\mathcal{H} - \mathbf{l}^T\dot{\mathbf{x}} + \mathbf{m}^T\mathbf{C})dt \qquad (5\text{-}10)$$

$$\begin{aligned} 0 = dJ = &\left(\frac{\partial\phi}{\partial t}dt_f + \frac{\partial\phi}{\partial\mathbf{x}}d\mathbf{x}\right)_{t=t_f} + \mathcal{L}_{t=t_f}dt_f + \left(\frac{\partial\theta}{\partial t}dt_i + \frac{\partial\theta}{\partial\mathbf{x}}d\mathbf{x}\right)_{t=t_i} \\ &+ \mathcal{L}_{t=t_i}dt_i + \int_{t_o}^{t_f}\Big\{\left(\frac{\partial\mathcal{L}}{\partial\mathbf{x}} + \mathbf{l}^T\frac{\partial\mathbf{f}}{\partial\mathbf{x}} + \mathbf{m}^T\frac{\partial\mathbf{C}}{\partial\mathbf{x}}\right)\delta\mathbf{x} \\ &+ \left(\frac{\partial\mathcal{L}}{\partial\mathbf{u}} + \mathbf{l}^T\frac{\partial\mathbf{f}}{\partial\mathbf{u}} + \mathbf{m}^T\frac{\partial\mathbf{C}}{\partial\mathbf{u}}\right)\delta\mathbf{u} - \mathbf{l}^T\delta\dot{\mathbf{x}}\Big\}dt \end{aligned} \qquad (5\text{-}11)$$

A few remarks: This equation contains no terms for the differential changes in $\mathbf{f}$ and $\dot{\mathbf{x}}$ because differential changes in $\mathbf{f}$ exactly cancel with differential changes in $\dot{\mathbf{x}}$ due to their equality, Equation 5-1. The differential recognizes variations in the state, the control, and the derivative of the state -- there are no control derivative terms -- at a *fixed* time, t.

We now simplify the integral term $\int_{t_o}^{t_f}\mathbf{l}^T\delta\dot{\mathbf{x}}dt$. For any variables y and v, $\int ydv = yv - \int vdy$. Applying this to $\int\mathbf{l}^T\delta\dot{\mathbf{x}}dt$ over the interval $\langle t_o,t_f\rangle$, and taking into account discontinuities in $\dot{\mathbf{x}}$ at the interior point, this gives

$$\begin{aligned} \int_{t_o}^{t_i^-}\mathbf{l}^T\delta\dot{\mathbf{x}}dt + \int_{t_i^-}^{t_f}\mathbf{l}^T\delta\dot{\mathbf{x}}dt = &\ \mathbf{l}^T\delta\mathbf{x}\Big|_{t_o}^{t_i^-} - \int_{t_o}^{t_i^-}\dot{\mathbf{l}}\delta\mathbf{x}dt \\ &+ \mathbf{l}^T\delta\mathbf{x}\Big|_{t_i^+}^{t_f} - \int_{t_i^+}^{t_f}\dot{\mathbf{l}}^T\delta\mathbf{x}dt \end{aligned} \qquad (5\text{-}12)$$

But since $\mathbf{x}$ is continuous in the interval, the right hand side of Equation 5-12 becomes

$$\lambda^T \delta x\Big|_{t_o}^{t_i^-} + \lambda^T \delta x\Big|_{t_i^+}^{t_f} - \int_{t_i^+}^{t_f} \dot{\lambda}^T \delta x\,dt = \lambda^T(t_i^-)\delta x(t_i^-) - \lambda^T(t_o)\delta x(t_o)$$

$$+ \lambda^T(t_f)\delta x(t_f) - \lambda^T(t_i^+)\delta x(t_i^+) - \int_{t_o}^{t_f} \dot{\lambda}^T \delta x\,dt \qquad (5\text{-}13)$$

We eliminate δx terms by solving for δx from the following equations for the differential, dx:

$$dx(t_f) = \delta x(t_f) + \dot{x}(t_f)dt_f \qquad (5\text{-}14a)$$

$$dx(t_i) = \begin{cases} \delta x(t_i^-) + \dot{x}(t_i^-)dt_i & (5\text{-}14b) \\ \delta x(t_i^+) + \dot{x}(t_i^+)dt_i & (5\text{-}14c) \end{cases}$$

or,
$$\delta x(t_f) = dx(t_f) - \dot{x}(t_f)dt_f \qquad (5\text{-}15a)$$

$$\delta x(t_i^-) = dx(t_i) - \dot{x}(t_i^-)dt_i \qquad (5\text{-}15b)$$

$$\delta x(t_i^+) = dx(t_i) - \dot{x}(t_i^+)dt_i \qquad (5\text{-}15c)$$

Using Equations 5-15, and noting that the variation in the initial conditions is zero, the right hand side of Equation 5-13 becomes

$$[\lambda^T(t_i^-) - \lambda^T(t_i^+)]dx(t_i) - \lambda^T(t_i^-)\dot{x}(t_i^-) + \lambda^T(t_i^+)\dot{x}(t_i^+)$$

$$+ \lambda^T(t_f)dx(t_f) - \lambda^T(t_f)\dot{x}(t_f)dt_f - \int_{t_o}^{t_f} \dot{\lambda}^T \delta x\,dt \qquad (5\text{-}16)$$

Finally, substituting for $\dot{x}$ using the dynamic relationships $x(t_i^-) = f_{t_i^-}$, $x(t_i^+) = f_{t_i^+}$, and $x(t_f) = f_{t_f}$, the workable form for $\int_{t_o}^{t_f} \lambda^T \delta\dot{x}\,dt$ becomes

$$\int_{t_0}^{t_f} \lambda^T \delta\dot{x}\,dt = [\lambda^T(t_i^-) - \lambda^T(t_i^+)]dx(t_i) - \lambda^T(t_i^-)f_{t_i^-}dt_i$$

$$+ \lambda^T(t_i^+)f_{t_i^+}dt_i + \lambda^T(t_f)dx(t_f) - \lambda^T(t_f)f_{t_f}dt_f$$

$$- \int_{t_o}^{t_f} \dot{\lambda}^T \delta x\,dt \qquad (5\text{-}17)$$

Substituting this result into the cost function differential, collecting like terms, and writing all suffixes as subscripts,

$$dJ = \left\{\left(\frac{\partial\phi}{\partial t} + \mathcal{L}_{t_f} + 1^T_{t_f} f_{t_f}\right)dt_f + \left(\frac{\partial\phi}{\partial x} - 1^T_{t_f}\right)dx\right\}_{t=t_f}$$

$$+ \left\{\left(\frac{\partial\theta}{\partial t} + \mathcal{L}_{t_i} + 1^T_{t_i-} f_{t_i-} - 1^T_{t_i+} f_{t_i+}\right)dt_i + \left(\frac{\partial\theta}{\partial x} - 1^T_{t_i-} + 1^T_{t_i+}\right)dx\right\}_{t=t_i}$$

$$+ \int_{t_o}^{t_f}\left\{\left(\frac{\partial\mathcal{L}}{\partial x} + 1^T\frac{\partial f}{\partial x} + m^T\frac{\partial C}{\partial x} + \dot{1}^T\right)\delta x + \left(\frac{\partial\mathcal{L}}{\partial u} + 1^T\frac{\partial f}{\partial u} + m^T\frac{\partial C}{\partial u}\right)\delta u\right\}dt \qquad (5\text{-}18)$$

To achieve J = 0 (minimization of the cost function), we choose 1 such that the coefficients of variations in the state, control, and time -- dx, δx, δu, and dt -- equal zero over the entire interval $\langle t_o, t_f \rangle$. Doing this yields the following conditions for optimality:

1. $$1^T_{t_f} = \frac{\partial\phi}{\partial x} \qquad (5\text{-}19)$$

2. $$\dot{1}^T = -\frac{\partial\mathcal{L}}{\partial x} - 1^T\frac{\partial f}{\partial x} - m^T\frac{\partial C}{\partial x} = -\frac{\partial\mathcal{H}}{\partial x} - m^T\frac{\partial C}{\partial x} \qquad (5\text{-}20)$$

3. $$0 = \frac{\partial\mathcal{L}}{\partial u} + 1^T\frac{\partial f}{\partial u} + m^T\frac{\partial C}{\partial u} = \frac{\partial\mathcal{H}}{\partial u} + m^T\frac{\partial C}{\partial u} \qquad (5\text{-}21)$$

4. $$0 = \frac{\partial\phi}{\partial t}_{t=t_f} + \mathcal{L}_{t_f} + 1^T_{t_f} f_{t_f} \qquad (5\text{-}22)$$

5a. $$1_{t_i-} = 1_{t_i+} + \frac{\partial\theta}{\partial x} \qquad (5\text{-}23)$$

5b. $$0 = \frac{\partial\theta}{\partial t}_{t=t_i} + \mathcal{L}_{t_f} + 1^T_{t_i-} f_{t_i-} - 1^T_{t_i+} f_{t_i+} \qquad (5\text{-}24)$$

The sufficient condition -- that the second variation of J to changes in x, u, and t must be positive -- is not treated here. It is noted below that this condition holds for the helicopter application problem.

Equation 5-19, together with Equations 5-20 and 5-21 without the m term, are the classic Euler-Lagrange equations for fixed end-time optimal control problems. Equations 5-23 and 5-24 are the optimizing conditions when the end time and interior point times are allowed to vary; i.e., these are the optimizing conditions for open end- and interior-time problems. Equation 5-23 defines the discontinuity in the adjoint history $\lambda(t)$ at the interior point time t_i. Equation 5-19 specifies a final time adjoint condition, and because $\mathbf{x}$ is specified at t_o, this is a two point boundary value problem and necessitates an iterative solution (Section 5.3).

5.2 Interpretation for Helicopter Trajectories

The cost function used for the helicopter trajectory optimization is linear-quadratic -- the helicopter dynamics are linear and the cost function penalties are quadratic norms of the state and control weighted by conformable positive-definite weighting matrices. Positive-definitiveness of the weighting matrices assures that the stationary point (found via cost function minimization) is a minimum stationary point. Mathematically, positive-definitiveness assures that the second variation of the cost function is positive at the stationary point. The method of using quadratic weighting matrices with linear dynamics is analagous to the method used in developing a linear-quadratic regulator.

This section discusses each term of the cost function in the context of the helicopter problem.

5.2.1 Dynamic Constraint

The dynamics of the helicopter can be viewed as a dynamic constraint which restricts the state accelerations to a given function of the state and control. The dynamic equation is $\dot{x} = Ax + Bu$. For the purpose of trajectory optimization, these dynamics are augmented in three ways: (1.) to include perturbation positions; (2.) to include the addition of auxilary propulsion to the helicopter; and (3.) to account for control rate limits. These three items are discussed separately.

5.2.1.1 Augmenting the dynamics to include change in position

Just as the perturbation rates and attitude, $[u,w,q,\theta]$, must be added to their respective trim values, $[U_o\ W_o\ Q_o\ \theta_o]$, so too must the perturbation positions, $[x\ y]$, be calculated and added to their trim values, $[X_o\ Y_o]$. Perturbation variables u, w, q, θ are defined in a body axis system (Figure 3-1), so that perturbation positions from trim must be resolved to the trim axis: $x = u\cos\theta$ and $y = w\cos\theta$. The dynamics are augmented to include these perturbation states:

$$\begin{bmatrix} \dot{u} \\ \dot{w} \\ \dot{q} \\ \dot{\theta} \\ \dot{x} \\ \dot{y} \end{bmatrix} = \left[\begin{array}{cccc|c} & & A & & 0 \\ \hline \cos\theta & 0 & 0 & 0 & \\ 0 & \cos\theta & 0 & 0 & 0 \end{array}\right] \begin{bmatrix} u \\ w \\ q \\ \theta \\ x \\ y \end{bmatrix} + \begin{bmatrix} B \\ \\ 0 \end{bmatrix} \begin{bmatrix} \theta_c \\ B_{1s} \end{bmatrix} \qquad (5\text{-}25)$$

θ in the $\cos\theta$ terms makes these augmented dynamics "slightly" nonlinear.

5.2.1.2 Inclusion of Auxilary Propulsion

In the current longitudinal framework, the two physical

controls of the helicopter are the swashplate controls: collective and longitudinal cyclic. Addition of an auxilary propulsive device would institute another control, which is included in the dynamics as follows:

$$\begin{bmatrix} \dot{u} \\ \dot{w} \\ \dot{q} \\ \dot{\theta} \\ \dot{x} \\ \dot{y} \end{bmatrix} = \left[\begin{array}{cccc|c} & & A & & 0 \\ & & & & \\ & & & & \\ & & & & \\ \hline \cos\theta & 0 & 0 & 0 & \\ 0 & \cos\theta & 0 & 0 & 0 \end{array}\right] \begin{bmatrix} u \\ w \\ q \\ \theta \\ x \\ y \end{bmatrix} + \left[\begin{array}{c|c} & X_T \\ B & 0 \\ & 0 \\ & 0 \\ \hline & 0 \\ 0 & 0 \end{array}\right] \begin{bmatrix} \theta_c \\ B_{1s} \\ T \end{bmatrix} \tag{5-26}$$

It is assumed that the auxiliary propulsion system provides purely longitudinal thrust. Thus, as Equation 5-26 shows, the only nonzero control derivative in the third column of the augmented B matrix is the derivative which directly affects horizontal acceleration, $\dot{u}$. This is obviously a very simplified approach. A much better understanding of the auxiliary propulsion unit and its aerodynamic and inertial effects on the helicopter is needed before its effects on any of the stability and control derivatives can be quantified. As for X_T, there is little data available on stability derivatives for longitudinal thrusters on helicopters or VTOL aircraft. A value for X_T is best determined by sizing it according to the desired acceleration level. This is discussed in Sections 2.3.1 and 6.1.

5.2.1.3 Control Rate Limits

As noted in Section 5.1, the cost function constrains the controls to fall within their saturation limits. This is, of course, a realistic necessity since a helicopter (or any other system) has physical limits on its control power. But it is also

necessary to constrain the control *rates*, since the hydraulic actuators impose a delay on the command input. These limits are included in the optimization as follows.

Consider the scalar control u, and assume it behaves as a first-order system:

$$\dot{u} = -\frac{1}{\tau}u + \frac{1}{\tau}u_{com} \tag{5-27}$$

For a unit step input, the response is

$$u = (1 - e^{-t/\tau}) \tag{5-28}$$

$$\text{and} \quad \dot{u} = \frac{1}{\tau}e^{-t/\tau} \quad \text{so} \quad \dot{u}_{max} = \frac{1}{\tau} \tag{5-29}$$

This means that the control is rate-limited by $\pm\frac{1}{\tau}$. Employing this method of rate-limiting has two particular advantages. Firstly, this first-order lag realistically models the actuator dynamics of the swashplate (Figure 5-1). The actuator lag time-constant is τ in the equations above. Secondly, rate-limiting the controls in the dynamics means that a rate-limit constraint does not have to be explicitly included in the cost function. Including such a constraint would add more complexity to the cost function and increase the optimization computation time. If the constraint was explicitly included, it would be appended to the cost function with an influence vector in a fashion similar to that done for the control constraint. [4] This would, however, necessitate back-differencing the control history to compute the control rate.

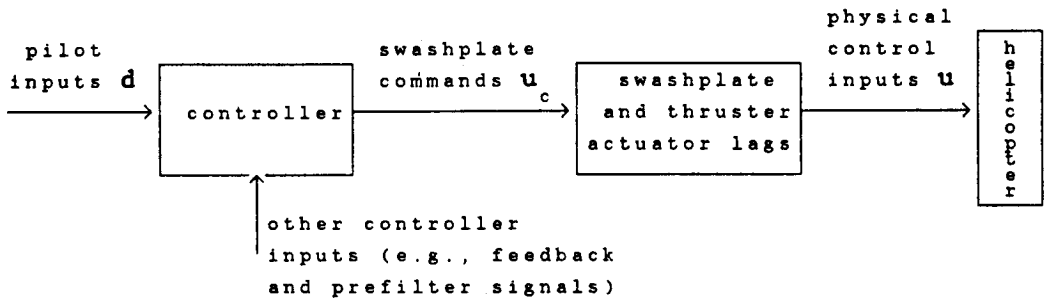

Figure 5-1 Actuator lags

Each of the three controls is rate-limited by a first-order system with an appropriate time-constant. These control dynamics are appended to the dynamics of Equation 5-26. The physical controls, θ_c, B_{1s}, and T now become part of the state vector and the commanded controls now serve as the control vector.

$$\begin{bmatrix} \dot{u} \\ \dot{w} \\ \dot{q} \\ \dot{\theta} \\ \dot{\theta}_c \\ \dot{B}_{1s} \\ \dot{T} \\ \dot{x} \\ \dot{y} \end{bmatrix} = \left[\begin{array}{cccc|ccc|c} & & A & & & B & & 0 \\ \hline & & & & -\tau_0^{-1} & 0 & 0 & \\ & & 0 & & 0 & -\tau_B^{-1} & 0 & 0 \\ & & & & 0 & 0 & -\tau_T^{-1} & \\ \hline \cos\theta & 0 & 0 & 0 & & & & \\ 0 & \cos\theta & 0 & 0 & & 0 & & 0 \end{array}\right] \begin{bmatrix} u \\ w \\ q \\ \theta \\ \theta_c \\ B_{1s} \\ T \\ x \\ y \end{bmatrix}$$

$$+ \left[\begin{array}{ccc} & 0 & \\ \hline \tau_0^{-1} & 0 & 0 \\ 0 & \tau_B^{-1} & 0 \\ 0 & 0 & \tau_T^{-1} \\ \hline & 0 & \end{array}\right] \begin{bmatrix} \theta_c \\ B_{1s} \\ T \end{bmatrix} \qquad (5\text{-}30)$$

We now let $\dot{x} = Ax + Bu$ represent this augmented system. This is precisely the dynamic constraint, $\dot{x} = f[x,u]$, used in the cost function.

5.2.2 Flying Qualities Constraints

The Hamiltonian penalyzes state and control excursions from zero throughout the flight. We can loosely say that the Hamiltonian quantitatively characterizes the desired "flying qualities" of the flight. Consider the quadratic Hamiltonian

$$\mathcal{H}[x,u] = \frac{1}{2}x^T K_x x + x^T K_{xu} u + \frac{1}{2}u^T K_u u \qquad (5\text{-}31)$$

The first term penalizes excursions of the state. Term three penalyzes control excursions and term two penalyzes state-control excursions. Excursions of a particular variable are penalyzed by assigning a positive weight to the corresponding element(s) of the appropriate weighting matrix. Because the Hamiltonian is integrated, and because the optimization procedure works to minimize the Hamiltonian, those state and control elements which are weighted must necessarily be driven toward zero. That is, their excursions (from zero) are minimized. Motions of state and control elements with zero weight are unrestricted -- though of course the dynamic constraint and other applicable constraints still apply.

For example, it is often desired to restrict the pitch rate and pitch attitude of the helicopter throughout the trajectory. In this case, the [3,3] and [4,4] elements of the K_x matrix are assigned positive weights. Intuition and experience dictate that it is usually only necessary to assign values to the diagonal

elements. In all cases, however, it must be remembered that the weighting matrix of the Hamiltonian -- the one formed by augmenting $\mathbf{x}$ and $\mathbf{u}$ -- has to be symmetric positive-definite. Determining the value of a weighting element is a matter of "engineering judgement." One develops a "feel" for sizing these weights according to their observed influence in the resulting optimal trajectory.

One final point about the weighting matrices. This analysis uses constant, time-invariant matrices. Matrices that are a function of time are probably not realistically necessary. Matrices that are a function of the state and/or control -- perturbation or nominal -- may be effective. However, if a weighting matrix is a function of a perturbation variable, the optimality conditions that result from the partial derivative of the Hamiltonian with respect to this variable will be slightly changed.

At this point, with dynamic constraints and flying qualities constraints, the cost function is

$$J = \int_{t_o}^{t_f} \left\{ \frac{1}{2}\mathbf{x}^T K_x \mathbf{x} + \mathbf{x}^T K_{xu} \mathbf{u} + \mathbf{u}^T K_u \mathbf{u} + \mathbf{l}^T(A\mathbf{x}+B\mathbf{u}) - \mathbf{l}^T\dot{\mathbf{x}} \right\} dt \qquad (5\text{-}32)$$

5.2.3 Interior and Final Point Constraints

Most NOE maneuvers are associated with achieving a specified velocity or position at a specified time, or within minimum time. Therefore, it is necessary to be able to specify the state vector at a point in the trajectory. This ability equates mathematically to constraining the state to equal a specified value at this specified time.

Again, quadratic constraints are used for the interior and final point constraints. Denoting $\mathbf{x}_{fd}$ as the desired state vector at the final time t_f, the error between the actual state and the desired state at t_f is $\mathbf{x}_f - \mathbf{x}_{fd}$. Using the weighting matrix K_f, we can construct a quadratic penalty of the final state error:

$$\phi[\mathbf{x}(t_f), t_f] = \frac{1}{2}(\mathbf{x}_f - \mathbf{x}_{fd})^T K_f (\mathbf{x}_f - \mathbf{x}_{fd}) \tag{5-33}$$

Similarly, for (multiple) interior points,

$$\sum_i^I \theta[\mathbf{x}(t_i), t_i] = \frac{1}{2}\sum_i^I (\mathbf{x}_i - \mathbf{x}_{id})^T K_i (\mathbf{x}_i - \mathbf{x}_{id}) \tag{5-34}$$

Including these constraints, the cost function is now

$$J = \frac{1}{2}(\mathbf{x}_f - \mathbf{x}_{fd})^T K_f (\mathbf{x}_f - \mathbf{x}_{fd}) + \frac{1}{2}\sum_i^I (\mathbf{x}_i - \mathbf{x}_{id})^T K_i (\mathbf{x}_i - \mathbf{x}_{id})$$
$$+ \int_{t_o}^{t_f} \left\{ \frac{1}{2}\mathbf{x}^T K_x \mathbf{x} + \mathbf{x}^T K_{xu} \mathbf{u} + \mathbf{u}^T K_u \mathbf{u} + \mathbf{l}^T(A\mathbf{x} + B\mathbf{u}) - \mathbf{l}^T \dot{\mathbf{x}} \right\} dt \tag{5-35}$$

5.2.4 Control Constraints

The swashplate controls and the thruster control have minimum and maximum saturation limits. These limits cannot be exceeded, and a hard constraint must therefore be imposed on the controls. Adjoining the control constraint to the cost function assures that the constraint will not be violated.

The control limits are simply

$$\mathbf{u}_{min} \leq \mathbf{u} \leq \mathbf{u}_{max}$$

$$\text{or,} \quad \theta_{c_{min}} \leq \theta_c \leq \theta_{c_{max}}$$

$$B_{1s_{min}} \leq B_{1s} \leq B_{1s_{max}} \tag{5-36}$$

$$T_{min} \leq T \leq T_{max}$$

Written functionally as a constraint,

$$C[u(t),t] = \begin{bmatrix} u-u_{max} \\ -u+u_{min} \end{bmatrix} \leq 0 \qquad (5\text{-}37)$$

This constraint is adjoined to the cost function with m(t) exactly as the dynamic constraint was adjoined with 1(t). Note that the dimension of m is twice the dimension of the control, u.

With the addition of the control constraint, the cost function takes its completed form:

$$J = \tfrac{1}{2}(x_f - x_{fd})^T K_f (x_f - x_{fd}) + \tfrac{1}{2}\sum_i^I (x_i - x_{id})^T K_i (x_i - x_{id})$$
$$+ \int_{t_o}^{t_f} \left\{ \tfrac{1}{2} x^T K_x x + x^T K_{xu} u + u^T K_u u + 1^T (Ax+Bu) - 1^T \dot{x} + m^T C \right\} dt \qquad (5\text{-}38)$$

5.2.5 Optimality Conditions

Applying the optimality conditions derived in Section 5-1 to this linear-quadratic cost function yields the following optimality conditions for the helicopter optimal trajectory problem:

1. $$1_{t_f} = \left(\frac{\partial \phi}{\partial x}\right)^T = K_f (x_f - x_{fd}) \qquad (5\text{-}39)$$

2. $$\dot{1} = \left(-\frac{\partial \mathcal{H}}{\partial x} - m^T \frac{\partial C}{\partial x}\right)^T = -K_x x - K_{xu} u - A^T 1 \qquad (5\text{-}40)$$

3. $$0 = \mathcal{H}_u^* = \frac{\partial \mathcal{H}}{\partial u} + m^T \frac{\partial C}{\partial u} = K_{xu}^T x + K_u u + B^T 1 + m^T C_u \qquad (5\text{-}41)$$

where for three controls, $C_u = \text{diag}[1\ 1\ 1\ -1\ -1\ -1]$

$$4.\quad 0 = \frac{\partial \phi}{\partial t}_{t=t_f} + \mathcal{L}_{t_f} + 1^T_{t} f_{t_f}$$

$$= (x^T K_x x + x^T K_{xu} u + u^T K_u u)_{t_f} + 1^T_{t_f}(Ax+Bu)_{t_f} \qquad (5\text{-}42)$$

$$5a.\quad 1_{t_i^-} = 1_{t_i^+} + \frac{\partial \theta}{\partial x} = 1_{t_i^+} + K_i(x_i - x_{id}) \qquad (5\text{-}43)$$

$$5b.\quad 0 = \frac{\partial \theta}{\partial t}_{t=t_i} + \mathcal{L}_{t_i} + 1^T_{t_i^-} f_{t_i^-} - 1^T_{t_i^+} f_{t_i^+}$$

$$- (x^T K_x x + x^T K_{xu} u + u^T K_u u)_{t_i} + 1^T_{t_i^-}(Ax+Bu)_{t_i^-} - 1^T_{t_i^+}(Ax+Bu)_{t_i^+} \qquad (5\text{-}44)$$

5.3 Optimal Trajectory Computation Algorithm

The numerical solution method used to solve the trajectory optimization problem is the second-order gradient, or steepest descent, method. [4,32] This is an iterative method that improves the control history, u(t), on each iteration. Improvement connotes minimizing the cost, thereby coming closer to satisfying the optimality conditions.

The following flow diagram shows the logistics of the steepest descent algorithm used for the trajectory optimization. A discussion of component functions of the algorithm follows the flow diagram.

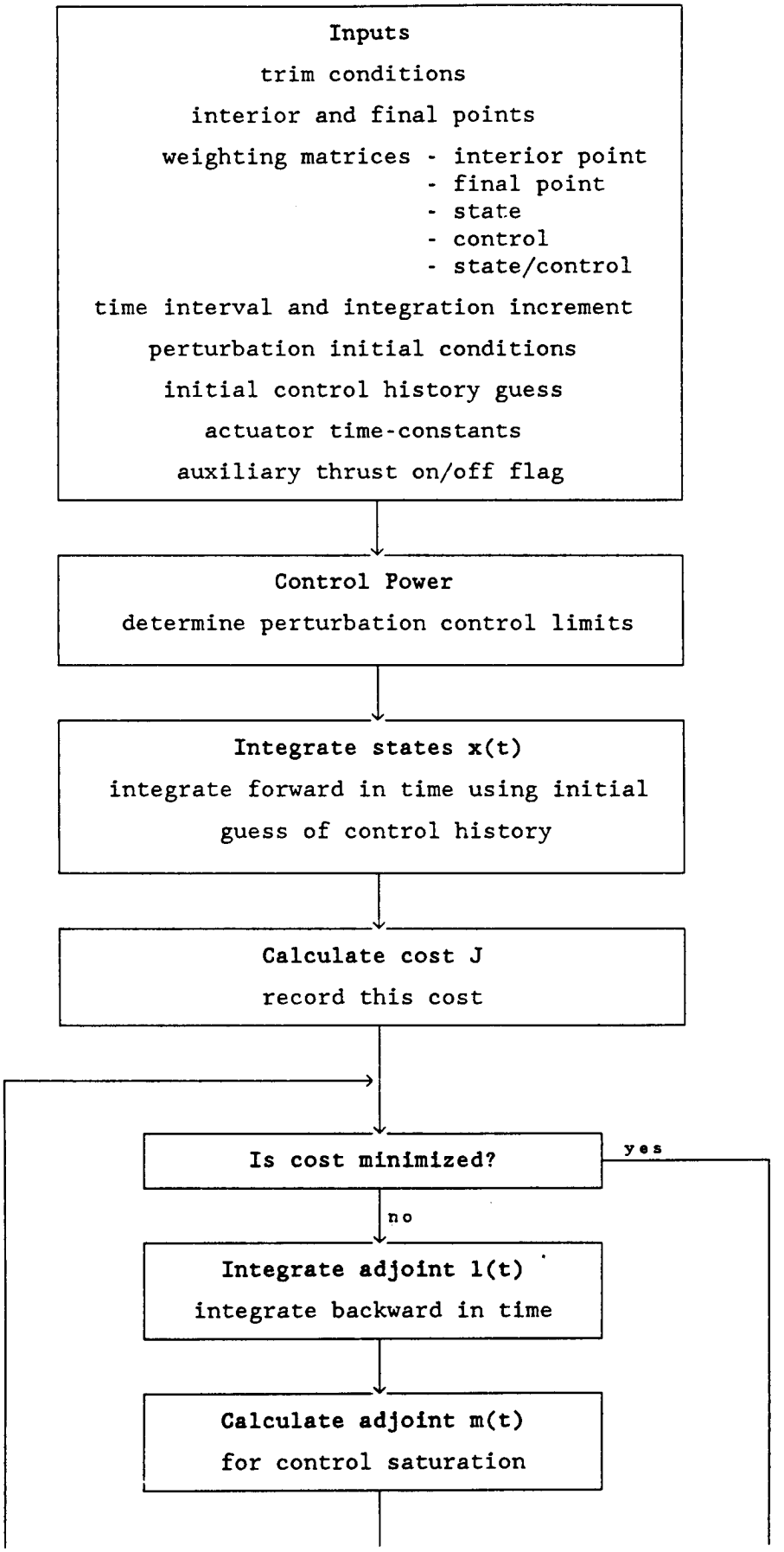
Inputs
trim conditions
interior and final points
weighting matrices - interior point
- final point
- state
- control
- state/control
time interval and integration increment
perturbation initial conditions
initial control history guess
actuator time-constants
auxiliary thrust on/off flag
Control Power
determine perturbation control limits
Integrate states x(t)
integrate forward in time using initial
guess of control history
Calculate cost J
record this cost
Is cost minimized?
yes
no
Integrate adjoint l(t)
integrate backward in time
Calculate adjoint m(t)
for control saturation

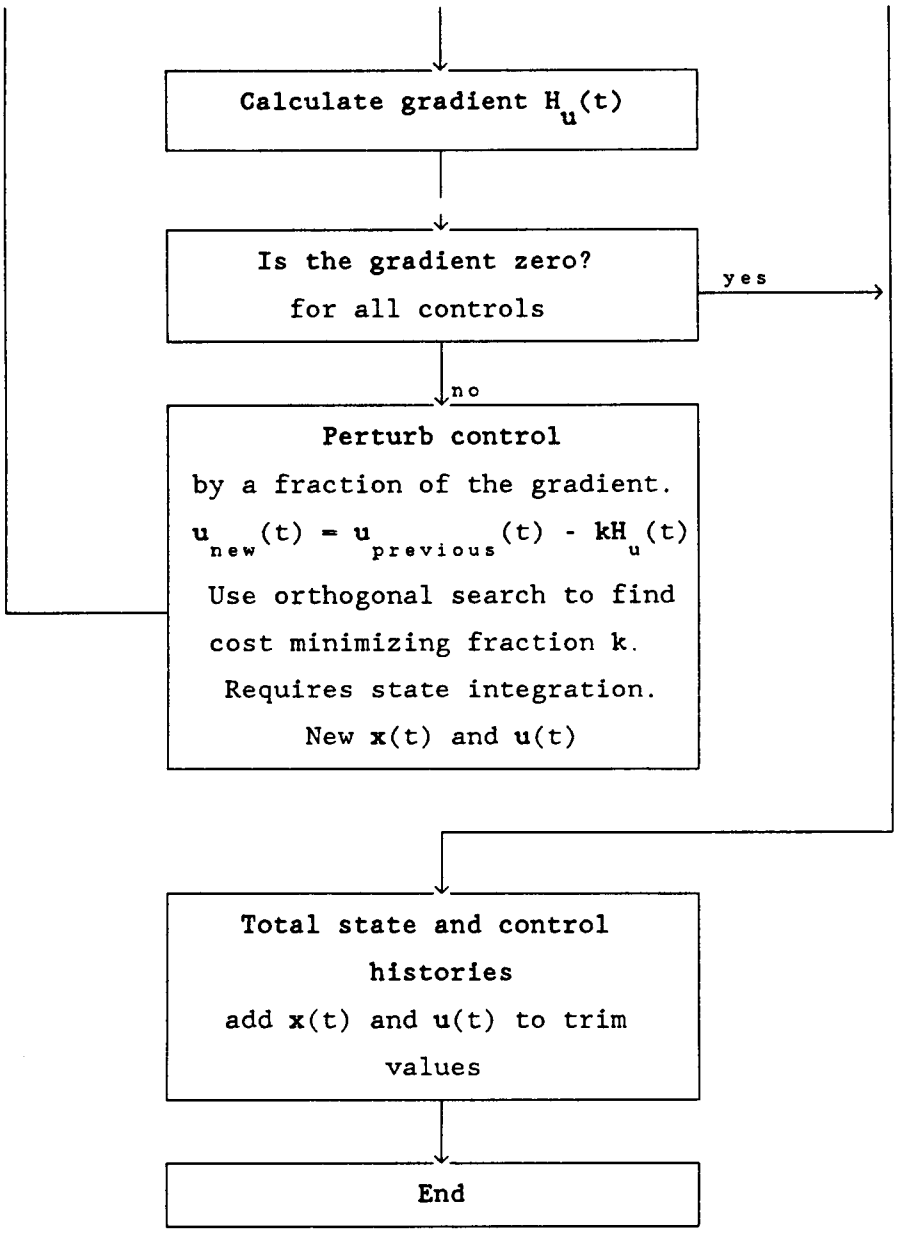

Figure 5-2 Flow Diagram of Trajectory Optimization Algorithm

5.3.1 Inputs

Each interior and final point is specified by the time at which it occurs, and by the values of each state element at that time. Obviously, t_f is the time for the final point. Initially, the interior point times must be guessed. Equations 5-42 and 5-44 are the optimality conditions which dictate how these initial guesses

should be changed for minimum-time problems. That is, these conditions are used as a gradient to adjust the interior and final point times until the new times result in trajectory histories which satisfy the equalities of Equations 5-42 and 5-44. In practice, finding the times for minimum-time problems is difficult. Rather than employ these optimality conditions in an outer-loop iteration around the optimization problem, once an optimal (but not minimum time) trajectory has been computed, the "tweaking" of these times is left to the user. The rationale is that the outer-loop iteration would have to choose a fraction of the interior point time gradient with which to perturb the interior point time. Choosing the correct fraction is very difficult, and a bad choice could mean considerable time to convergence, if convergence occurs at all. The user performs essentially the same outer-loop process by observing the completed trajectory and control histories, and deciding how much, if any, he wants to try to improve the trajectory by changing the interior point times. Mechanically, this means respecifying the interior point times and rerunning the optimization. The time to rerun the optimization is short, since presumably the new interior point times are not radically different form the existing times, so that the new optimal control history does not differ greatly from the existing history. The most efficient method is for the user to change the interior point times.

There is virtually no limit to the number of interior points that can be specified -- the limit is the number of time steps taken in the interval, minus the ones for t_o and t_f, or $(t_o-t_f)/(\text{integration increment}) - 1$. In practice, it would never

be necessary to specify this many interior points. State elements which are *not* to be constrained at interior or final points are assigned an arbitrary value, but their corresponding weighting matrix elements *must* be zero.

The integrand weighting matrices (K_x, K_{xu}, K_u) must be conformable with the state and control vectors. They must also be selected such that they form a Hamiltonian whose second derivative with respect to the control ($\mathcal{H}_{uu}$) is positive. In other words,

$$\begin{bmatrix} K_x & K_{xu} \\ K_{xu}^T & K_u \end{bmatrix}$$ must be symmetric positive semi-definite.

In many applications, K_x and K_{xu} are null matrices, so that K_u cannot be null. Elements of K_u are usually small; the identity matrix is a good choice for K_u.

Trim conditions are [U_o (ft/sec), W_o (ft/sec), Q_o (deg/sec), θ_o (deg)]. Perturbation initial conditions should always be zero.

The time interval $<t_o, t_f>$ is from t_o=0 to t_f. For minimum-time problems, determination of minimum t_f is best left to the user via the method discussed above for interior point times, for the reasons given.

The integrations in this study are performed digitally and are therefore discrete. Integrations are performed at 40 Hz, or every .025 seconds. The lower limit should be small enough to properly calculate the fastest dynamics. In this study, the fastest dynamics are the actuator dynamics, which have time constants of .08 seconds.

The better the initial estimate of the control history, the less time the optimization will take. The example of Section 7.4 shows how the trajectory converges to the optimal history from the initial history. The initial history can be quite dissimilar from the optimal history and still converge, as long as the pitch attitude is not driven to excessive amplitudes (near 90° and larger). And, it of course makes sense to specify control values for the initial estimated control history which are within the saturation limits. This initial control history *must* have time entries consistent with the specified time interval and integration increment.

The perturbation control limits are determined from the trimmed stick positions and the absolute authority limits of each control. The perturbation control, in terms of stick movement, is the inches of stick available from the trimmed position to these minimum and maximum limits. Perturbation stick movements are determined by finding the trimmed stick position (in inches) using the trimmed swashplate angle (in degrees) and the total stick and swashplate travels. For the longitudinal cyclic, this gives:

$$\left[\frac{B_{ls_{trim}} - B_{ls_{min}}}{B_{ls_{max}} - B_{ls_{min}}}\right]_{deg} = \left[\frac{B_{ls_{trim}} - B_{ls_{min}}}{B_{ls_{max}} - B_{ls_{min}}}\right]_{inches} \qquad (5\text{-}45)$$

or, solving for $B_{ls_{trim,inches}}$:

$$B_{ls_{trim,inch}} = \left[\frac{B_{ls_{trim}} - B_{ls_{min}}}{B_{ls_{max}} - B_{ls_{min}}}\right]_{deg} \times \left(B_{ls_{max}} - B_{ls_{min\,in}}\right) + B_{ls_{min,in}} \qquad (5\text{-}46)$$

The perturbation stick travel is then

$$B_{ls_{max,inches}} = \left(B_{ls_{max}} - B_{ls_{trim\ inches}}\right) \tag{5-47a}$$

$$B_{ls_{min,inches}} = \left(B_{ls_{min}} - B_{ls_{trim\ inches}}\right) \tag{5-47b}$$

Similarly, for the collective perturbation stick travel:

$$\theta_{c_{max,inches}} = \left(\Theta_{c_{max}} - \Theta_{c_{trim\ inches}}\right) \tag{5-48a}$$

$$B_{c_{min,inches}} = \left(\Theta_{c_{min}} - \Theta_{c_{trim\ inches}}\right) \tag{5-48b}$$

Note that the total permissible perturbation stick travel is equal to the total stick displacement; the trim position acts merely to define the perturbation "zero reference" position. Because the trim conditions used in this study are for conventional helicopters, the trimmed horizontal thruster position must be taken to equal zero. Minimum and maximum thrust perturbation movements are therefore the same as the total minimum and maximum movements.

Finally, the user selects the auxiliary propulsion option by setting a flag either on or off. An off flag zeros the control derivative column in the B matrix ($X_T = 0$).

5.3.2 State Integration

The state equation, $\dot{\mathbf{x}} = \mathbf{Ax} + \mathbf{Bu}$, is integrated forward in time from $\mathbf{x}_o$ using a fourth-order Runge-Kutta procedure. The integration increment is constant and specified by the user. The stability and control derivative matrices are scheduled according to flight condition and thus are computed each time the integrator

moves to compute $\overset{s}{\dot{x}}$. There are two entries in the state time history at interior point times. The second entry is necessary to account for discontinuities in $\dot{x}$ and l that occur at interior points (see Equation 5-43).

5.3.3 Cost Calculation

The integral of the cost function is computed by rectangular integration. The interior and final point costs are calculated using simple matrix mathematics.

The cost of control alone is computed and retained. It is used within the optimization algorithm as a measure for evaluating whether the cost function has been sufficiently minimized. Sufficiency is established when the total cost has been reduced to a level where the cost of control makes up most (90%) of the total cost. Recall that we want to determine the control input histories necessary to fly the trajectory, and we are therefore not interested in restricting control excursions (K_u is small). This means that when the trajectory is optimal, undesirable state excursions will be zero, and the (minimum) total cost will be comprised only of the cost of control, and thus the reason for using control cost as a minimization sufficiency measure.

5.3.4 Adjoint Integration

The adjoint equation (Equation 5-40) is integrated backward in time from l_f (Equation 5-39) using a fourth-order, constant increment, Runge-Kutta procedure. Equation 5-40 contains the A matrix, which is a function of flight condition and therefore computed each time the integrator moves to compute $\dot{l}$. The

integration routine places two entries at interior point times to account for discontinuities in 1 at t_i's (see Equation 5-43). 1(t) necessarily has the same number of time entries as **x**(t) and **u**(t).

5.3.5 Control Saturation Adjoint Vector

Each element of the adjoint, or influence, vector, m(t), can take on positive or zero values throughout the interval. Elements of m equal zero for an unsaturated control. An element becomes positive when its corresponding control is saturated. When the control is saturated, its element in m(t) is solved using Equation 5-41. Because a fraction of this equation, i.e. the gradient $\mathcal{H}_u^*$, is used to perturb the control, and because $\mathcal{H}_u^* = 0$ when the control is saturated, any improvement in the cost by perturbing the control would violate the constraint. When (and if) the element of m *begins* to turn negative, this signifies that the cost can be improved (reduced) by *unsaturating* the control, i.e., by perturbing the control by a fraction of the now nonzero gradient.

5.3.6 Control Gradient Calculation

Equation 5-41 is used to calculate the gradient, $\mathcal{H}_u'$, for each scalar control. (When the control element is unsaturated, $m_i C_i = 0$, and the gradients $\mathcal{H}_u$ and $\mathcal{H}_u'$ are the same). The control gradient can take on positive, negative, and zero values at each (discrete) point in its time history, depending on which direction (positive or negative) and how far the control is from its optimal value. See the discussion in Section 5.3.7 below for its application.

5.3.7 Control Perturbation

When the cost function is minimized, the gradient for each control equals zero over the entire interval, satisfying equation 5-41. However, to minimize the cost function requires numerical techniques because $\dot{\mathbf{x}}(t)$ and $\dot{\mathbf{l}}(t)$ are integrated in opposite directions in time, posing a two point bondary value problem. The steepest-descent method for solving this problem perturbs the most recent control history estimate by a fraction of the gradient history. The gradient gives the direction (positive or negative) and the *relative* magnitudes across time of the amount by which each control element should be perturbed. However, because this is a two point boundary value problem, which means the gradient expression is not "correct" until it exactly equals zero (which occurs when the cost is minimized and $\mathbf{x}(t)$, $\mathbf{u}(t)$, and $\mathbf{l}(t)$ are optimal), the gradient indeed provides only relative magnitudes, requiring that it be scaled by an "appropriate" fraction across the interval. As well, it cannot be expected that the same fraction is "appropriate" for each control element. Each element's fraction does, of course, apply over the entire interval.

The "appropriate" fractions for the control gradient elements are the ones which generate a new (perturbed) control history, $\mathbf{u}_{new}(t) = \mathbf{u}_{previous}(t) - k\mathbf{H}_{u}(t)$, which minimizes the cost within the *present* iteration of the trajectory optimization algorithm. [2,32] The search for the best fraction vector is an iterative

procedure which takes place within *each* major iteration of the trajectory optimization algorithm. Its logistics for the three controls case are shown in the flow diagram below. The iteration takes place within the **Perturb Control** block of Figure 5-2. Component functions are explained following the diagram.

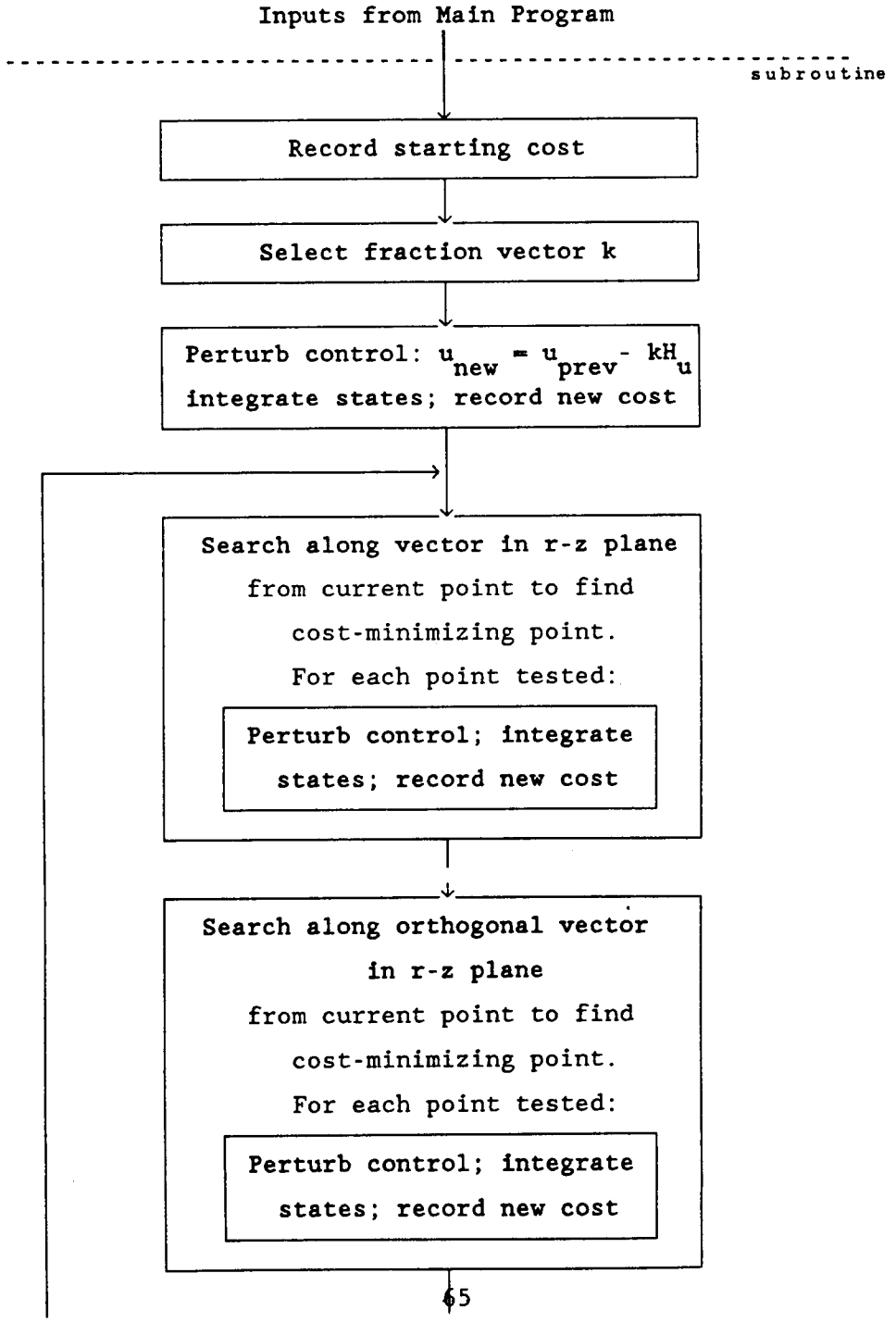

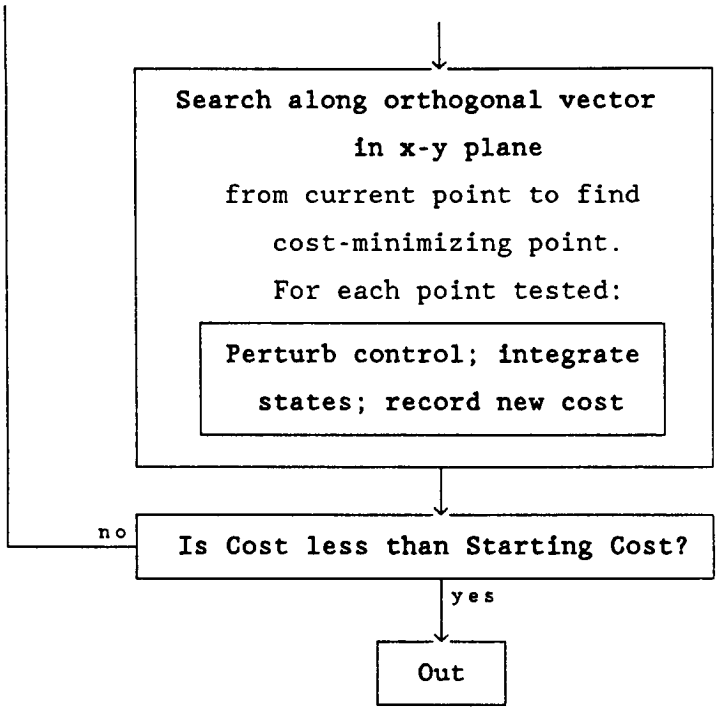

Figure 5-3 Flow Diagram for Fraction Vector Search

5.3.7.1 Selecting fraction vector k

To minimize the cost, we want to move the controls in the direction opposite the slope of their gradients [4], by a fraction of their gradients; i.e., we want to subtract $kH_u(t)$. And since the sign of the gradient tells us its direction, elements of k will always be positive (or zero).

Two options are available for selecting the fraction vector with which to begin this algorithm. One option is simply to use the vector which resulted from the previous search. A second method is employed when either: (1.) the current search is the first search within the first major iteration step (so that a fraction vector does not currently exist) or, (2.) the fraction vector from the previous search generates a control which yields a cost that is much greater than the current recorded cost. This second method takes, as the fraction for each control, 0.9% of the

quotient of the average absolute value of the control over the entire interval, and the maximum of the absolute value of its gradient over the entire interval.

5.3.7.2 Perturb Control

Once the control is perturbed -- $u_{new}(t) = u_{previous}(t) - kH_u(t)$ -- the state integration and cost calculation are performed using exactly the same functions called by the main program.

5.3.7.3 Search Routine

For m controls, the search routine searches the positive m-space by seaching along a starting search vector within this positive seach space, and then systematically searching along m-1 orthogonal vectors. The search moves to an orthogonal vector once the cost-minimizing point along the current vector has been found. This procedure is common, and treated in many texts [2,32]. A simple example best illustrates how the routine works.

Figure 5-4 plots cost contours versus fraction elements for a two control case. The fraction elements, k_1^* and k_2^*, which minimize the cost, are to be found. Starting at point A, vector 1 is searched for the $[k_1,k_2]$ pair which minimizes the cost along vector 1; this is achieved at point B. Then vector 2, which is orthogonal to vector 1, is searched, and the minimizing fraction pair is found at C. Then vector 3 is searched, et cetera, and the process continues until point $[k_1^*,k_2^*]$ is reached.

To determine which direction to search along a given axis (from its nominal point), the costs of points on each side of the nominal point, but very close to it, are computed. The direction of lesser cost is then searched. The routine defines two search lengths along every search vector, one on each side of the

starting point (see Figure 5-4), that extend from the starting point to the axes which the vector ultimately intersects, or to infinity. Costs are computed for four equally spaced points along this length. Of course, the search along the current vector stops when the cost increases, and if three points were investigated along that vector, a quadratic (least-squares) fit is performed to determine the point of minimum cost. An orthogonal search then proceeds from that point.

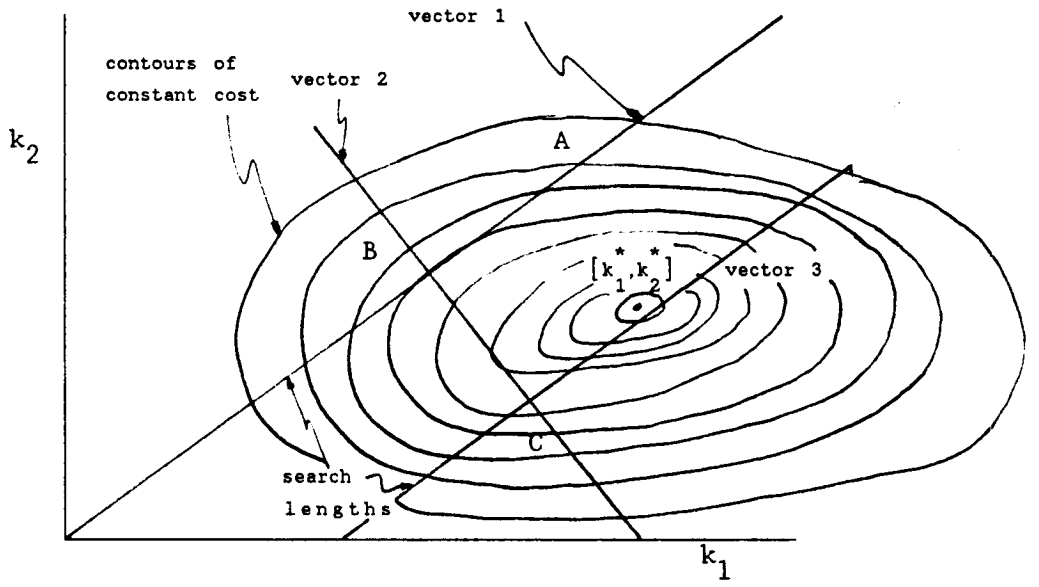

Figure 5-4 Two-dimensional Gradient Search Vector Example

Both the cost contours and the gradient change after each major iteration step, because $\mathbf{x}(t)$ and $\mathbf{u}(t)$ have changed. Therefore, the same point (set of fraction elements) may not reduce the cost on the next major iteration. Nevertheless, this point becomes the starting point for the orthogonal search.

As one might expect, the greatest reduction in cost usually occurs after m vector searches, where m is the number of controls. Take, for example, Figure 5-4 again. In this two control case,

searches along the first two search vectors (vectors 1 and 2) reduce the cost more than all the subsequent searches. Because the integration and cost calculations take considerable time, and because they are performed for each point that is checked along a vector, the search routine checks to see if the cost after m vector searches is less than the starting cost (from the previous major step). If it is, the search ends. Though the cost may be further reduced by more searches, this cost reduction (usually small) is not worth the computation time, and it is therefore advantageous to recalculate the gradient (next major step) which should yield more substantial reductions in the cost. Of course, if the cost has not been reduced after m tries, another m vector searches are performed before going to the next major step.

For this application, m = 3, and a vector search is carried out in the positive x-y-z space (or we could call it the k_1-k_2-k_3 space). The progression that this algorithm takes is to first search the r-z plane, which is the plane made by the z axis and the resultant vector r in the x-y plane. The second search vector is the vector orthogonal to the first vector in the r-z plane. There is an infinity of choices for the third vector, which is a vector orthogonal to the first two. The choice in this study is to use the vector in the plane parallel to the x-y axis at the point of intersection of the previous two vectors; i.e., at z = constant.

Determining the orientation of the intitial search vector is also a matter of choice. Eight distinct search vector orientations are possible in each plane, as shown in Figure 5-5. Unless a gradient element is zero over the entire interval, or a

control is not operating (e.g., when the auxiliary thruster is off), the vector from the origin (vector 1 in Figure 5-5) is taken as the initial search vector in each plane. In the special cases noted above, or in cases where the search along a vector terminates at an axis, the search vectors will be those vectors on, or parallel to, the representative axis.

The algorithm codes the eight different vector types by their search lengths and angle of orientation at a given search point. The code changes systematically according to the orthogonalization of the vector. For problems with more than three controls, it may then become advantageous to replace this technique with a more general technique, such as a Graham-Schmidt orthogonalization method [2].

This procedure changes from one to three of the fractions each time the search routine moves to a new point. This tends to make the orthogonalization process and vector length computations somewhat complex. A parallel search system -- one that varies each fraction element independently, i.e., one that searches parallel to each fraction axis -- would be trivial, and greatly reduce complexity (and therefore some computation time). This method was tried, but found to be inadequate. It is not as time efficient as the current algorithm. And, because it varies one element at a time, it tends to spend a lot of time in the "ridges" of the cost function contours.

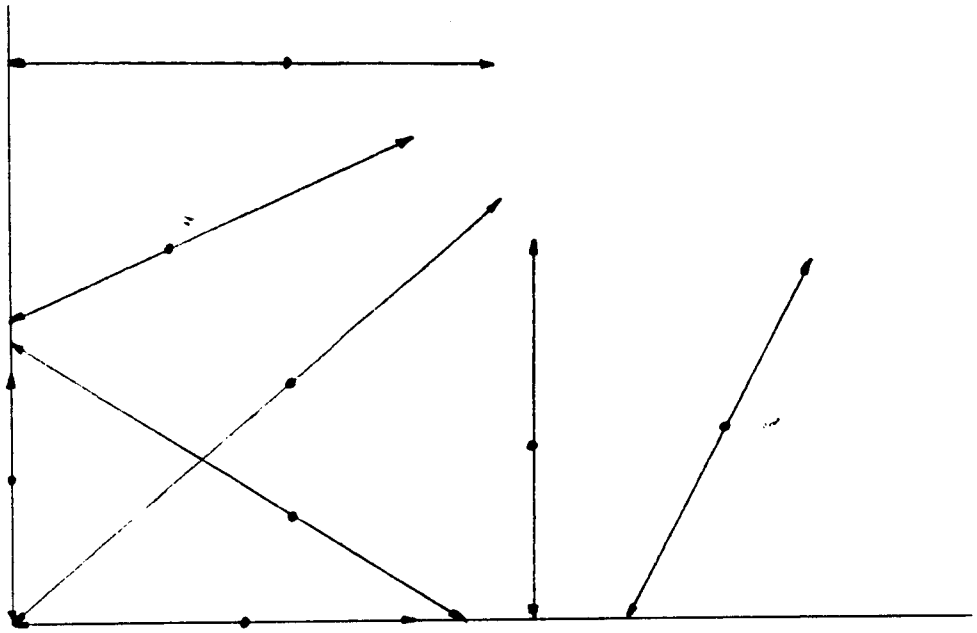

Figure 5-5 Possible Search Vector Orientations in a Plane

Chapter VI

CONTROLLERS FOR THE AH-1G TRIMMED AT HOVER

This chapter provides practical numerical examples of the development of the feedforward and feedback gains for an implicit and explicit model-following controller for longitudinal control of the AH-1G in the hover flight regime. The ideal response model reflects the desired handling qualities criteria for a longitudinal velocity-command controller operating near hover in an NOE environment; numerical criteria data are taken from the references cited in Section 2.5.

The development procedure includes the following analyses: input-output frequency response magnitude and phase analyses; eigenvalue placement and associated damping; and step input time history analyses. These analyses were used in designing each controller at each of the twenty-two trim points. Since it is rare that a controller can be developed which exactly meets the prescribed numerical handling qualities criteria, acceptable deviations, or "conditions of acceptability" were defined around these criteria. The controller was judged to be satisfactorily developed once the results of the frequency, eigenvector, and time history analyses met these conditions. These conditions also establish a common ground for comparing different controller structures. The conditions are defined in Section 6.4. Section 6.5 discusses the methodology for selecting weighting matrices' elements and the sensitivity of the closed-loop dynamics to these

elements. The examples below are for the hover trim condition, which was found to be the most difficult condition (of the twenty-two trim conditions investigated) for satisfying the handling qualities criteria.

6.1 Dynamics of the AH-1G and the Handling Qualities Model

The longitudinal model dynamics, $\dot{x} = Ax + Bu$, are

$$\begin{bmatrix} \dot{u} \\ \dot{w} \\ \dot{q} \\ \dot{\theta} \end{bmatrix} = \begin{bmatrix} -.33 & 0 & 0 & 0 \\ 0 & -.4 & 0 & 0 \\ 0 & 0 & 0 & 0 \\ 0 & 0 & 1 & 0 \end{bmatrix} \begin{bmatrix} u \\ w \\ q \\ \theta \end{bmatrix} + \begin{bmatrix} 0 & .33 \\ .4 & 0 \\ 0 & 0 \\ 0 & 0 \end{bmatrix} \begin{bmatrix} w_{com} \\ u_{com} \end{bmatrix}$$

It is obvious, in this simple model, that the u and w responses are completely uncoupled and have first-order responses with time-constants of $\frac{1}{.33}$ and $\frac{1}{.40}$ seconds, respectively. q and θ equal zero over all time since the perturbation initial condition vector, $\mathbf{x}_o$, is a null vector and since q and θ are unforced; this means Q and Θ remain at their trim values, Q_o and θ_o.

The linearized longitudinal dynamics, $\dot{x} = Ax + Bu$, of the AH-1G near hover (U_o=1.69 ft/sec, W_o=-.02 ft/sec, Q_o= 0 deg/sec, θ_o=-.73 deg) are

$$\begin{bmatrix} \dot{u} \\ \dot{w} \\ \dot{q} \\ \dot{\theta} \end{bmatrix} = \begin{bmatrix} -.0276 & -.0164 & 1.319 & -32.17 \\ -.12 & -.3836 & .31 & .4099 \\ .0005 & -.0035 & -.23 & 0 \\ 0 & 0 & 1 & 0 \end{bmatrix} \begin{bmatrix} u \\ w \\ q \\ \theta \end{bmatrix} + \begin{bmatrix} -.2635 & 1.296 & 2 \\ -12.66 & 0 & 0 \\ .00367 & -.1624 & 0 \\ 0 & 0 & 0 \end{bmatrix} \begin{bmatrix} \theta_c \\ B_{1s} \\ T \end{bmatrix} \quad (6\text{-}1)$$

The B matrix of the dynamics of the conventional helicopter has been augmented with a third column which incorporates the effects of the auxiliary propulsion system. The "2" in this third column is the control derivative for the auxilary propulsor's

contribution to the X-force (see Section 6.1.1 below). If the third column of B is null, meaning that no auxilary propulsion is employed, elements of the feedforward and feedback gain matrices corresponding to the thrust control will equal zero. This is shown by example for each controller.

6.1.1 Inclusion of the Auxiliary Thruster in the Dynamics

As discussed in Section 2.4, the advantages incurred using auxiliary propulsion come in the ability to achieve higher rates of acceleration and deceleration. We therefore derive the values for the thruster elements in the dynamic equation from the desired acceleration level, 0.3g to .35g.

In this simplified representation of the auxiliary thruster, the thruster contributes only to horizontal longitudinal body-axis acceleration/deceleration, i.e., to $\dot{u}$ (see Equation 6-1). It was assumed that there are no changes in any of the stability derivatives or any of the control derivatives for the conventional helicopter; and, the first element in the third column of the augmented B matrix is the only non-zero element in that column, representing the control derivative X_T.

The general expression for the dynamics of the thruster is then

$$\dot{u} = X_T T \qquad (6\text{-}2)$$

or, $$X_T = \dot{u}/T \qquad (6\text{-}3)$$

We express the travel of the thruster control in inches, and assign its range to be commensurate with the ranges of the collective and cyclic: T can travel ±5 inches. For full control deflection at ±.3g, this yields

$$X_T = \frac{.3g(32.174\ ft/sec^2/g)}{5\ inches} = 1.93 \cong 2\ \frac{ft}{s^2 \cdot in}$$

The AH-1G's actuator lag time-constants for both the cyclic and collective inputs are 0.08 seconds; 0.08 seconds is also used for the auxiliary thruster's actuator lag time-constant.

6.2 Implicit Model-Following Controller Design

6.2.1 Designs Including Auxiliary Propulsion

The controller gains for the AH-1G with auxiliary propulsion installed are derived first.

The Q and R matrices that result in a contoller which exhibits the desired handling qualities are

$$Q=\begin{bmatrix} 30 & 0 & 30 & 30 \\ 0 & 150 & 0 & 0 \\ 30 & 0 & 3000 & 0 \\ 30 & 0 & 0 & 3000 \end{bmatrix} \quad \text{and} \quad R=\begin{bmatrix} 1 & 0 & 0 \\ 0 & 2 & 1 \\ 0 & 1 & 1 \end{bmatrix}$$

The resulting weighting matrices are

$$W_{xx}=\begin{bmatrix} 6.332 & .7422 & 6.601 & -367.3 \\ .7422 & .442 & -3.164 & 15.88 \\ 6.601 & -3.164 & 48.38 & -1032 \\ -367.3 & 15.88 & -1032 & 31080 \end{bmatrix} \quad W_{uu}=\begin{bmatrix} 24030 & -8.818 & -15.59 \\ -8.818 & 39.76 & 69.02 \\ -15.59 & 69.02 & 121 \end{bmatrix}$$

$$W_{xu}=\begin{bmatrix} 224.9 & 12.68 & 22.37 \\ 101.9 & -.6924 & -1.192 \\ -596.9 & 35.9 & 65.31 \\ -527.4 & -1094 & -1930 \end{bmatrix} \quad W_{du}=\begin{bmatrix} -626.4 & 0 & 0 \\ -3.118 & 13.6 & 24 \end{bmatrix}$$

$$W_{xd}=\begin{bmatrix} -5.94 & 4.475 \\ -2.652 & -.2384 \\ 15.35 & 13.06 \\ 20.29 & -386.1 \end{bmatrix}.$$

The steady-state Riccati matrix, P, and influence matrix S are

$$P = \begin{bmatrix} .02348 & .00015 & -.9413 & -2.404 \\ .00015 & .00072 & -.1268 & -.0545 \\ -.9413 & -.1268 & 43.14 & 102.4 \\ -2.404 & -.0545 & 102.4 & 249.9 \end{bmatrix} \quad S = \begin{bmatrix} .02315 & .9285 \\ -.0004 & -.0156 \\ .04818 & .3082 \\ .00968 & -.0322 \end{bmatrix}$$

The resulting feedback and feedforward gains are

$$C_1 = \begin{bmatrix} .00948 & .00423 & -.0244 & -.0324 \\ .1979 & .01949 & -3.4 & -1.8 \\ .07365 & -.02042 & 2.41 & -15.01 \end{bmatrix} \quad C_2 = \begin{bmatrix} .02607 & -.000001 \\ -.0605 & -.0028 \\ .01263 & -.1946 \end{bmatrix}$$

The resulting closed-loop dynamics are $\dot{x} = (A-BC_1)x + (BC_2)d$:

$$\begin{bmatrix} \dot{u} \\ \dot{w} \\ \dot{q} \\ \dot{\theta} \end{bmatrix} = \begin{bmatrix} -.3993 & .00029 & .904 & .1716 \\ -.000028 & -.33 & .00176 & .00267 \\ .0326 & -.0003 & -.7821 & -.2928 \\ 0 & 0 & 1 & 0 \end{bmatrix} \begin{bmatrix} u \\ w \\ q \\ \theta \end{bmatrix} + \begin{bmatrix} .00185 & .3927 \\ .33 & .000098 \\ -.00002 & -.00045 \\ 0 & 0 \end{bmatrix} \begin{bmatrix} u_{com} \\ w_{com} \end{bmatrix}$$

The open-loop eigenvalues (A matrix) and closed-loop eigenvalues ($A-BC_1$ matrix) are

open-loop	closed-loop
.1205 ± .2645i	-.3902 ± .3726i
-.4411 ± .1927i	-.4019
	-.33

Two of the open-loop eigenvalues are unstable. All four closed-loop eigenvalues are stable. Of the closed-loop eigenvalues, two have been properly placed at -.4 and -.33 on the real axis; they have been driven to the roots of the model. The two other eigenvalues have complex parts ($\zeta = 0.52$); the frequency plots (Figures 6-1 and 6-3) and step input time histories (Figures 6-2 and 6-4) show that they do not comprise the dominant modes of the closed-loop dynamic response, though they are nevertheless sufficiently damped. Inspection of the Bode plots and step input histories in Figures 6-3 and 6-4 show that the vertical response to a vertical command input exactly tracks the response of the

first-order model to the same command; the responses of the other states are insignificant.

The u to u_{com} response of the controller (Figures 6-1 and 6-2) also emulates the model response very well; the horizontal velocity response, u, to a step input in u_{com} tracks the model response almost exactly, and no pitching motion results from this command. The ability of the helicopter to translate forward without a nose-down attitude is attributed to the auxiliary thruster; for the conventional helicopter, discussed below, the u to u_{com} response is accompanied by a nose-down attitude.

6.2.2 Designs Without Auxiliary Propulsion

For the conventional helicopter, the gains are computed in exactly the same manner as illustrated above, with the following two changes in the inputs: the open-loop B matrix is not augmented with the auxiliary propulsion dynamics, and the weighting matrices which ultimately provide the desired handling qualities are:

$$Q = \begin{bmatrix} 900 & 0 & 100 & 100 \\ 0 & 150 & 0 & 0 \\ 100 & 0 & 0 & 0 \\ 100 & 0 & 0 & 0 \end{bmatrix} \qquad R = \begin{bmatrix} 200 & 0 \\ 0 & 10 \end{bmatrix}$$

The resulting controller gains are

$$C_1 = \begin{bmatrix} .00955 & .00417 & -.0302 & -.0477 \\ .2923 & -.0122 & .3504 & -25.35 \\ 0 & 0 & 0 & 0 \end{bmatrix} \qquad C_2 = \begin{bmatrix} .02595 & -.0036 \\ .003917 & -.257 \\ 0 & 0 \end{bmatrix}$$

(The third row of gains contains zeros because the auxiliary propulsion is "off").

The closed-loop eigenvalues are $\begin{matrix} -.088 \pm 2.016. \\ -.4002 \\ -.3305 \end{matrix}$ Again, two of the poles have been properly placed at the poles of the model. The frequency and step input response plots are shown in Figures 6-5 to 6-8. Figure 6-5 shows a large amplitude response of q (and θ) at a frequency of 2 rad/sec to a u_c input, and Figure 6-6 shows the presence of the lightly damped mode in the pitch response to u_c inputs; the pitch rate feedback gain to u_c is only 0.35 compared with -21 in the augmented helicopter's feedback matrix.

This lightly damped mode does not meet the criterion set forth in Table 2-1. However, as noted above, it is not always possible to satisfy each criterion. In this example, increasing the damping of this mode (by increasing the values of the Q[1,3], Q[1,4], Q[3,1], and Q[4,1] weights) lengthened the time-constant of the horizontal velocity response to a horizontal velocity step input command, as shown in Figure 6-6a. Because this study used a velocity-command controller, the velocity response criterion was judged to be a more important than the damping criterion. Section 6-3 lists the order and importance of satisfying the handling qualities criteria that was followed in this study during the controller design.

Comparison of the responses in Figures 6-1 through 6-8 for the conventional and thruster-augmented helicopters with implicit model-following controllers shows that both controllers exhibit good vertical velocity command responses. For horizontal velocity command inputs, the conventionally equipped helicopter has underdamped pitching motion as it accelerates horizontally away from hover. The controller for the augmented helicopter met all

the response criteria, and therefore provided decoupled horizontal and vertical velocity command responses and insignificant pitch response.

6.3 Explicit Model-Following Controller

6.3.1 Designs Without Auxiliary Propulsion

Because the previous section showed the Ricatti matrix and closed loop matrices only for the controller design which included auxiliary propulsion, for the sake of completeness in showing the design synthesis the order of the previous section is reversed, and the controller gains for the AH-1G *without* auxiliary propulsion installed are derived first.

The Q and R matrices that result in a contoller which exhibits the desired handling qualities are

$$Q = \begin{bmatrix} 20 & 0 & 0 & 0 \\ 0 & 20 & 0 & 0 \\ 0 & 0 & 0 & 0 \\ 0 & 0 & 0 & 0 \end{bmatrix} \quad \text{and} \quad R = \begin{bmatrix} 100 & 0 \\ 0 & 1 \end{bmatrix}$$

The steady-state Riccati matrix, P_1, and influence matrices P_2 and S are

$$P_1 = \begin{bmatrix} 5.9488 & -.1244 & 20.127 & -28.65 \\ -.1244 & 3.3042 & -.3286 & .75468 \\ 20.127 & -.3286 & 196.53 & 35.77 \\ -28.65 & .75468 & 35.77 & 943.87 \end{bmatrix}$$

$$P_2 = \begin{bmatrix} -5.529 & .07940 & 0 & 0 \\ .05084 & -3.333 & 0 & 0 \\ -19.651 & .16556 & 0 & 0 \\ 18.07 & .39948 & 0 & 0 \end{bmatrix} \quad S = \begin{bmatrix} -.0172 & .43669 \\ .19412 & -.00404 \\ -.0719 & .4337 \\ .07277 & -11.224 \end{bmatrix}$$

C-2

The resulting gains are

$$C_1 = \begin{bmatrix} .00808 & -.41785 & -.0042 & -.0187 \\ 4.4409 & -.10787 & -5.831 & -42.94 \\ 0 & 0 & 0 & 0 \end{bmatrix}$$

$$C_2 = \begin{bmatrix} .00742 & .42157 & 0 & 0 \\ -3.975 & .07601 & 0 & 0 \\ 0 & 0 & 0 & 0 \end{bmatrix} \qquad C_3 = \begin{bmatrix} -.0245 & -.00062 \\ -.0106 & .49551 \\ 0 & 0 \end{bmatrix}$$

The closed-loop dynamics are $\dot{x} = (A-BC_1)x - (BC_2)x_m + (BC_3)d$:

$$\begin{bmatrix} \dot{u} \\ \dot{w} \\ \dot{q} \\ \dot{\theta} \end{bmatrix} = \begin{bmatrix} -5.7828 & .01328 & 8.875 & 23.48 \\ -.1098 & -5.6717 & .2564 & .17334 \\ .7217 & -.0195 & -1.177 & -6.974 \\ 0 & 0 & 1 & 0 \end{bmatrix} \begin{bmatrix} u \\ w \\ q \\ \theta \end{bmatrix}$$

$$+ \begin{bmatrix} 5.1534 & 1.101 & .00894 & -.2564 \\ .76506 & 56.261 & -.0006 & -.0033 \\ -.64577 & -.0075 & -.001 & .00002 \\ 0 & 0 & 1 & 0 \end{bmatrix} \begin{bmatrix} u \\ w \\ q \\ \theta \end{bmatrix}_m + \begin{bmatrix} -.00727 & .6424 \\ .31036 & -.0078 \\ .00163 & -.08147 \\ 0 & 0 \end{bmatrix} \begin{bmatrix} u_{com} \\ w_{com} \end{bmatrix}$$

The augmented dynamic equation is,

$$\begin{bmatrix} \dot{x} \\ \dot{x}_m \end{bmatrix} = \begin{bmatrix} A-BC_1 & -BC_2 \\ 0 & F \end{bmatrix} \begin{bmatrix} x \\ x_m \end{bmatrix} + \begin{bmatrix} BC_3 \\ G \end{bmatrix} d$$

and the closed-loop eigenvalues are the eigenvalues of the augmented state matrix $\begin{bmatrix} A-BC_1 & -BC_2 \\ 0 & F \end{bmatrix}$. The open-loop eigenvalues (A matrix) and closed-loop eigenvalues are

open-loop	.1205 ±.2645i	closed-loop	-.2911 ± 1.892i
	-.4411 ±.1927i		-6.3726
			-5.6767
			-.40
			-.33
			0
			0

The last four closed-loop roots are those of the prefilter (i.e., the model), and the first four are those of the closed-loop helicopter, all of which are stable. Bode plots are shown in

Figures 6-9 and 6-11. The oscillatory modes (ζ = 0.15) can be seen in the time histories, Figures 6-10 and 6-12. Like the implicit controller for the conventional helicopter, this controller does not meet the damping criterion but was chosen over a controller which traded off greater damping for a longer horizontal velocity response time-constant (the time-constant was judged to be the more important of these two criteria for velocity-command controllers). Figures 6-11 and 6-12 show that the w to w_{com} response tracks the model response exactly.

6.3.2 Designs Including Auxiliary Propulsion

X_T now has a non-zero value; the thruster is "on." The Q and R matrices are

$$Q = \begin{bmatrix} 10000 & 0 & 0 & 0 \\ 0 & 500 & 0 & 0 \\ 0 & 0 & 0 & 0 \\ 0 & 0 & 0 & 0 \end{bmatrix} \qquad R = \begin{bmatrix} 2000 & 0 & 0 \\ 0 & 2000 & 1800 \\ 0 & 1800 & 2000 \end{bmatrix}$$

The resulting controller gains are

$$C_1 = \begin{bmatrix} -.1160 & -.4697 & .1809 & .4863 \\ -.8200 & -.0016 & -22.59 & -36.47 \\ 2.929 & -.0273 & 15.45 & 14.28 \end{bmatrix}$$

$$C_2 = \begin{bmatrix} .11944 & .47337 & 0 & 0 \\ 1.1376 & .01843 & 0 & 0 \\ -3.024 & .0097 & 0 & 0 \end{bmatrix} \qquad C_2 = \begin{bmatrix} -.0245 & -.00597 \\ -.0082 & .350 \\ .0034 & -.109 \end{bmatrix}$$

The closed-loop eigenvalues are $-2.03 \pm 1.27i$, -4.607, -6.4, $-.40$, $-.33$, 0, 0. The dominant mode is complex and satisfies the damping criteria (ζ = 0.85). The other two roots have been driven far to the left along the

real axis. This controller satisfies the handling qualities criteria very well. The Bode plots and step input time histories for this controller are shown in Figures 6-13 through 6-16. The ability of the auxiliary thruster to reduce the forward pitch and oscillation of the helicopter out of hover is evident in the pitch rate/attitude time history of Figure 6-14.

The explicit controller for the helicopter equipped with auxiliary propulsion provided u and w responses which track the model responses very well. However, though the controller met all the handling qualities criteria, it was not possible to design an explicit controller which equaled the ability of the implicit controller (for the augmented helicopter) to meet these criteria and also to provide unnoticeable pitching motion response to a horizontal velocity step input command.

6.3 Conditions of Acceptability for Controller Analysis

For the model dynamics of Section 6.1, the controllers of Sections 6.2 and 6.3 were judged to be acceptable and comparable in their abilities to satisfy the handling qualities criteria when they met the following conditions; these conditions were evaluated in the order given below:

- The u/u_c and w/w_c frequency magnitude responses remained within ±0.1 decibels of the model response from 0 to 1 rad/sec.
- There were no peaks in these magnitude responses, and any valleys were confined to a 1 rad/sec span.

o The u/u_c and w/w_c frequency phase responses remained within ±4 degrees of the model response from 0 to 1 rad/sec.

o Any deviation in phase from the model was confined to -45° to -100° on the phase plot.

o All input-output frequency magnitude responses other than u/u_c and w/w_c remained below -20 decibels for at least 5 rad/sec of the 0-6 rad/sec bandwidth and below -10 decibels over the entire band.

o The time response of u to a step input in u_c and w to a step in w_c remained within ±10% of the time responses of the model to these same two inputs over the 5 second history.

o The coupled responses, u to w_c and w to u_c, were confined within ±0.05 ft/sec from zero over the 5 second time history.

o Closed-loop eigenvalues were confined to the 0-6 rad/sec bandwidth.

o The damping criterion ($\zeta \geq 0.5$) was satisfied as long as it did not result in a system which violated any of conditions above. For both the implicit and explicit controllers without auxiliary propulsion, this criterion could not be met. This suggests that satisfactory damping using these controller structures is only possible when auxiliary propulsion is employed.

o Pitch rate and pitch attitude time history responses were minimized while adhering to the conditions above.

6.5 Selecting Controller Weighting Matrices.

The elements of the Q and R matrices are parameters which must be chosen to yield a controller which provides the desired closed-loop properties. The following rules of thumb for selecting appropriate weighting matrices resulted from the

development of the controllers outlined in this study. Many of the rules discussed below are clearly seen in Figure 6-17, which plots root loci for the explicit controller (auxiliary propulsion installed) of Section 6-3 for various weighting matrices.

o In general, the diagonal elements dictate the dominate response characteristics of the system. A few off-diagonal terms may occasionally be used to refine some aspects of the response, as discussed below.

o The [1,1] and [2,2] elements of Q weight the u and w responses. They were varied independently to achieve the desired frequency magnitude and phase responses and time history responses. The magnitude of these elements varied from one controller to the next (from 20 to 10,000 in the examples in Sections 6.2 amd 6.3) and from one trim point to the next, but their influence in the frequency and time responses was easily discernible, so that the correct order of magnitude was quickly determined. These two weights affected only the response of their corresponding state variables, and once the correct order of magnitude was determined, changes within this order had virtually zero effect on the eigenvalue locations. These two parameters alone provided the desired decoupled velocity-command responses.

o The [3,3] and [4,4] elements of Q showed little influence in the responses, except for the augmented helicopter's implicit controller. Occasionally, a unity weight was assigned to these elements to reduce pitching motions. For the implicit controller, at many trim conditions it was imperitive to weight the [1,3], [1,4], [3,1], and [4,1] elements of Q to reduce excessive

responses in q and θ to u_{com} inputs. Once the [1,1] element was determined, these elements were found to be less than or equal to the [1,1] element.

o The control weighting matrix, R, effectively controls the pole locations of the less dominant poles. In general, R did not strongly affect the dominant roots, and therefore it did not strongly influence the frequency and time responses of the system. In those cases where this influence was observed, the implicit controller was more susceptible to changes in the state responses from increasing R than was the explicit controller.

o The unity matrix was a good choice for R. When (a) pole(s) were out of bounds of the 6 rad/sec frequency band, one or more of the diagonal elements of R was increased to pull the pole(s) back in bounds. A few tries showed which elements influenced which poles, and the magnitude of the proper element was adjusted to properly place the pole; often the poles were effectively placed by simply assigning the same scaling factor to all elements.

o For the auxiliary thrusted helicopter, assigning a positive weight to the cross-coupled elements of R for the longitudinal cyclic and auxiliary thruster (elements [2,3] and [3,2]) provided an easy means of increasing the damping ratio of the dominant complex roots. The value of this weight was equal to or slightly less than, but of the same order of magnitude as,the smaller value of the [2,2] and [3,3] elements.

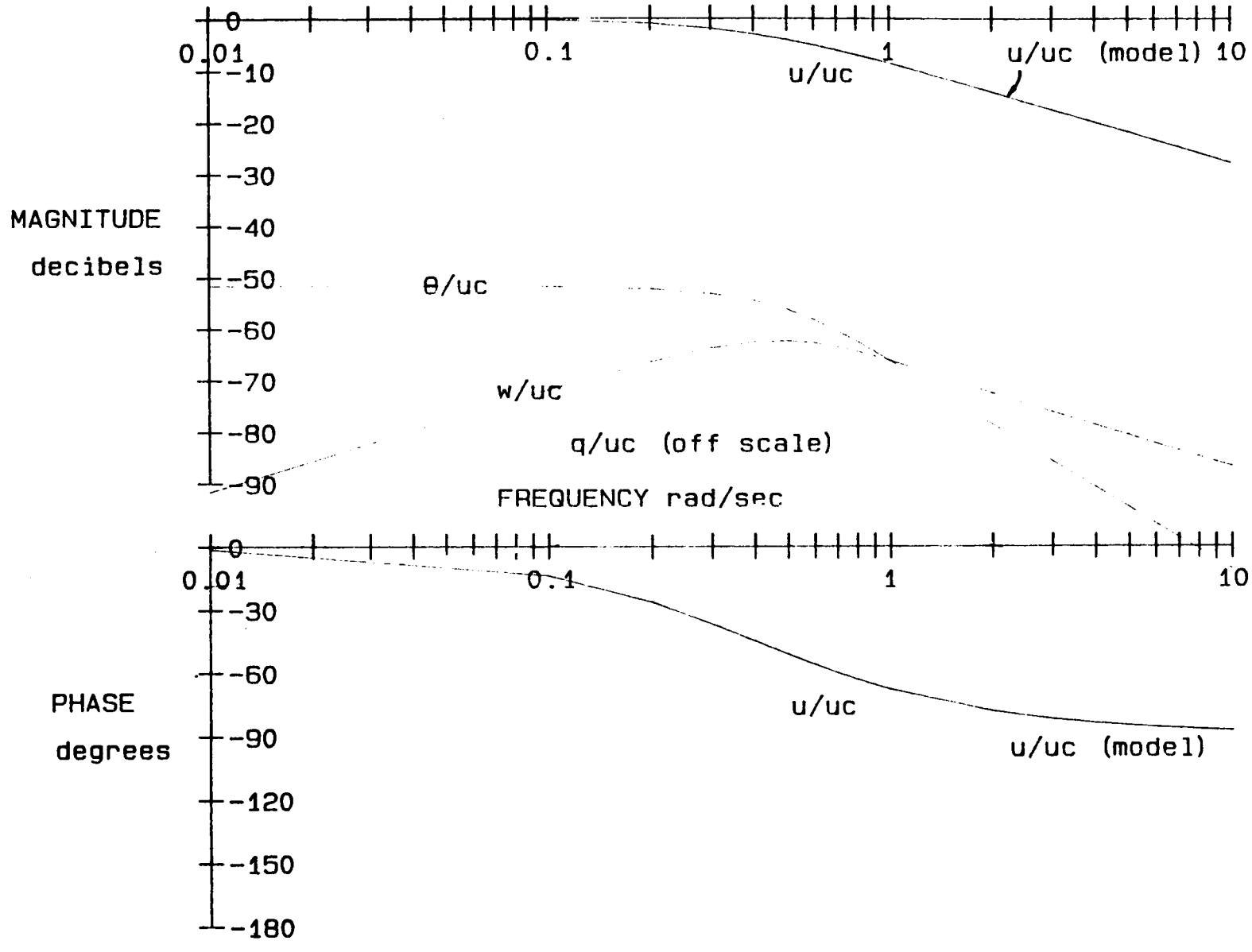

Figure 6-1

Implicit Controller: Hover, Aux Prop ON, u-command frequency response

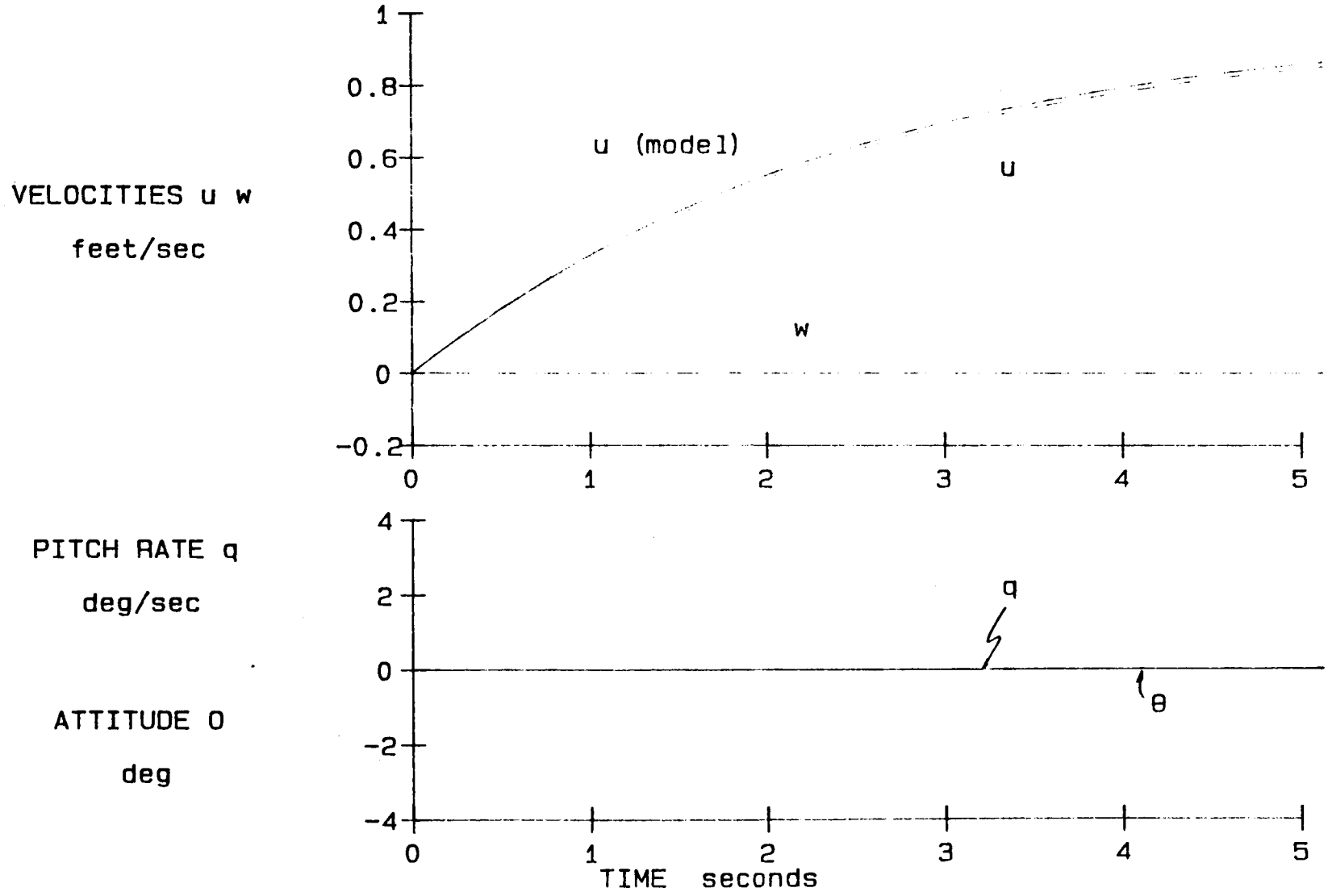

Figure 6-2

Implicit Controller: Hover, Aux Prop ON, u-command step response

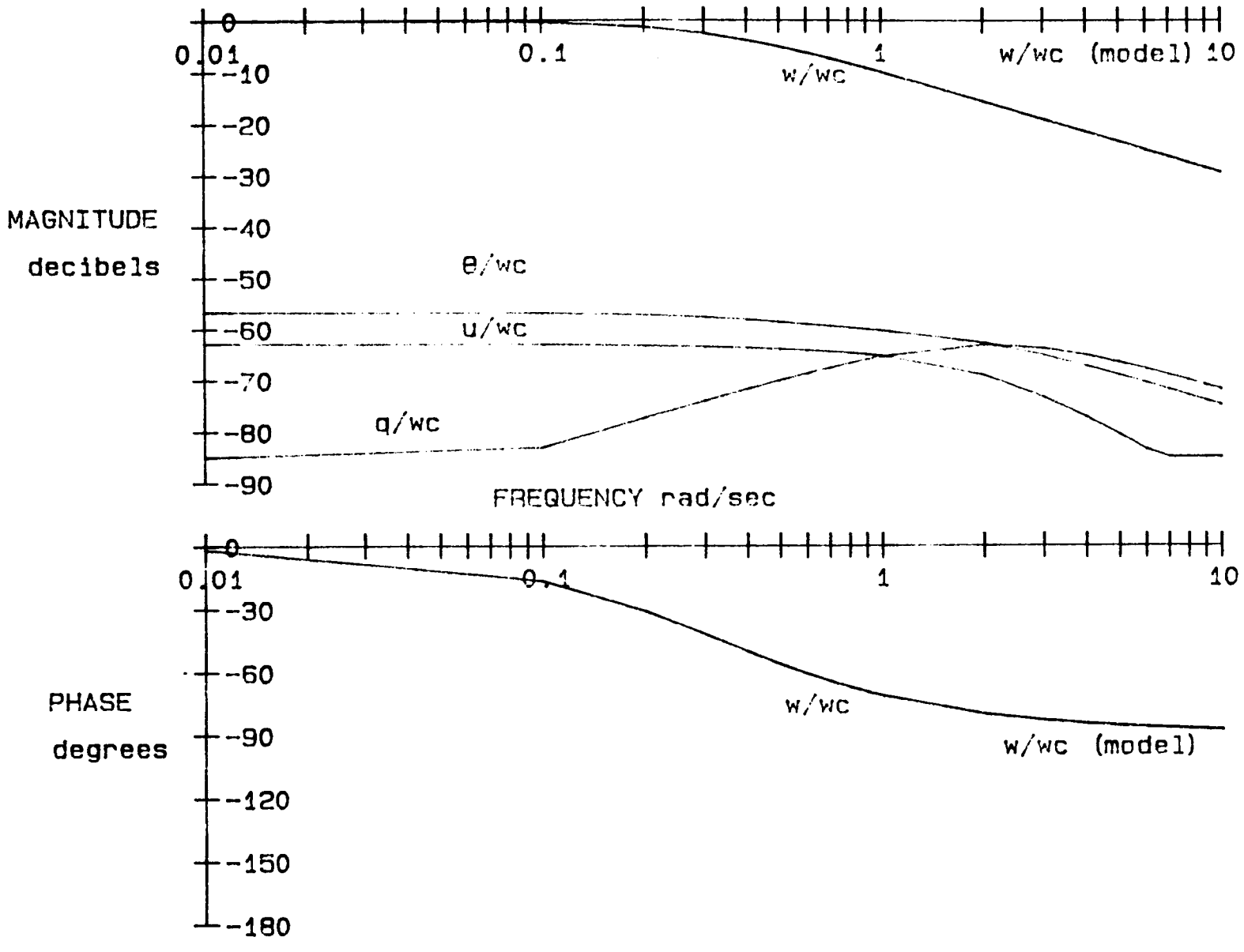

Figure 6-3

Implicit Controller: Hover, Aux Prop ON, w-command frequency response

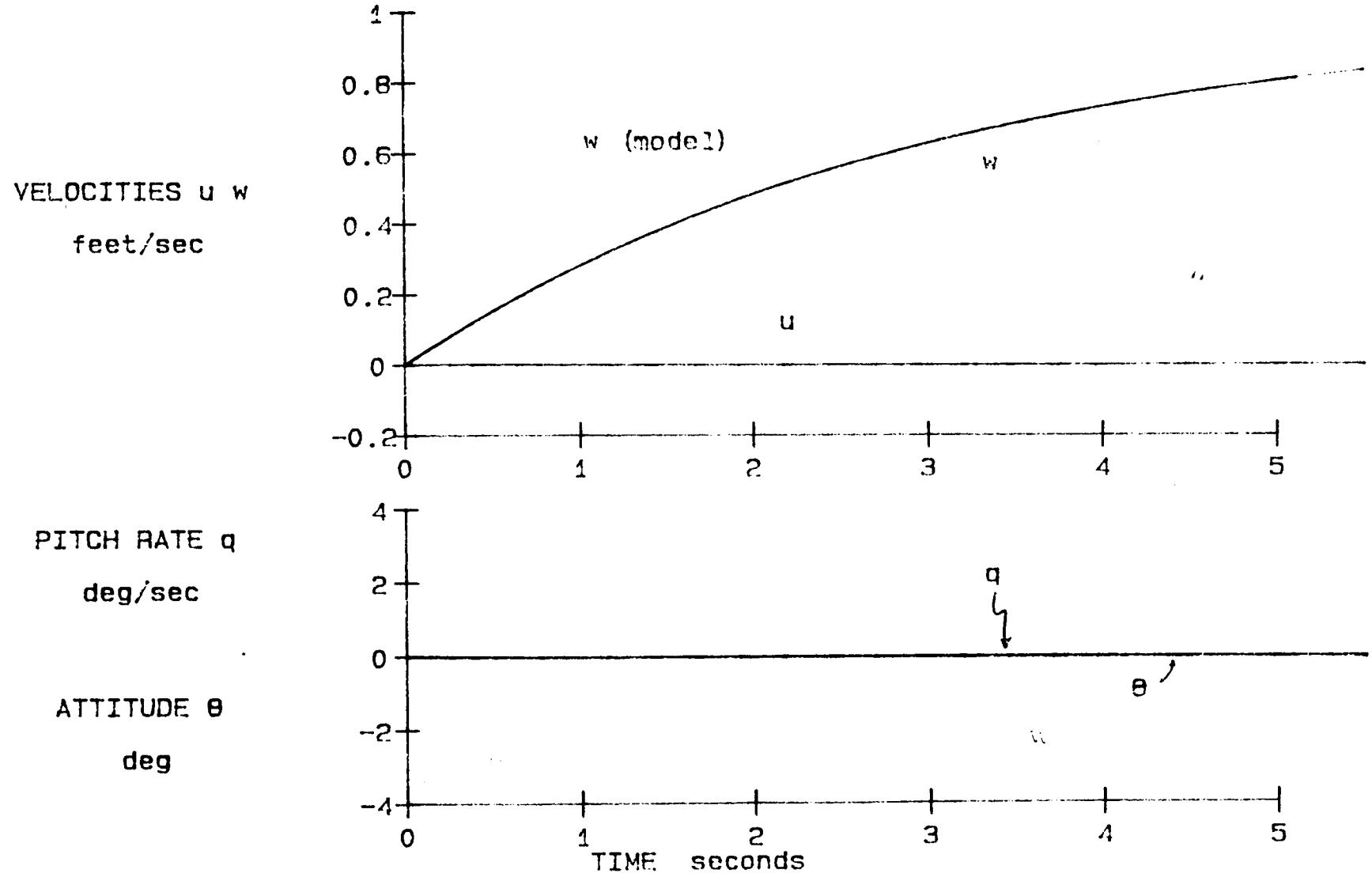

Figure 6-4

Implicit Controller: Hover, Aux Prop ON, w-command step response

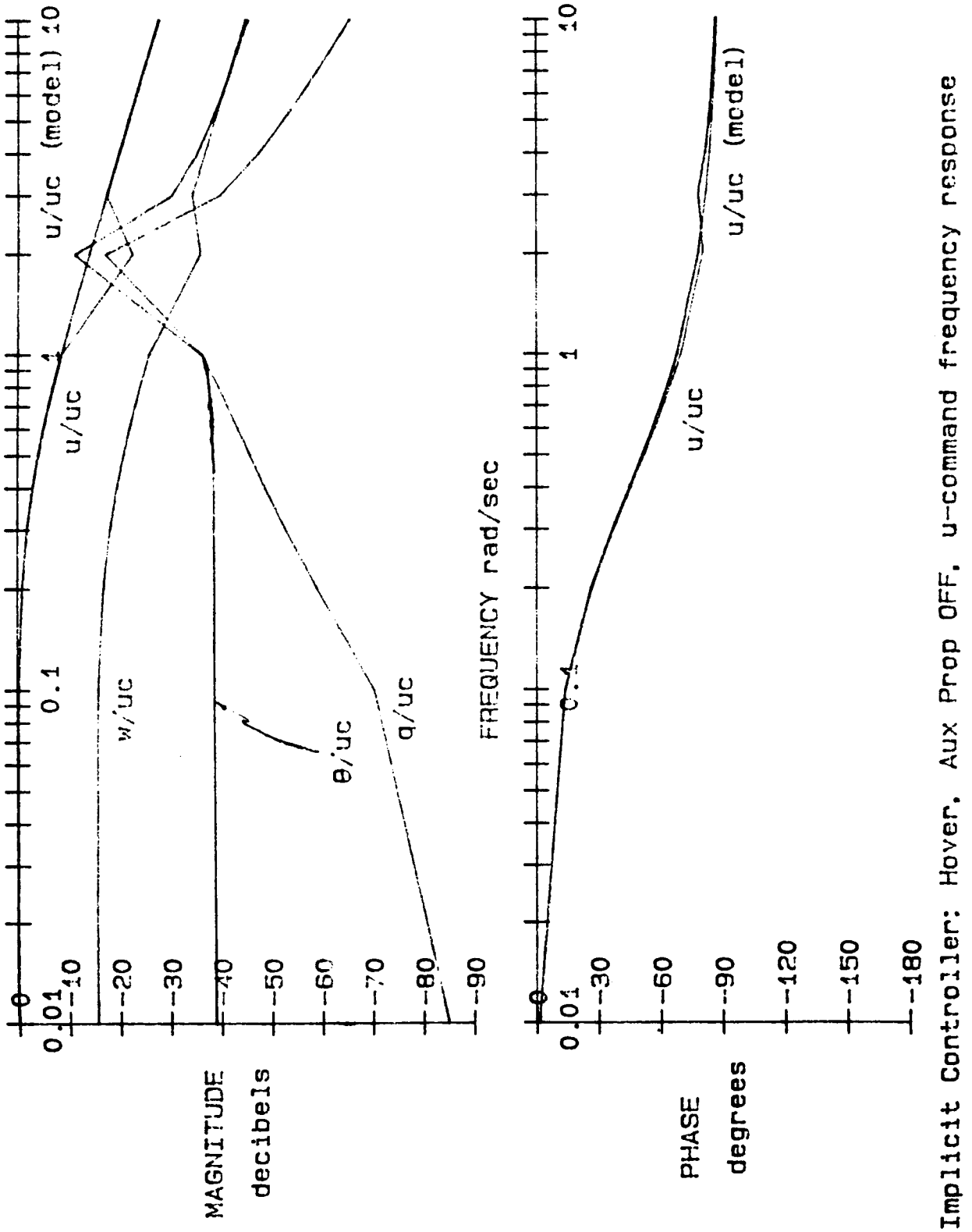

Figure 6-5

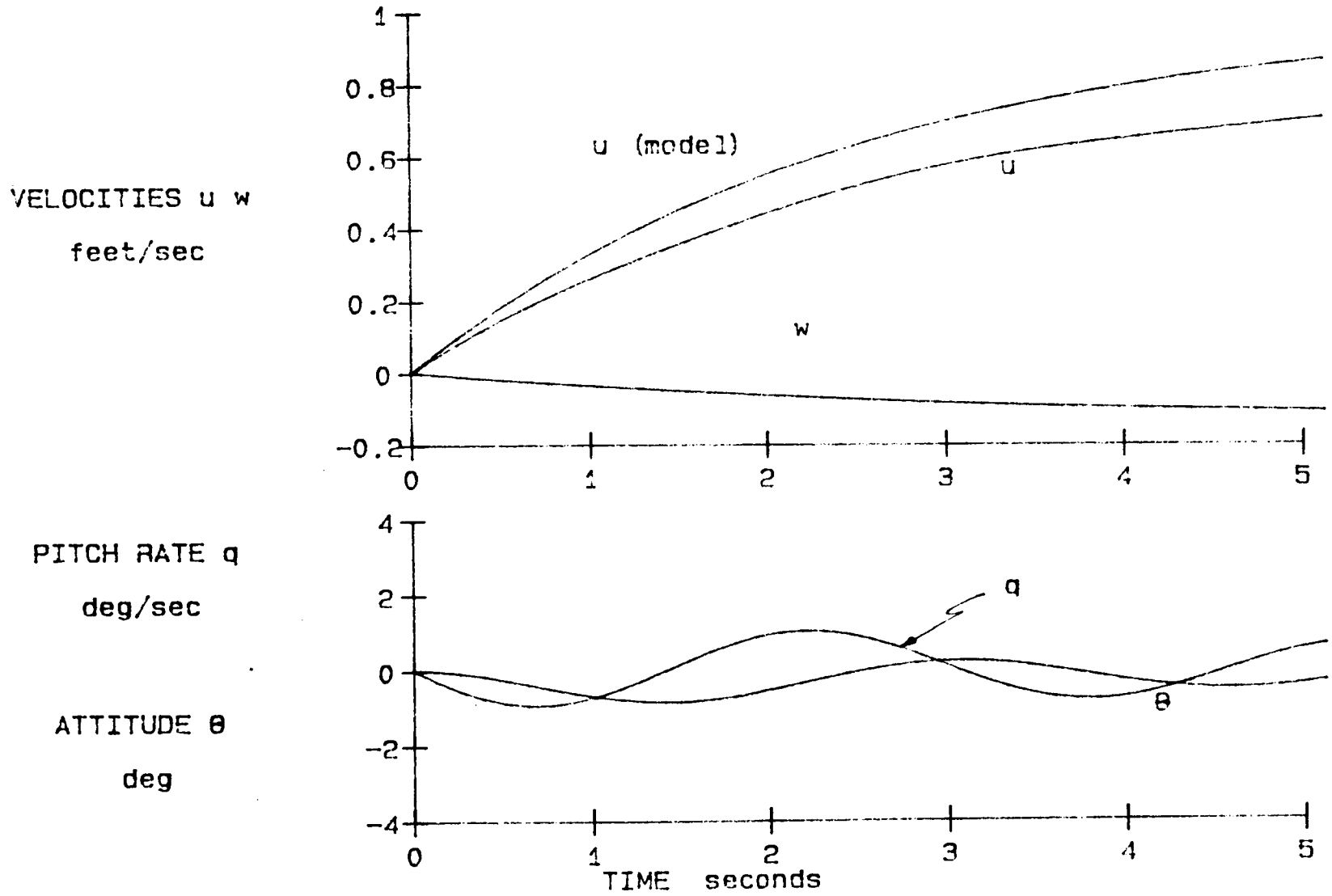

Figure 6-6

Implicit Controller: Hover, Aux Prop OFF, u-command step response

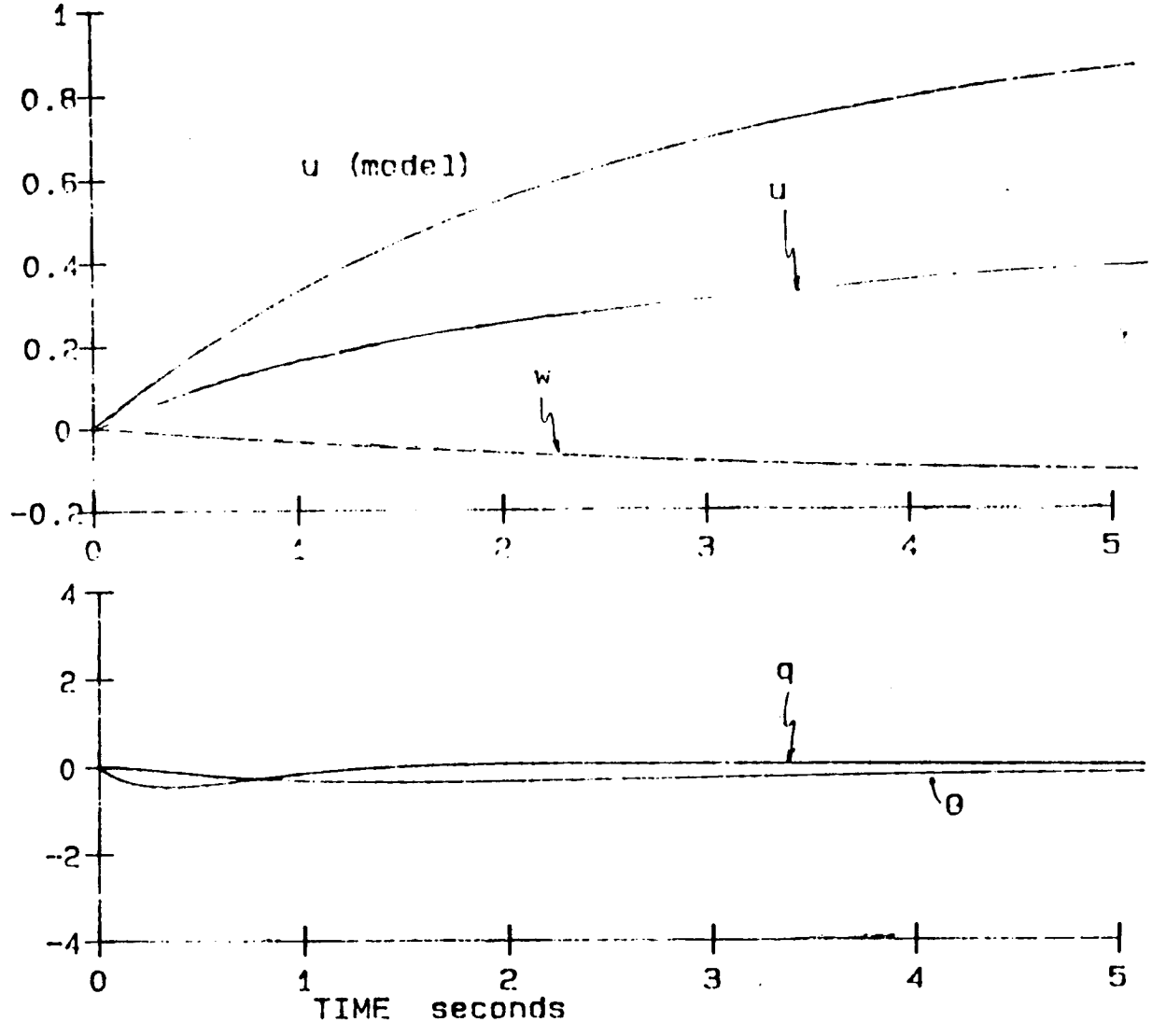

Figure 6-39

Implicit Controller: Hover, Aux Prop OFF, u-command step response

(effect of increasing the damping for the controller of Figure 6-6)

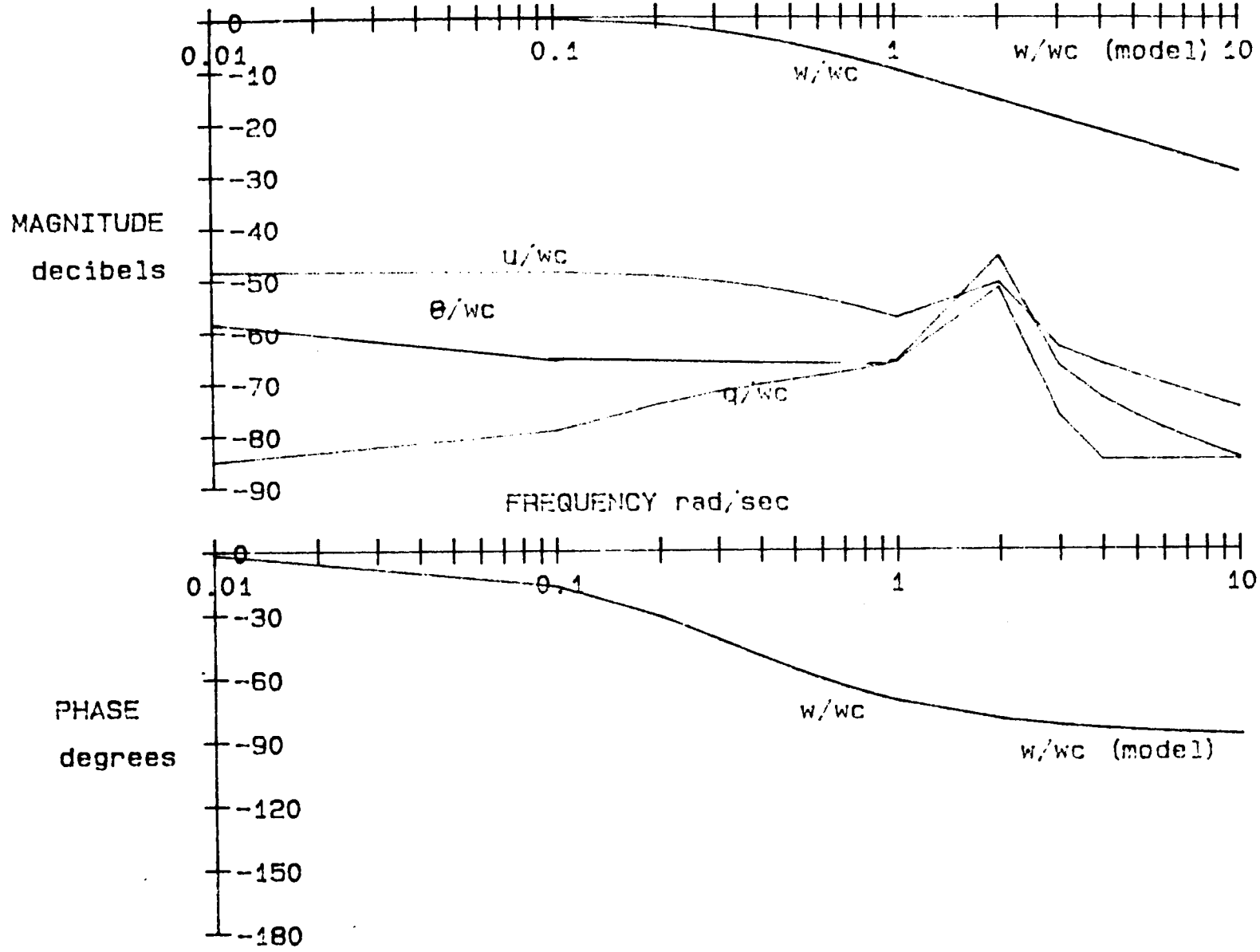

Figure 6-7

Implicit Controller: Hover, Aux Prop OFF, w-command frequency response

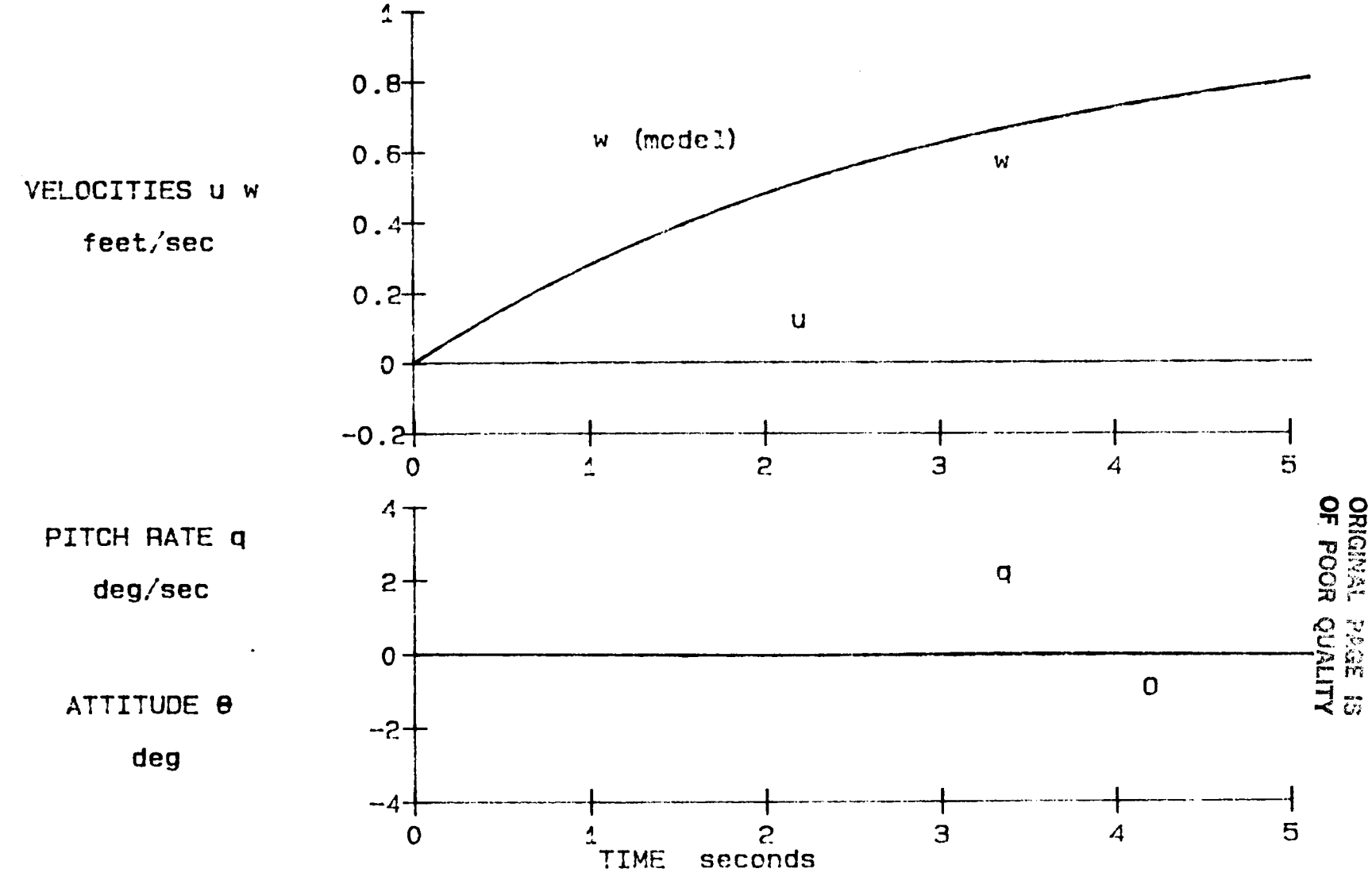

Figure 6-8

Implicit Controller: Hover, Aux Prop OFF, w-command step response

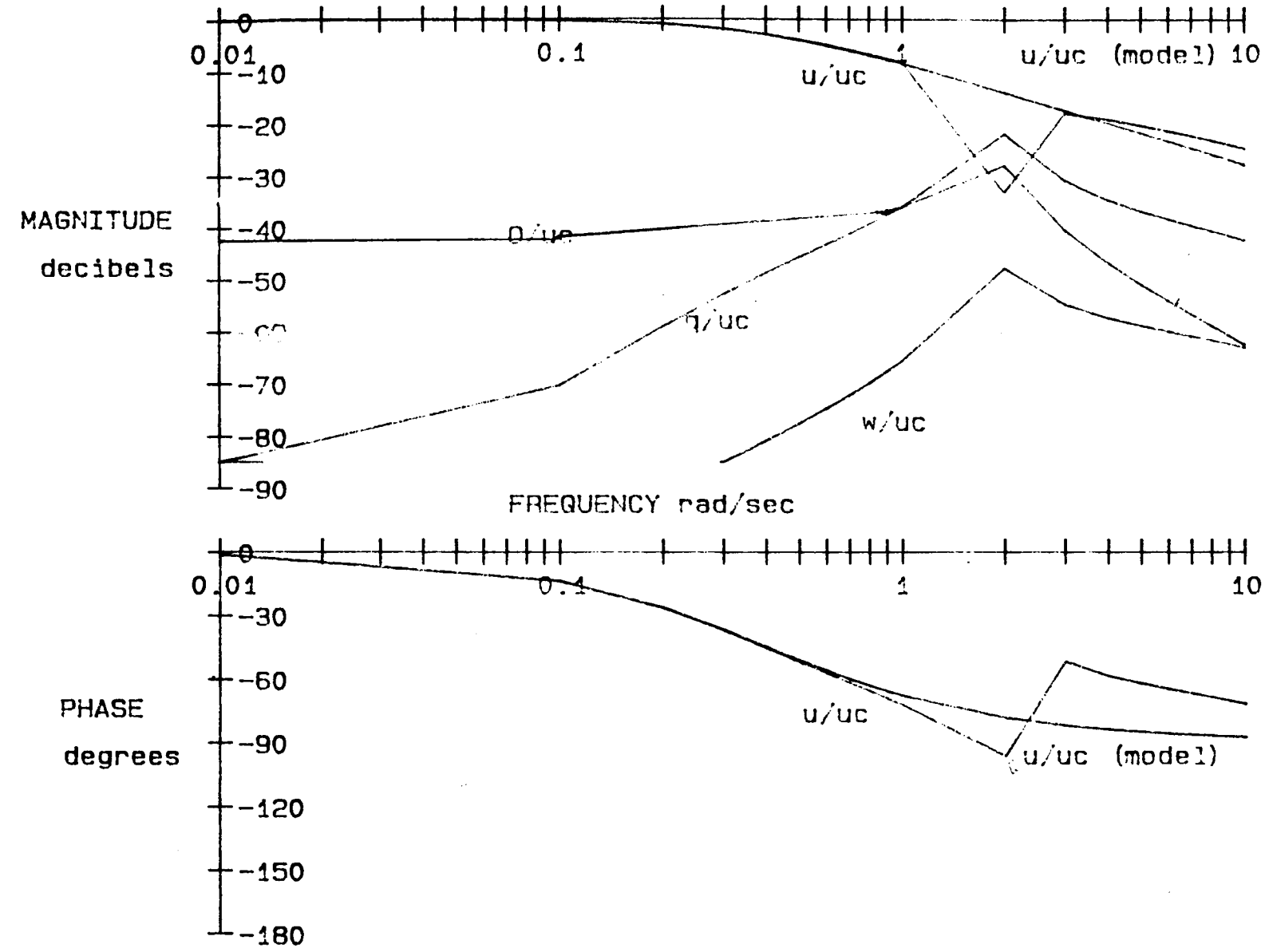

Figure 6-9

Explicit Controller: Hover, Aux Prop OFF, u-command frequency response

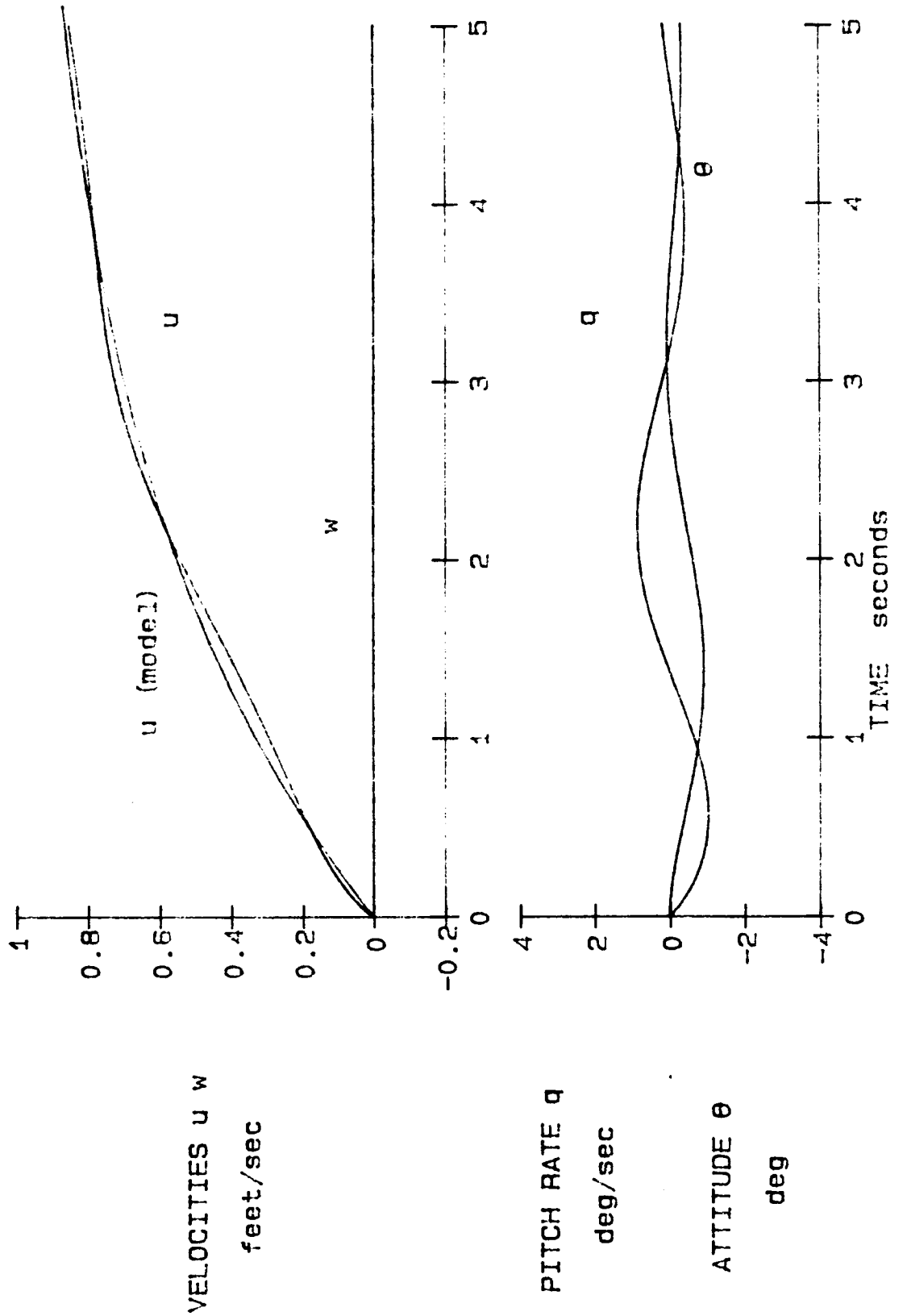

Figure 6-10

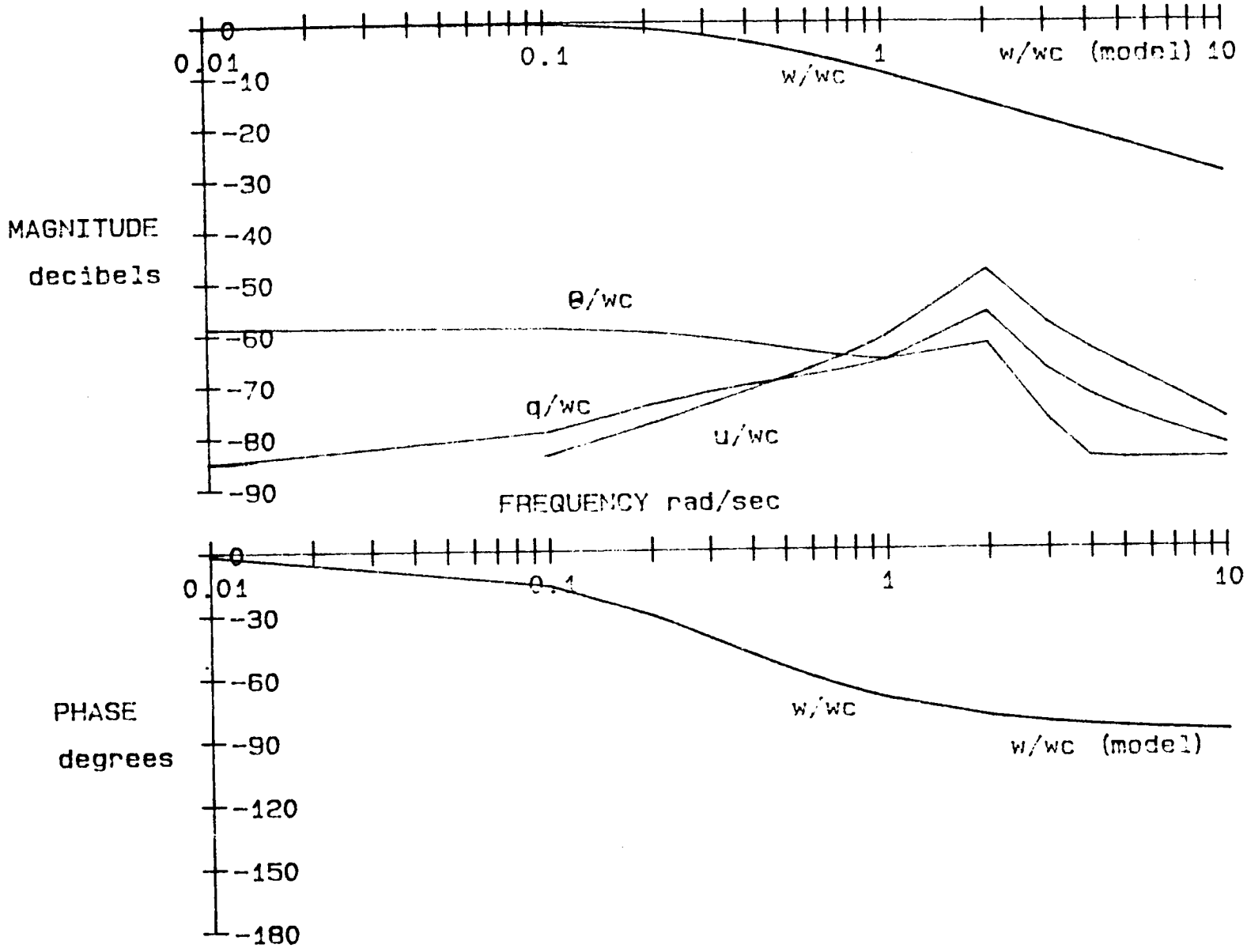

Figure 6-11

Explicit Controller: Hover, Aux Prop OFF, w-command frequency response

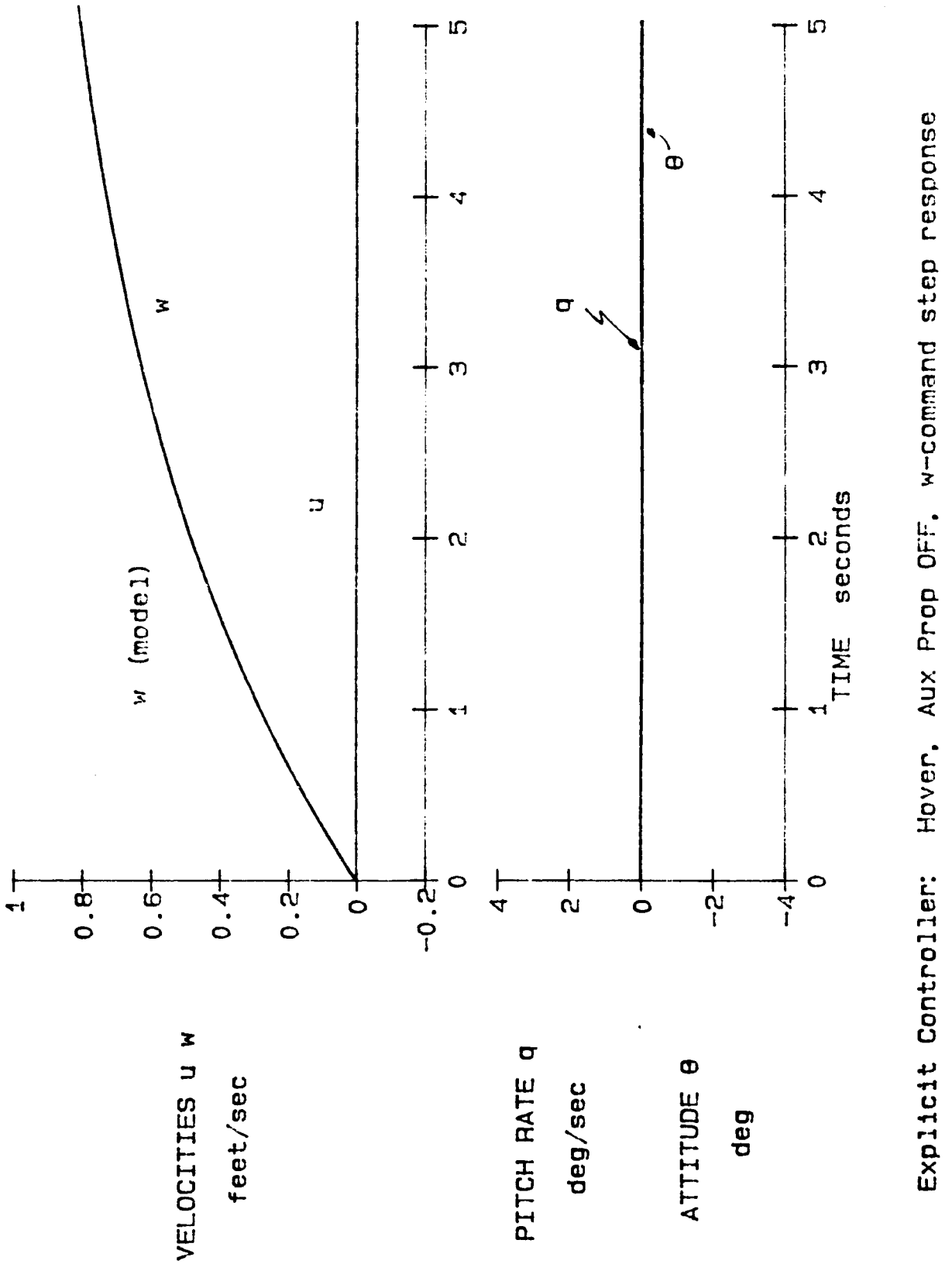

Explicit Controller: Hover, Aux Prop OFF, w-command step response

Figure 6-12

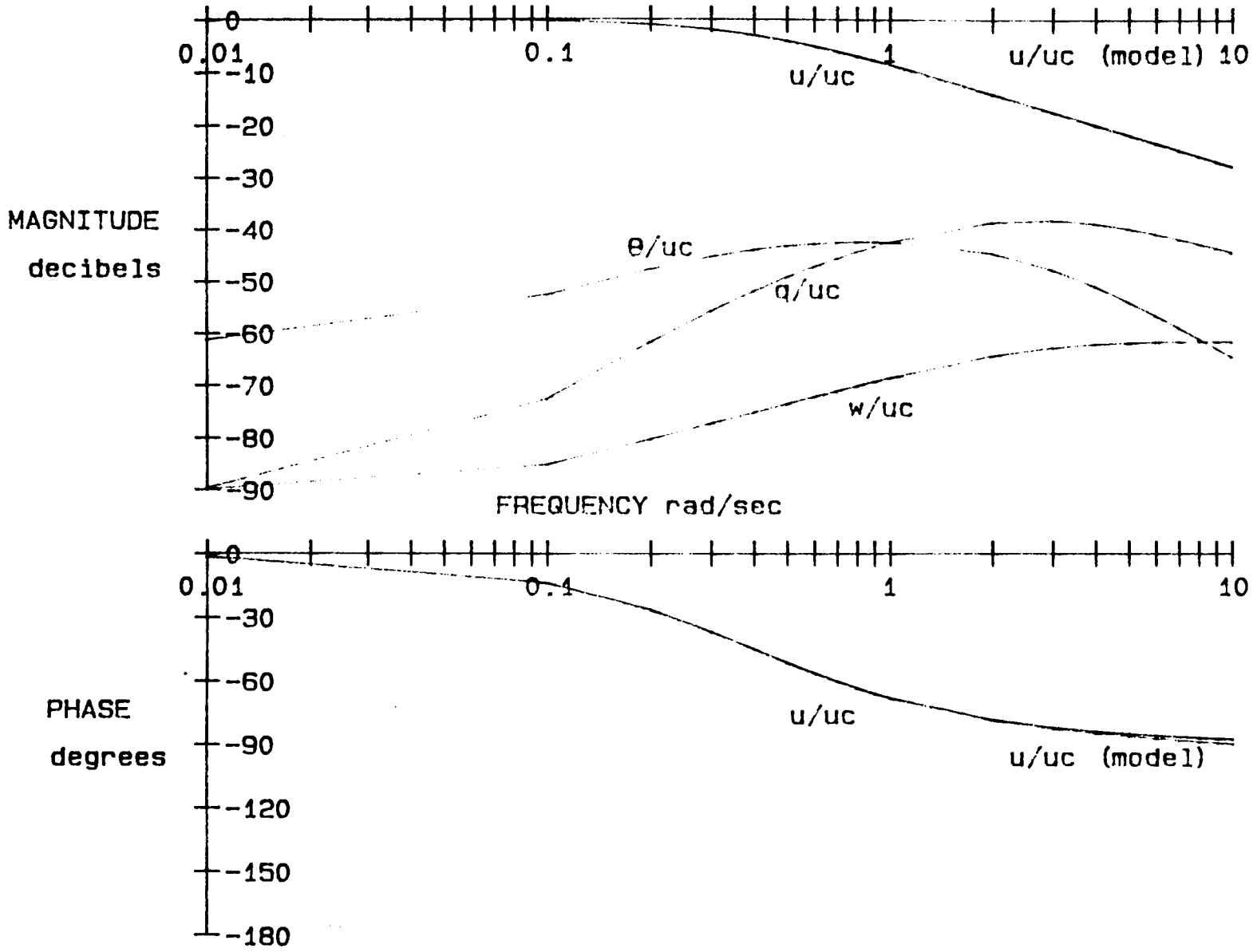

Figure 6-13

Explicit Controller: Hover, Aux Prop ON, u-command frequency response

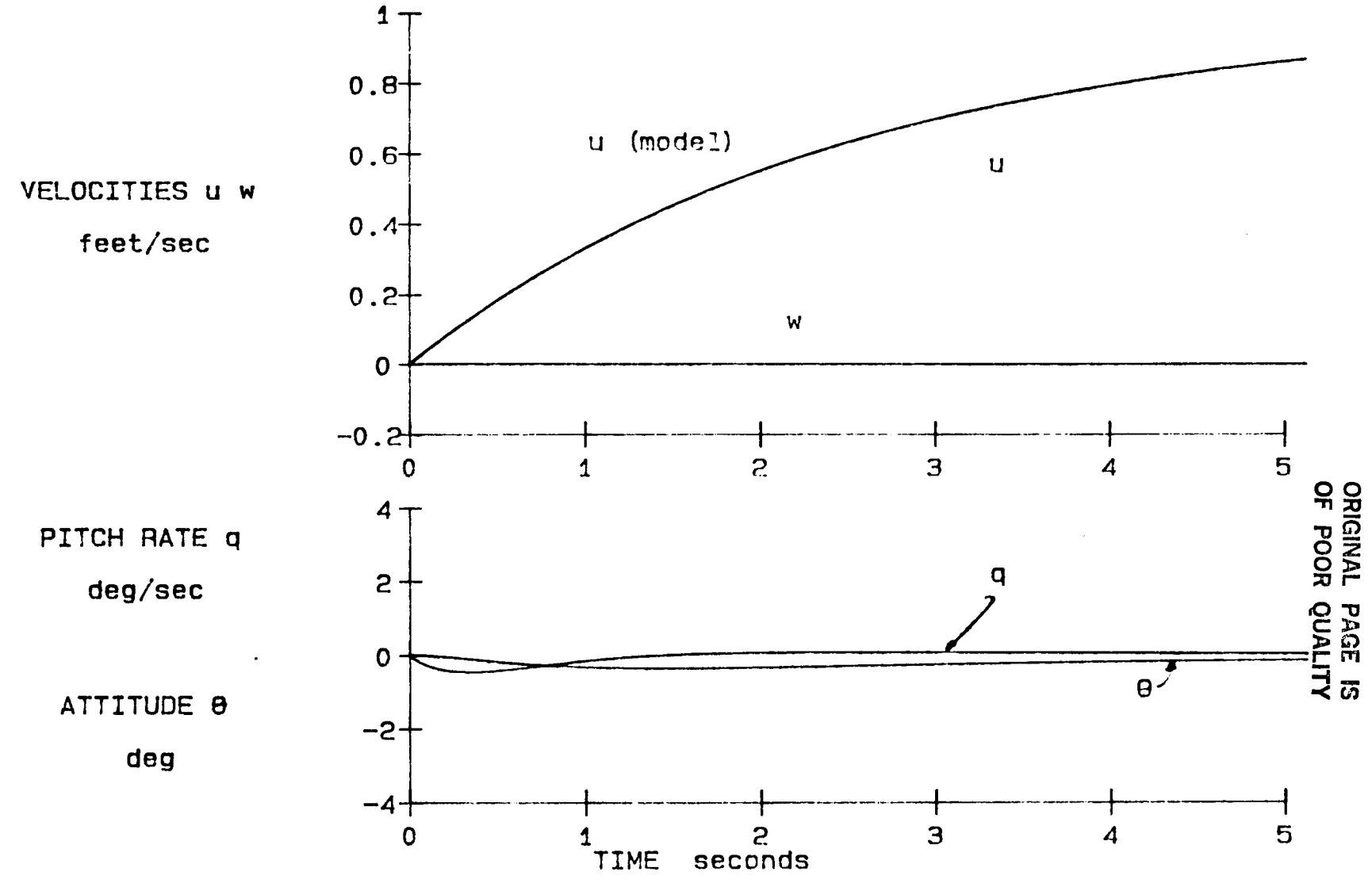

Figure 6-14

Explicit Controller: Hover, Aux Prop ON, u-command step response

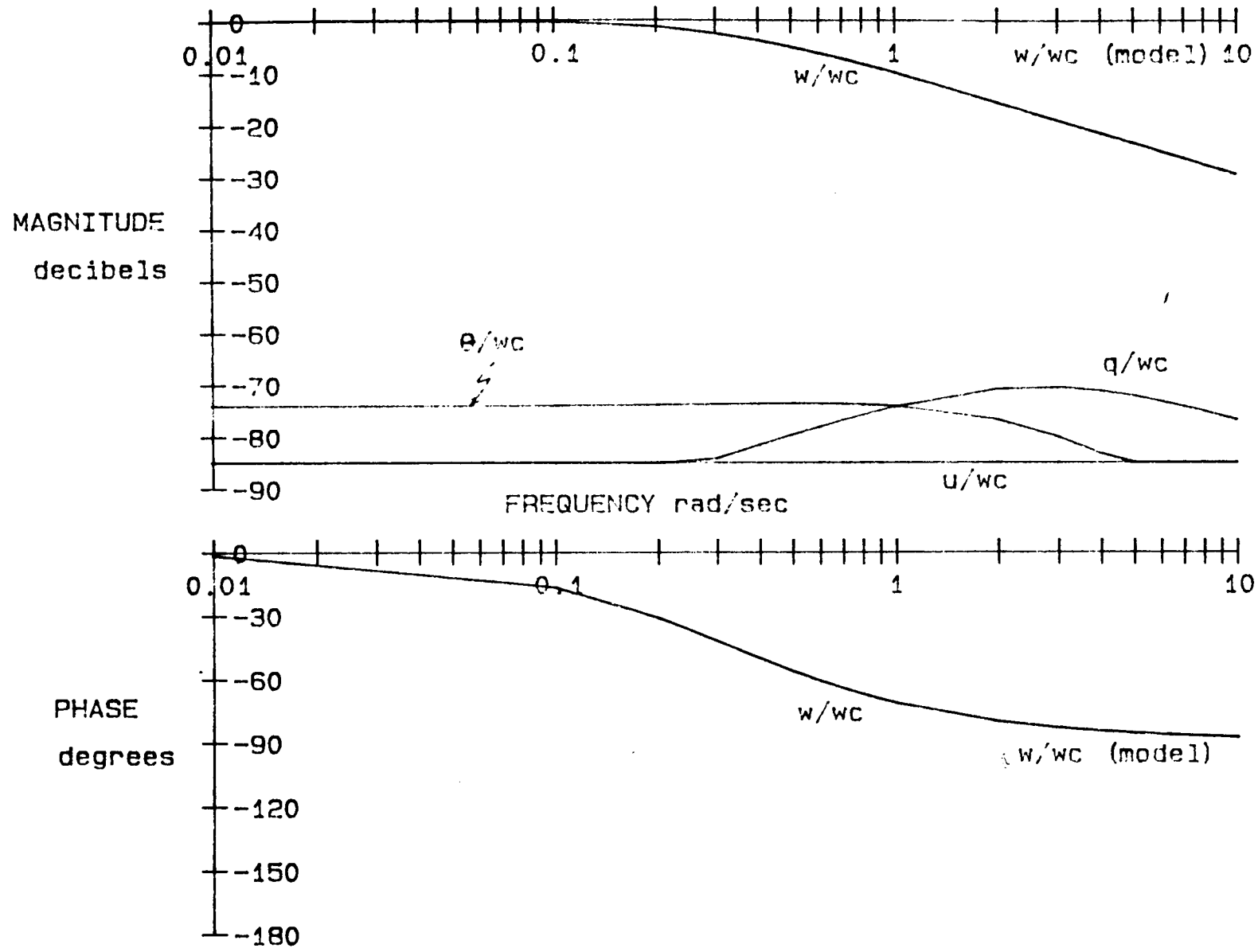

Figure 6-15

Explicit Controller: Hover, Aux Prop ON, w-command frequency response

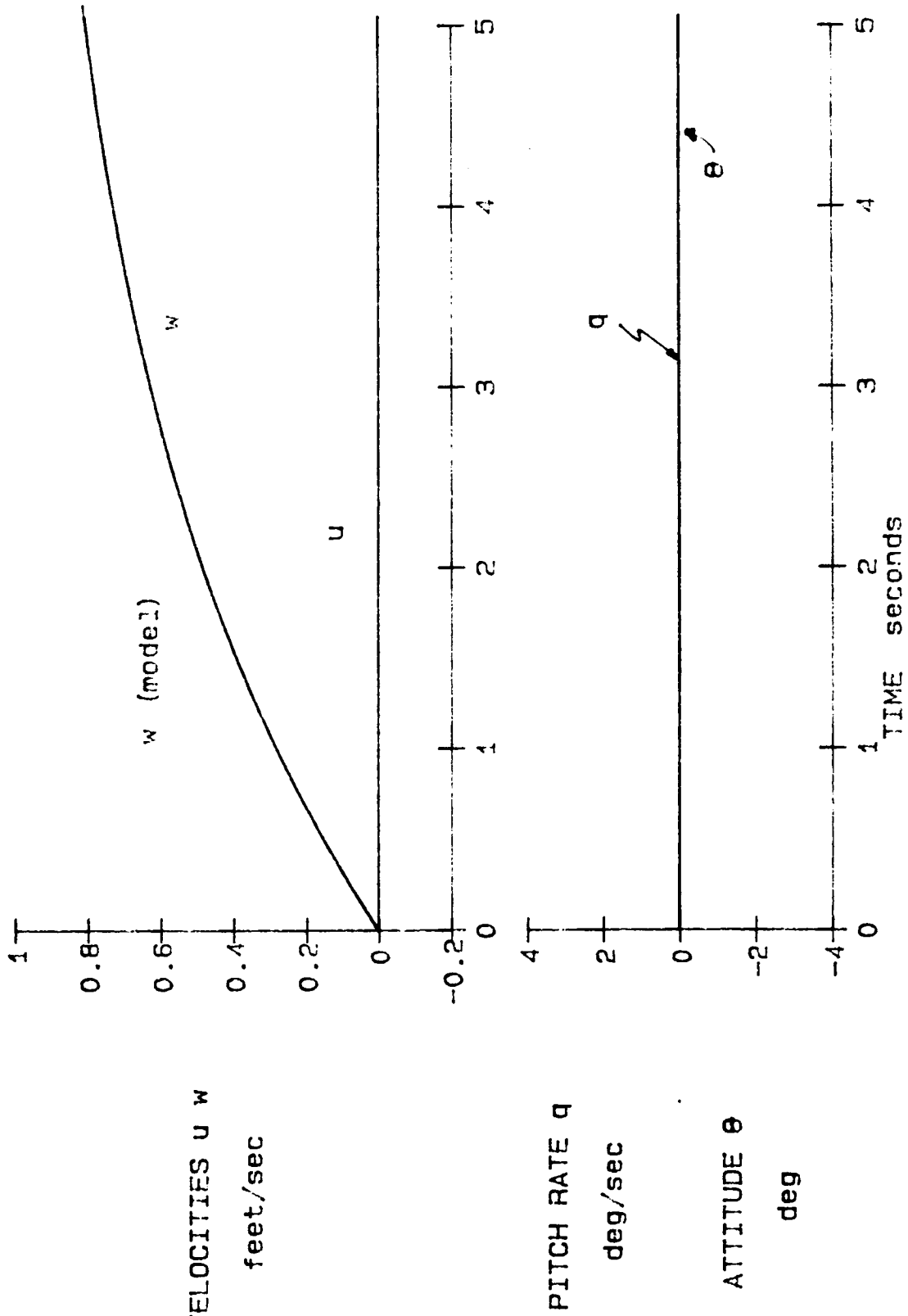

Explicit Controller: Hover, Aux Prop ON, w-command step response

Figure 6-16

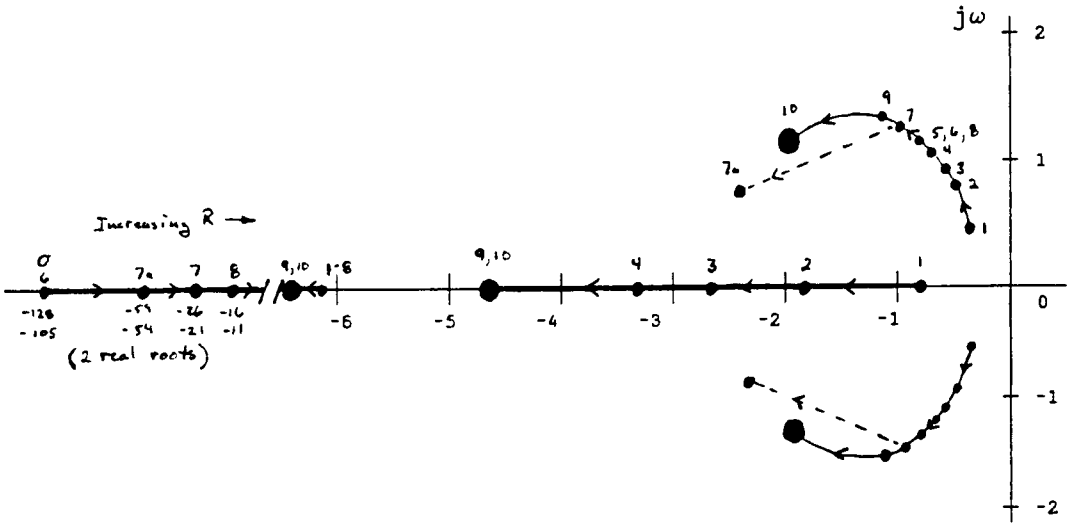

Figure 6-17: Root Loci versus Q and R for Explicit Controller (auxiliary propulsion installed)
Numbers refer to the pairs of Q and R matrices.
"x" denotes the helicopter's open-loop roots.

Q and R matrices:

1 $\begin{bmatrix} 1 & 0 & 0 & 0 \\ 0 & 500 & 0 & 0 \\ 0 & 0 & 0 & 0 \\ 0 & 0 & 0 & 0 \end{bmatrix}$ $\begin{bmatrix} 2000 & 0 & 0 \\ 0 & 2000 & 0 \\ 0 & 0 & 2000 \end{bmatrix}$

2 $\begin{bmatrix} 500 & 0 & 0 & 0 \\ 0 & 500 & 0 & 0 \\ 0 & 0 & 0 & 0 \\ 0 & 0 & 0 & 0 \end{bmatrix}$ $\begin{bmatrix} 2000 & 0 & 0 \\ 0 & 2000 & 0 \\ 0 & 0 & 2000 \end{bmatrix}$

3 $\begin{bmatrix} 1500 & 0 & 0 & 0 \\ 0 & 500 & 0 & 0 \\ 0 & 0 & 0 & 0 \\ 0 & 0 & 0 & 0 \end{bmatrix}$ $\begin{bmatrix} 2000 & 0 & 0 \\ 0 & 2000 & 0 \\ 0 & 0 & 2000 \end{bmatrix}$

4 $\begin{bmatrix} 3000 & 0 & 0 & 0 \\ 0 & 500 & 0 & 0 \\ 0 & 0 & 0 & 0 \\ 0 & 0 & 0 & 0 \end{bmatrix}$ $\begin{bmatrix} 2000 & 0 & 0 \\ 0 & 2000 & 0 \\ 0 & 0 & 2000 \end{bmatrix}$

5 $\begin{bmatrix} 10000 & 0 & 0 & 0 \\ 0 & 500 & 0 & 0 \\ 0 & 0 & 0 & 0 \\ 0 & 0 & 0 & 0 \end{bmatrix}$ $\begin{bmatrix} 2000 & 0 & 0 \\ 0 & 2000 & 0 \\ 0 & 0 & 2000 \end{bmatrix}$

6 $\begin{bmatrix} 10000 & 0 & 0 & 0 \\ 0 & 500 & 0 & 0 \\ 0 & 0 & 0 & 0 \\ 0 & 0 & 0 & 0 \end{bmatrix}$ $\begin{bmatrix} 5 & 0 & 0 \\ 0 & 5 & 0 \\ 0 & 0 & 5 \end{bmatrix}$

7 $\begin{bmatrix} 10000 & 0 & 0 & 0 \\ 0 & 500 & 0 & 0 \\ 0 & 0 & 0 & 0 \\ 0 & 0 & 0 & 0 \end{bmatrix}$ $\begin{bmatrix} 50 & 0 & 0 \\ 0 & 50 & 0 \\ 0 & 0 & 50 \end{bmatrix}$

7a $\begin{bmatrix} 10000 & 0 & 0 & 0 \\ 0 & 500 & 0 & 0 \\ 0 & 0 & 0 & 0 \\ 0 & 0 & 0 & 0 \end{bmatrix}$ $\begin{bmatrix} 50 & 0 & 0 \\ 0 & 50 & 49 \\ 0 & 49 & 50 \end{bmatrix}$

8 $\begin{bmatrix} 10000 & 0 & 0 & 0 \\ 0 & 500 & 0 & 0 \\ 0 & 0 & 0 & 0 \\ 0 & 0 & 0 & 0 \end{bmatrix}$ $\begin{bmatrix} 200 & 0 & 0 \\ 0 & 200 & 0 \\ 0 & 0 & 200 \end{bmatrix}$

9 $\begin{bmatrix} 10000 & 0 & 0 & 0 \\ 0 & 500 & 0 & 0 \\ 0 & 0 & 0 & 0 \\ 0 & 0 & 0 & 0 \end{bmatrix}$ $\begin{bmatrix} 2000 & 0 & 0 \\ 0 & 2000 & 1000 \\ 0 & 1000 & 2000 \end{bmatrix}$

10 $\begin{bmatrix} 10000 & 0 & 0 & 0 \\ 0 & 500 & 0 & 0 \\ 0 & 0 & 0 & 0 \\ 0 & 0 & 0 & 0 \end{bmatrix}$ $\begin{bmatrix} 2000 & 0 & 0 \\ 0 & 2000 & 1800 \\ 0 & 1800 & 2000 \end{bmatrix}$

Chapter VII

SELECTED NOE TRAJECTORIES

Three representative longitudinal NOE maneuvers are defined in this chapter. The optimal control input histories for each maneuver are determined using the trajectory optimization algorithm. These trajectories, or maneuvers, are used in Chapter VIII to evaluate the controllers developed in Chapter VI, and to evaluate the use of longitudinal auxiliary propulsion.

The collective and longitudinal cyclic ranges of stick travel for the AH-1G are [1]:

θ_c: 0 to 10.7 inches $\quad\quad$ B_{1s}: -7.5 to 5.7 inches

7.1 Pop-up/Dash/Descent

This maneuver, shown in Figure 7-1 is employed primarily when moving from one hiding point to the next. For example, the helicopter, hidden by tree cover, ascends above tree height, dashes across the tree-tops, and descends back to hover in a new clearing. The maneuver is done in minimal time.

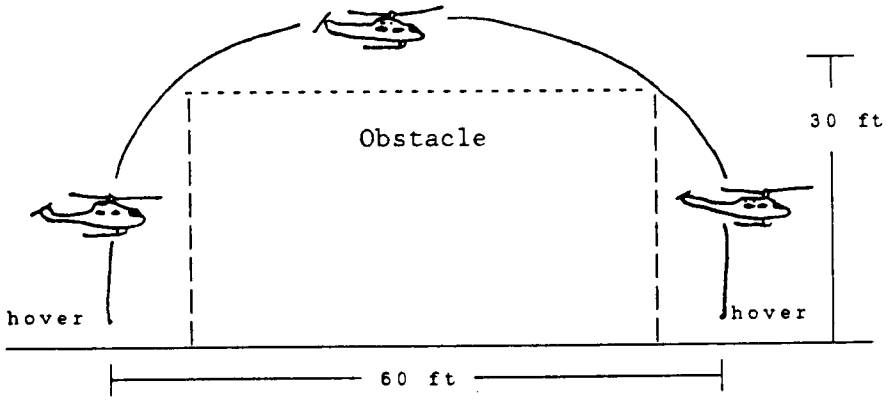

Figure 7-1

With auxiliary propulsion installed, the minimum time in which the maneuver can be effectively completed is 4.6 seconds. Table 7-1 shows the specified values of the states at the interior and final point times, the trim states, the available control power at this trim condition, and the cost function weighting matrices. The specified control values (of the controls in the augmented state vector) at interior and final points are arbitrary since the corresponding weighting elements are zero; the weights *must* be zero since we do not want to penalyze control excursions.

interior and final points

time sec	u ft/s	w ft/s	q deg/s	θ deg/s	θ_c in	B1 in	T in	ΔX ft	ΔY** ft	[aux prop off,on]
1.25,1.25	0	0	0	0	0	0	0	0	30	
4.80,3.60	0	0	0	0	0	0	0	60	30	
5.90,4.60	0	0	0	0	0	0	0	60	0	

trim conditions

U_o ft/s	W_o ft/s	Q_o deg/s	θ_o deg	$\theta^*_{c_o}$ in	$B^*_{1s_o}$ in	T^*_o in	X_o ft	Y_o ft
1.69	-0.02	0	-0.73	5.3	-.39	0	0	10

cost function weighting matrices

state: diag [0 0 400 400 0 0 0 0 0]

control: diag [1 1 1]

state-control: null matrix

interior point weighting matrices

diag [150 0 400 400 0 0 0 150 150]

final point weighting matrix

diag [150 150 400 400 0 0 0 150 150]

control power (inches)

θ_c: -5.3, +5.4 B_{1s}: -7.1, +6.1 T: -5, +5

*θ_{c_o} and B_{1s_o} refer to stick trim; corresponding swashplate trim angles are 14.83 and -.76 degrees.

**ΔY is defined positive upward

Table 7-1

Figures 7-3, 7-4, and 7-5 show the spatial position and position histories, velocities, and control inputs for a conventional helicopter performing the pop-up maneuver. Figures 7-6, 7-7, and 7-8 show the same plots for the auxiliary propulsion equipped helicopter.

Auxiliary propulsion is a major advantage in this type of maneuver. The conventionally equipped helicopter has large nose-down attitudes; after one second of vertical climb, the helicopter pitches nose down to accelerate; the attitude returns to trim during deceleration (Figure 7-4). The path that the helicopter takes during the second half of its trajectory is not as square as it is for the augmented helicopter. "Cutting the corner" off this path is necessary to avoid excessively high pitch attitudes. If a more square path is desired, the forward speed of the helicopter must be further reduced before descending; this will, of course, increase the total time to complete the maneuver.

This maneuver is a high agility task. As one expects, we find that the stick motions span their entire ranges (Figures 7-5 and 7-8). Comparing these two figures shows the impact of the auxiliary thruster. For the conventional helicopter, the longitudinal cyclic saturates at its maximum during the dash, and then is pulled back strongly for the deceleration. For the auxiliary thrusted helicopter, the thruster saturates for acceleration and deceleration, and the amount of cyclic is reduced. The collective saturates for the thrusted helicopter because the maneuver is performed more quickly.

The pitch attitude for the conventional helicopter is more extreme than for the augmented helicopter. The pitch rates for

both cases are understandably high, but fall within the acceptable limit of 0.69 rad/sec^2: 0.56 for the conventional helicopter, and 0.49 for the augmented helicopter.

7.2 Bob-up at 40 knots

The bob-up entails "hurdling" an object while flying at a moderate to high speed, as shown in Figure 7-2.

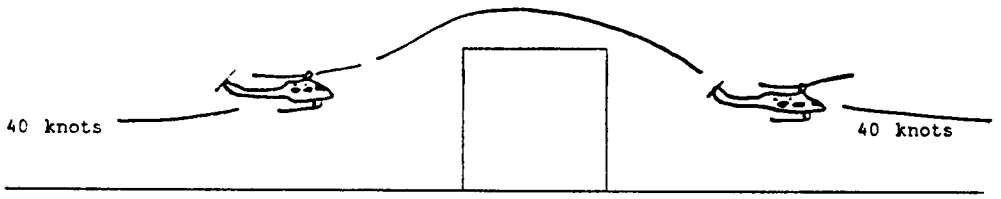

Figure 7-2

Table 7-2 specifies the geometry and flying qualities for this maneuver. Both the conventional and auxiliary-equipped missions are accomplished in 2.5 seconds.

interior and final points

time sec [aux prop off,on]	u ft/s	w ft/s	q deg/s	θ deg/s	θ_c in	Bls in	T in	ΔX ft	ΔY ** ft
1.0 ,1.0	0	0	0	0	0	0	0	0	20
1.5 ,1.5	0	0	0	0	0	0	0	0	20
2.5 ,2.5	0	0	0	0	0	0	0	0	0

trim conditions

U_o	W_o	Q_o	θ_o	$\theta^*_{c_o}$	$B^*_{1s_o}$	T^*_o	X_o	Y_o
ft/s	ft/s	deg/s	deg	in	in	in	ft	ft
67.48	-2.13	0	-1.81	3.75	-.04	0	0	10

cost function weighting matrices

state: diag [150 0 400 400 0 0 0 150 0]

control: diag [1 1 1]

state-control: null matrix

interior point weighting matrices

diag [150 0 400 400 0 0 0 150 150]

final point weighting matrix

diag [150 150 400 400 0 0 0 150 150]

control power (inches)

θ_c: -3.7, +10.0 B_{1s}: -7.5, +5.7 T: -5, +5

*θ_{c_o} and B_{1s_o} refer to stick trim; corresponding swashplate trim angles are 12.77 and -.10 degrees.

**ΔY is defined positive upward

Table 7-2

Figures 7-9, 7-10, and 7-11 show the spatial position and

position histories, velocities, and control inputs for a conventional helicopter performing the bob-up maneuver. Figures 7-12, 7-13, and 7-14 show the same plots for the auxiliary propulsion-equipped helicopter.

Both the conventional and augmented helicopter were constrained to remain very near their trimmed horizontal velocity; this was effectively accomplished. The use of auxiliary propulsion decreases the amount of cyclic required; therefore, the pitch attitude for the augmented helicopter at the end of the maneuver is slightly less than the attitude for the conventional helicopter (the attitudes are well within the acceptable range). In either case, the pilot would have to reduce the pitch attitude at the end of the maneuver (alternatively, we could have weighted the constraint on the final pitch attitude more heavily). There is no time advantage in using auxiliary propulsion here. There is a slight advantage in reducing the pitching motion during the maneuver.

In both cases, the vertical velocity, W, is almost perfectly symmetric about its trim level over the interval, that is, it increases smoothly then decreases smoothly back to trim. The collective is increased, then decreased below its trim value to retard the vertical ascent, then increased above trim for the final half second to slow the descent speed to zero.

The maximum pitch rate never exceeds the 0.69 rad/sec^2 limit; the maximum rates (absolute value) are 0.27 and 0.4 rad/sec^2 for the conventional and augmented helicopter, respectively.

7.3 Glideslope

The glideslope is typically associated with descending from a moderate to high-speed cruise at an altitude of several hundred feet to a near-earth hover. The glideslope to ship deck landing is a common trajectory employing the glideslope. This study uses a very simplified glideslope. No particular glideslope path or angle is specified; the maneuver simply requires transition from flight at 40 knots and 250 feet altitude to a near-earth hover 250 feet along the horizontal earth axis.

Table 7-3 specifies the geometry and flying qualities for this maneuver. Figures 7-15, 7-16, and 7-17 show the spacial position and position histories, velocities, and control inputs for a conventional helicopter performing the glideslope maneuver. Figures 7-18, 7-19, and 7-20 show the same plots for the auxiliary propulsion equipped helicopter.

The advantage of using auxiliary propulsion is evident in trying to fly the glideslope in minimum time while not exceeding the pitch attitude limits. The maneuver takes one second longer for the conventional helicopter than for the augmented helicopter (7 versus 6 seconds), and the pitch attitude is worse. In fact, as can be seen in Figure 7-16, the nose-up pitch attitude for the conventional helicopter at the end of the glideslope is not favorable; it exceeds the 10° limit. The spacial histories are nearly identical, as are the translational velocities histories, so the thruster provides the ability to rapidly decelerate while maintaining satisfactory attitude.

The maximum absolute pitch rates over the trajectory are well within the allowable range, as should be expected. These values

are 0.22 and 0.17 rad/sec^2 for the conventional and augmented helicopter, respectively.

interior and final points

time	u	w	q	θ	θ_c	B1s	T	ΔX	ΔY**
sec	ft/s	ft/s	deg/s	deg/s	in	in	in	ft	ft
[aux prop off,on]									
7.0 ,6.0	-67.5	2.13	0	0	0	0	0	0	-250

trim conditions

U_o	W_o	Q_o	θ_o	$\theta^*_{c_o}$	$B^*_{1s_o}$	T^*_o	X_o	Y_o
ft/s	ft/s	deg/s	deg	in	in	in	ft	ft
67.48	-2.13	0	-1.81	3.75	-.04	0	0	250

cost function weighting matrices

state: diag [0 0 400 400 0 0 0 0 0]

control: diag [1 1 1]

state-control: null matrix

interior point weighting matrices

not applicable

final point weighting matrix

diag [150 150 400 400 0 0 0 150 150]

control power (inches)

θ_c: -3.7, +10.0 B_{1s}: -7.5, +5.7 T: -5, +5

*θ_{c_o} and B_{1s_o} refer to stick trim; corresponding swashplate trim angles are 12.77 and -.10 degrees.

**ΔY is defined positive upward

Table 7-3

7.4 Example of Path Evolution using the Trajectory Optimization

Figure 7-21 shows three "paths" during different stages of the trajectory optimization for the pop-up/dash/descent maneuver (with auxiliary propulsion). The initial control history yields a path that is very far from the desired trajectory. As the cost is minimized, the geometric specifications are met, as are the flying qualities criteria. The optimization of the other trajectories of this section converge similarly to their optimal path.

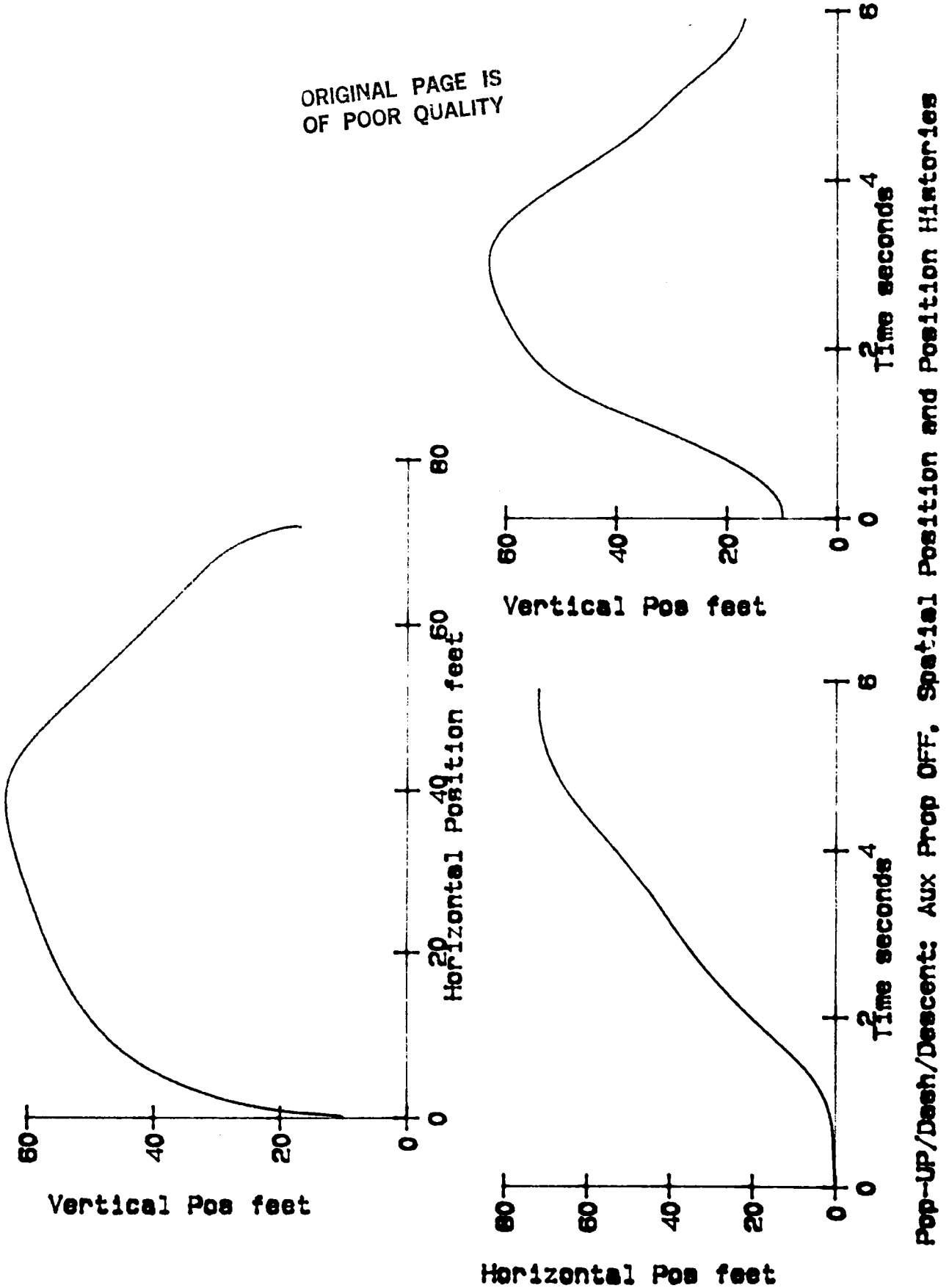

Figure 7-3

Figure 7-4

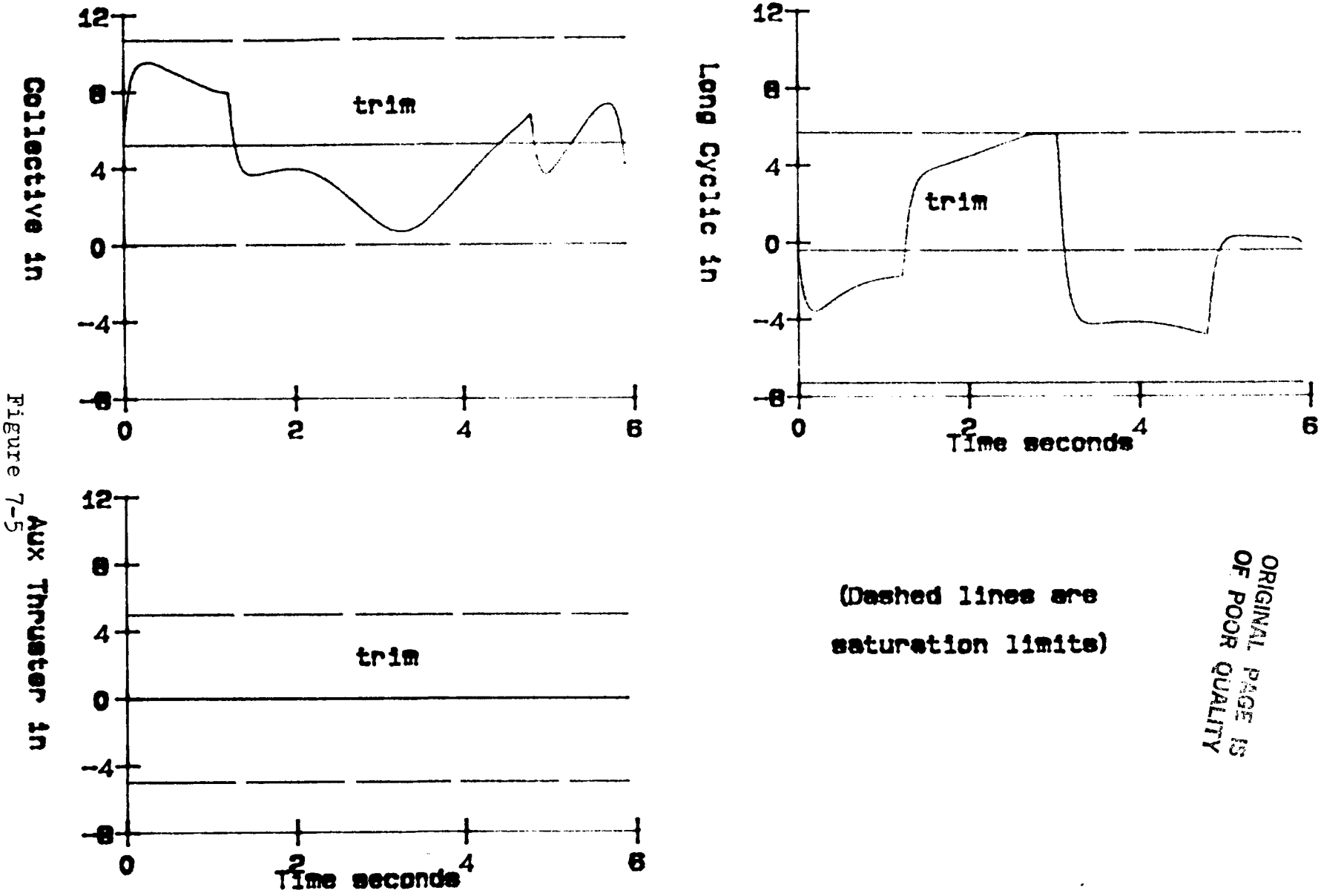

(Dashed lines are saturation limits)

Pop-up/Dash/Descent: Aux Prop OFF, Control Input Time Histories

Figure 7-5

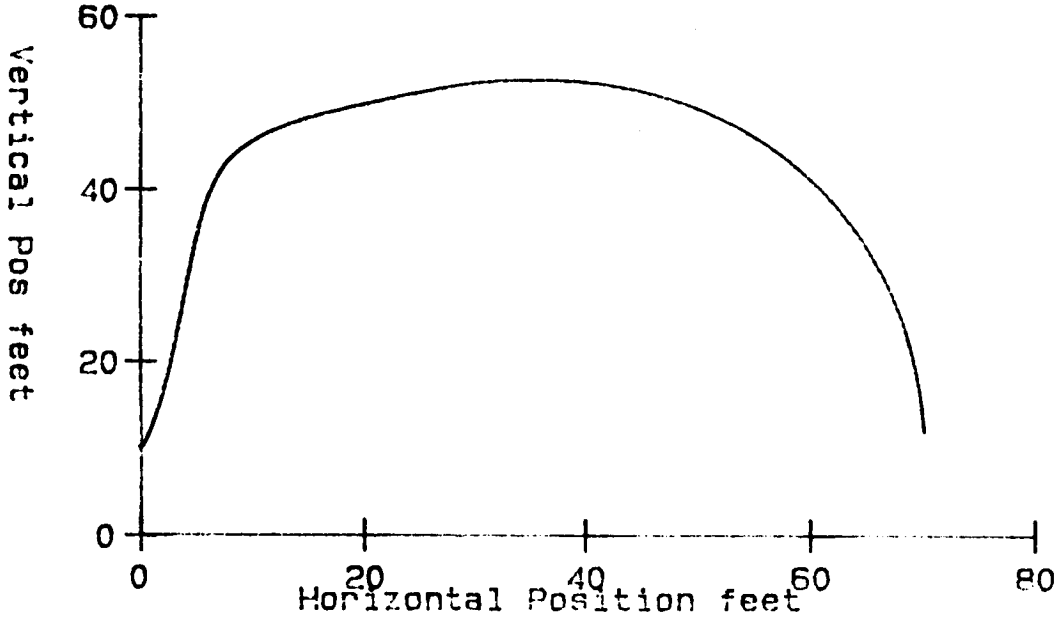

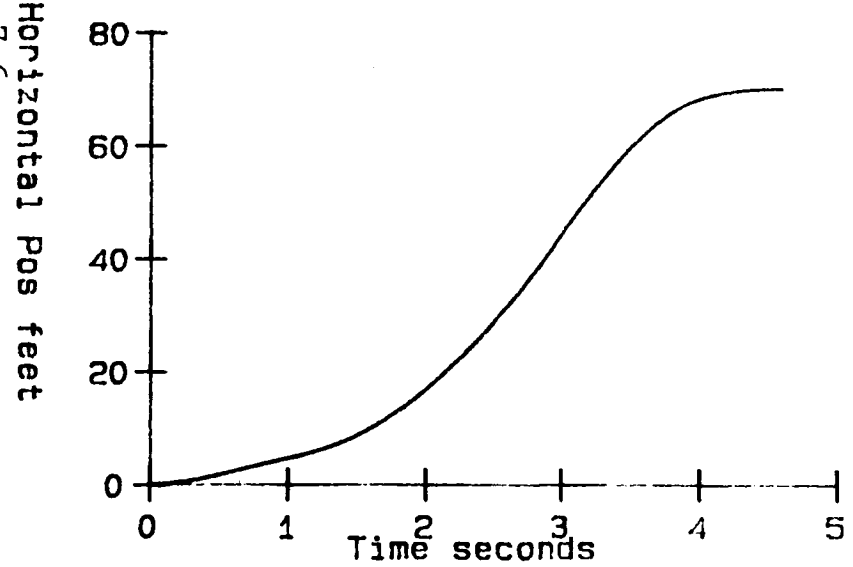

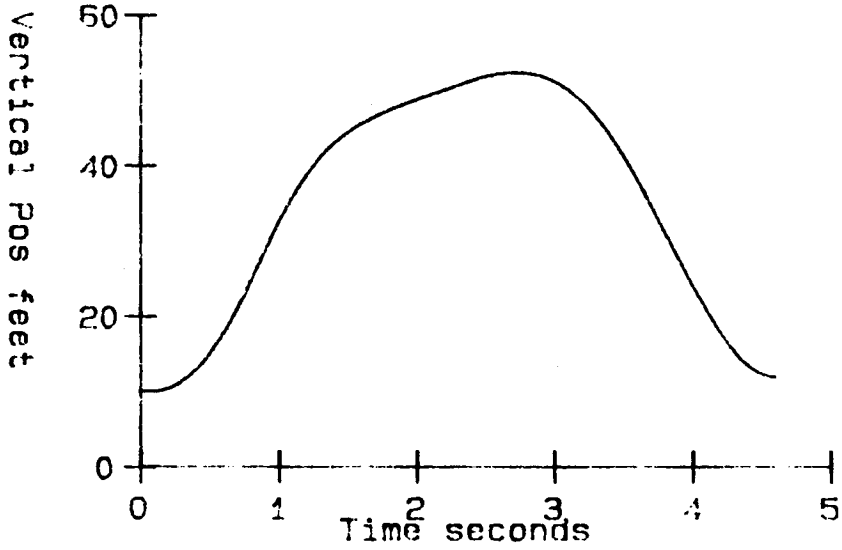

Figure 7-6
116

Pop-UP/Dash/Descent: Aux Prop ON, Spatial Position and Position Histories

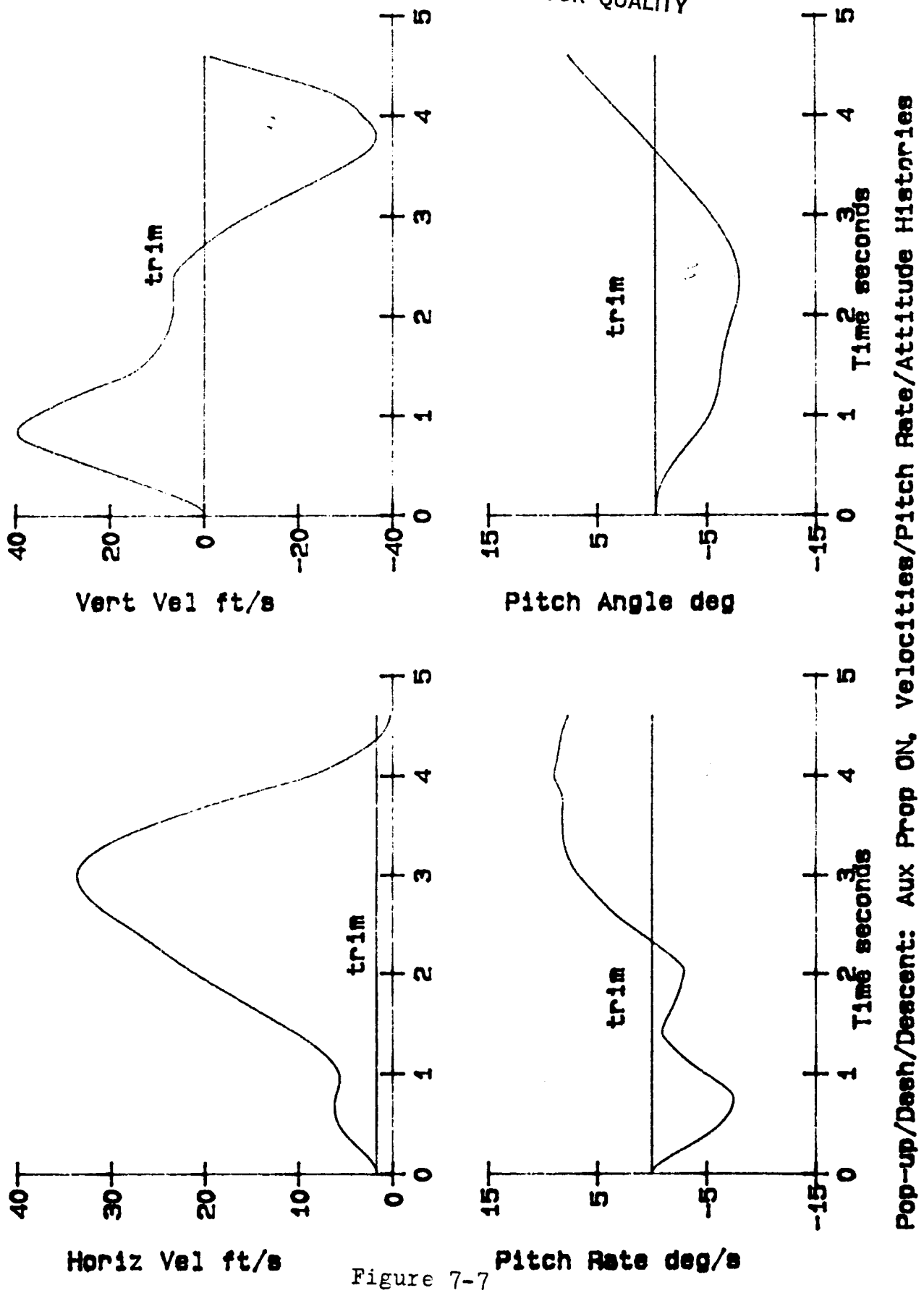

Figure 7-7

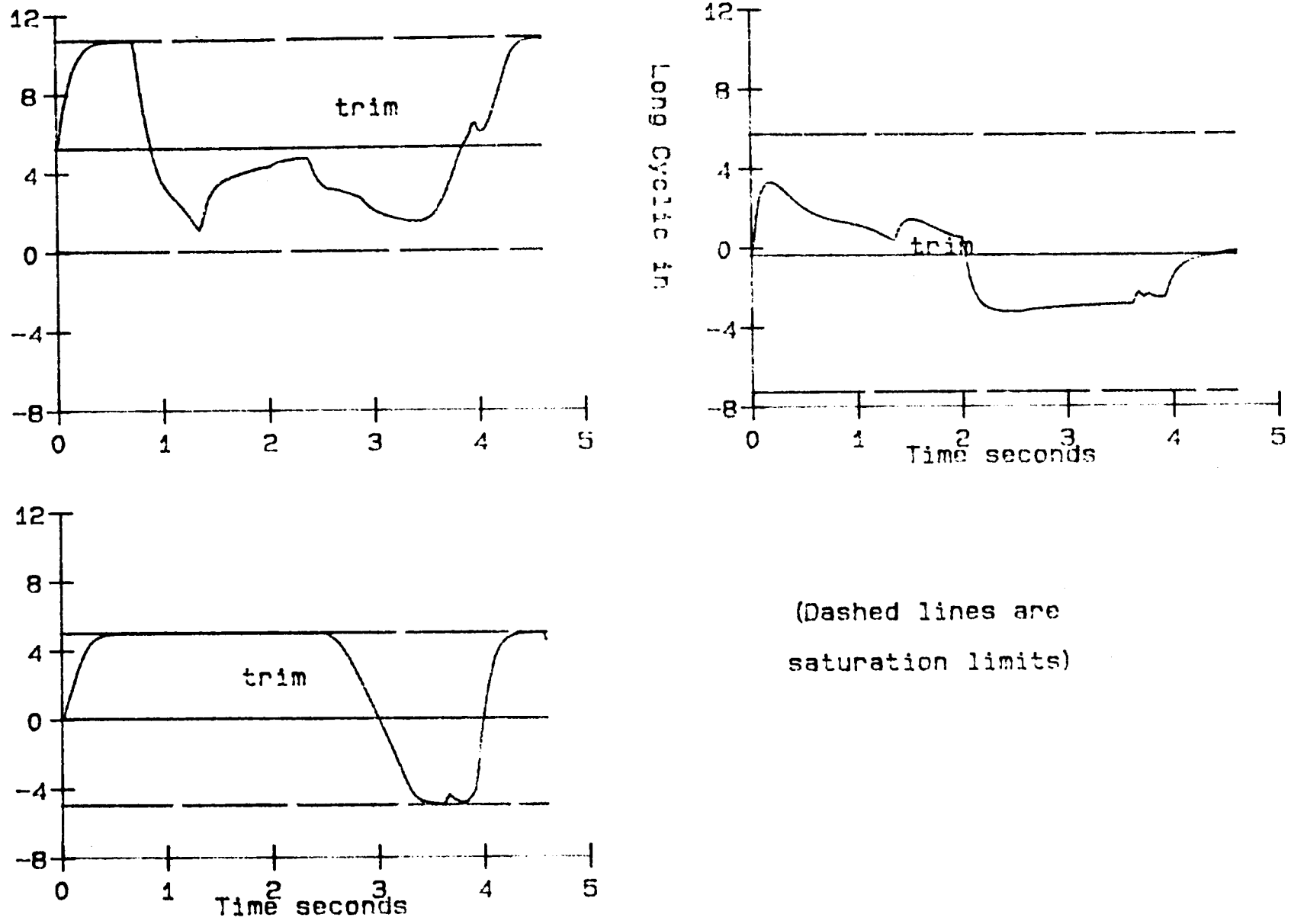

Figure 7-8
Pop-up/Dash/Descent: Aux Prop ON, Control Input Time Histories

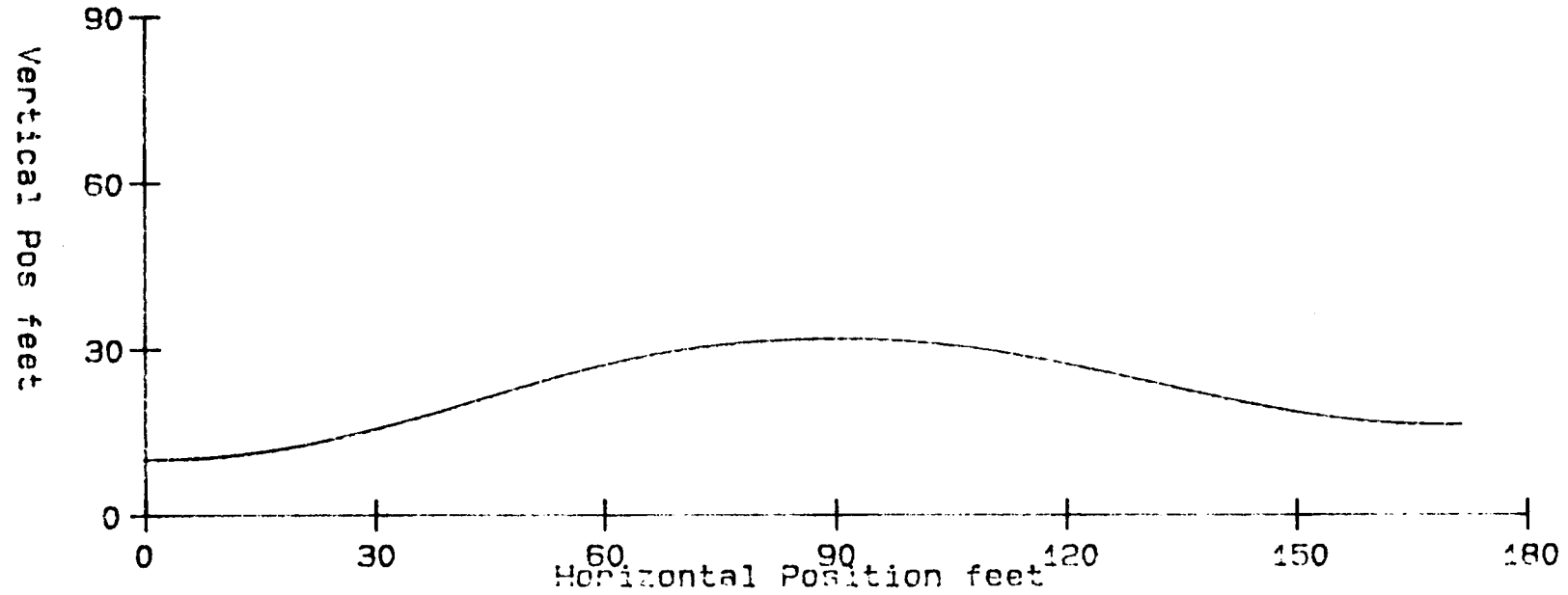

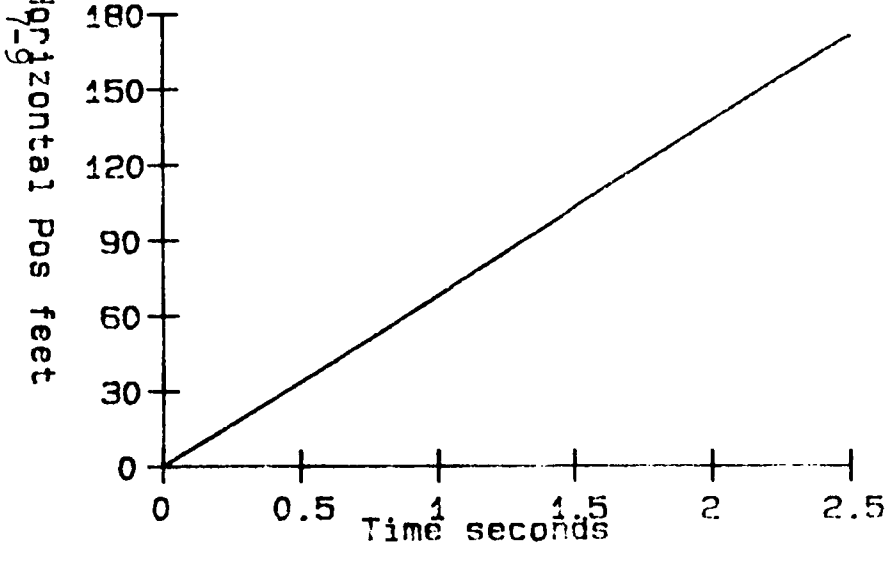

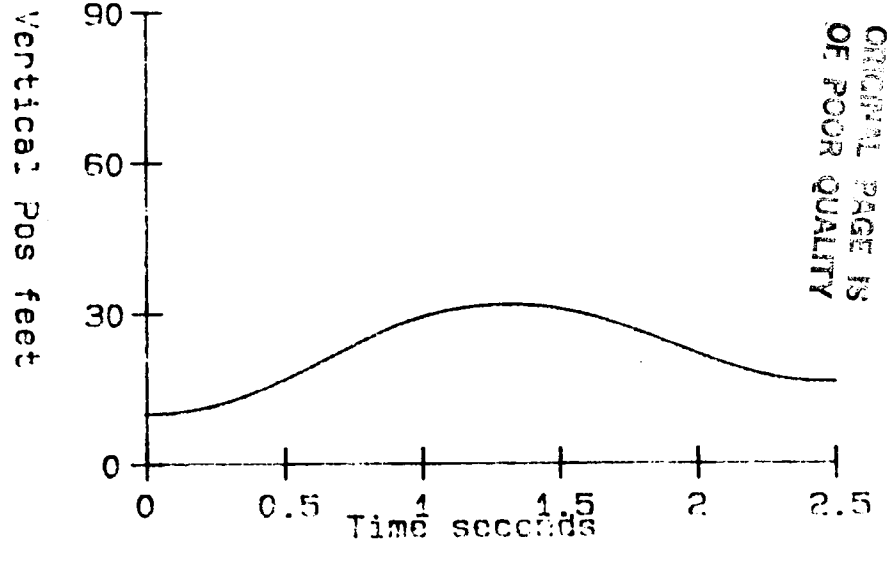

Figure 7-9
119

Bob-up at 40 knots: Aux Prop OFF, Spatial Position and Position Histories

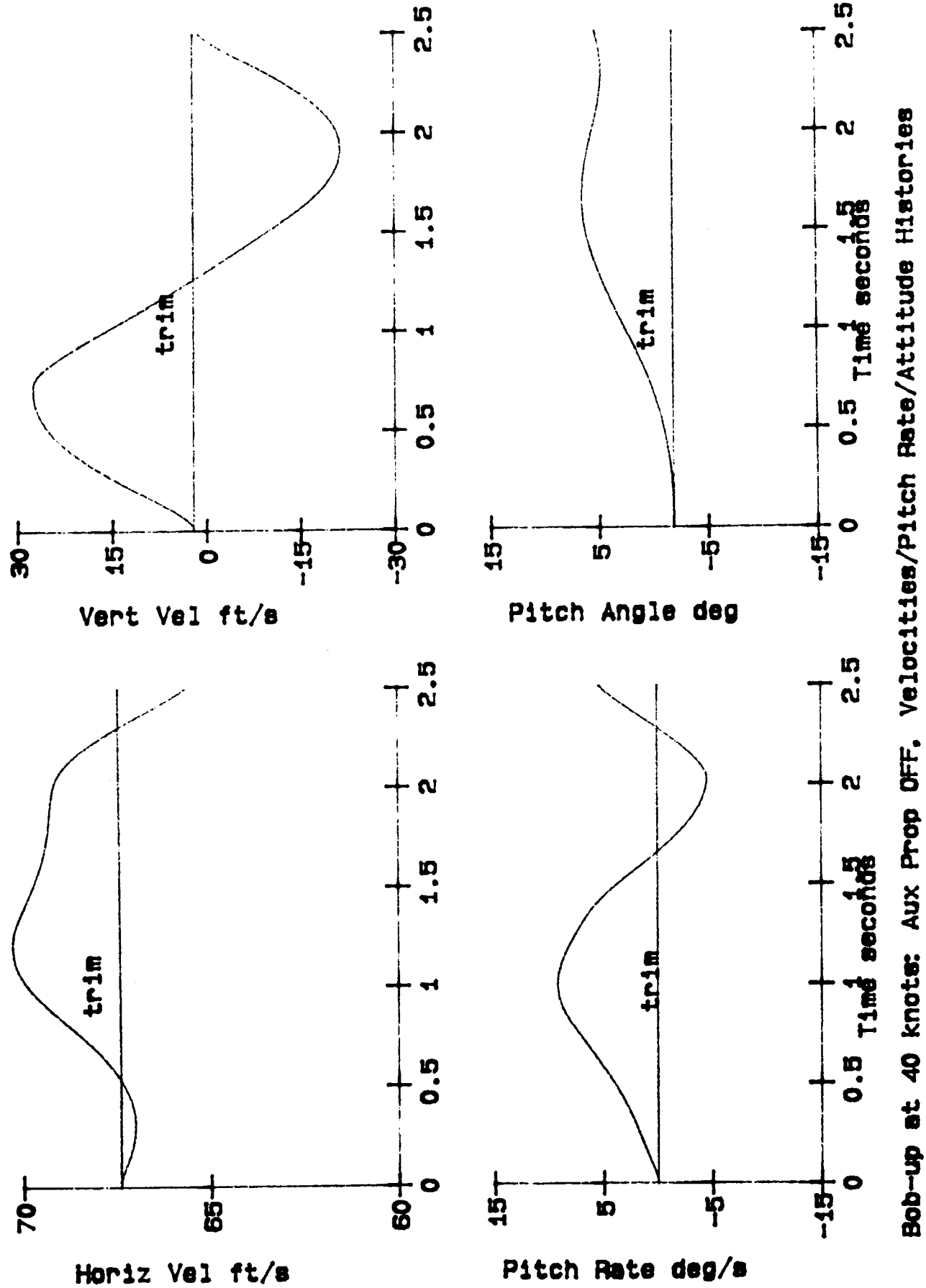

Bob-up at 40 knots: Aux Prop OFF. Velocities/Pitch Rate/Attitude Histories

Figure 7-10

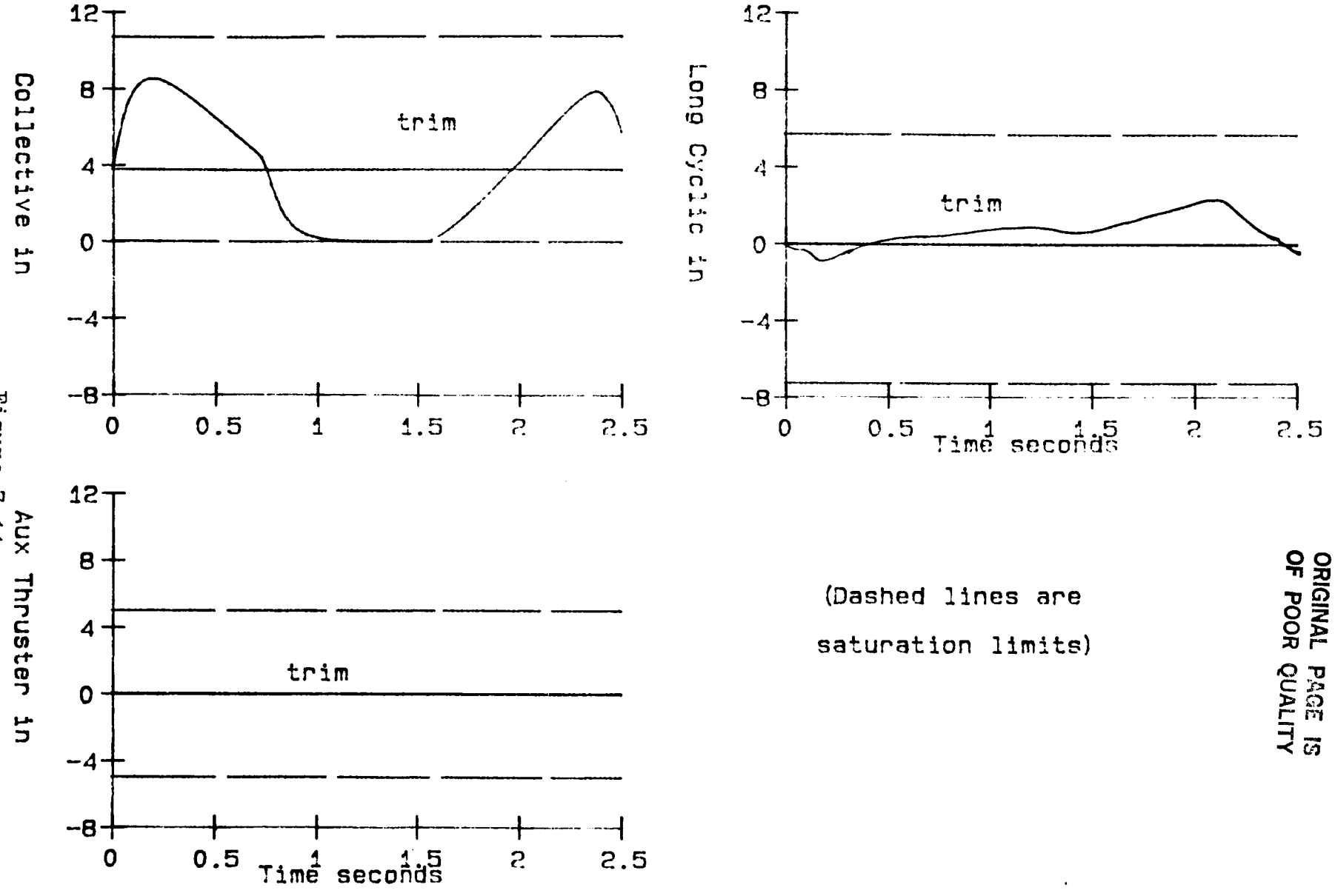

Figure 7-11

Bob-up at 40 knots: Aux Prop OFF, Control Input Time Histories

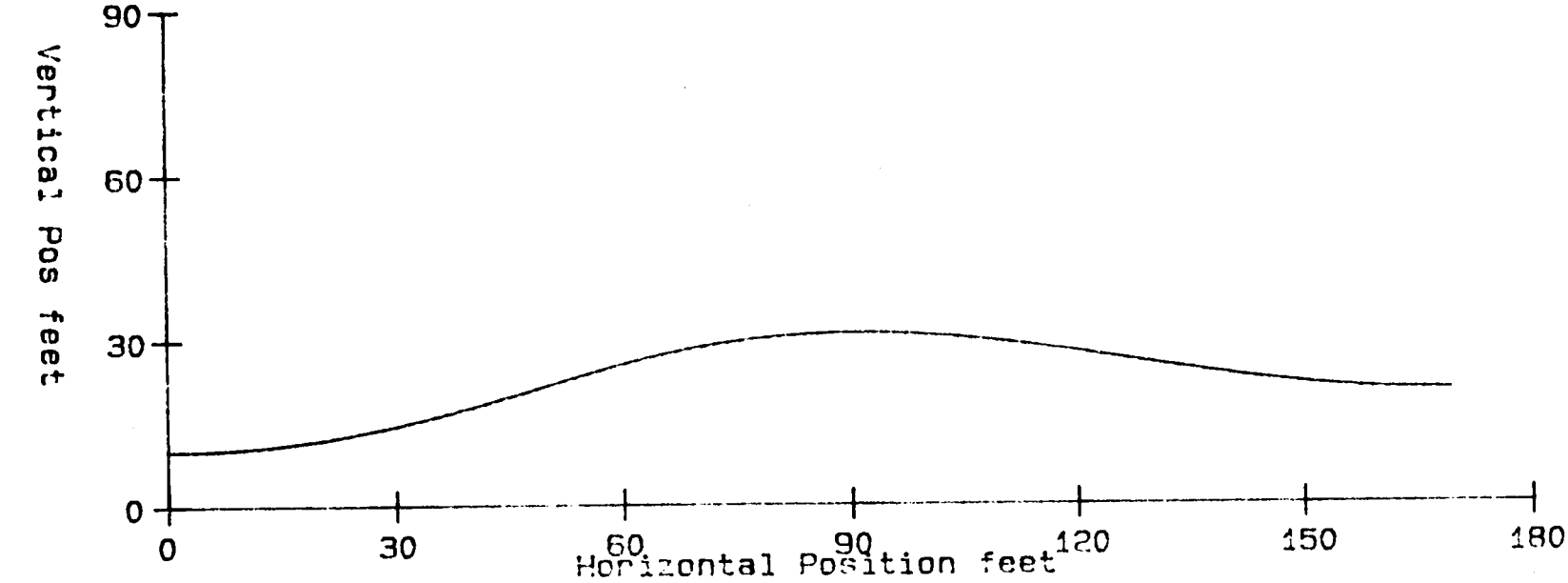

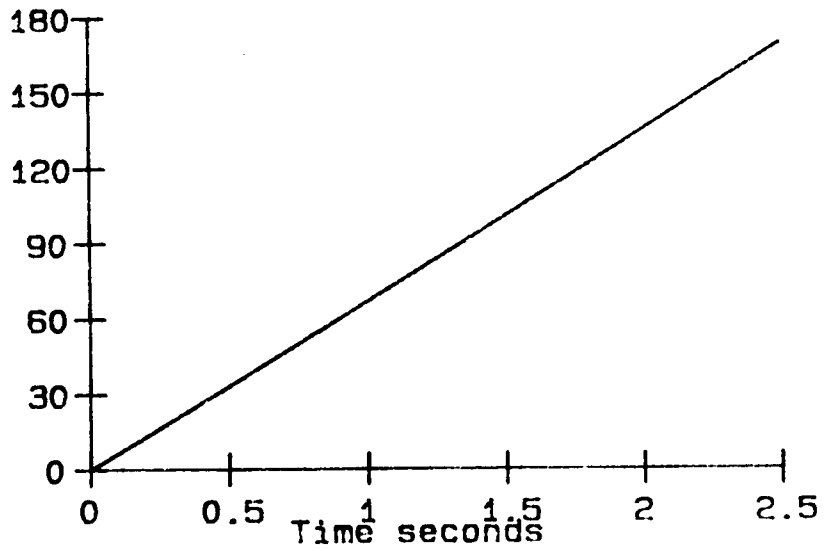

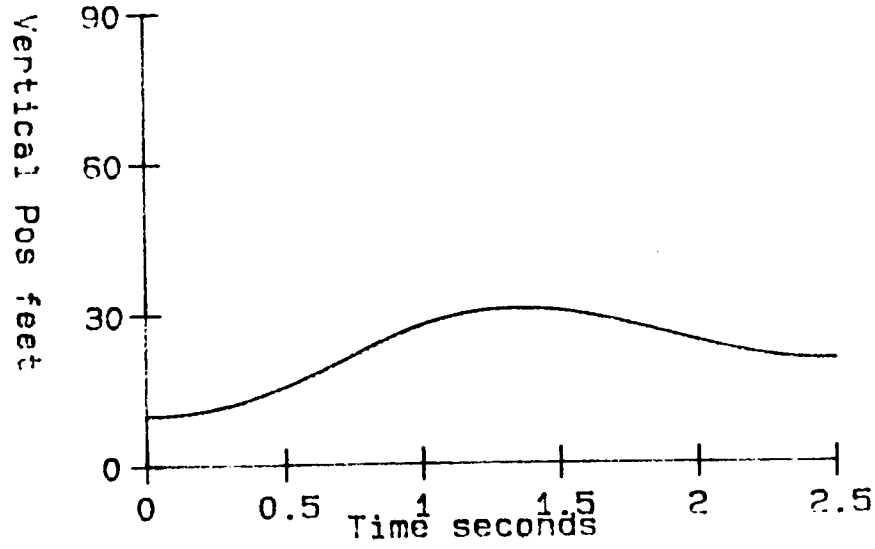

Figure 7-12
Bob-up at 40 knots: Aux Prop ON, Spatial Position and Position Histories

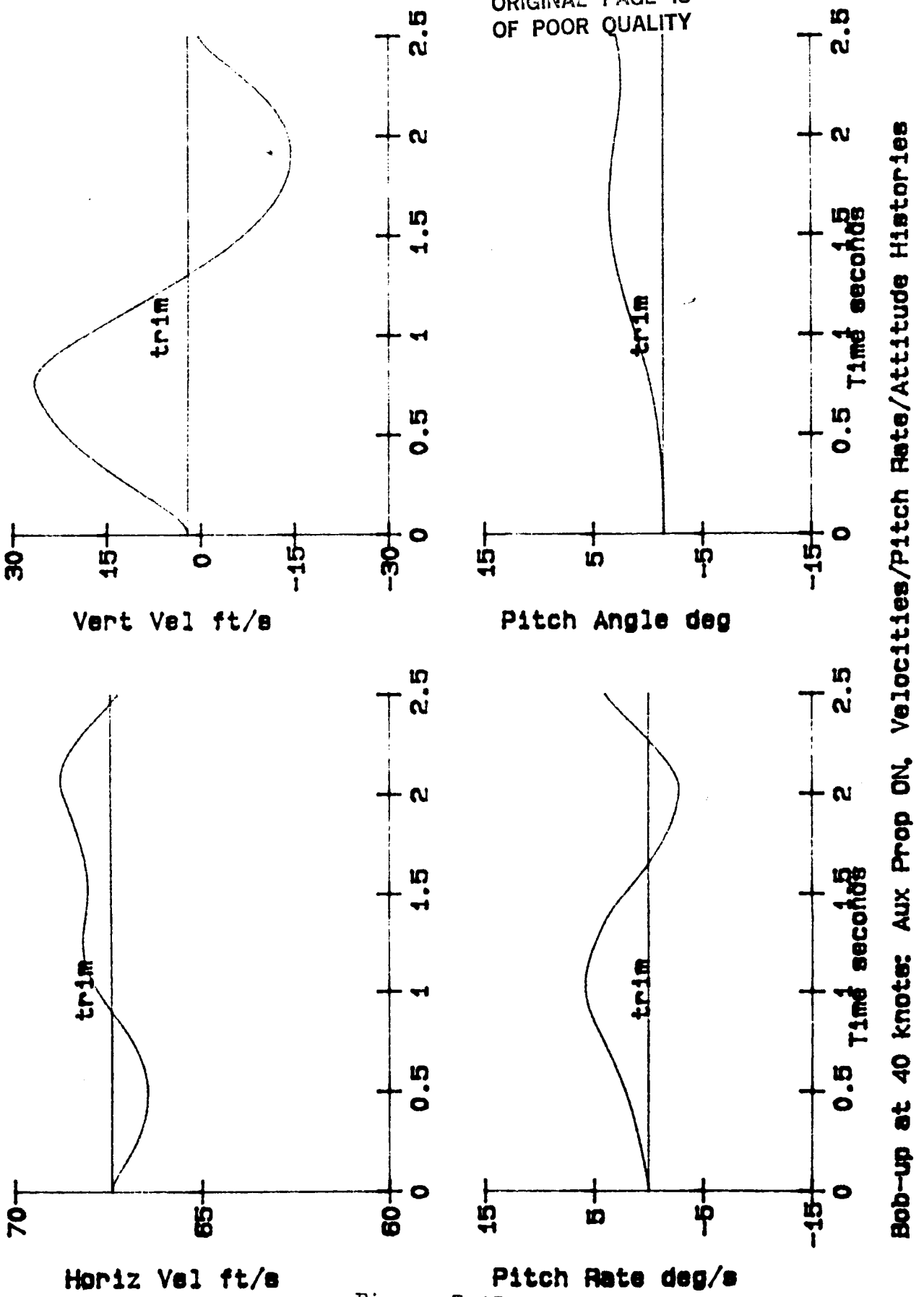

Figure 7-13

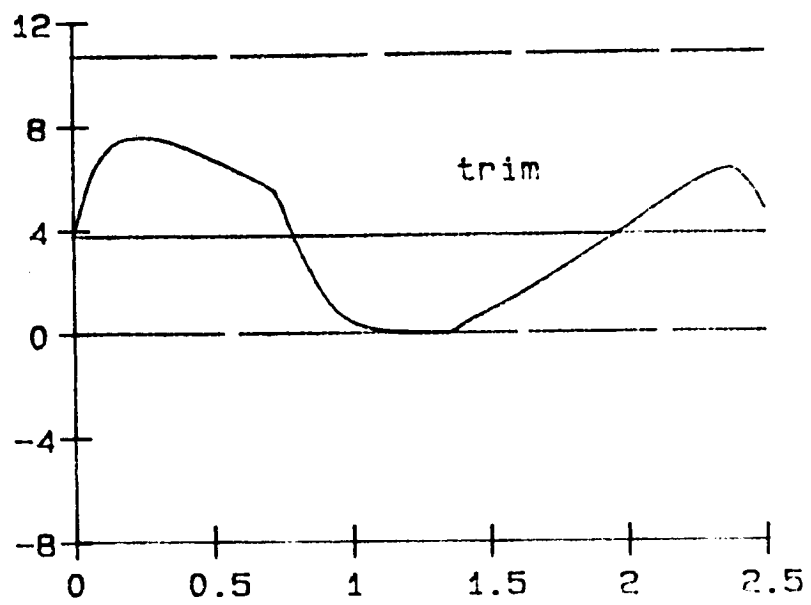

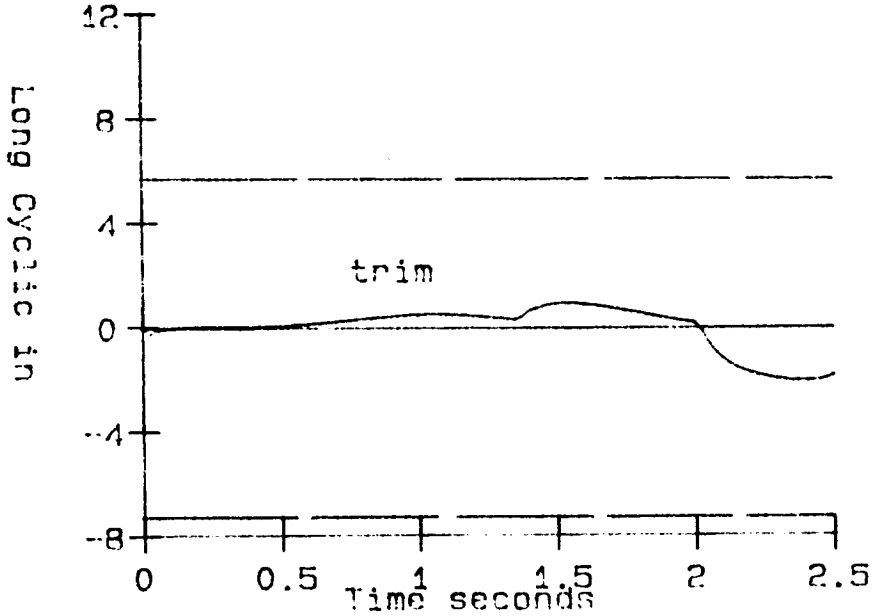

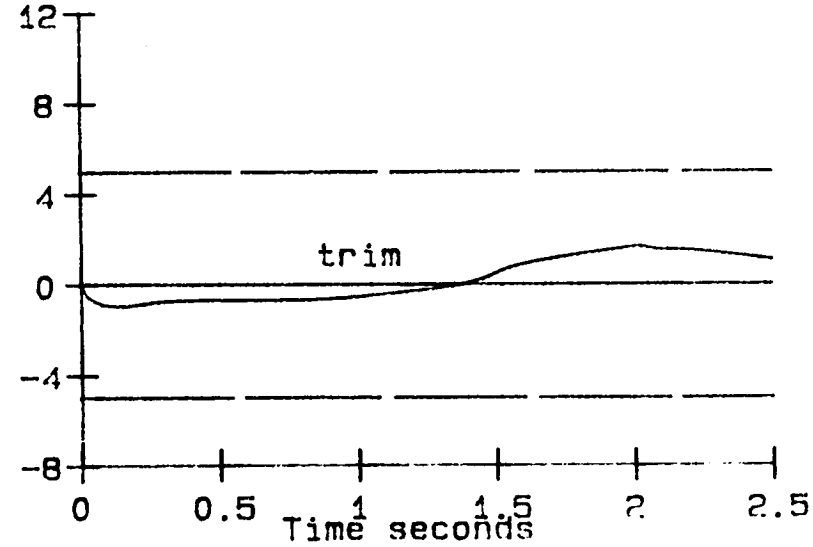

(Dashed lines are saturation limits)

Figure 7-14
124

Bob-up at 40 knots: Aux Prop ON, Control Input Time Histories

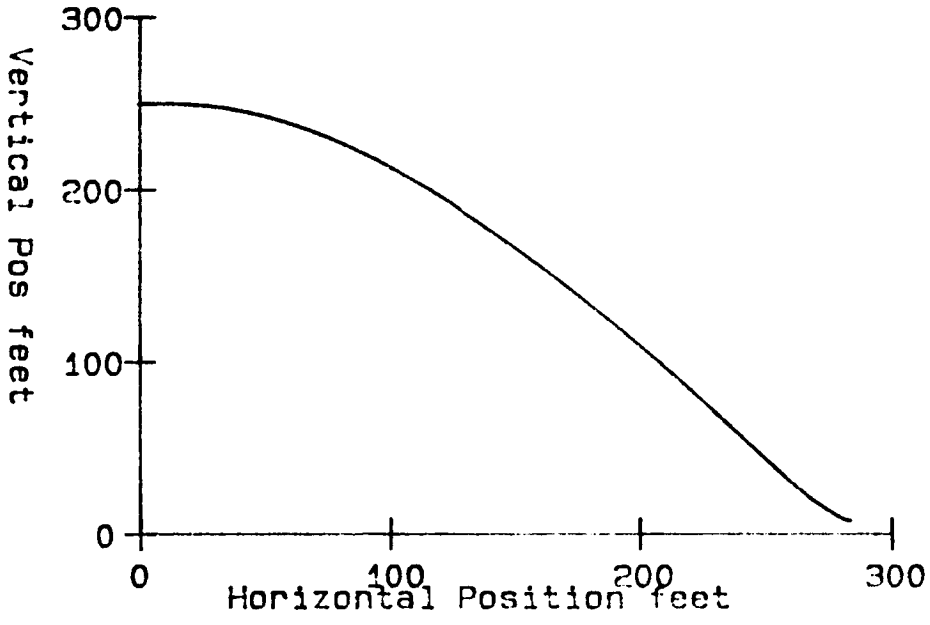

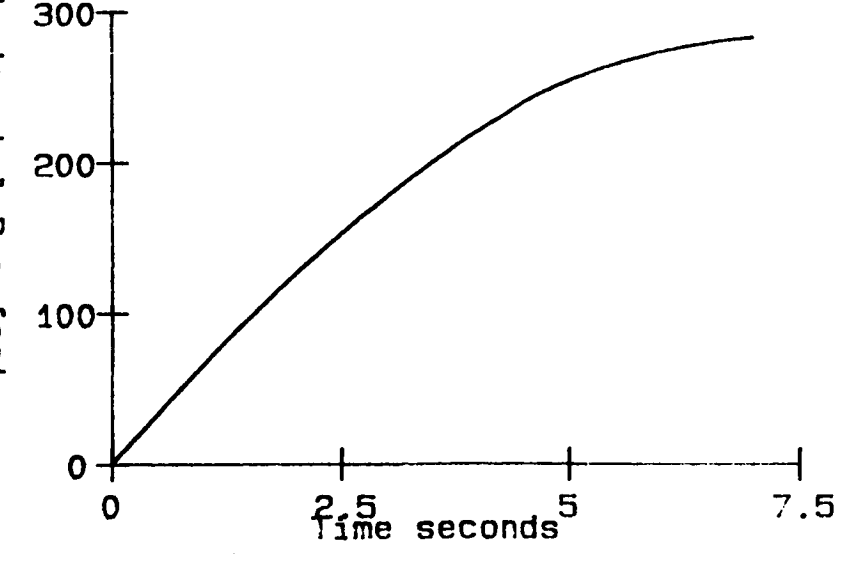

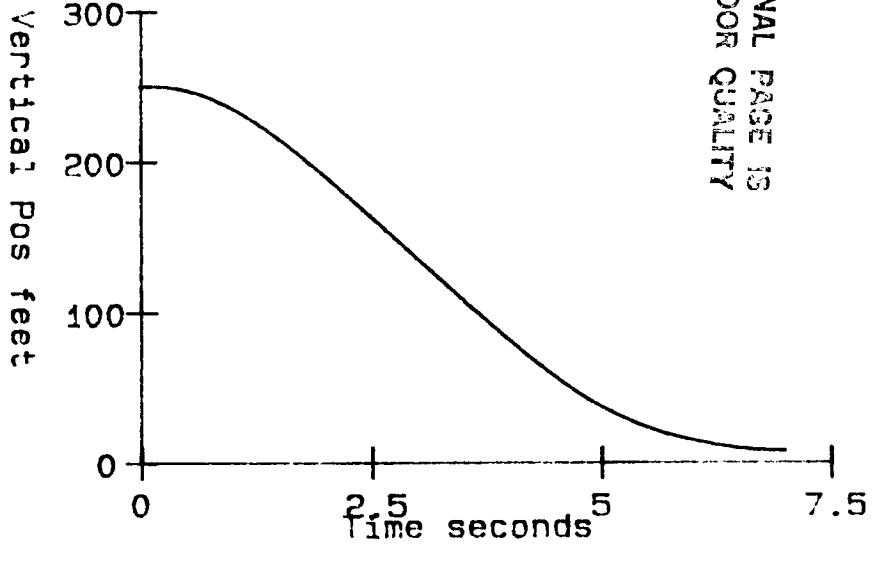

Figure 7-15
Glideslope: Aux Prop OFF, Spatial Position and Position Histories

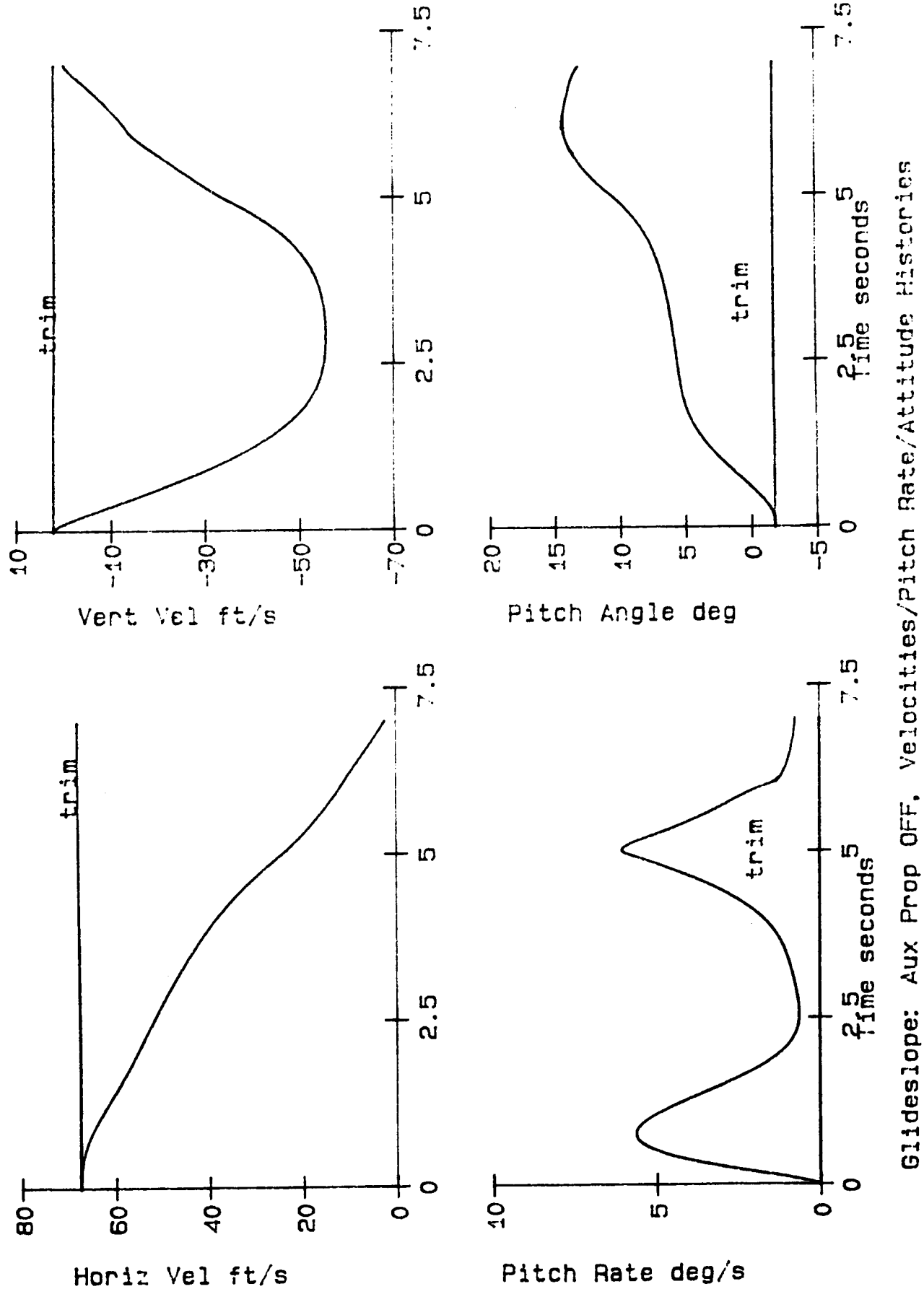

Figure 7-16

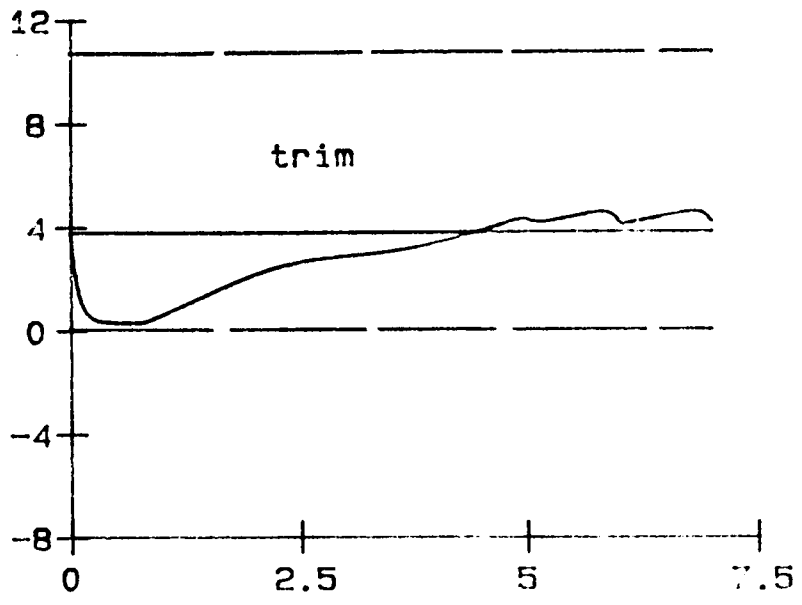

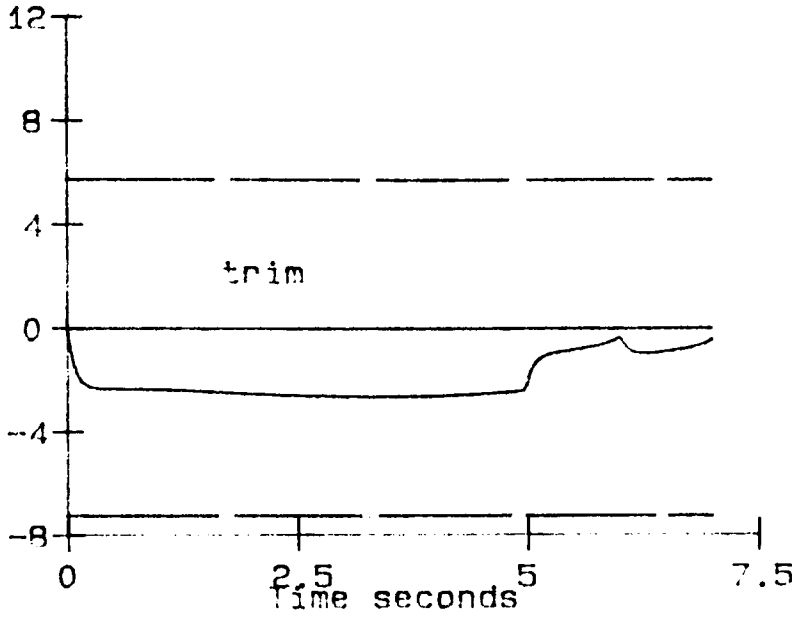

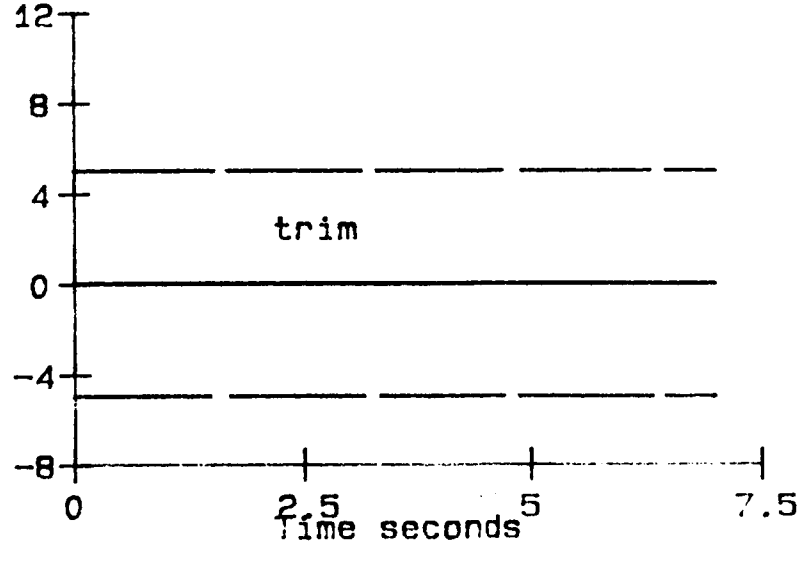

(Dashed lines are saturation limits)

Figure 7-17

Glideslope: Aux Prop OFF, Control Input Time Histories

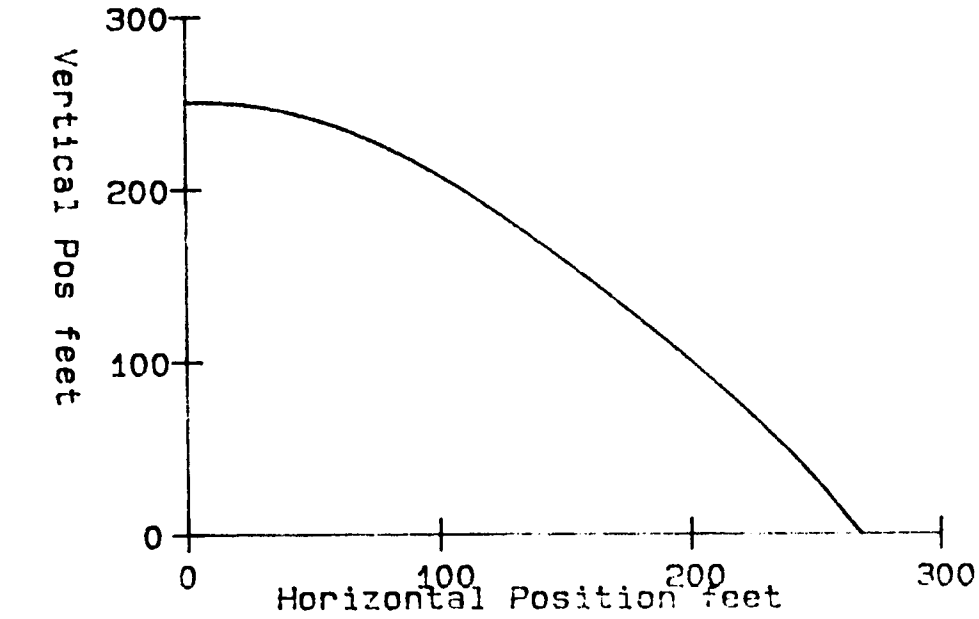

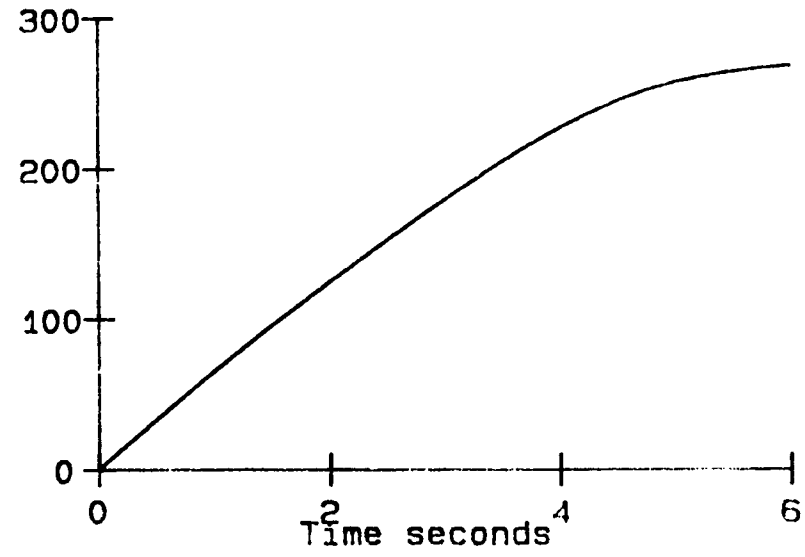

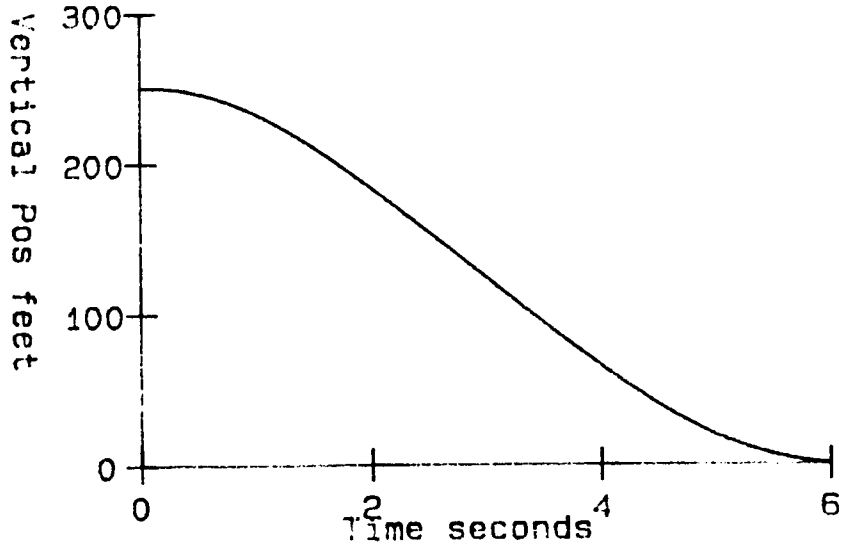

Figure 7-18
128

Glideslope: Aux Prop ON, Spatial Position and Position Histories

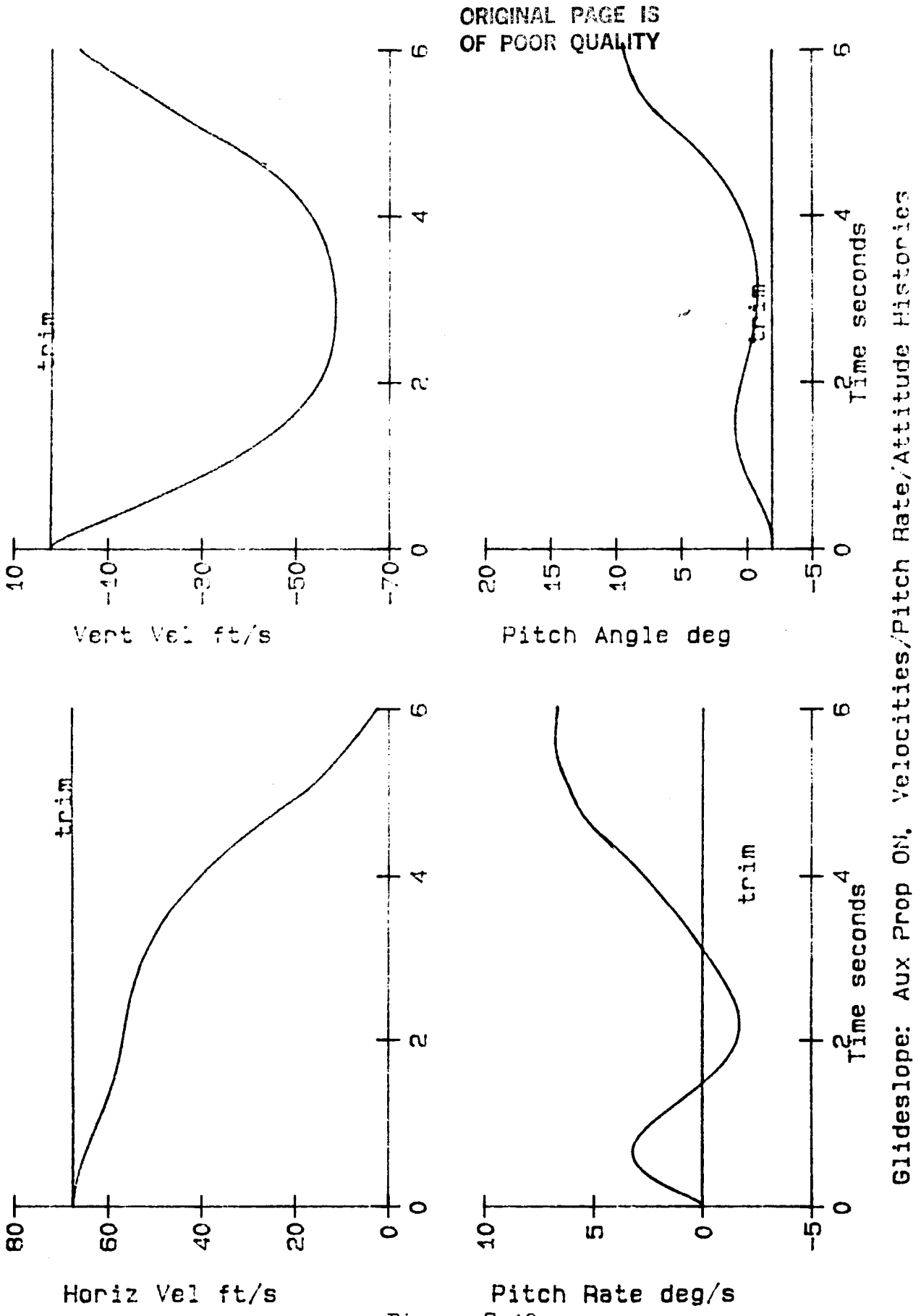

Figure 7-19

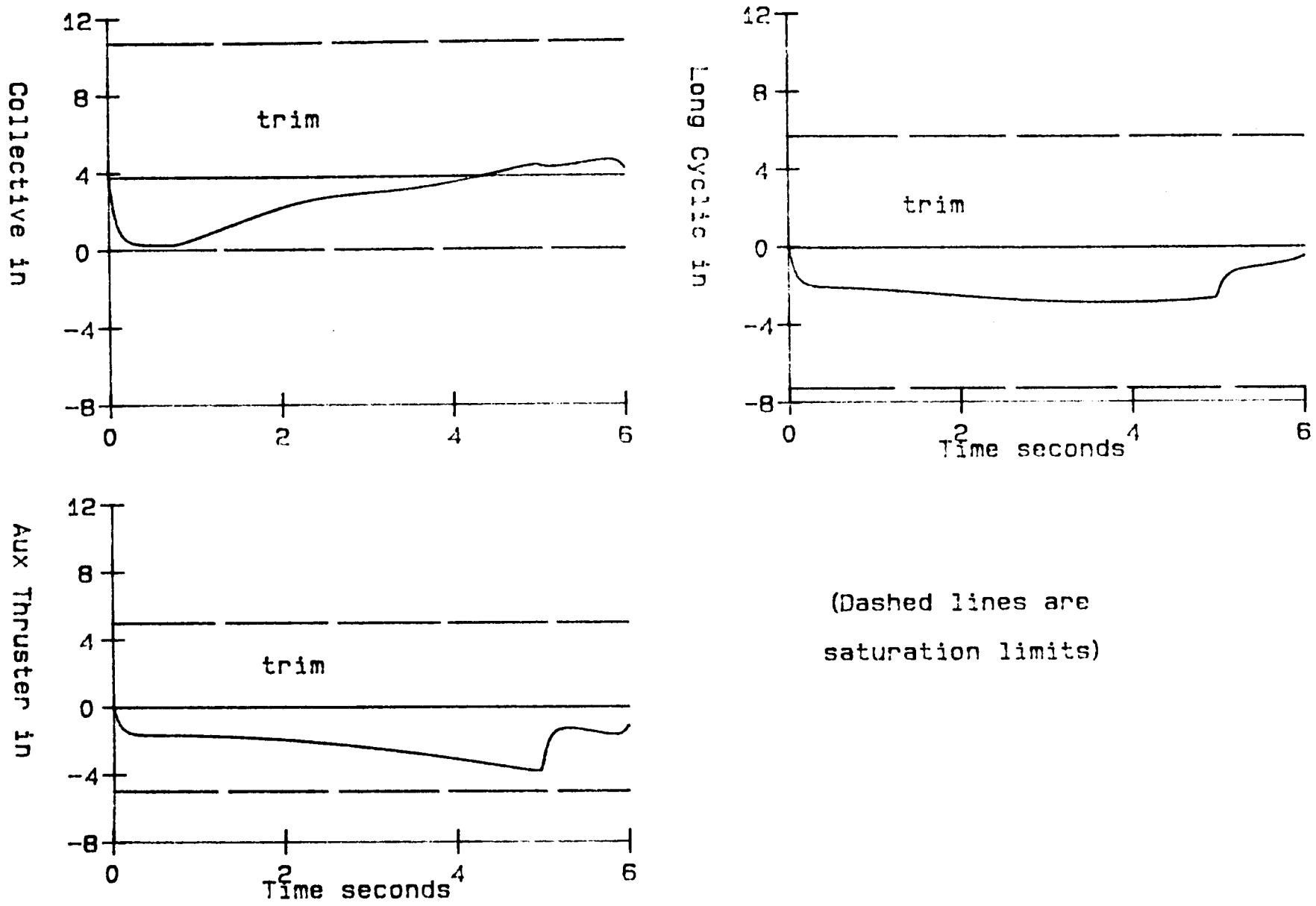

Figure 7-20

Glideslope: Aux Prop ON, Control Input Time Histories

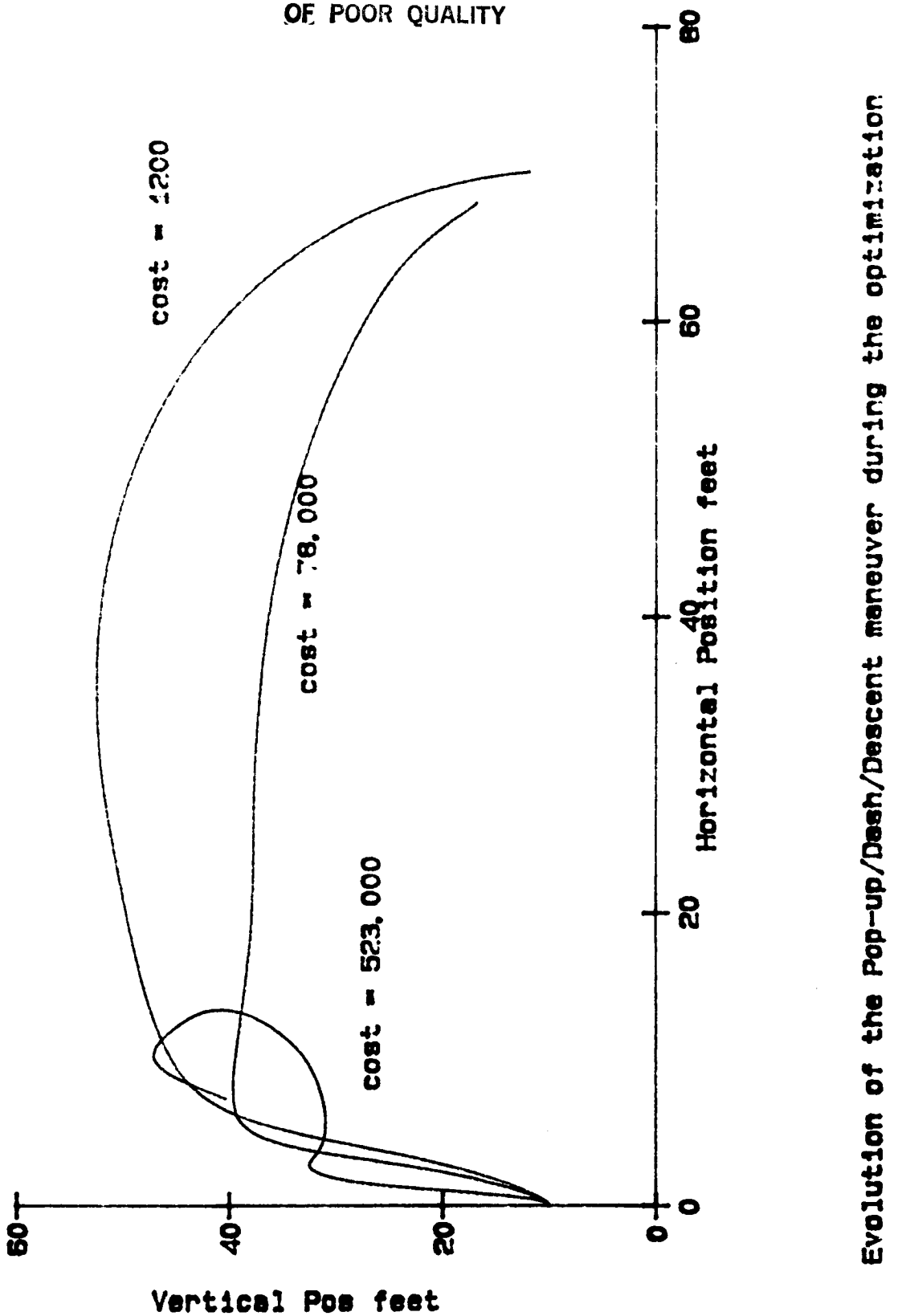

Evolution of the Pop-up/Dash/Descent maneuver during the optimization

Figure 7-21

Chapter VIII

EVALUATION OF IMPLICIT AND EXPLICIT CONTROLLERS

The three maneuvers used for evaluation in this chapter are those maneuvers which were defined in Chapter VII. The optimal control input histories and state histories for these maneuvers (Chapter VII) are referred to often in the following discussion of the pilot command input histories.

8.1 Pop-up Maneuver

The pilot input histories for the implicit and explicit controllers are shown in Figures 8-1 and 8-2, respectively, for the conventional helicopter, and in Figures 8-3 and 8-4 for the helicopter equipped with auxiliary propulsion. A summary of the pilot workloads for this task is contained in Table 8-1.

8.1.1 Without Auxiliary Propulsion

For the implicit controller, the command inputs are choppy, and definitely coupled. Both stick motions reverse direction several times throughout the trajectory, and the rates of change are appreciable. Therefore, the pilot workload is very high. The explicit controller's command inputs are smooth. The vertical velocity command rises and then falls back to trim, in accordance with the desired shape of the pop-up and descent. The horizontal velocity command increases for the dash portion of the task, though it seems to remain unusually high at the end of the trajectory.

8.1.2 With Auxiliary Propulsion

The implicit controller, as for the case above, should be judged unacceptable. The explicit controller again accepts smooth, low pilot workload inputs. The horizontal velocity command this time, however, seems unusually low over the entire trajectory (Figure 8-4), especially considering the amount of positive cyclic and thruster input used throughout the maneuver (Figure 7-8).

8.2 Bob-up Maneuver

The pilot input histories for the implicit and explicit controllers are shown in Figures 8-5 and 8-6, respectively, for the conventional helicopter, and in Figures 8-7 and 8-8 for the helicopter equipped with auxiliary propulsion. A summary of the pilot workloads for this task is contained in Table 8-1.

8.2.1 Without Auxiliary Propulsion

The implicit model-following controller requires pilot inputs (Figure 8-5) that are not distinctively different from the swashplate inputs (Figure 7-11); there is a lot of movement in each stick, as witnessed in the command inputs and the rate of command inputs. Consequently, the pilot workload is relatively high. Furthermore, we notice that this controller has not decoupled the translational velocities very well.

The explicit model-following controller, on the other hand, shows excellent controller characteristics. Figure 8-6 plots the pilot inputs using this controller. The vertical velocity input

is a very smooth bell-shaped curve. This command input reflects the curvature of the trajectory and the vertical velocity history (Figures 7-9 and 7-10); that is, the vertical response to the vertical command input is direct and predominately uncoupled. At the completion of the maneuver, when the helicopter is at its trim altitude and cruise speed, the W_{com} stick has been returned to its trimmed location. Only minor horizontal velocity compensatory command is necessary, and this input is also very smooth.

These smooth pilot inputs result in very low pilot workloads (see Table 8-1). The ability of the explicit controller to accept smooth inputs, mix them, and output the necessary "choppy" swashplate and thruster histories is quite pleasing.

8.2.2 With Auxiliary Propulsion

There is very little change in the pilot input histories for the thruster-equipped helicopter (because very little thruster power is needed to meet the specifications of this maneuver). The same results concluded above apply to this controller.

8.3 Glideslope Maneuver

The pilot input histories for the implicit and explicit controllers are shown in Figures 8-9 and 8-10, respectively, for the conventional helicopter, and in Figures 8-11 and 8-12 for the helicopter equipped with auxiliary propulsion. A summary of the pilot workloads for this task is contained in Table 8-1.

8.3.1 Without Auxiliary Propulsion

The swashplate inputs for this maneuver are somewhat choppy (Figure 7-11). The pilot inputs for the implicit controller are

also choppy, whereas the explicit controller accepts smooth inputs. The smoothness of these inputs for the explicit controller, and the relative simple nature of this task results in very low pilot workload.

8.3.2 With Auxiliary Propulsion

Again, the implicit controller does not provide good controller characterisitics. The explicit controller is very good; the pilot histories differ from those above only in that the vertical velocity command at the end of the trajectory becomes positive to curtail the high descent rate which was made possible via the auxiliary thruster.

In all of the cases presented above, the pilot workload for the explicit controller is considerably less than the workload for the implicit controlle The difference in workloads between maneuvers is attributed to the relative degree of agility inherent in the maneuver.

Both controllers exhibited good frequency responses. It appears, therefore, that the explicit controller was able to accept smoother pilot inputs because of its use of a prefilter. The explicit controller attempted to match the actual and model *state* histories, whereas the implicit controller attempted to match the *state rate* histories; state rate matching required that the pilot input histories were similar to swashplate inputs so that the integrated state rates resulted in the correct state histories. Since the explicit controller matched state histories, the pilot inputs were required to satisfy the *integrated* model

dynamics, and resulted in commands that were smooth and proportional to the desired velocities.

Maneuver/ Aux Prop, Controller	Pilot Workload Cost		Open-loop Control Cost			Normalized Cost	
	$\dot{W}_{com}$	$\dot{U}_{com}$	$\dot{\theta}_c$	$\dot{B}_{1s}$	$\dot{T}$	$\frac{\dot{W}_{com}}{\dot{\theta}_c}$	$\frac{\dot{U}_{com}}{\dot{B}_{1s}}$
Pop-up/Off							
Implicit	23	550	357	526	NA	.07	1.05
Explicit	8	85	357	526	NA	.02	.20
Pop-up/On							
Implicit	22	126	331	232	336	NA	NA
Explicit	7	52	331	232	336	NA	NA
Bob-up/Off							
Implicit	21	140	238	190	NA	.09	.74
Explicit	12	44	238	190	NA	.05	.23
Bob-up/On							
Implicit	18	66	171	74	65	NA	NA
Explicit	10	32	171	74	65	NA	NA
Glideslope/Off							
Implicit	10	19	176	135	NA	.06	.14
Explicit	2	31	176	135	NA	.01	.23
Glideslope/On							
Implicit	4	60	162	108	133	NA	NA
Explicit	4	21	162	108	133	NA	NA

Table 8-1

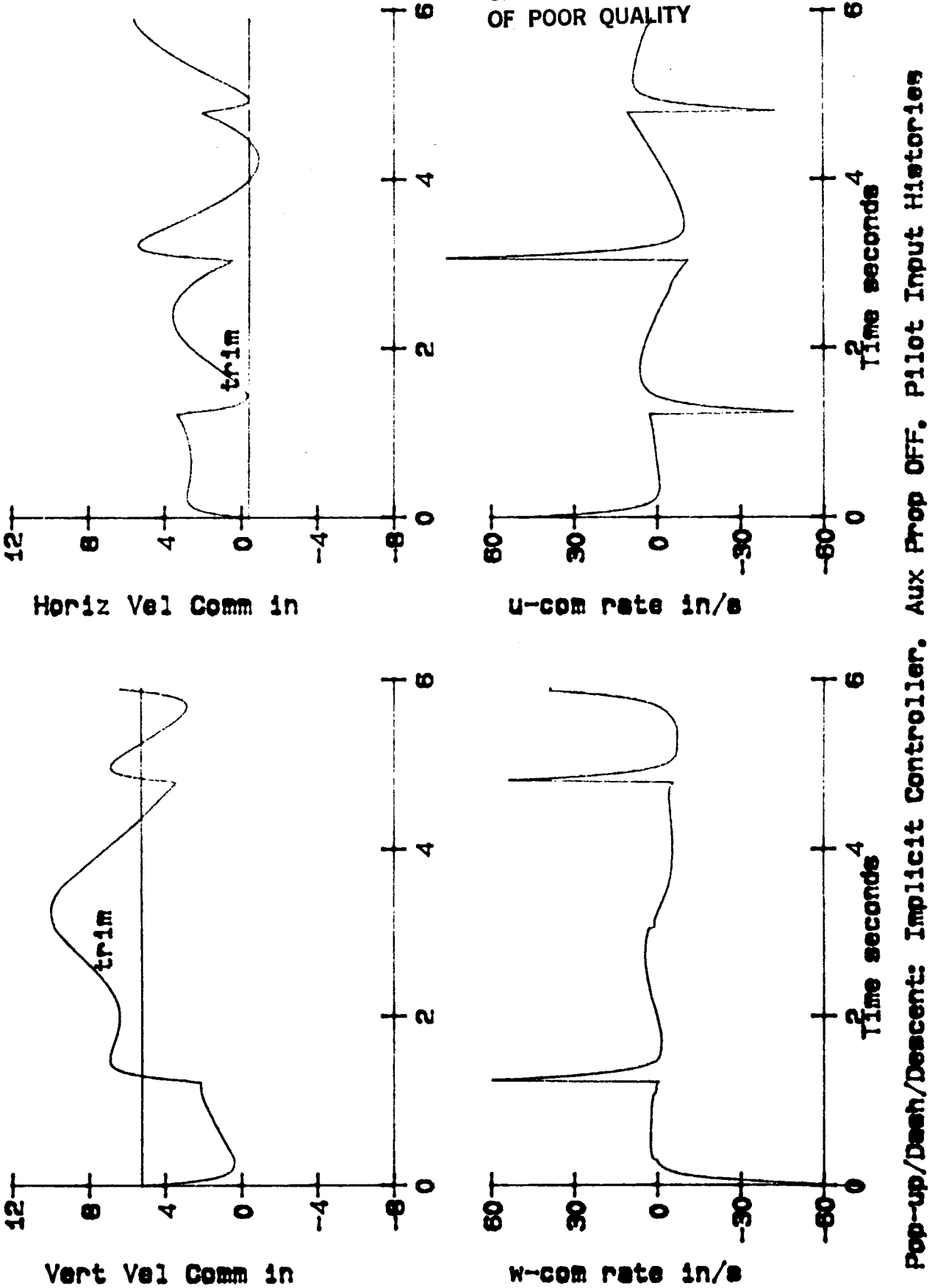

Figure 8-1

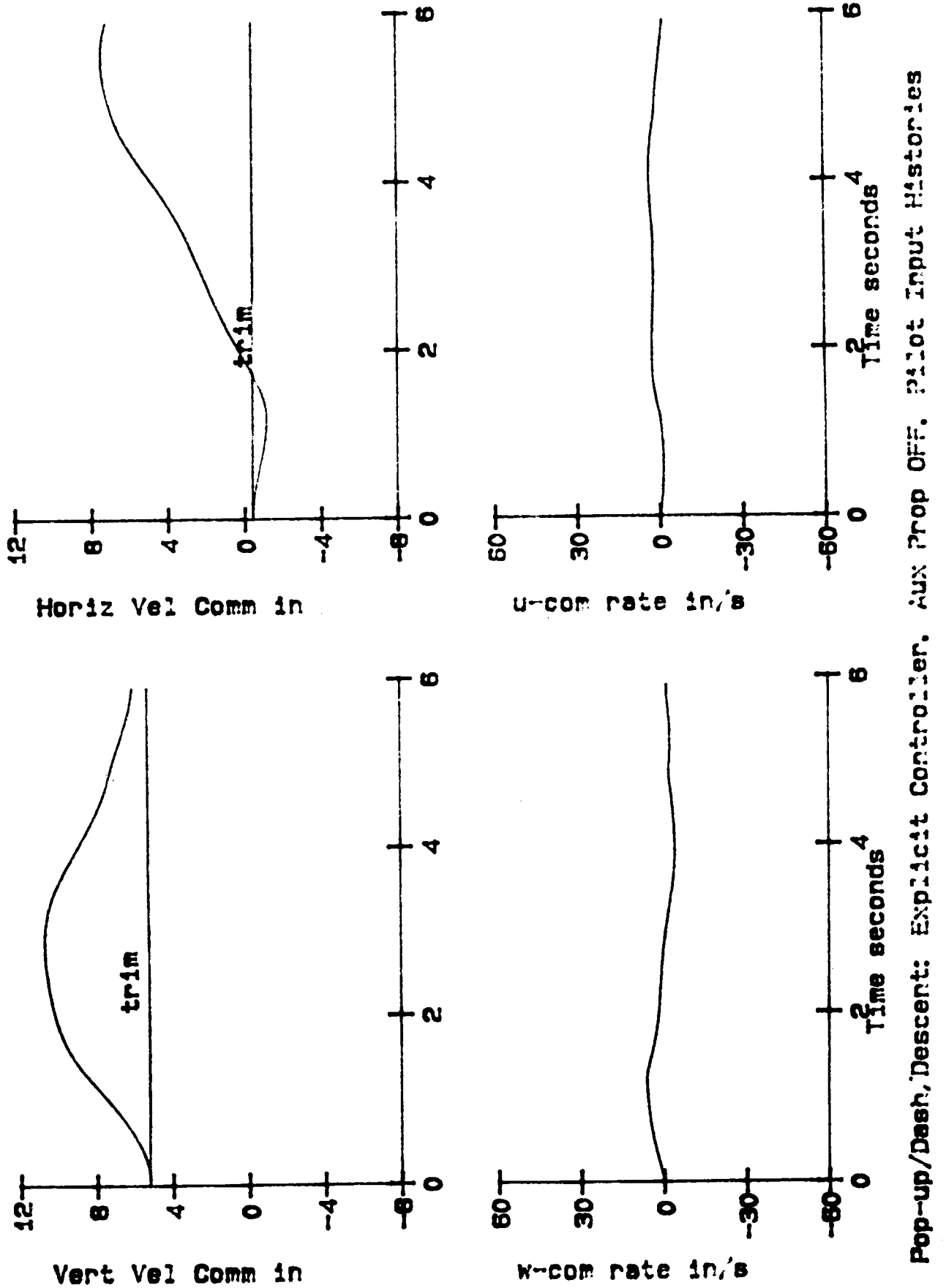

Figure 8-2

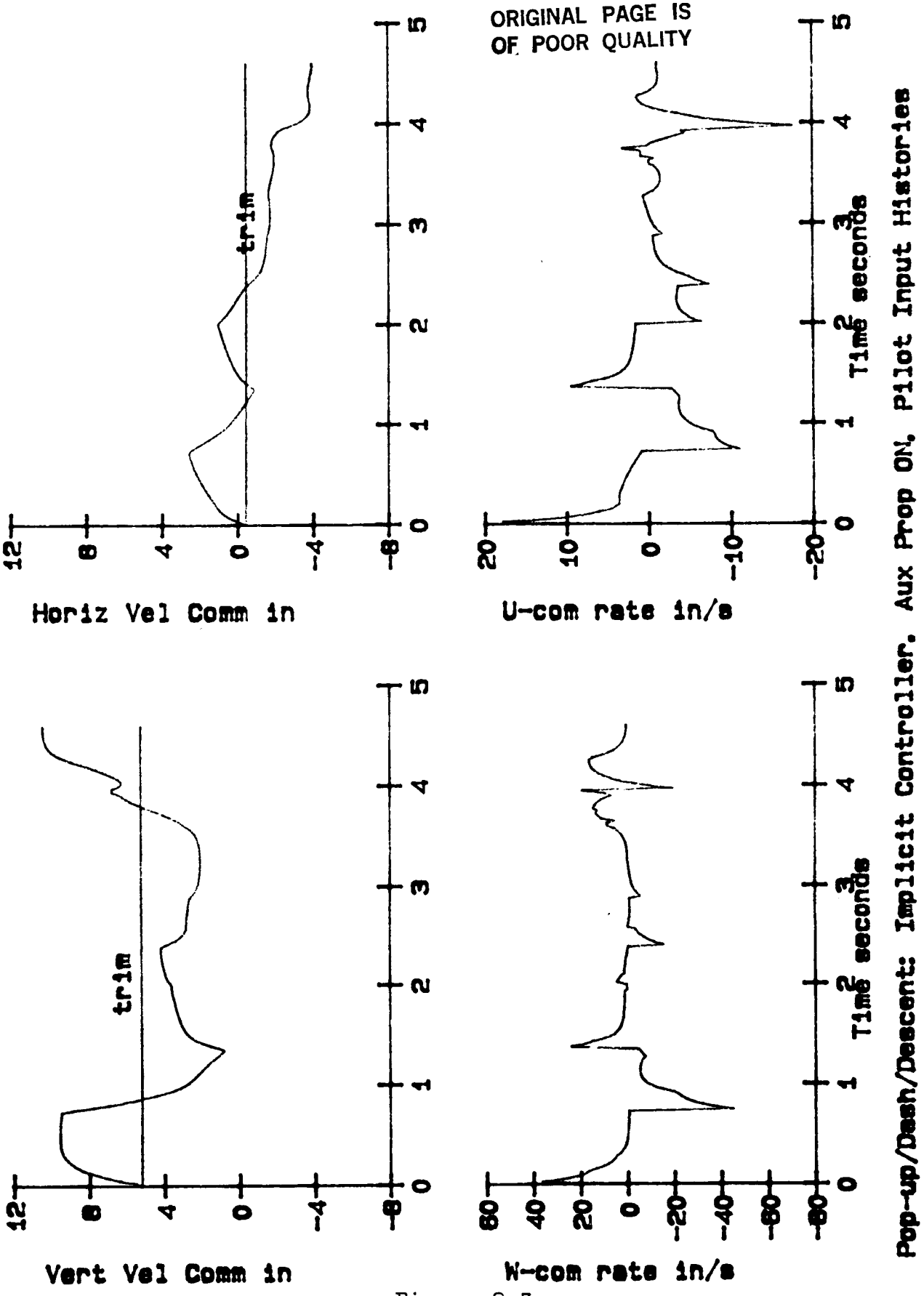

Figure 8-3

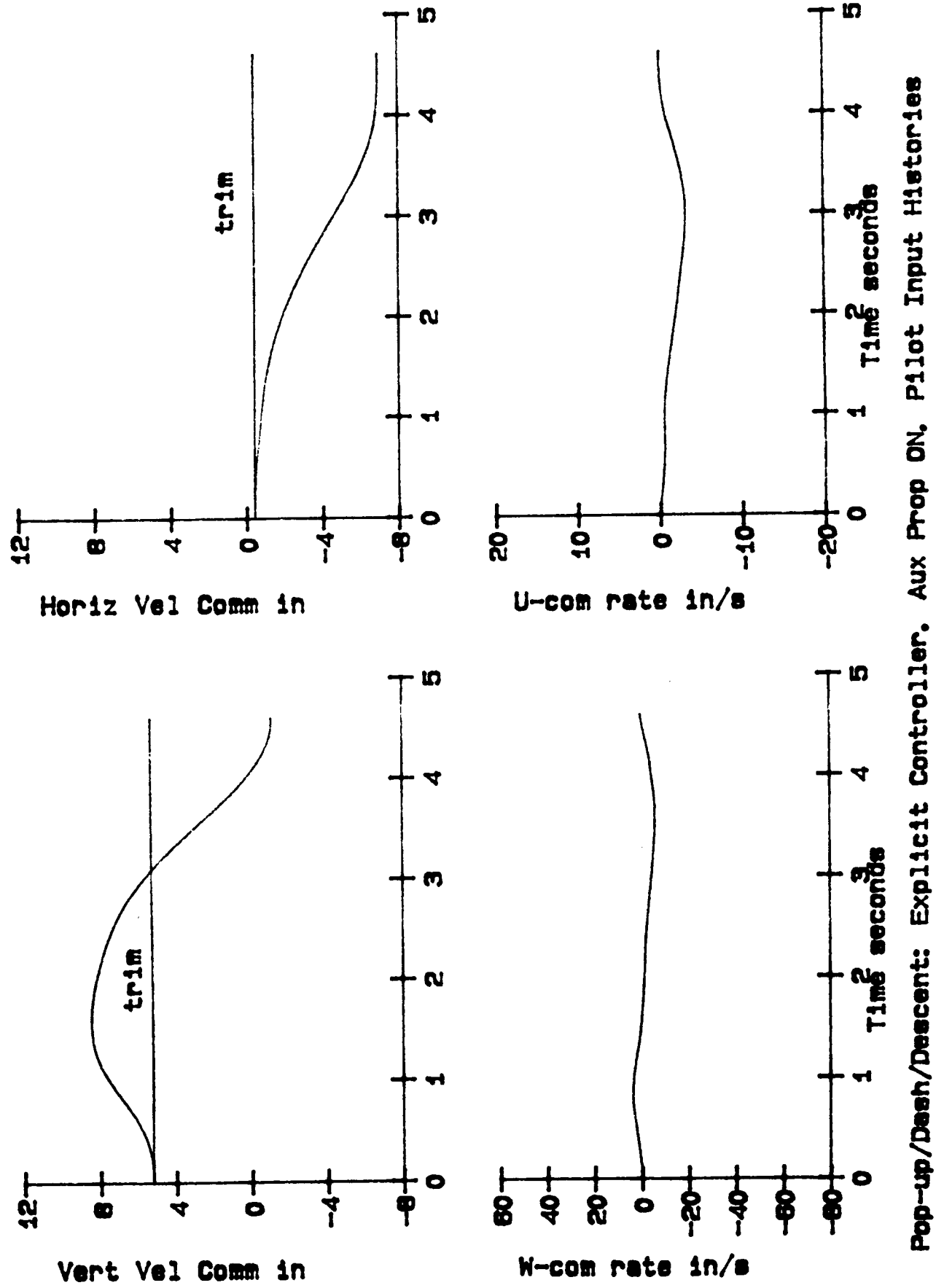

Figure 8-4

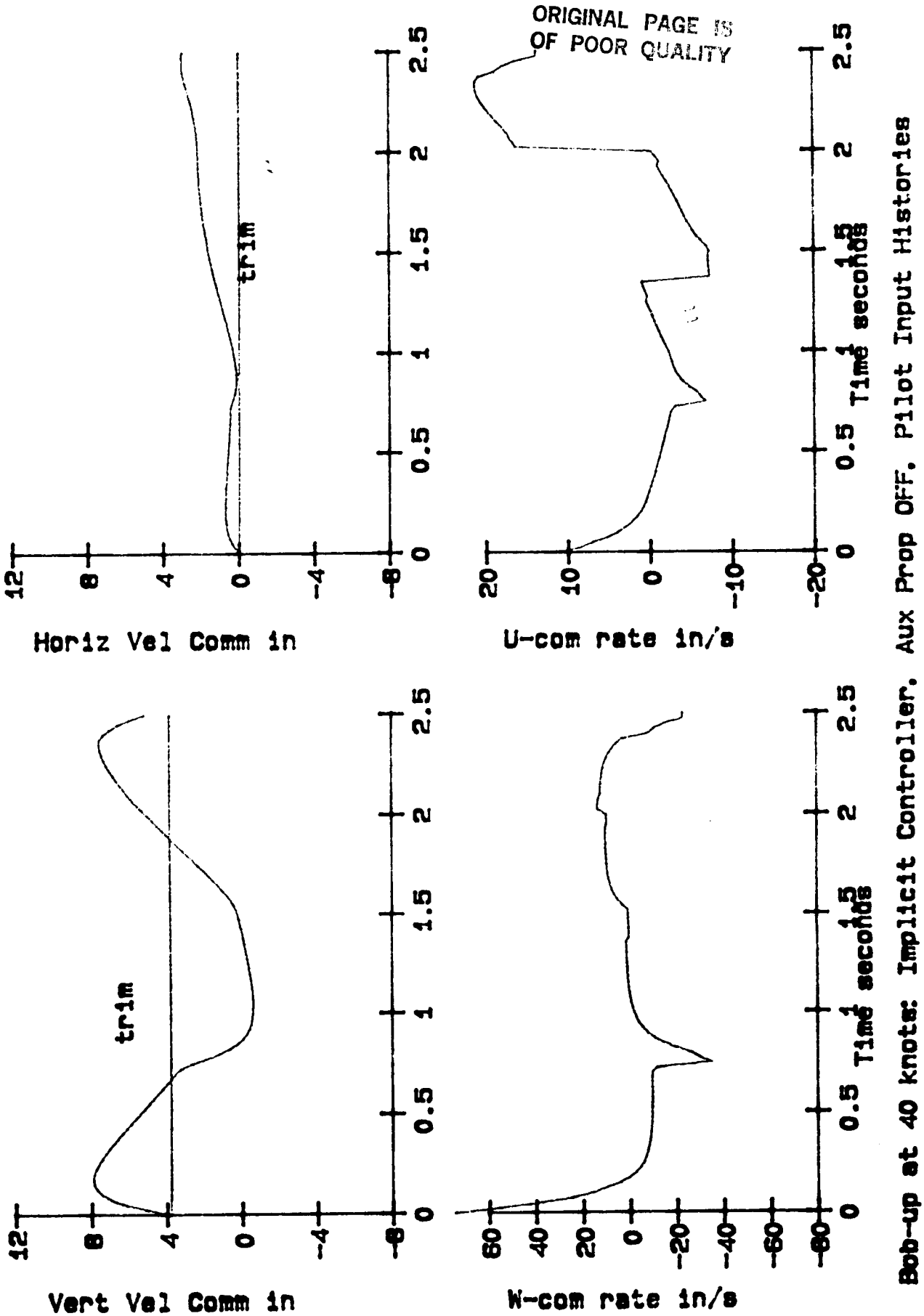
ORIGINAL PAGE IS
OF POOR QUALITY
trim
Horiz Vel Comm in
U-com rate in/s
trim
Vert Vel Comm in
W-com rate in/s
Time seconds
Time seconds
Bob-up at 40 knots: Implicit Controller, Aux Prop OFF, Pilot Input Histories

Figure 8-5

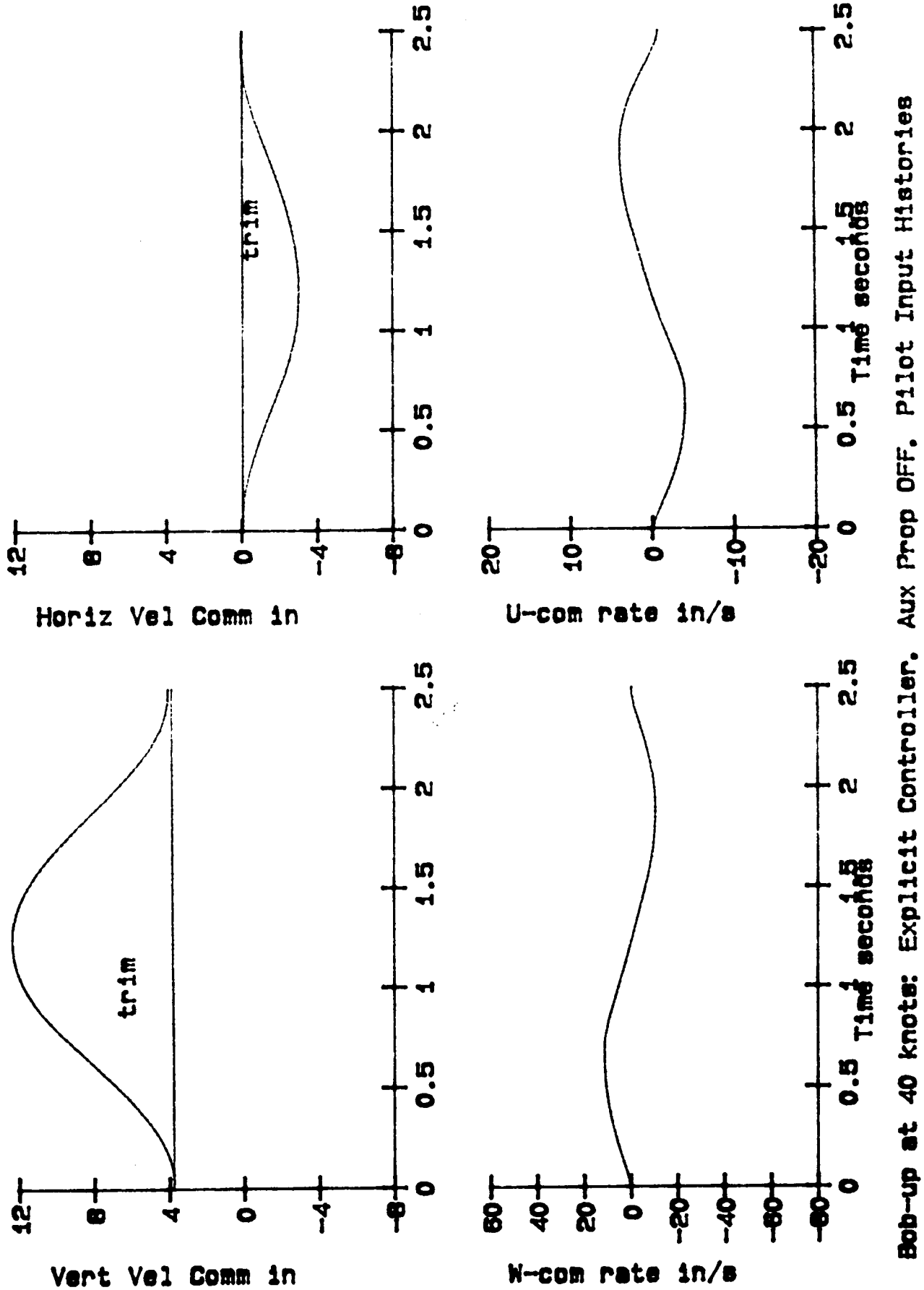

Figure 8-6

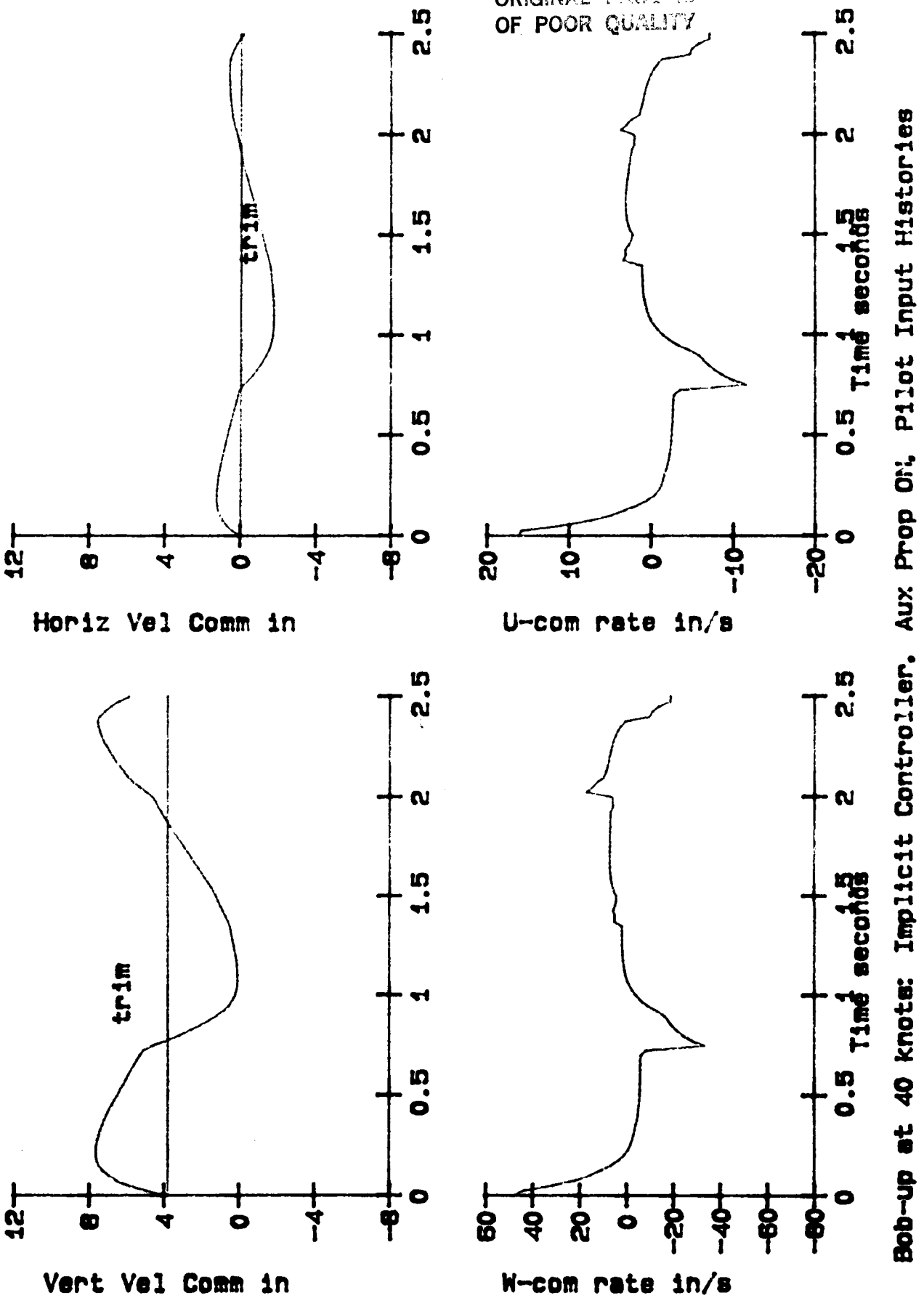

Figure 8-7

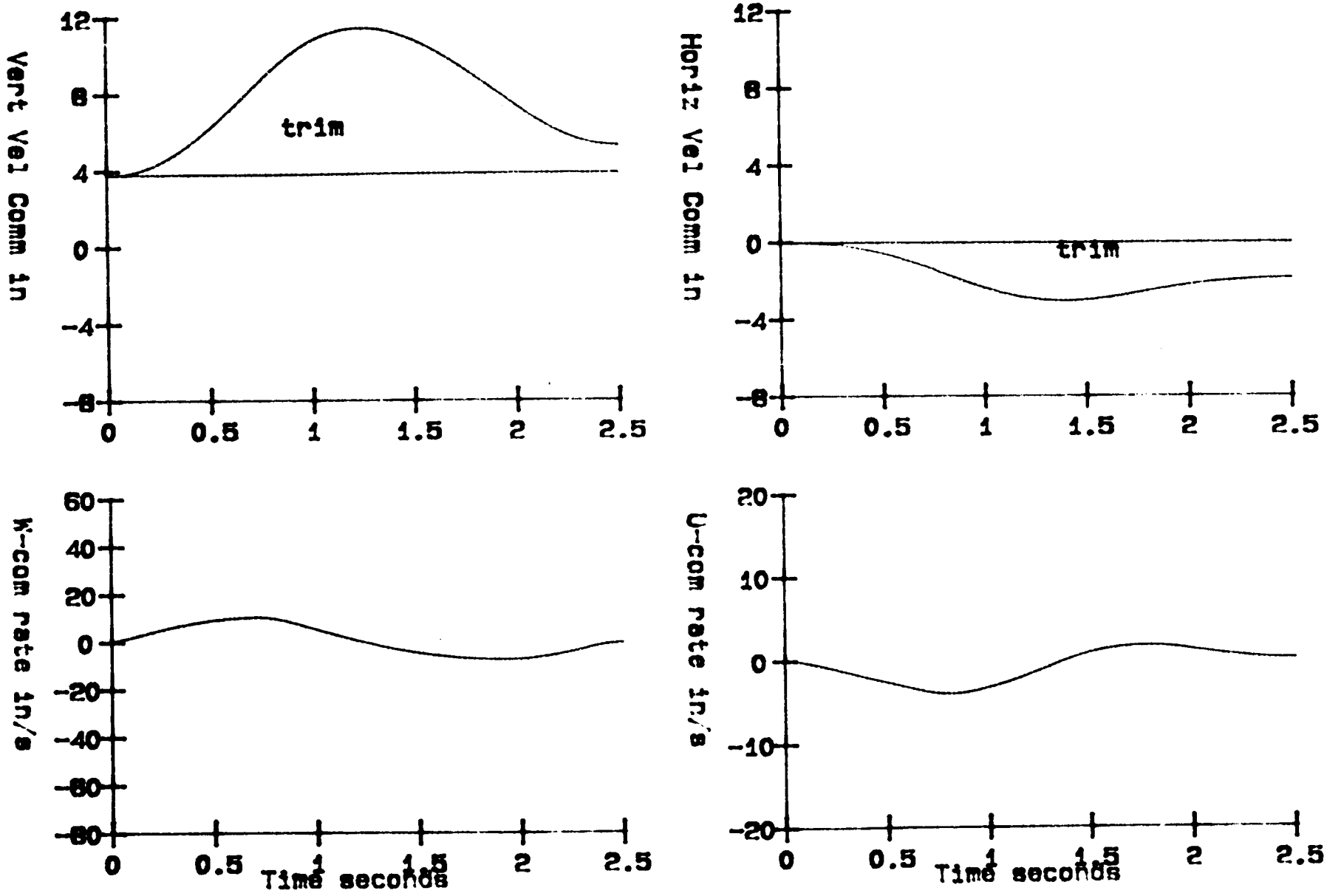

Figure 8-8

Bob-up at 40 knots: Explicit Controller, Aux Prop On, Pilot Input Histories

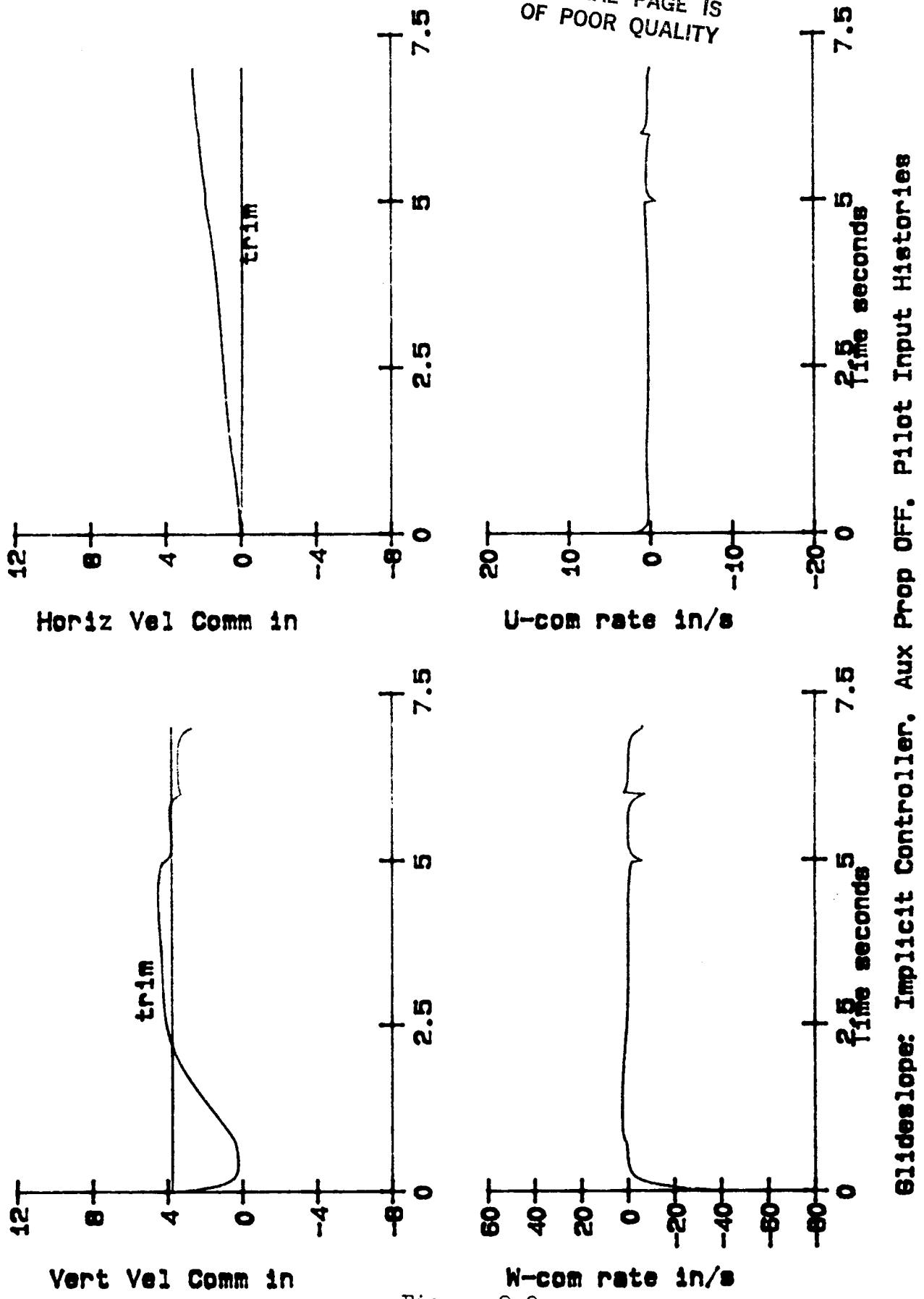

Figure 8-9

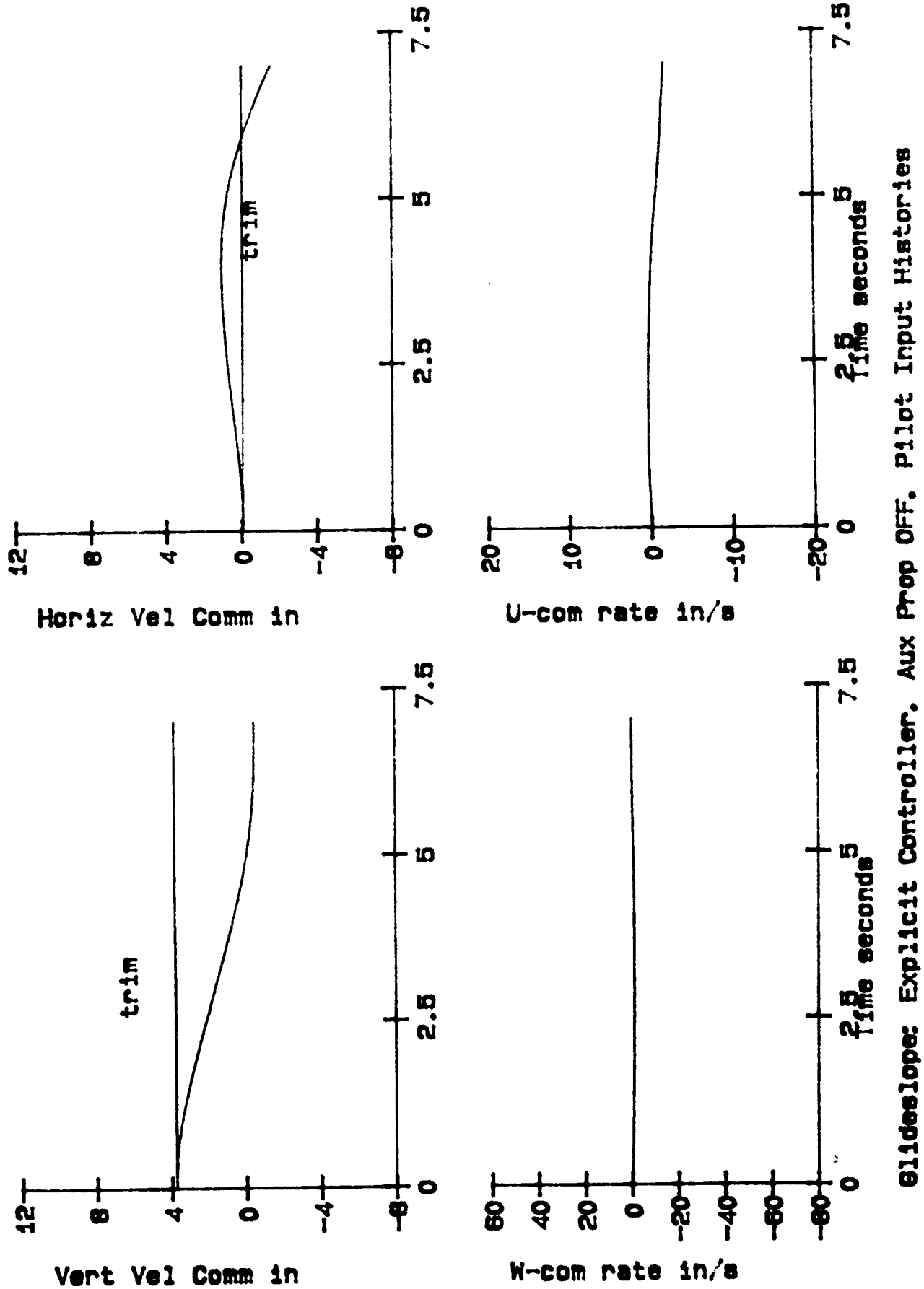

Figure 8-10

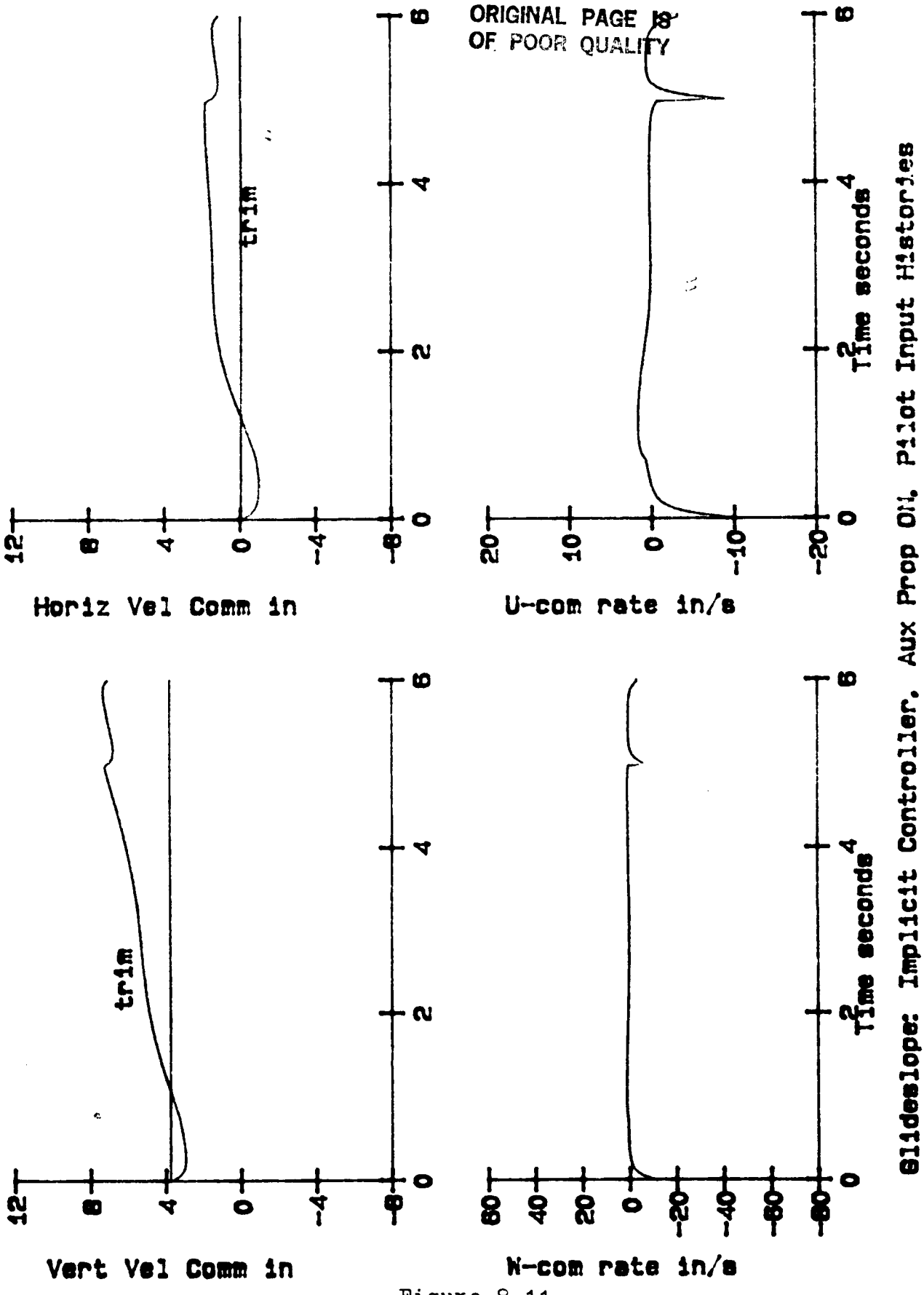

Glideslope: Implicit Controller, Aux Prop Oil Pilot Input Histories

Figure 8-11

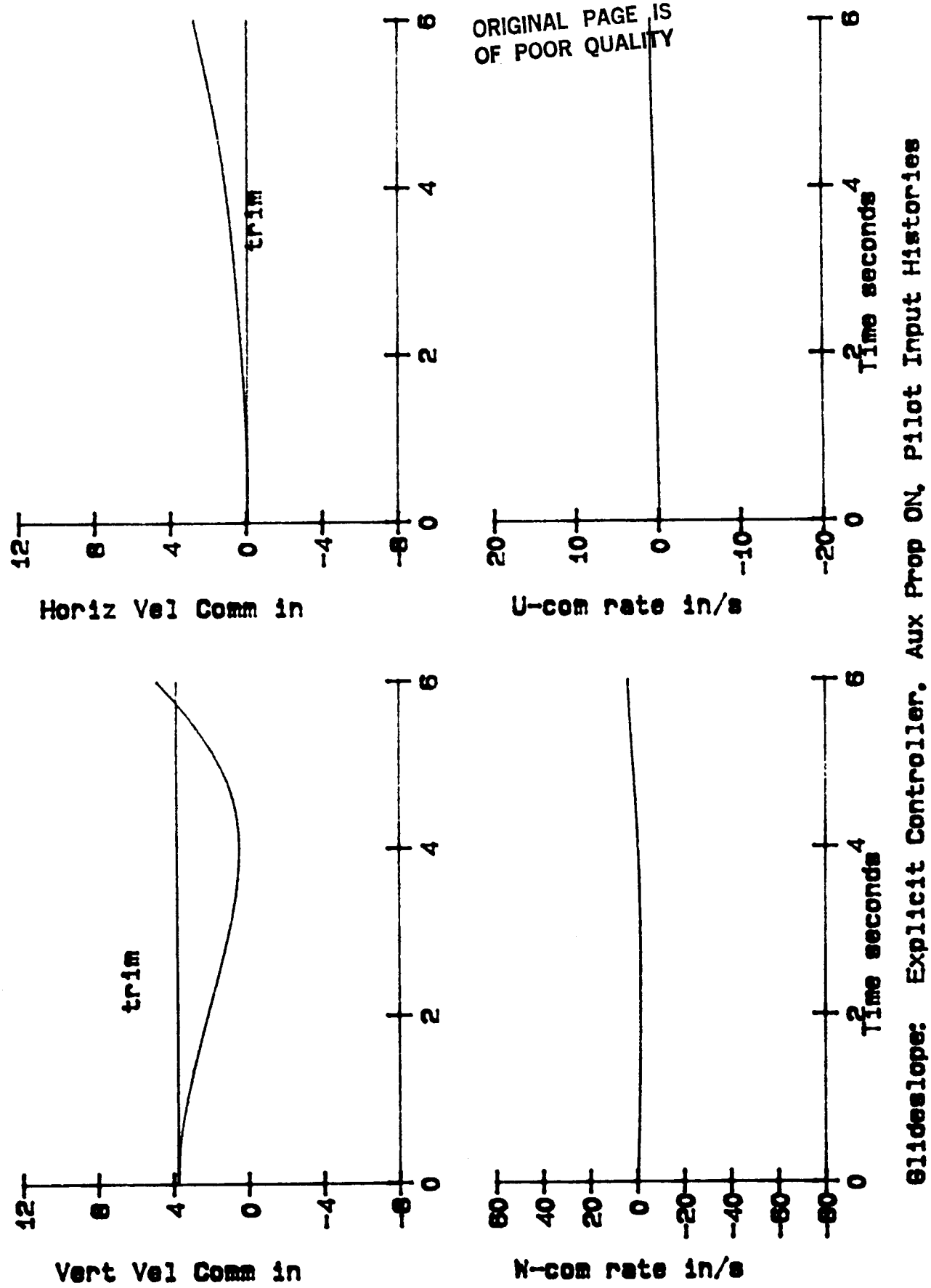

Figure 8-12

Chapter IX

CONCLUSIONS AND RECOMMENDATIONS

Implicit and explicit model-following controllers have been investigated for use with the longitudinal degrees of freedom of an attack-type helicopter operating in a NOE environment. A computational trajectory optimization method was employed to evaluate these controllers, and to access the advantages incurred using auxiliary propulsion on helicopters operating in this environment. The auxiliary control power was sized according to desired acceleration potential. The contollers and longitudinal propulsion advantages were judged in terms of their resulting handling qualities, flying qualities, and pilot workload.

A velocity-command controller, with decoupled command inputs, is preferred for these types of NOE tasks, which typically require high levels of helicopter agility. The explicit model-following controller uses a prefilter of model dynamics in the feedforward loop of the controller. This controller was superior to the implicit model-following controller in all cases tested, and was much easier to design because the same Q and R matrices were applicable for all trim conditions. Both could be designed to satisfactorily meet the prescribed handling qualities criteria using primarily diagonal weighting matrices. The explicit controller, however, required far less pilot workload. The explicit controller's command inputs reflected the direction, duration, and relative magnitude of the desired horizontal and

vertical velocity responses. This was true for the conventionally equipped helicopter, and for the thruster augmented helicopter, where the two command inputs were effectively mixed to provide inputs to the three helicopter controls (collective, cyclic, and thruster).

The auxiliary propulsor is very effective for NOE operations because (1) it increases the acceleration/deceleration potential of the helicopter, thereby decreasing the time to complete the task, and (2) the thruster-generated acceleration does not require excessive pitch motion, which is detrimental for navigation, target acquisition, and hiding.

The trajectory optimization method provides a straightforward and efficient way to determine the optimal control input histories, which can be employed to then evaluate attributes of various controllers, propulsion systems, and perhaps other components of the helicopter. This study uses a soft constraint on the helicopter's pitch attitude and pitch rate. In retrospect, it may be more effective to use a hard constraint so as to absolutely limit the rate and attitude. In the current method, early stages of the optimization may yield rates and attitudes which are definitely unacceptable, and extreme attitudes may lead to divergence of the optimization.

The controller gains are scheduled throughout the flight envelope. This is necessary to account for changes in the flight condition throughtout the trajectory. However, some gains change very little with flight condition, and some have negligible influence. This, in fact, was verified during early stages of this study, when the gains at the trimmed condition were used

throughout the entire trajectory. Therefore, further work in this area should be directed to correlating the most influencial gains with flight condition, and scheduling accordingly. For implementation in the aircraft, this will be necessary to reduce computational storage and real-time processing, and expense.

Appendix A

Helicopter Equations of Motion

The most basic starting point in developing the dynamic equations of motion for the helicopter (or for any body) is to apply Newton's Second Law to the forces and moments acting on the helicopter, as described in reference 23. The helicopter is assumed to be a perfectly rigid body. Using a body-axis reference frame (Figure A-1), this yields the six degree of freedom expressions for helicopter motion. These equations relate the translational and angular accelerations to the aerodynamic, inertial, and gravitational terms. This study is concerned with the longitudinal equations of motion, and therefore the lateral-directional motion equations are not presented.

Other assumptions employed in this derivation are that

1. the helicopter has constant mass and mass distribution.
2. the helicopter is flying at speeds low enough and distances short enough that the Earth can be considered flat; the body-axis frame then need not be related to rotation about the Earth's geocenter, and the inertial reference frame is therefore the flat Earth axis.
3. quasisteady flow applies.

The dynamics of the helicopter are presented in a body-axis frame. This is an axis system affixed to the body (Figure A-1). The X_B axis is forward through the nose of the helicopter; Y_B points out the right side; and Z_B points *down* through the body of

the helicopter. P, Q, and R designate rotational rates about the X_B, Y_B, and Z_B axes, respectively. The origin of this axis system is the helicopter's center of gravity. The XZ plane is assumed to be a plane of symmetry. Figure A-1 also shows the Earth-referenced frame: X_I points right; Y_I points out of the page; and Z_I points in the gravity (g) direction. Typically, it is necessary to consider the inertial to body transformation matrix which relates these two reference frames. However, since we are dealing only with the linearized longitudinal motion equations, it is more succinct to state the simple result of the transformation linearization than to develop the transformation which is, for the most part, unused. (The result, $q=\dot{\theta}$, is included and explained below with the linearized longitudinal equations of motion).

The nonlinear longitudinal dynamic equations of motion are

$$\mathbb{X} = m(\dot{U} + QW - RV + g\sin\Theta) = ma_x \qquad \text{(A-1a)}$$

$$\mathbb{Z} = m(\dot{W} + PV - QU - g\cos\Theta\sin\Theta) = ma_z \qquad \text{(A-1b)}$$

$$\mathbb{M} = \dot{Q}I_y + PR(I_x - I_z) - R^2I_{xz} + P^2I_{xz} \qquad \text{(A-1c)}$$

m is the mass of the helicopter. Subscripted I and a are the moment of inertia and acceleration, respectively, along the axis (or in the plane) of the subscript variable. The equations represent the balance between the inertial and gravitational terms, and all aerodynamic and propulsive terms represented by the generalized symbols $\mathbb{X}$, $\mathbb{Z}$, and $\mathbb{M}$.

Since only the longitudinal degrees of freedom are of interest, these equations are rewritten without their lateral-directional terms (the lateral-directional terms are set to zero):

$$\mathbb{X} = m(\dot{U} + QW + g\sin\Theta) \tag{A-2a}$$

$$\mathbb{Z} = m(\dot{W} - QU - g\cos\Theta) \tag{A-2b}$$

$$\mathbb{M} = \dot{Q}I_y \tag{A-2c}$$

These nonlinear equations are linearized by accounting for dynamic motion as small perturbations about an operating, or trim, point. The subscript $(\ )_o$ denotes trim. We write the total motion of each state as the sum of its trim value plus its perturbation value, i.e., we take the first two terms in a Taylor Series expansion.

$$\begin{aligned} U &= U_o + dU = U_o + u & \mathbb{X} &= X_o + dX = X_o + X \\ W &= W_o + dW = W_o + w & \mathbb{Z} &= Z_o + dZ = Z_o + Z \\ Q &= Q_o + dQ = Q_o + q & \mathbb{M} &= M_o + dM = M_o + M \\ \Theta &= \theta_o + d\theta = \theta_o + \theta \end{aligned} \tag{A-3}$$

In trim, nominal translational and rotational accelerations are zero: $\dot{U}_o = \dot{W}_o = \dot{Q}_o = 0$. Therefore,

$$U = U_o + u = u \quad W = W_o + w = w \quad Q = Q_o + q = q \tag{A-4}$$

and the trim equations are

$$X_o = m(Q_o W_o + g\sin\theta_o) \tag{A-5a}$$

$$Z_o = m(Q_o U_o - g\cos\theta_o) \tag{A-5b}$$

$$M_o = 0 \tag{A-5c}$$

Rewriting Equations A-2 using Equations A-3 and the derivative of Equations A-4,

$$\begin{aligned} X_o + X &= m[\dot{u} + (Q_o+q)(W_o+w) + g\sin(\theta_o+\theta)] \\ &= m[\dot{u} + Q_o W_o + Q_o w + W_o q + qw + g\sin\theta_o\cos\theta + g\cos\theta_o\sin\theta] \end{aligned} \tag{A-6a}$$

$$Z_o + Z = m[\dot{w} - (Q_o+q)(U_o+u) - g\cos(\theta_o+\theta)]$$

$$= m[\dot{w} - Q_oU_o - Q_ou - U_oq - qu - g\cos\theta_o\cos\theta + g\sin\theta_o\sin\theta] \quad \text{(A-6b)}$$

$$M_o + M = \dot{q}I_y \quad \text{(A-6c)}$$

This linearization technique assumes small perturbations, so that a small angle approximation is used: $\cos\theta \cong 1$ and $\sin\theta \cong \theta$. We also assume the products of perturbation variables are negligible. Using these two approximations, Equations A-6 are

$$X_o + X = m[\dot{u} + Q_oW_o + Q_ow + W_oq + g\sin\theta_o + g\cos\theta_o\theta] \quad \text{(A-7a)}$$

$$Z_o + Z = m[\dot{w} - Q_oU_o - Q_ou - U_oq - g\cos\theta_o + g\sin\theta_o\theta] \quad \text{(A-7b)}$$

$$M_o + M = \dot{q}I_y \quad \text{(A-7c)}$$

Subtracting the trim expressions, Equations A-5, from Equations A-7 yields the linearized (perturbation) equations:

$$X = m[\dot{u} + Q_ow + W_oq + g\cos\theta_o\theta] \quad \text{(A-8a)}$$

$$Z \quad m[\dot{w} - Q_ou - U_oq + g\sin\theta_o\theta] \quad \text{(A-8b)}$$

$$M = \dot{q}I_y \quad \text{(A-8c)}$$

or,
$$\frac{X}{m} = \dot{u} + Q_ow + W_oq + g\cos\theta_o\theta \quad \text{(A-9a)}$$

$$\frac{Z}{m} = \dot{w} - Q_ou - U_oq + g\sin\theta_o\theta \quad \text{(A-9b)}$$

$$\frac{M}{I_y} = \dot{q} \quad \text{(A-9c)}$$

Recall that X, Z, amd M represent the perturbation aerodynamic and propulsive forces and moment.

The linearization of the inertial/body transformation yields the simple expression $q=\dot{\theta}$. This means that pitch attitude, θ, is the direct integral of pitch rate, q. Thus, the independent perturbation variables in the longitudinal degrees of freedom are

$$= m[\dot{w} - Q_o U_o - Q_o u - U_o q - qu - g\cos\theta_o \cos\theta + g\sin\theta_o \sin\theta] \quad \text{(A-6b)}$$

$$M_o + M = \dot{q} I_y \quad \text{(A-6c)}$$

This linearization technique assumes small perturbations, so that a small angle approximation is used: $\cos\theta \cong 1$ and $\sin\theta \cong \theta$. We also assume the products of perturbation variables are negligible. Using these two approximations, Equations A-6 are

$$X_o + X = m[\dot{u} + Q_o W_o + Q_o w + W_o q + g\sin\theta_o + g\cos\theta_o \theta] \quad \text{(A-7a)}$$

$$Z_o + Z = m[\dot{w} - Q_o U_o - Q_o u - U_o q - g\cos\theta_o + g\sin\theta_o \theta] \quad \text{(A-7b)}$$

$$M_o + M = \dot{q} I_y \quad \text{(A-7c)}$$

Subtracting the trim expressions, Equations A-5, from Equations A-7 yields the linearized (perturbation) equations:

$$X = m[\dot{u} + Q_o w + W_o q + g\cos\theta_o \theta] \quad \text{(A-8a)}$$

$$Z = m[\dot{w} - Q_o u - U_o q + g\sin\theta_o \theta] \quad \text{(A-8b)}$$

$$M = \dot{q} I_y \quad \text{(A-8c)}$$

or,

$$\frac{X}{m} = \dot{u} + Q_o w + W_o q + g\cos\theta_o \theta \quad \text{(A-9a)}$$

$$\frac{Z}{m} = \dot{w} - Q_o u - U_o q + g\sin\theta_o \theta \quad \text{(A-9b)}$$

$$\frac{M}{I_y} = \dot{q} \quad \text{(A-9c)}$$

Recall that X, Z, amd M represent the perturbation aerodynamic and propulsive forces and moment.

The linearization of the inertial/body transformation yields the simple expression $q=\dot{\theta}$. This means that pitch attitude, θ, is the direct integral of pitch rate, q. Thus, the independent perturbation variables in the longitudinal degrees of freedom are

u, w, and q. With this in mind, we express X, Z, and M in terms of their sensitivities to changes in these independent state variables, and to changes in the longitudinal perturbation controls θ_c and B_{1s} (collective and cyclic, respectively):

$$X = \frac{\partial X}{\partial u}u + \frac{\partial X}{\partial w}w + \frac{\partial X}{\partial q}q + \frac{\partial X}{\partial \theta_c}\theta_c + \frac{\partial X}{\partial B_{1s}}B_{1s} \qquad \text{(A-10a)}$$

$$Z = \frac{\partial Z}{\partial u}u + \frac{\partial Z}{\partial w}w + \frac{\partial Z}{\partial q}q + \frac{\partial Z}{\partial \theta_c}\theta_c + \frac{\partial Z}{\partial B_{1s}}B_{1s} \qquad \text{(A-10b)}$$

$$M = \frac{\partial M}{\partial u}u + \frac{\partial M}{\partial w}w + \frac{\partial M}{\partial q}q + \frac{\partial M}{\partial \theta_c}\theta_c + \frac{\partial M}{\partial B_{1s}}B_{1s} \qquad \text{(A-10c)}$$

Dividing the force equations (X and Z) by m, and the moment equation (M) by I_y, the the resulting coefficients of the state variables are what are commonly referred to as the stability derivatives, and the control coefficents are the control derivatives.

$$\frac{X}{m} = \frac{1}{m}\frac{\partial X}{\partial u}u + \frac{1}{m}\frac{\partial X}{\partial w}w + \frac{1}{m}\frac{\partial X}{\partial q}q + \frac{1}{m}\frac{\partial X}{\partial \theta_c}\theta_c + \frac{1}{m}\frac{\partial X}{\partial B_{1s}}B_{1s}$$

$$= X_u u + X_w w + X_q q + X_{\theta_c}\theta_c + X_{B_{1s}}B_{1s} \qquad \text{(A-11a)}$$

$$\frac{Z}{m} = \frac{1}{m}\frac{\partial Z}{\partial u}u + \frac{1}{m}\frac{\partial Z}{\partial w}w + \frac{1}{m}\frac{\partial Z}{\partial q}q + \frac{1}{m}\frac{\partial Z}{\partial \theta_c}\theta_c + \frac{1}{m}\frac{\partial Z}{\partial B_{1s}}B_{1s}$$

$$= Z_u u + Z_w w + Z_q q + Z_{\theta_c}\theta_c + Z_{B_{1s}}B_{1s} \qquad \text{(A-11b)}$$

$$\frac{M}{I_y} = \frac{1}{I_y}\frac{\partial M}{\partial u}u + \frac{1}{I_y}\frac{\partial M}{\partial w}w + \frac{1}{I_y}\frac{\partial M}{\partial q}q + \frac{1}{I_y}\frac{\partial M}{\partial \theta_c}\theta_c + \frac{1}{I_y}\frac{\partial M}{\partial B_{1s}}B_{1s}$$

$$= M_u u + M_w w + M_q q + M_{\theta_c}\theta_c + M_{B_{1s}}B_{1s} \qquad \text{(A-11c)}$$

Equating Equations A-9 and A-11, collecting like terms and rearranging, yields

$$\dot{u} = X_u u + (X_w - Q_o)w + (X_q - W_o)q - g\cos\theta_o\theta + X_{\theta_c}\theta_c + X_{B_{1s}}B_{1s} \qquad \text{(A-12a)}$$

$$\dot{w} = (Z_o+U_o)u + Z_w w + (Z_q+U_o)q - g\sin\theta_o\theta + Z_{\theta c}\theta_c + Z_{B1s}B_{1s} \quad \text{(A-12b)}$$

$$\dot{q} = M_u u + M_w w + M_q q + M_{\theta c}\theta_c + M_{B1s}B_{1s} \quad \text{(A-12c)}$$

Writing Equations A-12 in matrix form, and including the dynamics for θ, we have a general expression for the linear longitudinal dynamics of the helicopter:

$$\begin{bmatrix} \dot{u} \\ \dot{w} \\ \dot{q} \\ \dot{\theta} \end{bmatrix} = \begin{bmatrix} X_u & X_u-Q_o & X_q-W_o & -g\cos\theta_o \\ Z_u+Q_o & Z_w & Z_q+U_o & -g\sin\theta_o \\ M_u & M_w & M_q & 0 \\ 0 & 0 & 1 & 0 \end{bmatrix} \begin{bmatrix} u \\ w \\ q \\ \theta \end{bmatrix}$$

$$+ \begin{bmatrix} X_{\theta c} & X_{B1s} \\ Z_{\theta c} & Z_{B1s} \\ M_{\theta c} & M_{B1s} \\ 0 & 0 \end{bmatrix} \begin{bmatrix} \theta_c \\ B_{1s} \end{bmatrix} \quad \text{(A-13)}$$

This matrix equation takes the form

$$\dot{\mathbf{x}} = \mathbf{A}\mathbf{x} + \mathbf{B}\mathbf{u} \quad \text{(A-14)}$$

where A is the stability derivative matrix, B is the control derivative matrix, **x** is the state vector, and **u** is the control vector.

$$\mathbf{x} = \begin{bmatrix} u \\ w \\ q \\ \theta \end{bmatrix} \qquad \mathbf{u} = \begin{bmatrix} \theta_c \\ B_{1s} \end{bmatrix}$$

$$\dot{w} = (Z_o + U_o)u + Z_w w + (Z_q + U_o)q - g\sin\theta_o \theta + Z_{\theta c}\theta_c + Z_{B1s}B_{1s} \quad \text{(A-12b)}$$

$$\dot{q} = M_u u + M_w w + M_q q + M_{\theta c}\theta_c + M_{B1s}B_{1s} \quad \text{(A-12c)}$$

Writing Equations A-12 in matrix form, and including the dynamics for θ, we have a general expression for the linear longitudinal dynamics of the helicopter:

$$\begin{bmatrix} \dot{u} \\ \dot{w} \\ \dot{q} \\ \dot{\theta} \end{bmatrix} = \begin{bmatrix} X_u & X_u - Q_o & X_q - W_o & -g\cos\theta_o \\ Z_u + Q_o & Z_w & Z_q + U_o & -g\sin\theta_o \\ M_u & M_w & M_q & 0 \\ 0 & 0 & 1 & 0 \end{bmatrix} \begin{bmatrix} u \\ w \\ q \\ \theta \end{bmatrix} + \begin{bmatrix} X_{\theta c} & X_{B1s} \\ Z_{\theta c} & Z_{B1s} \\ M_{\theta c} & M_{B1s} \\ 0 & 0 \end{bmatrix} \begin{bmatrix} \theta_c \\ B_{1s} \end{bmatrix} \quad \text{(A-13)}$$

This matrix equation takes the form

$$\dot{\mathbf{x}} = \mathbf{A}\mathbf{x} + \mathbf{B}\mathbf{u} \quad \text{(A-14)}$$

where A is the stability derivative matrix, B is the control derivative matrix, $\mathbf{x}$ is the state vector, and $\mathbf{u}$ is the control vector.

$$\mathbf{x} = \begin{bmatrix} u \\ w \\ q \\ \theta \end{bmatrix} \qquad \mathbf{u} = \begin{bmatrix} \theta_c \\ B_{1s} \end{bmatrix}$$

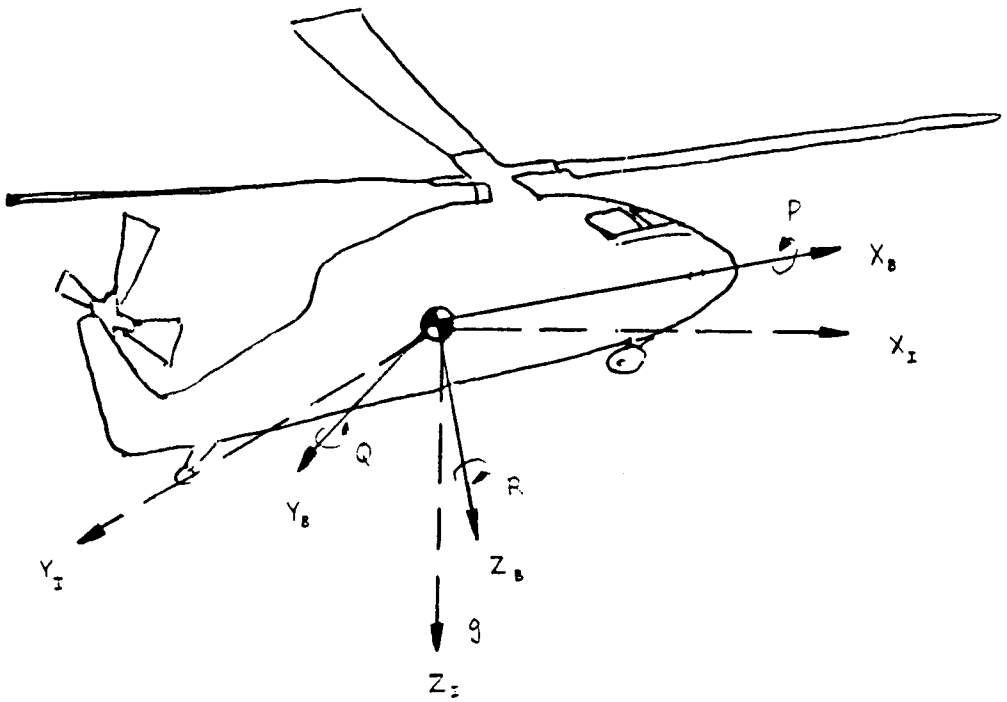

Figure A-1: Body Axis System

Appendix B

AH-1G Stability/Control Derivatives and Scheduling

	trim			stability and control derivatives			
#	U_o	W_o	θ_o	X_u	X_w	X_q	Z_u
1	1.69	[illegible]	-0.73	-0.0276	-0.0164	1.[illegible]	-0.1208
2	16.87	-0.33	-1.1	-0.0276	-0.0164	1.2985	-0.208
3	33.74	-0.93	-1.59	-0.0276	-0.0164	1.2985	-0.2485
4	67.48	-2.13	-1.81	-0.0276	-0.0164	1.2986	-0.1638
5	101.19	-3.98	-2.25	-0.0276	-0.0164	1.2986	-0.106
6	134.87	-6.35	-2.71	-0.0276	-0.0164	1.2986	-0.0731
7	168.49	-9.83	-3.34	-0.0276	-0.0164	1.2986	-0.052
8	201.96	-14.97	-4.24	-0.0276	-0.0164	1.2986	-0.0387
9	235.19	-22.82	-5.54	-0.0276	-0.0164	1.2986	-0.0294
10	1.38	-27.95	2.83	-0.0276	-0.0164	1.2986	-0.0497
11	94.21	-37.12	1.13	-0.0276	-0.0164	1.2986	-0.0444
12	164.47	-37.86	-1.04	-0.0276	-0.0164	1.2986	-0.0148
13	98.26	24.51	-3.86	-0.0276	-0.0164	1.2986	-0.1501
14	167.24	22.75	-5.09	-0.0276	-0.0164	1.2986	-0.0969
15	0.23	10	-1.26	-0.0276	-0.0164	1.2986	-0.0979
16	0.6	19.99	-1.72	-0.0276	-0.0164	1.2986	-0.1162
17	0.02	-10	0.11	-0.0276	-0.0164	1.2986	-0.067
18	0.45	-19.99	1.4	-0.0276	-0.0164	1.2986	-0.0555
19	98.9	-21.79	-1.04	-0.0276	-0.0164	1.2986	-0.0801
20	100.43	-13.04	-1.73	-0.0276	-0.0164	1.2986	-0.094
21	101.14	5.27	-2.65	-0.0276	-0.0164	1.2986	-0.1176
22	100.22	14.56	-3.13	-0.0276	-0.0164	1.2986	-0.1296

#	Z_w	Z_q	M_u	M_w	M_q	$X_{\theta c}$	X_{Bls}
1	-0.6786	-1.38	5E-4	-3.3E-3	-0.2345	-0.256	1.296
2	-0.406	-1.38	2E-4	-2.6E-3	-0.2289	-0.261	1.296
3	-0.5022	-1.38	4E-4	-1.8E-3	-0.2289	-0.4393	1.296
4	-0.7094	-1.38	1.7E-3	-2.3E-3	-0.2805	-0.5435	1.296
5	-0.6377	-1.38	1.9E-3	-3E-3	-0.3244	-0.6761	1.296
6	-0.5243	-1.38	2.2E-3	-4.2E-3	-0.3656	-0.6883	1.296
7	-0.9517	-1.38	2.6E-3	-5.8E-3	-0.3849	-0.6101	1.296
8	-1.0451	-1.38	2.9E-3	-8E-3	-0.4074	-0.4126	1.296
9	-1.0862	-1.38	3.4E-3	-0.0106	-0.4162	-0.1154	1.296
10	-0.5069	-1.38	-1E-4	-0.0135	-0.3009	0.6176	1.296
11	-0.8153	-1.38	8E-4	-0.0144	-0.2218	0.1958	1.296
12	-0.9681	-1.38	3.4E-3	-0.0105	-0.2293	0.0992	1.296
13	-0.7429	-1.38	1.4E-3	-5.7E-3	-0.4218	-0.9503	1.296
14	-0.9799	-1.38	1.2E-3	-8E-3	-0.5269	-1.1951	1.296
15	-0.84	-1.38	1.8E-3	-3.2E-3	-0.2888	-0.2499	1.296
16	-0.3045	-1.38	3.4E-3	-3.3E-3	-0.3153	-0.395	1.296
17	-0.4134	-1.38	7E-4	-6.1E-3	-0.2564	5.6E-3	1.296
18	-0.4633	-1.38	4E-4	-9.8E-3	-0.279	0.2091	1.296
19	-0.8255	-1.38	2.4E-3	-5.3E-3	-0.2421	-0.3293	1.296
20	-0.8305	-1.38	2.2E-3	-3.8E-3	-0.2836	-0.5114	1.296
21	-0.8337	-1.38	1.7E-3	-2.9E-3	-0.3663	-0.7519	1.296
22	-0.828	-1.38	1.3E-3	-2.5E-3	-0.396	-0.8992	1.296

#	$Z_{\theta c}$	Z_{Bls}	$M_{\theta c}$	M_{Bls}
1	-12.761	0.1799	7.6E-3	-0.1624
2	-12.359	0.427	8.5E-3	-0.1624
3	-12.166	0.8473	0.0259	-0.1624
4	-13.284	1.8147	0.0804	-0.1624
5	-15.009	2.9518	0.0267	-0.1624
6	-16.435	4.2224	0.0195	-0.1624
7	-17.99	5.5388	6.2E-3	-0.1624
8	-18.728	6.8995	-0.0206	-0.1624
9	-19.793	8.4228	-0.0621	-0.1624
10	-13.207	0.1308	-0.0871	-0.1624
11	-15.043	2.8635	-0.052	-0.1624
12	-17.489	5.4483	-0.0574	-0.1624
13	-14.605	2.6669	0.0735	-0.1624
14	-17.256	5.3634	0.067	-0.1624
15	-12.794	0.1131	-2.9E-3	-0.1624
16	-12.687	0.1661	0.014	-0.1624
17	-12.811	0.1569	-0.0203	-0.1624
18	-12.99	0.1432	-0.0556	-0.1624
19	-15.085	2.972	1.3E-3	-0.1624
20	-15.034	2.9918	0.0153	-0.1624
21	-14.838	2.9607	0.0337	-0.1624
22	-14.677	2.8437	0.0475	-0.1624

Scheduling

The stability and control derivatives were scheduled according to the flight velocities U and W. Modal analyses [3,27] showed that the derivatives X_u, X_w, X_q, Z_q, X_{B1s}, and M_{B1s}, and variations in these derivatives, did not significantly affect the open-loop dynamic characteristics of the AH-1G. Thesefore, the average value of each derivative over the twenty-two trim conditions listed in Reference 1 was used throughout the entire flight envelope (see data above).

The remaining stability and control derivatives were scheduled in a two-dimensional format by first curve-fitting the derivatives with respect to U, and then with respect to W. That is, they were scheduled as functions of U and W. Curve-fitting was either linear or quadratic, and the function for one derivative may have been composed of several distinct curves; all functions were continuous for all U and W.

These non-constant derivatives were easily scheduled as functions of U by fitting curves to the data points. This method was also employed for scheduling with respect to W, except for the M_u, M_w, M_q, and Z_w derivatives. Because these derivatives varied considerably for different values of W, and because of the limited data set, curve-fitting was not directly possible. To facilitate scheduling, the effect of flight condition on these derivatives was rationalized by examining the equations that describe them in terms of their contributing aerodynamic forces and moments. By rationalizing the effects of flight velocities on rotor inflow, rotor angle of attack, thrust coefficient, and rotor flap, and

then looking at their effects on the derivatives, the derivatives were written as functions of U and W.

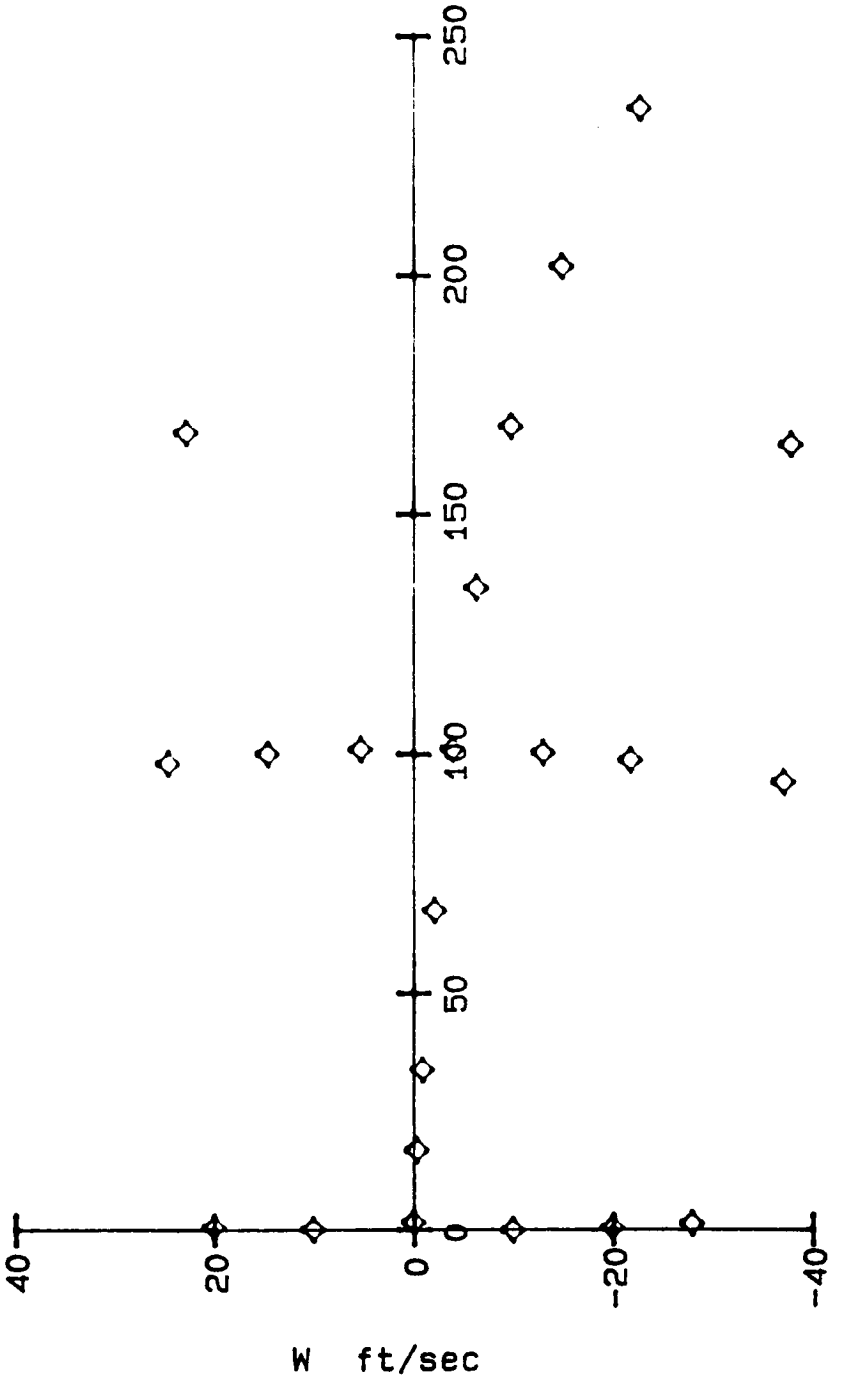

Figure B-1: Trim points in the U-W plane (Ref 1)

Appendix C

Solution of the Steady-state Riccati Equation

Reference [26] provides a detailed description of the following diagonalization procedure for solving the steady-state Riccati equation.

The equation has the form $\dot{P} = -PM - M^T P + PNP + K$ and a solution is sought for P at steady-state, i.e., when $\dot{P} = 0$. M, N, K, and P have dimension $n \times n$.

Define the $2n \times 2n$ matrix

$$Z = \begin{bmatrix} M & -N \\ K & -M^T \end{bmatrix}$$

It is assumed that Z has 2n distinct eigenvalues. For each eigenvalue λ, there is an eigenvalue $-\lambda$; none of the eigenvalues have zero real parts. The eigenvalues of Z which are negative (stable), are the eigenvalues of the steady-state closed-loop optimal controller. The diagonal modal matrix Λ contains the eigenvalues of Z with positive real parts. Z can be diagonalized as

$$Z = W \begin{bmatrix} \Lambda & 0 \\ 0 & -\Lambda \end{bmatrix} W^{-1}$$

Partitioning W into $n \times n$ submatrices, $W = \begin{bmatrix} W_{11} & W_{12} \\ W_{21} & W_{22} \end{bmatrix}$,

the steady-state solution of the Riccati equation is

$$P = W_{22} W_{12}^{-1}$$

Appendix D

Controller Gains at All Trim Points

Trim numbers correspond to those in Appendix B. Numbers in the "Q" and "R" columns refer to the number which designates the Q and R weighting matrices used to develop the controller; these numbered matrices are listed at the end of the appendix.

Implicit Controller -- conventional helicopter (no auxiliary prop)

#	$C_{1_{1,1}}$	$C_{1_{1,2}}$	$C_{1_{1,3}}$	$C_{1_{1,4}}$	$C_{1_{2,1}}$	$C_{1_{2,2}}$	$C_{1_{2,3}}$
1	9.55E-3	4.17E-3	-0.0302	-0.0477	0.2923	-0.0122	0.3504
2	0.01662	9.655E-3	-1.243	-0.06829	0.2941	-0.0105	8.203E-3
3	0.03358	0.01581	-2.622	-1.199	0.3015	-8.238E-3	0.7826
4	0.05413	0.02534	-5.021	-3.745	0.3083	-2.441E-3	-1.077
5	0.07353	0.03492	-8.262	-6.383	0.3115	6.515E-3	-7.383
6	0.0947	0.03558	-8.224	-8.127	0.3282	8.231E-3	-0.01948
7	0.1115	0.03603	-9.723	-10.24	0.3294	1.433E-3	-0.6637
8	0.1225	0.03557	-11.7	-12.59	0.3245	-2.035E-3	-2.916
9	0.1284	0.03388	-14.56	-15.42	0.3121	-7.613E-3	-7.278
10	0.01043	9.809E-3	0.02087	-0.5927	0.199	6.743E-3	-16.08
11	0.06234	0.02736	-11.32	-9.278	0.2749	-0.01911	-25.13
12	0.09309	0.02893	-16.4	-14.78	0.2819	-0.0189	-21.76
13	0.08491	0.03714	-12.52	-6.397	0.3615	0.02046	-28.98
14	0.137	0.04391	-20.7	-11.43	0.4047	0.02565	-34.46
15	8.51E-3	4.082E-4	0.09057	-0.05538	0.2921	-0.0129	-6.865
16	9.563E-3	-2.562E-3	0.06279	-0.07279	0.2937	-0.01394	-14.61
17	7.079E-3	6.631E-3	0.1123	-0.05975	0.173	3.634E-3	-8.845
18	8.836E-3	8.828E-3	0.07595	-0.3259	0.2035	2.144E-3	-12.25
19	0.06854	0.03131	-9.46	-7.975	0.2978	-7.93E-3	-13.76
20	0.07209	0.03302	-8.109	-7.032	0.3097	-1.72E-3	-6.807
21	0.07934	0.03552	-8.465	-6.141	0.335	9.317E-3	-8.349
22	0.08238	0.03646	-10.44	-6.295	0.3479	0.01481	-18.07

#	$C1_{2,4}$	$C1_{3,1}$	$C1_{3,2}$	$C1_{3,3}$	$C1_{3,4}$	$C2_{1,1}$	$C2_{1,2}$
1	-25.35	0	0	0	0	0.02595	-3.6E-3
2	-25.41	0	0	0	0	0.02356	0.02183
3	-25.6	0	0	0	0	0.02738	-0.01271
4	-26.92	0	0	0	0	0.02486	-0.02683
5	-29.72	0	0	0	0	0.02272	-0.0740?
6	-29.21	0	0	0	0	0.02322	-0.117?
7	-30.94	0	0	0	0	0.0211	-0.1624
8	-33.29	0	0	0	0	0.01782	-0.2073
9	-36.64	0	0	0	0	0.0144	-0.2397
10	-25.5	0	0	0	0	0.02804	-1.594E-3
11	-45.27	0	0	0	0	0.01471	-0.1114
12	-45	0	0	0	0	0.01019	-0.1815
13	-30.36	0	0	0	0	0.02718	-0.0774?
14	-34.53	0	0	0	0	0.0259	-0.1402
15	-25.1	0	0	0	0	0.02583	5.285E-4
16	-25.09	0	0	0	0	0.02573	1.662E-3
17	-26.62	0	0	0	0	0.02631	-2.336E-4
18	-27.16	0	0	0	0	0.02716	-9.694E-4
19	-37.86	0	0	0	0	0.02081	-0.1173
20	-38.01	0	0	0	0	0.02364	-0.1134
21	-29.53	0	0	0	0	0.02545	-0.07628
22	-29.43	0	0	0	0	0.02629	-0.07727

#	$C2_{2,1}$	$C2_{2,2}$	$C2_{3,1}$	$C2_{3,2}$	Q	R
1	3.917E-3	-0.257	0	0	1	11
2	4.906E-3	-0.2505	0	0	1	11
3	7.799E-3	-0.285	0	0	4	11
4	5.234E-3	-0.287	0	0	5	11
5	2.668E-3	-0.3496	0	0	5	12
6	0.01059	-0.4275	0	0	5	12
7	7.173E-3	-0.4947	0	0	5	12
8	1.157E-3	-0.5547	0	0	5	12
9	-4.326E-3	-0.5805	0	0	5	12
10	-6.975E-4	-0.3792	0	0	1	11
11	-0.03831	-0.5655	0	0	6	12
12	-0.02571	-0.5637	0	0	6	13
13	0.02358	-0.3762	0	0	6	13
14	0.0217	-0.4293	0	0	6	13
15	5.633E-3	-0.3091	0	0	1	11
16	9.491E-3	-0.3117	0	0	1	11
17	-2.506E-3	-0.2506	0	0	6	13
18	-4.443E-4	-0.3733	0	0	1	11
19	-6.446E-3	-0.5662	0	0	6	13
20	7.036E-3	-0.539	0	0	6	13
21	0.01558	-0.3601	0	0	6	13
22	0.01945	-0.3681	0	0	6	13

Explicit Controller -- conventional helicopter (no auxiliary prop)

#	$C1_{1,1}$	$C1_{1,2}$	$C1_{1,3}$	$C1_{1,4}$	$C1_{2,1}$	$C1_{2,2}$	$C1_{2,3}$
1	8.1E-4	-0.0418	-4.23E-3	-0.0187	4.44	-0.109	-5.83
2	-0.0852	-4.43	-1.05	0.261	4.44	-0.127	-5.93
3	0.0341	-4.43	-2.7	-1.2	4.44	-1.25E-4	-6.55
4	0.332	-4.41	-5.58	-5.08	4.44	0.318	-7.53
5	0.587	-4.38	-8.03	-8.94	4.41	0.589	-8.53
6	0.11	-0.377	-8.92	-4.32	9.58	2.37	-140
7	0.155	-0.362	-10.9	-6.73	9.22	3.34	-163
8	0.2	-0.344	-12.4	-9.74	8.76	4.23	-177
9	0.241	-0.327	-13.7	-14.1	8.21	5.04	-181
10	1.04	-4.44	6.45	-35.6	4.1	0.215	-20.1
11	0.157	-0.386	-5.42	-9.39	9.12	1.34	-108
12	0.222	-0.36	-10	-16.8	8.52	3.49	-161
13	0.0353	-0.386	-6.58	-0.845	9.95	0.655	-118
14	0.108	-0.368	-11.3	-2.64	9.63	2.46	-194
15	-0.0764	-4.44	0.142	-0.0175	4.45	-0.0932	-9.5
16	-0.16	-4.45	0.147	0.0612	4.45	-0.171	-14.5
17	0.221	-4.44	1.34	-3.95	4.38	0.0489	-9.36
18	0.615	-4.44	3.76	-16.4	4.26	0.137	-15.2
19	0.0915	-0.386	-6.29	-4.69	9.64	1.34	-106
20	0.0721	-0.387	-6.57	-3.19	9.76	1.34	-106
21	0.0553	-0.386	-6.7	-1.57	9.87	1.12	-111
22	0.0463	-0.386	-6.69	-1.13	9.91	0.91	-115

#	$C1_{2,4}$	$C1_{3,1}$	$C1_{3,2}$	$C1_{3,3}$	$C1_{3,4}$	$C2_{1,1}$	$C2_{1,2}$
1	-42.9	0	0	0	0	7.41E-3	0.422
2	-43.3	0	0	0	0	0.103	4.44
3	-45.8	0	0	0	0	-1.53E-3	4.44
4	-43.2	0	0	0	0	-0.265	4.43
5	-51.6	0	0	0	0	-0.484	4.41
6	-293	0	0	0	0	-0.0694	0.409
7	-385	0	0	0	0	-0.0959	0.399
8	-379	0	0	0	0	-0.117	0.377
9	-446	0	0	0	0	-0.126	0.355
10	-259	0	0	0	0	-0.713	4.34
11	-752	0	0	0	0	-0.0791	0.401
12	-714	0	0	0	0	-0.0947	0.374
13	-103	0	0	0	0	-0.0202	0.419
14	-148	0	0	0	0	-0.0809	0.409
15	-26.1	0	0	0	0	0.0847	4.45
16	-22.3	0	0	0	0	0.168	4.44
17	-109	0	0	0	0	-0.17	4.44
18	-189	0	0	0	0	-0.448	4.41
19	-497	0	0	0	0	-0.0473	0.414
20	-365	0	0	0	0	-0.0394	0.417
21	-180	0	0	0	0	-0.0356	0.419
22	-133	0	0	0	0	-0.0292	0.418

#	$C_{2_{1,3}}$	$C_{2_{1,4}}$	$C_{2_{2,1}}$	$C_{2_{2,2}}$	$C_{2_{2,3}}$	$C_{2_{2,4}}$	$C_{2_{3,1}}$
1	0	0	-3.97	0.075	0	0	0
2	3.65E-5	-2.18E-4	-3.97	0.0989	-6.9E-3	1.5E-4	0
3	-1.37E-4	-1.64E-4	-3.95	-0.0286	-6.9E-3	1.41E-4	0
4	-6.59E-4	-1.21E-4	-3.91	-0.385	-6.89E-3	8.5E-5	0
5	-1.11E-3	-9.33E-5	-3.85	-0.601	-6.84E-3	6.44E-5	0
6	-3.85E-5	-2.07E-6	-6.71	-2.46	-2.96E-3	4.42E-5	0
7	-5.32E-5	-3.26E-6	-6.09	-3.53	-2.85E-3	5.85E-5	0
8	-6.67E-5	-4.58E-6	-5.38	-4.51	-2.71E-3	7.86E-5	0
9	-7.87E-5	-5.08E-6	-4.94	-5.42	-2.56E-3	8.92E-5	0
10	-1.02E-3	-7.45E-4	-2.09	-0.837	-6.55E-3	4.1E-4	0
11	-3.73E-5	-1.29E-5	-3.29	-2.81	-2.89E-3	1.39E-4	0
12	-6.39E-5	-9.06E-6	-2.95	-4.58	-2.71E-3	1.29E-4	0
13	-1.47E-5	-4.74E-7	-8.81	-0.61	-3.05E-3	3.26E-5	0
14	-3.93E-5	-2.21E-7	-8.08	-2.38	-2.91E-3	5.13E-5	0
15	-1.09E-4	-2.62E-4	-4.16	0.0801	-6.91E-3	7.38E-5	0
16	-8.52E-5	-2.56E-4	-4.2	0.162	-6.92E-3	8.05E-5	0
17	-3.18E-4	-4E-4	-3.32	-0.199	-6.86E-3	1.8E-4	0
18	-6.64E-4	-6.04E-4	-2.61	-0.522	-6.73E-3	2.83E-4	0
19	-2.78E-5	-6.08E-6	-5.26	-1.88	-3.01E-3	5.64E-5	0
20	-2.44E-5	-2.81E-6	-6.33	-1.54	-3.04E-3	4.11E-5	0
21	-2.09E-5	-1.39E-6	-7.99	-1.14	-3.05E-3	3.64E-5	0
22	-1.82E-5	-9.31E-7	-8.47	-0.89	-3.05E-3	3.49E-5	0

#	$C_{2_{3,2}}$	$C_{2_{3,3}}$	$C_{2_{3,4}}$	$C_{3_{1,1}}$	$C_{3_{1,2}}$	$C_{3_{2,1}}$	$C_{3_{2,2}}$
1	0	0	0	-0.0245	-6.22E-4	-0.0106	0.496
2	0	0	0	-0.0264	-3.07E-3	-7.09E-3	0.499
3	0	0	0	-0.0272	0.0132	-9.1E-3	0.526
4	0	0	0	-0.0257	0.0572	-0.0126	0.551
5	0	0	0	-0.025	0.101	-0.0163	0.587
6	0	0	0	-0.0198	0.0416	-0.0186	2.98
7	0	0	0	-0.0174	0.0638	0.0152	3.25
8	0	0	0	-0.0144	0.0899	0.0675	3.54
9	0	0	0	-0.0105	0.124	0.125	3.95
10	0	0	0	-3.16E-3	0.354	0.23	2.26
11	0	0	0	-0.0131	0.0791	0.676	6.07
12	0	0	0	-5.66E-3	0.134	0.494	5.64
13	0	0	0	-0.0231	7.24E-3	-0.0341	1.17
14	0	0	0	-0.02	0.0264	-0.0233	1.63
15	0	0	0	-0.0259	-3.15E-4	-4.91E-3	0.311
16	0	0	0	-0.0258	-1.71E-3	-8.12E-3	0.268
17	0	0	0	-0.0263	0.0479	0.0185	1.15
18	0	0	0	-0.0215	0.177	0.103	1.82
19	0	0	0	-0.02	0.0426	0.101	4.53
20	0	0	0	-0.0212	0.09	-0.0132	3.55
21	0	0	0	-0.0221	0.0152	-0.0329	1.94
22	0	0	0	-0.0225	0.0107	-0.0329	1.48

#	$C_{3_{3,1}}$	$C_{3_{3,2}}$	Q	R
1	0	0	7	12
2	0	0	7	12
3	0	0	7	12
4	0	0	7	12
5	0	0	7	12
6	0	0	7	12
7	0	0	7	12
8	0	0	7	12
9	0	0	7	12
10	0	0	7	12
11	0	0	7	12
12	0	0	7	12
13	0	0	7	12
14	0	0	7	12
15	0	0	7	12
16	0	0	7	12
17	0	0	7	12
18	0	0	7	12
19	0	0	7	12
20	0	0	7	12
21	0	0	7	12
22	0	0	7	12

Implicit Controller -- auxiliary propulsion installed

#	$C_{1_{1,1}}$	$C_{1_{1,2}}$	$C_{1_{1,3}}$	$C_{1_{1,4}}$	$C_{1_{2,1}}$	$C_{1_{2,2}}$	$C_{1_{2,3}}$
1	9.48E-3	4.28E-3	-0.0244	-0.0824	0.1979	0.01949	-21.54
2	0.01662	9.775E-3	-1.245	-0.04958	0.2277	-5.608E-3	-6.653
3	0.03029	0.01605	-2.989	-1.037	0.2257	-2.71E-3	-7.694
4	0.04102	0.02646	-6.228	-3.032	0.2118	5.379E-3	-9.912
5	0.05066	0.03677	-9.2	-4.652	0.2007	0.01519	-11.81
6	0.03678	0.04065	-10.95	-3.832	0.1067	0.02182	-9.955
7	0.03479	0.04451	-12.62	-4.525	0.09887	0.02724	-9.506
8	0.03393	0.04824	-13.9	-5.082	0.08824	0.03179	-8.84
9	0.02906	0.04947	-15.04	-5.428	0.07026	0.0301	-8.468
10	4.471E-3	0.01266	-6.287E-5	0.1246	0.1279	0.0233	-16.11
11	0.0144	0.04181	-9.421	-2.585	0.04681	0.04946	-15.56
12	0.0142	0.04758	-13.67	-4.231	0.04314	0.03758	-13.39
13	0.04073	0.03968	-10.27	-3.037	0.1469	0.03279	-18.03
14	0.05051	0.04986	-15.77	-4.738	0.1396	0.04368	-19.34
15	8.58E-3	4.164E-4	0.09156	-0.05577	0.2415	-9.153E-3	-9.264
16	9.668E-3	-2.58E-3	0.06169	-0.07606	0.2488	-0.01064	-14.73
17	6.409E-3	6.949E-3	0.1073	4.588E-3	0.191	-1.654E-3	-8.397
18	5.329E-3	0.01025	0.07021	0.06144	0.1543	0.01045	-13.39
19	0.02215	0.03842	-8.955	-2.831	0.07739	0.02584	-11.44
20	0.02615	0.03716	-8.803	-2.852	0.09217	0.01791	-10.18
21	0.03538	0.03851	-9.122	-3.022	0.1274	0.02347	-11.46
22	0.03834	0.03923	-9.637	-3.038	0.1381	0.02802	-14.22

#	$C1_{2,4}$	$C1_{3,1}$	$C1_{3,2}$	$C1_{3,3}$	$C1_{3,4}$	$C2_{1,1}$	$C2_{1,2}$
1	-25.59	0.07365	-0.02043	12.81	-1.421	0.02607	-7E-6
2	-22.05	0.05949	-4.849E-3	4.238	-3.559	0.02659	-6.42E-6
3	-22.02	0.06366	-4.698E-3	4.777	-3.772	0.02492	-0.08034
4	-21.71	0.07656	-5.852E-3	5.631	-4.498	0.01682	-0.05089
5	-21.55	0.08795	-7.3E-3	6.357	-5.236	0.01118	-0.06884
6	-13.6	0.1262	-0.01051	7.05	-8.325	-0.03099	2.284
7	-13.46	0.1304	-0.01433	8.4	-8.473	0.05719	1.07
8	-13.26	0.1355	-0.01865	10.86	-8.489	0.1393	0.9777
9	-12.77	0.1277	-0.01949	12.39	-8	0.01054	-0.06933
10	-22.14	0.1122	-0.03017	24.54	-3.573	0.02607	-4.721E-5
11	-13.31	0.1551	-0.04062	29.17	-7.445	-9.713E-3	-0.01998
12	-13.02	0.1576	-0.03276	28.12	-7.639	-0.03292	-0.08462
13	-14.04	0.1137	-6.533E-3	-5.801	-8.647	-0.09121	0.7143
14	-14.02	0.1234	-8.484E-3	-7.039	-9.548	-0.02845	0.4546
15	-22.08	0.05108	-4.688E-3	0.7705	-3.556	0.02603	1.352E-6
16	-22.08	0.0482	-4.483E-3	-1.13	-3.556	0.02604	2.118E-5
17	-22.1	0.07763	-0.01042	10.19	-3.563	0.02603	-2.189E-5
18	-22.12	0.09769	-0.02021	17.94	-3.569	0.02604	-3.603E-5
19	-13.47	0.1366	-0.01933	17.53	-7.751	7.224E-4	-0.08507
20	-13.25	0.1156	-0.01013	9.342	-7.464	0.01902	-0.08873
21	-13.73	0.117	-7.979E-3	1.77	-8.294	-0.09349	1.159
22	-13.91	0.1146	-7.217E-3	-2.097	-8.476	-0.07782	0.7704

#	$C2_{2,1}$	$C2_{2,2}$	$C2_{3,1}$	$C2_{3,2}$	Q	R
1	-0.01558	0.4559	0.01263	-0.443	2	10
2	-0.03314	-0.5343	0.02172	0.1041	2	10
3	-0.05089	-0.4647	0.03118	0.06254	2	10
4	-0.05531	-0.3735	0.03303	5.121E-3	2	10
5	-0.05177	-0.3248	0.03073	-0.02845	2	10
6	-0.1366	8.125	0.1336	-5.896	2	10
7	0.117	3.26	-0.081	-2.537	2	10
8	0.3259	2.615	-0.2382	-2.147	2	10
9	-0.01393	-0.169	0.0254	-6.973E-3	2	10
10	0.02353	-0.5298	-9.823E-3	0.08622	2	10
11	-0.1635	-0.1012	0.1433	-0.1687	3	14
12	-0.1609	-0.1074	0.1415	-0.159	3	14
13	-0.5514	3.469	0.3747	-2.511	3	14
14	-0.1449	1.393	0.09903	-1.124	3	14
15	-0.06283	-0.229	0.03793	-0.0614	2	10
16	-0.2276	0.5566	0.13	-0.494	2	10
17	0.01641	-0.5542	-7.228E-3	0.1095	2	10
18	0.02011	-0.5381	-8.794E-3	0.09475	2	10
19	-0.1041	-0.4105	0.08335	0.08597	3	14
20	-0.0151	-0.1841	0.01273	0.01117	3	14
21	-0.5458	5.467	0.3721	-3.88	3	14
22	-0.4765	3.669	0.3221	-2.634	3	14

Explicit Controller -- auxiliary propulsion installed

#	$C1_{1,1}$	$C1_{1,2}$	$C1_{1,3}$	$C1_{1,4}$	$C1_{2,1}$	$C1_{2,2}$	$C1_{2,3}$
1	-0.116	-0.47	0.181	0.489	-0.82	-1.61	-28.6
2	-0.589	-3.12	-1.01	0.997	-55.5	0.299	-38.3
3	-1.46	-3.1	-3.42	-0.997	-55	1.93	-38.5
4	-3.34	-2.92	-8.05	-3.92	-51.9	5.38	-35.7
5	-4.67	-2.69	-11.6	-5.9	-47.7	7.81	-36.9
6	0.11	-0.377	-8.92	-4.32	9.58	2.37	-140
7	0.155	-0.362	-10.9	-6.73	9.23	3.34	-163
8	0.2	-0.344	-12.4	-9.74	8.76	4.23	-177
9	0.241	-0.327	-13.7	-14.1	8.21	5.04	-181
10	0.845	-3.12	0.0171	0.0165	-59.9	-0.69	-45.7
11	0.157	-0.386	-5.42	-9.39	9.12	1.24	-108
12	0.222	-0.36	-10	-16.8	8.52	3.49	-161
13	0.0353	-0.386	-6.58	-0.845	9.95	0.655	-118
14	0.108	-0.369	-11.3	-2.64	9.63	2.46	-194
15	-0.624	-3.13	0.187	0.152	-52.2	0.415	-37
16	-1.08	-3.13	0.478	0.512	-47.8	0.44	-49.3
17	0.178	-3.13	0.0763	-0.116	-57.8	-0.0563	-38.3
18	0.552	-3.12	0.0598	-0.0614	-59.2	-0.385	-39.3
19	0.0915	-0.386	-6.29	-4.69	9.64	1.34	-106
20	0.0721	-0.387	-6.57	-3.19	9.76	1.34	-106
21	0.0558	-0.386	-6.7	-1.57	9.87	1.12	-111
22	0.0462	-0.386	-6.68	-1.13	9.91	0.91	-115

#	$C1_{2,4}$	$C1_{3,1}$	$C1_{3,2}$	$C1_{3,3}$	$C1_{3,4}$	$C2_{1,1}$	$C2_{1,2}$
1	-36.5	2.93	-0.0273	15.4	14.3	0.119	0.473
2	-50.6	63.2	-0.429	22.7	20.9	0.6	3.13
3	-50.3	62.7	-1.64	23.5	20.6	1.51	3.11
4	-46.3	59.9	-5.15	24.7	18.9	3.38	2.95
5	-45.4	56.1	-7.44	25.3	16.4	4.72	2.73
6	-299	0	0	0	0	-0.0694	0.409
7	-335	0	0	0	0	-0.0959	0.398
8	-379	0	0	0	0	-0.117	0.377
9	-446	0	0	0	0	-0.126	0.355
10	-43.5	66.2	0.775	43.1	13	-0.84	3.13
11	-752	0	0	0	0	-0.0791	0.401
12	-714	0	0	0	0	-0.0947	0.374
13	-103	0	0	0	0	-0.0202	0.419
14	-148	0	0	0	0	-0.0809	0.409
15	-54.9	60.7	-0.528	22.7	25.9	0.631	3.13
16	-60	57.2	-0.681	29.1	31.9	1.09	3.13
17	-47.1	64.9	0.0975	27.3	17	-0.171	3.14
18	-44.8	65.8	0.471	35.5	14.4	-0.546	3.13
19	-497	0	0	0	0	-0.0473	0.414
20	-365	0	0	0	0	-0.0394	0.417
21	-180	0	0	0	0	-0.0356	0.418
22	-133	0	0	0	0	-0.0292	0.418

#	$C_{2_{1,3}}$	$C_{2_{1,4}}$	$C_{2_{2,1}}$	$C_{2_{2,2}}$	$C_{2_{2,3}}$	$C_{2_{2,4}}$	$C_{2_{3,1}}$
1	0	0	1.14	0.0184	0	0	-3.02
2	0	0	55.9	-0.272	0	0	-63.3
3	0	0	55.5	-1.91	0	0	-62.9
4	0	0	52.3	-5.35	0	0	-60
5	0	0	48.1	-7.75	0	0	-56.2
6	-3.85E-5	-2.07E-6	-6.71	-2.48	-2.96E-3	4.42E-5	0
7	-5.32E-5	-3.26E-6	-6.09	-3.53	-2.85E-3	5.85E-5	0
8	-6.67E-5	-4.58E-6	-5.33	-4.51	-2.71E-3	7.86E-5	0
9	-7.97E-5	-5.08E-6	-4.34	-5.42	-2.56E-3	8.92E-5	0
10	0	0	60.1	0.754	0	0	-66.2
11	-3.73E-5	-1.28E-5	-3.28	-2.81	-2.89E-3	1.39E-4	0
12	-6.39E-5	-9.06E-6	-2.95	-4.58	-2.71E-3	1.29E-4	0
13	-1.47E-5	-4.74E-7	-8.81	-0.61	-3.05E-3	3.26E-5	0
14	-3.93E-5	-2.21E-7	-8.08	-2.38	-2.91E-3	5.13E-5	0
15	0	0	52.7	-0.396	0	0	-61
16	0	0	48.4	-0.425	0	0	-57.5
17	0	0	58.2	0.0982	0	0	-64.9
18	0	0	59.5	0.458	0	0	-65.8
19	-2.78E-5	-6.08E-6	-5.26	-1.88	-3.01E-3	5.84E-5	0
20	-2.44E-5	-2.81E-6	-6.33	-1.54	-3.04E-3	4.11E-5	0
21	-2.09E-5	-1.39E-6	-7.99	-1.14	-3.05E-3	3.64E-5	0
22	-1.82E-5	-9.31E-7	-8.47	-0.89	-3.05E-3	3.46E-5	0

#	$C_{2_{3,2}}$	$C_{2_{3,3}}$	$C_{2_{3,4}}$	$C_{3_{1,1}}$	$C_{3_{1,2}}$	$C_{3_{2,1}}$	$C_{3_{2,2}}$
1	0.119	0.473	0	0	1.14	0.0184	0
2	0.6	3.13	0	0	55.9	-0.272	0
3	1.51	3.11	0	0	55.5	-1.91	0
4	3.38	2.95	0	0	52.3	-5.35	0
5	4.72	2.72	0	0	48.1	-7.75	0
6	-0.0694	0.409	-3.85E-5	-2.07E-6	-6.71	-2.48	-2.96E-3
7	-0.0959	0.396	-5.32E-5	-3.26E-6	-6.09	-3.53	-2.85E-3
8	-0.117	0.377	-6.67E-5	-4.58E-6	-5.33	-4.51	-2.71E-3
9	-0.126	0.355	-7.87E-5	-5.08E-6	-4.34	-5.42	-2.56E-3
10	-0.84	3.13	0	0	60.1	0.754	0
11	-0.0791	0.401	-3.73E-5	-1.28E-5	-3.28	-2.81	-2.89E-3
12	-0.0947	0.374	-6.39E-5	-9.06E-6	-2.95	-4.58	-2.71E-3
13	-0.0202	0.419	-1.47E-5	-4.74E-7	-8.81	-0.61	-3.05E-3
14	-0.0809	0.409	-3.93E-5	-2.21E-7	-8.08	-2.38	-2.91E-3
15	0.631	3.13	0	0	52.7	-0.396	0
16	1.09	3.13	0	0	48.4	-0.425	0
17	-0.171	3.14	0	0	58.2	0.0982	0
18	-0.545	3.13	0	0	59.5	0.458	0
19	-0.0473	0.414	-2.78E-5	-6.08E-6	-5.26	-1.88	-3.01E-3
20	-0.0394	0.417	-2.44E-5	-2.81E-6	-6.33	-1.54	-3.04E-3
21	-0.0356	0.418	-2.09E-5	-1.39E-6	-7.99	-1.14	-3.05E-3
22	-0.0292	0.418	-1.82E-5	-9.31E-7	-8.47	-0.89	-3.05E-3

#	$C_{3_{3,1}}$	$C_{3_{3,2}}$	Q	R
1	3.4E-3	-0.1[illegible]	8	9
2	8.15E-3	-0.19[illegible]	8	9
3	0.0112	-0.15[illegible]	8	9
4	0.0121	-0.13[illegible]	8	9
5	0.0109	-0.10[illegible]	8	9
6	0	0	8	9
7	0	0	8	9
8	0	0	8	9
9	0	0	8	9
10	-5E-3	0.028[illegible]	8	9
11	0	0	8	9
12	0	0	8	9
13	0	0	8	9
14	0	0	8	9
15	6.6E-3	-0.24[illegible]	8	9
16	0.0174	-0.33[illegible]	8	9
17	-5.99E-3	-0.03[illegible]	8	9
18	-6.05E-3	-0.017[illegible]	8	9
19	0	0	8	9
20	0	0	8	9
21	0	0	8	9
22	0	0	8	9

Q and R matrices:

1 $\begin{bmatrix} 900 & 0 & 100 & 100 \\ 0 & 150 & 0 & 0 \\ 100 & 0 & 0 & 0 \\ 100 & 0 & 0 & 0 \end{bmatrix}$ 2 $\begin{bmatrix} 30 & 0 & 30 & 30 \\ 0 & 150 & 0 & 0 \\ 30 & 0 & 0 & 0 \\ 30 & 0 & 0 & 0 \end{bmatrix}$ 3 $\begin{bmatrix} 30 & 0 & 30 & 30 \\ 0 & 700 & 0 & 0 \\ 30 & 0 & 0 & 0 \\ 30 & 0 & 0 & 0 \end{bmatrix}$

4 $\begin{bmatrix} 900 & 0 & 100 & 100 \\ 0 & 750 & 0 & 0 \\ 100 & 0 & 0 & 0 \\ 100 & 0 & 0 & 0 \end{bmatrix}$ 5 $\begin{bmatrix} 900 & 0 & 100 & 100 \\ 0 & 900 & 0 & 0 \\ 100 & 0 & 0 & 0 \\ 100 & 0 & 0 & 0 \end{bmatrix}$ 6 $\begin{bmatrix} 900 & 0 & 100 & 100 \\ 0 & 3000 & 0 & 0 \\ 100 & 0 & 0 & 0 \\ 100 & 0 & 0 & 0 \end{bmatrix}$

7 $\begin{bmatrix} 20 & 0 & 0 & 0 \\ 0 & 20 & 0 & 0 \\ 0 & 0 & 0 & 0 \\ 0 & 0 & 0 & 0 \end{bmatrix}$ 8 $\begin{bmatrix} 10000 & 0 & 0 & 0 \\ 0 & 500 & 0 & 0 \\ 0 & 0 & 0 & 0 \\ 0 & 0 & 0 & 0 \end{bmatrix}$ 9 $\begin{bmatrix} 2000 & 0 & 0 \\ 0 & 2000 & 1800 \\ 0 & 1800 & 2000 \end{bmatrix}$

10 $\begin{bmatrix} 1 & 0 & 0 \\ 0 & 2 & 1 \\ 0 & 1 & 1 \end{bmatrix}$ 11 $\begin{bmatrix} 200 & 0 \\ 0 & 10 \end{bmatrix}$ 12 $\begin{bmatrix} 100 & 0 \\ 0 & 1 \end{bmatrix}$ 13 $\begin{bmatrix} 1 & 0 \\ 0 & 400 \end{bmatrix}$ 14 $\begin{bmatrix} 5 & 0 \\ 0 & 10 \end{bmatrix}$

REFERENCES

1. Heffley, Robert K., A Compilation and Analysis of Helicopter Handling Qualities Data, Vols 1 and 2, NASA CR 3145, 1979.

2. Stengel, Robert F., Stochastic Optimal Control, John Wiley & Sons, 1986.

3. Gessow, Alfred, and Myers, Garry C. Jr., Aerodynamics of the Helicopter, Frederick Ungar Publishing Co., 1967.

4. Bryson, Arthur E. Jr., and Ho, Yu-Chi, Applied Optimal Control, Hemisphere Publishing Corp., 1975.

5. Dorf, Richard C., Modern Control Systems, Addison-Wesley, 1981.

6. AGARD Report No. 577, V/STOL Handling Qualities Criteria, Vols 1 and 2, NATO-AGARD 1970.

7. Stengel, Robert F., Broussard, J.R., Berry, P.W., "Digital Controllers for VTOL Aircraft," IEEE Transactions on Aerospace and Electronic Systems, January 1978, pp. 54-63.

8. Stengel, Robert F., Broussard, J.R., Berry, P.W., "The Design of Digital-Adaptive Controllers for VTOL Aircraft," NASA CR 144912, March 1976.

9. Kriechbaum, Gerhard K.L., and Stineman, Russell W., "Design of Desirable Handling Qualities via Optimal Control," AIAA Conference, August 16-18, 1971.

10. Legge, P.J., Fortescue, P.W., Taylor, P., "Preliminary Investigation into the Addition of Auxiliary Longitudinal Thrust on Helicopter Agility," HMSO, 1981.

11. Landis, Kenneth H., and Glusman Steven I., "Developemnt of ADOCS Controllers and Control Laws," Vols 1 and 2, AVRADCOM, NAS2-10880, 1984.

C-3

12. Hoh, Roger H., Mitchell, David G., et al., "Background Information and User's Guide for Proposed Handling Qualities Requirements for Military Aircraft," NAS2-11304, 1985.

13. Hoh, Roger H., and Askenas, Irving L., "Handling Qualities and Display Requirements for Low Speed and Hover in Reduced Flight Visibility," American Helicopter Society (AHS) preprint No. 79-29, May 1979.

14. Key, David L., and Hoh, Roger H., "New Handling-Qualities Requirements and How They Can Be Met," AHS 43rd Annual National Forum, May 1987.

15. Glusman, S.I., Dabundo, C., Landis, K.H., "Evaluation of ADOCS Demonstrator Handling Qualities," AHS 43rd Annual National Forum, May 1987.

16. Curtiss, H.C. Jr., and Price, George, "Studies of Rotorcraft Agility and Maneuverability," Tenth European Rotorcraft Forum, August 1984.

17. Merrick, Vernon K., and Gerdes, Ronald M., "Design and Piloted Simulation of a VTOL Flight-Control System," Journal of Guidance, Control and Dynamics, May-June 1978, pp. 209-216.

18. Corliss, Lloyd, Greif, R.K., Gerdes, R.M., "Comparison of Ground-Based and In-Flight Simulation of VTOL Hover Control Concepts," Journal of Guidance, Control and Dynamics, May-June 1978, pp. 217-221.

19. Mitchell, David G., Hoh, R.H., Atencio, Adloph Jr., "Classification of Response-Types for Single-Pilot NOE Helicopter Combat Tasks," 43rd AHS Annual Forum, May 1987.

20. Gallagher, J.T., Saworotnow, I., Seeman, R., "A Model-Following Variable Stability System for the NASA ARC X-14B," Journal of Aircraft, July, 1972, pp. 461-469.

21. Tyler, J.S., Jr., "The Characteristics of Model-Following Systems as Synthesized by Optimal Control," IEEE Transactions on Automatic Control, October, 1964, pp. 485-498.

22. McKillip, Robert M., "Periodic Control of the Individual-Blade-Control Helicopter Rotor," Tenth European Rotorcraft Forum, August 28-31, 1984.

23. McRuer, Duane T., Askenas, Irving, Graham, Duane, Aircraft Dynamics and Automatic Control, Princeton University Press, 1973.

24. Levine, L.S., Warburton, F.W., Curtiss, H.C. Jr., "Assessment of Rotorcraft Agility and Manueverability with a Pilot-in-the-Loop Sinulation," 41st AHS Annual Forum, 1985.

25. Linden, A.W., and Biggers, J.C., "X-Wing Potential for Navy Applications," 41st AHS Annual Forum, 1985.

26. Kwaackernaak, Huibert, and Sivan, Raphael, Linear Optimal Control Systems, Wiley Interscience, 1972.

27. Porter, Brian, and Crossley, Roger, Modal Control: Theory and Applications, Barnes & Noble, 1972.

28. Goldstein, K.W., and Dooley, L.W., "V-22 Control Law Development," 42nd AHS Annual Forum, 1986.

29. Linden, A., and Ruddell, A., "An ABC Status Report," 37th AHS Annual Forum, 1981.

30. Kailath, Thomas, Linear Systems, Prentice-Hall, 1980.

31. Lewis, Michael S., and Mansur, Hossein, "A Simulator Investigation of Parameters Affecting Helicopter Hangling Qualities in Air Combat (HAC II)," 43rd AHS Annual Forum, 1987.

32. Athans, Michael, Dertouzos, M.L., Spann, R.N., et al, Systems, Networks and Computation: Multivariable Methods, McGraw-Hill, 1974.

33. Parlier, Charles A., "An Advanced Flight Control Concept for Single Pilot, Attack Helicopter Operations," 43rd AHS Annual Forum, 1987.